DOCTOR OF PHILOSOPHY

Mathematical Optimization of Catastrophic Risk Processes via Expectation-Maximization(EM) Algorithms

Chatoro, Marian

Award date:
2024

Awarding institution:
Coventry University

Coventry University
Centre for Financial and Corporate Integrity

Mathematical Optimization of Catastrophic Risk Processes via Expectation-Maximization(EM) Algorithms

Marian Chatoro

Supervisors: Prof Panagiotis Andrikopolous; Dr Jia Shao

A thesis submitted in partial fulfilment of the University's requirements for the degree of Doctor of Philosophy

Word Count: 55,049

January 18, 2024

Certificate of Ethical Approval

Applicant:	Marian Chatoro
Project Title:	Final Thesis: Mathematical Optimization of Catastrophic Risk Processes via Expectation-Maximization(EM) Algorithms

This is to certify that the above named applicant has completed the Coventry University Ethical Approval process and their project has been confirmed and approved as Low Risk

Date of approval:	20 Jun 2023
Project Reference Number:	P161478

Declaration

All sentences or passages quoted in this document from other people's work have been specifically acknowledged by clear cross-referencing to author, work and page(s). Any illustrations that are not the work of the author of this report have been used with the explicit permission of the originator and are specifically acknowledged. I understand that failure to do this amounts to plagiarism and will be considered grounds for failure.

Acknowledgments

I would like to acknowledge my supervisory and co-research team, both at Coventry University and externally , including Prof Panagiotis Andrikopolous; Dr Jia Shao; Prof Athanasios Pantelous; Dr Fei He; and Dr Sovan Mitra. Thank you for your invaluable help throughout this PhD journey, and for your patience in a difficult season.

I would also like to thank all of my family and friends, both in the UK and in Kenya, who played a crucial role in supporting me throughout my journey, and when I was at my weakest.

Finally, I would like to thank Coventry University, especially the Doctoral College and the researchers at the Centre for Financial and Corporate Integrity, the Centre for Business in Society, and the Sigma Mathematics Centre for their contributions to both supporting my PhD and their input towards improving my research.

Abstract

Recent climate observations and trends dictate multiple possibilities of future overall climate depending on the actions taken in the present. Some views can be optimistic, believing that human beings will soon make the necessary changes required for continued survival, while others are more pessimistic, believing that there is not much that can be done, and that life will end altogether on the planet as Earth slowly converts into a hot and barren wasteland. The answers are rarely clear-cut, but given the ability of human beings to research and understand the driving factors behind such processes, the possibility of optimizing our climate conditions for all of earth's inhabitants is always an option. It is for this reason that there are many who try to improve these conditions as best as they can, even if they are unsure if their efforts produce any tangible long-term results. To optimize our climate processes therefore, it has become important focus on long-term sustainability and renewal of optimal environments, and improvement of disaster risk resilience, especially for the more immediate climate risks.

This study intends to contribute to this long-term climate management, by first analysing the history, developments, and trends underlying climate processes, modelling these processes mathematically for the sake of comprehensiveness, and finally applying said models to not only improve climate-based catastrophic risk loss modelling, but also to price and analyse extreme disaster risk financing instruments.

In this manner, the study ensures a fuller view of climate processes and their interactions, generates more efficient catastrophic loss models, and improves model applicability to incorporate newer trends in climate change and climate risk financing, while ensuring better model efficiency in terms of both computational performance and tractability. In this manner, the study thus contributes to the very important need for better disaster resilience among communities and societies, a key goal of recent climate agreements, including the Sendai Framework for Disaster Risk Management (SFDRR). The results established here are useful for both practitioners, academics,

and development-based organisations handling issues of climate and disaster risk, disaster financing, and applied mathematics. In addition, any individual interested in climate impact, mitigation and adaptation can derive value from other elements of the study beyond just its results, including the historical and geological connections that have been discussed.

To this effect, therefore, the study focuses on the application of mathematical optimization, with the Expectation-Maximization (EM) algorithm in particular, to improve climate-based catastrophic loss modelling and pricing of catastrophic disaster risk financing instruments, and the catastrophe bond in particular. Three main studies are conducted, with the first aiming to assess the catastrophe bond market's efficiency by analysing the 'fairness' of its issuer-specific prices through multi-level random effects modelling, the second to provide a better mathematical optimization model for the heavy-tailed nature of catastrophic losses through finite mixture modelling, while the third and final study proposes a model that better incorporates dependence single-peril dependence structure in observed catastrophic losses by applying hidden Markov models. Apart from these three main studies, historical timelines and developments in climate and financial disaster risk management are also extensively discussed in the remaining sections.

Contents

List of Tables

List of Figures

Chapter 1

Introduction

"Unless there is a global catastrophe, mankind will remain a major environmental force for many millennia. A daunting task lies ahead" - Paul Crutzen, Nobel Prize winner and originator of Anthropocene as an epoch

In the year 2000, Nobel Prize winner Paul Crutzen and Eugene Stoermer proposed an epoch change, from the Holocene to the Anthropocene, a new geological time unit for which human activities had the most significant role in the formation of prevailing climate systems (Crutzen and Stoermer, 2021). Over twenty years since their recommendation, the proposal has gained much traction, with the increase in supporting evidence (see e.g., Ring et al., 2012; SOQS, 2019; Milfont et al., 2021) and the formation of a special working group to determine the specifics of such an epoch, including its estimated start date. The Anthropocene Working Group, as it is called, recently determined the start date of this epoch to be around 1950 CE, based on bottom-layer evidence from Crawford Lake in Canada (SOQS, 2019).

While the formal application for this new epoch is still under review, the theory is seeing much support from the scientific community, and even the world at large, especially as human-origin climate change effects continue to be observed worldwide. The soaring of greenhouse gas concentrations in the atmosphere within the past century and its resultant effects of the planet's aggregate temperature has also provided further proof for this phenomenon (see e.g., Brown, 1994; Nordell, 2003; Ibrahim Dincer, 2013; Intergovernmental Panel on Climate Change, 2018). As global warming is now linked to many of the observed climate extremes and trends including glacial melts and rising sea levels, heat waves, droughts, and flash floods (see e.g., Intergovernmental Panel on Climate Change, 2018; NASA, 2023); the reality of such a human-induced long-term climate effect is becoming increasingly difficult to dismiss. Currently, the only leftover scepticism has been shown to be a consequence of behavioural factors like the roles of gender, political conservatism, and other system justifying ideologies in limiting the acceptance of climate change evidence (see e.g., Milfont et al., 2021).

This study proceeds with these observations in mind, using these developments to assess the current state of our planet's resilience, and our disaster risk resilience tools. It assesses the effectiveness of the available disaster risk financing and insurance tools, with greater emphasis on insurance-linked securities, proposed to fill the gap in funding observed in the early 1990s after the occurrence of extreme loss events like Hurricane Andrew and the Northridge Earthquake (Froot, 1999a). In addition to assessing these resilience tools' effectiveness, the study also proposes more effective valuation techniques to incorporate sources of variability and changes or modifications in catastrophe loss distributions arising as a result of increased frequency and severity of loss events, seasonality, and dependence for catastrophic events.

To achieve these aims, this introduction flows through four key subsections; the first subsection focuses on the background and history of climate processes and events, trends, and climate research. The second subsection discusses the key challenges that are encountered in conducting climate research, and the research gaps observed in climate research, more especially in catastrophic events' loss modelling applications under current climate (change) trends. The third subsection discusses how this study intends to address the identified gaps, with the use of catastrophe loss modelling and valuation models that rely on expectation-maximization algorithms. We discuss three main issues; and their proposed solutions, with each question addressed in turn. Finally, the chapter concludes with an impact and contribution subsection; discussing the importance of this research projects to not only researchers and academics, but also the wider society, including to insurance institutions and security/stock analysts; governments and individuals seeking catastrophic risk insurance; and supranational organizations seeking to protect vulnerable communities from the effects of climate change and increased event risks.

We now begin with the background of climate events and processes, linking this background with the state of current climate research. Whether formalised as a geological time unit or not, the Anthropocene's evidential existence still serves as proof that the planet's future climate processes will be heavily and disproportionately influenced by human activity in the future, even with the current proposed changes to reduce this impact (see e.g., Maizland, 2022). As human energy consumption needs continue to grow (Ruijven et al., 2019), those practices aimed at meeting this energy demand will continue to place further strain on the planet, especially if said activities continually use pollution-heavy sources to achieve their targets. As an example, Mongolia's worsening winters due to climate change have necessitated an increase in the use of coal as a heating source for many households, especially those in its capital Ulaanbaatar, causing some of the worst pollution to the city and further exacerbating global warming (UNDP, 2023). As rising energy needs compete with finite resources, the effects of human-induced climate change will continue to be extensively felt and costlier to manage. Vulnerable communities are especially at risk, as most are normally already weakened by internal economic and socio-political events including land degradation, war, and previous famines, a phenomenon observed especially among nomadic herder communities like the Somali (see e.g., ICRC, 2021).

All is not completely bleak though, as climate observations have also shown that it is possible to survive this impending reality, as solutions still exist. In some cases, it has also been shown that conditions can be sustainably improved once the necessary changes are made (see e.g., Intergovernmental Panel on Climate Change, 2018; Quéré et al., 2021). In particular, the reduction in greenhouse gas emissions observed during the Covid-19 pandemic (Quéré et al., 2021) when many parts of the world were locked down signifies that it possible to reverse these warming effect. In addition, an observation of the current environmentally-thriving states of previously heavily degraded ancient civilization settlements of the ancient Maya, Inca, and the Khmer of Cambodia, also further proves that nature possesses an outstanding level of resilience, and only requires time away from human degrading activity. In fact, even the most toxic of environments, like the radiation polluted site of Chernobyl in Ukraine, has still managed to sustain some life since its abandonment after the 1986 disaster (Kovalchuk et al., 2004).

The planet requires time to sustain itself but rising energy demands have made it almost impossible for human beings to allow it the required time. Vulnerable communities, in particular, have rarely had a choice but to survive, as they lose not only their livelihoods due to increasingly unsupportive external environments, but are also then forced to migrate to urban centres (see e.g., ADB, 2021; ICRC, 2021; UNDP, 2023). These migrations then raise the urban populations of their cities of settlement, which in most cases further stresses the urban support system's resources (Pande, 2023). Despite this, many have recognised the need to restore a planetary sustainable state and have slowly begun enacting measures aimed towards accomplishing this (see e.g., Intergovernmental Panel on Climate Change, 2018; ADB, 2021; ICRC, 2021; UNDP, 2023).

Governments, supranational organisations, individuals, and other humanitarian organisations have been at the forefront; enacting climate sustainability policy, climate agreements, or making deliberate choice towards protecting the earth for its inhabitants, both present and future (see e.g., Intergovernmental Panel on Climate Change, 2018; ADB, 2021; ICRC, 2021; UNDP, 2023; Vesnic, 2023). Despite this, these stakeholders often have significant internal constraints that limit just how much they can reasonably accomplish; including the prioritization of basic need provision for their current populations or dependents; and a forced shift in focus to only providing for their local communities when resources are limited by other socio-political factors like wars; with an example being the recently observed grain shortages as a consequence of the Russia-Ukraine war (see e.g., Ben Hassen and El Bilali, 2022; Lin et al., 2023). Some governments e.g., the Indian government (see e.g., Ivanov et al., 2022) have moved to limit their grain exports, further exacerbating the grain crisis in import countries. The increased pace and resultant increase in costs associated with climate-based events has also significantly complicated, and in some cases, impeded mitigation and adaptation efforts (see e.g., Froot, 1999b; Vesnic, 2023).

The pace of climate events has meant that there is often little time to recover and pool resources before the next event hits, and that countries can no longer fully rely on humanitarian aid to meet their recovery needs, as this requires time to be sourced. Aid also seems to favour more 'trending' events over long-standing events. It has been noted, for example, that the efforts to gain aid for the Somalia famine in 2022, which has been shown to have led to over 43,000 deaths and 2.9 million internal displacements (WHO, 2023), were complicated as most aid shifted towards the Russia-Ukraine war, leading the Somali people even more vulnerable to the associated health risks. In addition, aid is dependent on said disasters not affecting the world on a more global scale, or on the absence of multi-disaster events that would affect both the donor and the receiver at the same time. This unreliability of financial aid then forces a protection seeker to look elsewhere for their disaster funding needs. In the past, this has mostly been via the use of the insurance markets.

This brings us to our second subsection, which focuses on disaster-based resilience-maximizing solutions that have historically been available to us; and why these solutions have, in the past three decades especially, increasingly begun to prove insufficient. We also briefly discuss the financial security that was introduced to cover this gap in extreme event insurance in the early 1990s, i.e., the catastrophe bond. We then address the challenges faced in the modelling of underlying catastrophic loss processes for such/similar instruments, and why such challenges need to be addressed for the continual reliability of such instruments as viable solutions for funding disaster recovery.

For centuries, insurance and reinsurance have been the most popular way to fund uncertain and extreme events (Trenerry, 1926; Coppola, 2006; Holland, 2009; Swiss Re, 2017). In recent decades, however, the increased frequency and severity of extreme events has overwhelmed the industry, making it difficult for the industry to offer comprehensive insurance for catastrophic events without risking their own solvency in turn. This capital flight observed especially after extreme events like Hurricane Andrew in

1992 and the Northridge earthquake in 1994 was the motivation behind an alternative source of capital that could better cover the insurance needs of protection seekers. The Insurance Linked Securities (ILS thereafter) market and its catastrophe bond market was developed as a result (Swiss Re, 2012).

Though small in scale when compared to traditional insurance and the reinsurance markets, its ability to provide an alternative source of capital when traditional markets are strained has made the ILS market, and the catastrophe bond market particularly, a key source of extreme-event risk financing (see e.g., Froot, 2001; Cummins, 2008; UNCDF, 2021). The market provides the necessary funding to aid short-term recovery efforts, whose costs have been on the rise with the increased frequency and severity of catastrophic events. Its key users have included both protection providers like insurance and reinsurance companies, and pure protection seekers, including governments, non-governmental organizations, and infrastructure-at-risk companies, including utility companies (Artemis, 2023). Investors in such financial assets are drawn from a wide range of fields, with institutional investors making up most of them.

The catastrophe bond market has been in existence since the early 1990s, and continues to broaden in both size and number of issues, as the catastrophe bond has proven the most popular of the available ILS instruments (UNISDR, 2004; Cummins, 2008; Artemis, 2023). As the instrument becomes one of the most important sources of extreme disaster funding, modelling efforts to expand its pricing capabilities under the changing climate and loss trends are becoming increasingly necessary. This is because the change in pacing and size of observed losses must be efficiently incorporated in order for these instruments to continue to be a reliable source of disaster risk financing. These increased frequencies, volatilities in both losses and prices, and loss dependencies, are just but a few of the factors to be incorporated into pricing models to allow for comprehensive and fair pricing.

The challenge arises, however, in the structure of the modelling process itself. The catastrophe bond pricing process, for example, applies comprehensive models that already incorporate other underlying models for each of the underlying loss severity processes, loss frequency processes, interest rate processes, and finally the bond pricing model itself (see e.g., Vaugirard, 2003a; Vaugirard, 2003b; Burnecki et al., 2005; Ma and Ma, 2013; Shao et al., 2017; Burnecki et al., 2019). The number of underlying variables increases the complexity and thus intractability of the modelling process, making it difficult to incorporate further trends that would further complicate the pricing process into the model. The increased computational complexity and model intractability can also render such models virtually unsolvable, as many of the formulas lack open solutions. Incorporating any trends or changes in extreme event processes can therefore prove to be an especially difficult task for these already complicated instruments.

This can be costly to protection seekers, as the inability to comprehensively model their key sources of risk could mean a failure to access recovery funding for their changing needs. In addition, investors have been shown to be unwilling to fund perils they do not fully understand or fund them at exceptionally high risk premiums in the catastrophe bond market (Bantwal and Kunreuther, 2000).

Having established the catastrophic loss modelling challenges, and why it is necessary that these be addressed, we focus this chapter's third subsection on the proposition of models that can effectively address the previously discussed issues. We discuss three main challenges and propose models to address each in turn. This study contributes towards improving the efficiency of the modelling process underlying catastrophe bond loss modelling and pricing, with the goal of improving its adaptability to observed loss trends and climate processes. The study focuses especially on improving the comprehensiveness, computational power and tractability of heavy-tailed loss models, loss dependency models, and protection seekers' pricing volatility models.

This is accomplished through the application of Expectation-Maximization (EM) algorithms, a class of local optimization algorithms formally proposed by Dempster et al. (1977) for the modelling of latent variables or missing data problems, and extensively used in other applications, including in gene sequencing, image processing, pattern recognition, and linguistics, among others (see e.g., Couvreur, 1997; Rabiner, 1989).

Since the three aforementioned effects of (i) volatility, (ii) heavy-tail characteristics, and (iii) dependency can be structured as missing or latent variable problems, the EM algorithms provide efficient and robust techniques to allow the incorporation of such effects without significantly affecting model tractability and complexity. These three main problems are considered in this study, and their respective EM-based models are further discussed below. The first effect considered is the *presence and extent of pricing volatility in the primary catastrophe bond market for bonds with similar underlying characteristics but issued by different cedents.* In an efficient market, these prices should be similarly priced despite their different issuers. This is because a catastrophe bond's risk stems not from the characteristics of the issuing party, but from the underlying catastrophic event and its risks, including its frequency and severity. Any significant observed volatility would then imply that issuer's reputation and standing within the catastrophe bond market still bears weight, with investors inadvertently penalising newer and less consistent issuers over older and more consistent issuers. This would further prove that the catastrophe bond market is still inefficient to some degree, with this specific type of inefficiency more likely caused by behavioural factors, as previously discussed by Bantwal and Kunreuther (2000).

This effect is tested in the first empirical chapter, Chapter 5 , using a large dataset of primary catastrophe bonds issued from the early stages of the market, i.e., January 1997 and until March 2020. The pricing volatility among issuers is assessed through a proposed random effects model (an application of Expectation-Maximization algorithms to variance component analysis), which analyses the variations in catastrophe bond premiums introduced by the differences between issuers. The results indicate that this effect exists and is significant. The testing is also extended to specific issuer characteristics, and the effect is found to be stronger (i) for smaller issuers based on issue size, (ii) for less consistent issuers based on their years of issue in the primary market, and (iii) for issuers whose primary business is insurance, as opposed to those whose primary business is reinsurance of a combination of primary businesses, including insurance, reinsurance, general risk management and consulting, labelled here as multiline issuers.

The second issue we examined and is covered in Chapter 6 , deals with the *improvement in the modelling of heavy-tailed catastrophic losses for the valuation and pricing of disaster risk financing instruments, that is, the catastrophe bond.* This is accomplished by the proposition of an EM-based approximation technique based on finite mixture modelling for Property Claims Services (PCS)'s industry loss data spanning the period beginning January 1985 and ending in April 2014.

The approximation model is applied to find the mixture distribution that best suits such heavy-tailed data from a set of heavy-tailed and general distributions; both for frequency distribution estimation and severity distribution estimations. The resulting model, which in this case is found to be the 2-component log-normal mixture for loss severity and the 3-component Poisson mixture model for the loss frequency, is then used to generate aggregate loss values that form the basis of the catastrophe bond pricing model. Finally, these results are applied to price two catastrophe bonds with different bond payoff functions and their prices plotted on 3-dimensional plots. The model is then compared with other similar, but non-EM-based mixture models that have been applied for the modelling of heavy-tailed data, including composite mixtures and pure composite models, and found to possess superior fit characteristics, among other factors including estimate stability and reliability, flexibility, and computational efficiency. The chosen model's fit statistics on a different but similarly heavy-tailed dataset (out-of-sample data) are also compared with these non-EM-based mixture models and found to be superior. This proves that the model is consistent in its optimization of heavy-tailed data regardless of the dataset considered and can be reliably used in real practice.

The third and final issue this study tackles in Chapter 7 is the *modelling of dependencies in catastrophe losses over time*, especially compounded by the observed climate-based and demographic impacts on extreme event loss frequencies and loss severity. The independence and identical distribution assumption, commonly used to simplify modelling processes, is discarded, and our loss processes are assumed to neither be independent nor identically distributed. The loss process is assumed to display both dependencies over time and seasonality, and this is tested and modelled by the proposed Baum-Welch (a special case of Expectation-Maximization(EM) algorithms) algorithm-based Hidden Markov Model. This standardized approach models loss clusters generated from such dependent and non-stationary processes as catastrophe 'states'. Using single-event data from Property Claims Services (PCS), the presence, extent, and distribution of these clusters is established through extreme value techniques. Hidden Markov Models are then used to identify the optimal dependent mixture models for both loss frequency and loss severity. To test this approach, we use a final sample of 3143 observations that consist of isolated meteorological event data. [1] The meteorological event data covers, for example, hurricanes, tropical storms, and other wind and thunderstorm events.

A number of both heavy-tailed and general distributions are tested with the most optimum loss models found to be the three-component Poisson dependent mixture for the loss frequency and the four-component log-normal dependent mixture for the loss severity. The dependent mixture Poisson model's results are then compared to a more common Poisson-based frequency model, i.e., the non-homogeneous Poisson frequency model based on the peak-over-threshold approach, with the latter's plots found to be a worse fit for the data compared to the dependent Poisson mixture model. Finally, a compound Poisson Markov-dependent mixture model is generated for the chosen distributions and aggregate losses generated from the model are used as input for the accompanying catastrophe bond valuation process.

The three models applied in these three assessments (i.e., Chapter 5, Chapter 6, and Chapter 7) prove the efficiency and applicability of EM-type algorithms to heavy-tailed problems, with improved fit statistics and stability of estimates when compared to similar Newton-Raphson based models.

Lastly, in this chapter's fourth and final subsection, we discuss the value and impact

[1] The selected dataset is drawn from a larger original dataset of 3951 individual observations that further included non-meteorological events including earthquakes and wildfires from the US-based Property Claims Service (PCS)

of this study to numerous stakeholders and the wider society. In this subsection, a case is made for why this study's contributions have a place in furthering our efforts towards the improvement of overall societal conditions, especially with regards to strengthening our disaster risk resilience capacities.

We begin by assessing the impact of this study on extreme event protection-seekers. These include individuals seeking to insure themselves from the effects of extreme events, governments seeking to boost resilience among their societies and supranational organisations seeking to ensure marginalised and vulnerable communities are not left at risk, especially since they normally bear the greatest losses due to conditions stemming from the lack of recovery and insurance funding and other resources when such disasters occur.

In times of increasing frequency and severity of catastrophic losses, it is especially important that protection-seekers can not only access such funding, but also access it at fair prices for the market to truly contribute towards improving insurance capacity for those at risk. This is as opposed to adding higher costs to already costly events because of mispricing or unreliable pricing risks. This study contributes to improving this outreach and access to funding for all those that may need such protection by proposing models to identify, quantify and improve the valuation of catastrophic loss processes.

The second group of stakeholders are the insuring institutions. These include insurance and reinsurance companies. As extreme events become more prevalent, these insurers find themselves having to struggle to maintain their solvency. As the principles of pooling and diversification begin to fail due to risk and loss concentration, the concept of insurance becomes difficult to profitably sustain for the insurer. Capital flight and funding limitations brought on by these increased extreme event risks also pose a challenge to traditional insurers. Under such conditions, there is a growing need to find and provide extended insurance funding alternatives, especially if the goal is to ensure the survival of such institutions.

Financial markets, through insurance-linked securities and especially catastrophe bonds have evolved to fill this gap. Yet these markets are still young and represent only a fraction of the mainstream insurance/reinsurance markets. Prior studies to improve valuation and product structuring, including this current study, contribute towards making such markets more accessible for all that may need its protection, especially in times where conventional insurance fails due to the nature of such losses.

Thirdly, we discuss the importance of this thesis to an alternative group of protection sellers not in the direct business of providing insurance, that is the security market investors. These are stakeholders whose objectives include seeking suitable returns on investment and identifying viable and niche return sources for themselves and for those companies, institutions, or individuals whose funds they manage, as well as seeking sources of diversification for their investments to minimize their underlying risk of their investment portfolios.

Insurance-linked security markets are known to be a great source of diversification as their returns are typically uncorrelated with those of other financial market sectors (Froot, 2001; Cummins et al., 2002; Cummins, 2008). Such markets also provide higher returns due to the riskier nature of the tradable instruments, making them a suitable investment for investors that seek high returns and potential speculators. Our study into improvement of valuation of insurance-linked securities is of importance to all investor seeking to understand the risk-return tradeoffs for these types of markets and tradable financial assets.

Finally, we discuss two groups of stakeholders who may perhaps be the most keenly interested in this study and its results. We begin with valuation companies and investment banks involved in insurance-linked securities' underwriting processes. The analysis, results and conclusions of this thesis are most directly useful to these end users since we are working under similar objectives, that is to provide a more accurate and suitable valuation process for such instruments. In line with the objective of this thesis, these institutions seek to gain and apply the information they gain or collect on catastrophic events' losses and occurrences to optimize the creation and valuation of catastrophic financing and insurance options for all the previously discussed stakeholders. They also seek to ensure prices reflect true conditions as best as possible, thereby reducing forecasting errors and promoting trust between sellers and buyers of such financial instruments.

Apart from the previous end users, the findings of this thesis are also of particular importance to academics, researchers, and consultants, especially in the field of extreme event disaster risk management. There are multiple objectives that these groups intend to meet, with the most applicable being discussed and linked to this study's objectives and contributions. In seeking to ensure that market processes are efficient and that all relevant instruments created truly suit their purpose, this thesis contributes towards the assessment of the efficiency of pricing among different issuers for similar bonds. This is done by proposing pricing processes that incorporate climate trends and their effects on observed losses, including dependence, seasonality, and heavier tails.

As this group of end users also seeks to propose new and more efficient financing and insurance tools for an ever-changing climate landscape, and ensure availability of protection for all including those vulnerable and unable to access funding by themselves, we address this gap in the current literature by pricing instruments that provide funding in the most extreme cases and are frequently used by organisations aiming to protect the most vulnerable communities, including supranational organisations, governments, and disaster funds. There is also the goal to ensure available instruments cover possible events comprehensively, leaving no gaps in funding or protection availability, which this study contributes to by ensuring better incorporation of heavy tail losses, dependence, and seasonality elements of catastrophic events; and the intention to provide industry stakeholders with more comprehensive and complete insight into all variables affecting catastrophic event processes and observed losses which we also add to by assessing key variables affecting pricing in the primary market and the degree to which behavioural factors like issuer-based effects would influence pricing of instruments believed to be uncorrelated with the issuing companies.

Finally, there is the aim to assess and critique present solutions and use this knowledge to propose even better future disaster risk funding solutions. By proposing the use of expectation-maximization-based algorithms that have better ability to pick out and isolate hidden effects that either could not be modelled through normal processes, or might be entirely ignored, this thesis contributes to the improvement of available disaster risk financing solutions and helps in reducing computational costs of the relevant modelling processes.

In conclusion, even beyond key stakeholders, this study retains the over-arching objective of providing better disaster risk management solutions for the sustainability and resilience of the planet, which in a sense, is the end-goal of all solution-seekers. It therefore not only accomplishes its task of proposing a new class of models for heavy-tailed data than can better incorporate and assess the trends in extreme event modelling and climate change science as well as their impact on the pricing of disaster risk financing instruments, but also contributes to the over-arching goal of planetary sustainability and disaster risk resilience.

The rest of the thesis is structured as follows. Chapters 2 and 3 give an overall historical background of both climate disaster risk and disaster risk management. Chapters 4 explains the origins and development of optimisation and the EM algorithm, while chapters 5, 6, and 7 apply the EM algorithm to catastrophic loss modelling, through multilevel random effects models, finite mixture models, and hidden Markov models respectively. The thesis concludes in chapter 8, where we discuss the implications of the findings including suggestions for future research.

Chapter 2

Geology, Natural Disasters and Disaster Risk Management

2.1 Geological History: Climate and Natural Disasters

"To focus solely on endings is to trade conclusions for the very beginnings that created them. And if this cycle should persist, we will likewise miss the beginning that will follow this ending." Craig D. Lounsbrough, Author

2.1.1 Introduction

The comprehension and appreciation of the geological roots underlying natural disaster occurrence necessitates understanding the structure of the planet and/or universe in both its current and previous states. For this to be achieved, knowledge of the processes underlying landscape, oceanic and atmospheric formation is essential to address the link between such events and creation and/or evolution. After all, occurrences bearing the label 'natural hazards', and consequently 'natural disasters' are rarely indistinguishable from occurrences underlying the formation of the universe and its ecosystems. This is because the universe is an interactive system, with its processes seemingly creating through destruction. Volcanic eruptions, for example, are responsible for lithospheric replenishment (Longo and Longo, 2013); wildfires for ecological diversity (Burton et al., 2008; Tang et al., 2021; Goldammer et al., 2005); and extinction and speciation that arise due to geological cycles, for evolution and diversity (Raup, 1994). Geological cycles, which include the tectonic cycle (Nance et al., 2014), the rock cycle (Abbott, 2022)(Abbott, 2016), the hydrological cycle (Oki, 2006), and the biogeochemical cycle (Galloway et al., 2014). Arneth et al. (2010) provide proof of this interconnectivity. The universe is also in a constant state of change, evolving due to both geological cycles and external influences like the role of its inhabitants, especially human beings (Le Treut et al., 2007). To understand the influences behind natural disasters therefore, it is necessary to understand this process of change.

The dichotomy of roles in natural events arises only due to these events' effect on the affected communities. Only in cases of significant exposure and in some cases coupled with limited capacity to handle such effects, is the source event then termed a natural hazard. The United Nations Office for Disaster Risk Reduction (UNDRR) defines a hazard as 'a process, phenomenon or human activity that may cause loss of life, injury or other health impacts, property damage, social and economic disruption, or environmental degradation' (UNDRR, 2016). When these threats arise from a natural process, then the hazard is referred to as a natural hazard (Hyndman and Hyndman, 2016). Examples of natural hazards according to the World Meteorological Organization (WMO) include droughts, tropical cyclones, air pollution, desert locusts, floods and flash floods, landslide or mudslide (mudflow), avalanche, dust-storms/sandstorms, thermal extremes, thunderstorms, lightning and tornadoes, forest or wild-land fires, heavy rain and snow, and strong winds; while the Unites States of America's (USA) Federal Emergency Management Agency (FEMA) includes earthquakes, tsunamis, and volcanic eruptions as additional processes. Other natural hazards stem from extra-terrestrial events e.g., asteroid and comet impacts.

The UNDRR also defines a disaster as 'a serious disruption of the functioning of a community or a society at any scale due to hazardous events interacting with conditions of exposure, vulnerability, and capacity, leading to one or more of the following: human, material, economic and environmental losses and impacts' (UNDRR, 2016).

This implies that only when the natural hazard results in the actual realization of a threat or disruption is it then referred to as a ‘natural disaster’, and once the level of loss and destruction is large enough, i.e., beyond a given minimum threshold[1], the disaster is then labelled a catastrophe (Hyndman and Hyndman, 2016). The following table displays the costliest global catastrophic events by economic losses[2] since 1900.

Table 2.1: *Top 10 Costliest Global Economic Loss Events (1900-2022)*

Date(s)	Event	Location	Economic Loss (Nominal $ billion)	Economic loss (2022 $ billion)
March 11, 2011	Tohoku Earthquake/Tsunami	Japan	235	314
January 16, 1995	Great Hanshin Earthquake	Japan	103	203
August, 2005	Hurricane Katrina	United States	125	190
May 12, 2008	Sichuan Earthquake	China	122	168
August, 2017	Hurricane Harvey	United States	125	152
September, 2017	Hurricane Maria	Puerto Rico, Caribbean	90	109

Continued on next page

[1]The risk management and consulting company Aon, for example, defines catastrophes as ‘natural disasters that cause at least $25 million in insured losses; or 10 deaths; or 50 people injured; or 2,000 filed claims or homes and structures damaged.’

[2]Economic loss, in this case, includes ‘any direct physical damage or direct net loss business interruption costs’, according to Aon.

Table 2.1 – continued from previous page

Date(s)	Event	Location	Economic Loss (Nominal $ billion)	Economic loss (2022 $ billion)
October, 2012	Hurricane Sandy	United States, Caribbean, Canada	77	99
September 2022	Hurricane Ian	United States, Cuba	96	96
September, 2017	Hurricane Irma	United States, Caribbean	77	93
January 17, 1994	Northridge Earthquake	United States	44	90

Source: Aon 2023 Catastrophe Insight

Of note is the observation that all the costliest natural disasters have occurred in the most recent two decades. This could either mean that natural disasters have increased in frequency, or the severity of losses from such disasters has increased. Alternatively, it could signify a parallel increase in both frequency and severity of natural disasters. This deduction is supported by evidence from earth's external environment, especially with regards to the observed changes in the climate system and its consequences (Botzen et al., 2010; Hansen et al., 2016). It has been shown in the most recent years that human-induced changes in climate have increased in scale (Eyring et al., 2021), and therefore a key goal to ensure society's sustainable future has been climate adaptation and disaster risk management. This has been evidenced mainly through the key 2015 climate-related agreements i.e., 2015's UN Sustainable Development Goals (SDG), the Paris Climate Agreement (Asselt et al., 2015; Falkner, 2016), and the Sendai Framework for Disaster Risk Reduction (Wahlström, 2015).

It has always been important to understand that as the universe is constantly changing, natural events will likely keep occurring. As such, knowledge of how to best adapt to and coexist with these occurrences is essential. Understanding a natural hazards' underlying processes and its origins enables the proposal of efficient and optimal solutions to any risks that could potentially arise as a result. Society's resilience is then not only strengthened, but through a deeper understanding of the risks introduced at each stage of the disaster processes, such risks can even be further converted into rewards, by harnessing the immense energy released through these processes and redirecting it to more efficient usage. This therefore ensures sustainable maximization of societal experience irrespective of the prevailing external state.

2.2 History and Natural Disasters

Throughout history, the field of disaster risk management has aimed to achieve this sustainability in one way or another, and using the resources available to civilization at the time. Before civilization began, hunter gatherer populations ruled the land. These were originally quite sparse in comparison to the land size, but as populations grew, increased competition for available resources began to lead to conflicts (Bogucki, 2008). Early civilizations arose consequently, i.e., out of the need to better manage their environmental states to ensure survival of their populations (Bogucki, 2008). Early forms of Disaster Risk Management (DRM) thus developed and continued evolving with each culture's needs. This led to improved practices in water management, plant and animal domestication, and general governance in the early societies of Mesopotamia (Mays, 2010), Ancient China (Gong et al., 2019; Chen, 2016), Crete (Mays, 2010), and the Indus valley (Mays, 2010), to name but a few. This also boosted skill diversification and availability of better tools for production (Bogucki, 2008).

Despite these developments, the solutions were not always enough, nor sustainable, since for many of these civilizations later failures would in a large proportion be attributable to climate change. This is because environments that supported agriculture and ensured society's safety were especially dynamic due to factors both internal to the ecosystems and human related after-effects of settlement. The Minoan civilization of Crete, for example, was made vulnerable by a combination of volcanic eruptions, earthquakes, and tsunamis, which eventually weakened them to attacks from their enemies (Antonopoulos, 1992). The Angkor civilization of Cambodia was weakened by drought-flood cycles (Penny et al., 2019); the ancient Mayans of Central America by deforestation, erosion, and environmental degradation; the Moche of Peru by drought-flood cycles and earthquakes; and Norse Greenland by the little ice age beginning around 1000 CE to 1500 CE (Leroy, 2020). These environmental factors were therefore frequently both responsible for the onset of civilizations and their eventual demise.

All this notwithstanding, however, Disaster Risk Management has existed in one form or another for as long as change has affected human existence and has continued to evolve to fit the requirements of the prevailing systems and civilizations. Disaster risks have been defined as 'a function of hazard, exposure, vulnerability, and capacity' by the Organization for Economic Cooperation and Development (OECD) (OECD, 2017). In this case, exposure is defined as 'a measurement of the value at risk of damage and loss', and vulnerability as 'conditions determined by physical, social, economic and environmental factors or processes which increase the susceptibility of an individual, a community, assets or systems to the impacts of hazards', according to the United Nations Office for Disaster Risk Reduction (UNDRR) (UNDRR, 2016). Capacity refers to 'the combination of all the strengths, attributes and resources available within an organization, community or society to manage and reduce disaster risks and strengthen resilience', (also) as defined by UNDRR. Disaster risk management can thus be formally defined as the application of disaster risk reduction processes for the prevention, reduction, and adaptation to new, existing, and residual disaster risks and the resulting losses (UNDRR, 2016).

Natural disasters were explained through myths, folklore, legends, and other forms of spirituality. [3] Overall, these creations served multiple purposes, including explaining

[3] A *myth* is a story, considered sacred, from the past, that explains either the origin of the universe

disasters, warning about disasters, coping with the effects of disasters both mental and physical, and seeking solutions to disasters. Other solutions were also sought in a consequent manner i.e., through sacrifices, chants, lamentations, and prayers (Bentzen, 2013).

These practices subsequently provided the foundation for later developments in disaster risk management. At the time, however, risk acceptance was the predominant risk management strategy (Cashman and Cronin, 2008), with divine providence relied upon more than mitigation. This could be because of the helplessness early civilizations would have experienced under such circumstances, further compounded by the lack of knowledge and/or tools to provide better understanding and management of disasters. Evidently, ancient civilizations' gods were frequently named after natural events for example, sun-gods, moon-gods, storm-gods, and disaster-gods, etc. Divine reliance has persisted to recent times, with any developments counter to the divine notions encountering resistance. According to Swiss Re (2017), as recently as the 19th century, insuring against death was still frowned upon, especially by religious leaders. These survival techniques pose several limitations, including, overlooking sustainable solutions in favour of erroneous beliefs that then compound disaster losses and ca-

and life or expresses a culture's moral values (Rosenberg, 1997). Examples include the myths depicting Ancient Greek gods (Graves, 1955); the Japanese creation myth of Izanagi and Izanami (Chamberlain, 1982); and the Ancient Egyptian myths of Anubis, Osiris etc. (Pinch, 2004). *Folktales* are fictional stories that are used to symbolically present different mechanisms humankind uses to cope with the world they inhabit (Rosenberg, 1997). Popular folktales include the tales of the Little Red Riding Hood (Ashliman, 2002) and Jack and the Beanstalk (Jacobs, 2005) from Europe; Anansi the Spider from West Africa (McDermott, 1987); and the Wonderful Wizard of Oz (Chaston, 2001) from North America. Finally, a *legend* defines a story based on an individual or subject that was or is believed to have lived or existed in the past. These heroes frequently serve as role models for their respective cultures, embodying the desirable values and virtues of a given community (Rosenberg, 1997). An example is the Luo community of East Africa's Legend of Lwanda Magere, a prophesied hero born with skin made of stone that no weapon could pierce, who subsequently freed the Luo's from the Lang'o, who had held them captive (Omtatah, 1991); or more famously, Gilgamesh of the ancient Mesopotamian epics (Dalley, 1998).

sualties for events that could otherwise have been better handled. In addition, the passivity arising due to a transfer of responsibility could also lead to the persistence or worsening of environmental degradation and pollution, key causes of climate change.

As civilizations expanded and human population increased over time, more individuals became exposed to natural hazards due to their areas of settlement and reduced resources to enable relocations from hazard-prone areas. In earlier civilizations, communities could easily relocate to more conducive geographical areas if their current settlements were deemed uninhabitable due to climactic and environmental effects. Proof of this can be deduced from the many abandoned historical cities e.g., the Incan lost cities of Machu Picchu in Peru (Rodríguez-Camilloni, 2009); the Khmer capital of Angkor (Chandler, 2003) in present-day Cambodia; and the ancient Mesopotamian cities of Ur, Lagash and Nippur etc. (McDaniel, 1968). Later civilizations did not have many resettlement options due to political and demographic factors, including land borders and population increase. In addition, such hazard-prone areas were, in most cases, the only locations that could support agriculture and society was therefore left no choice but to settle in such spots. Cities like San Salvador in El Salvador (Ilopango volcano (Suñe-Puchol et al., 2019)); Mexico City in Mexico (Popocatépetl volcano, Trans-Mexican Volcanic Belt (Granados and Jenkins, 2015)); Sicily (Etna volcano (Duncan et al., 1996)) and Naples (Vesuvius volcano (Everson, 2012)) in Italy, for example, are built in the shadow of active volcanoes or volcanic belts. This proximity has therefore meant that natural disaster occurrences generated increasing costs over time. As these costs arose, so did developments in disaster risk management since communities were faced with no alternatives but to develop means to adapt and protect themselves against such catastrophic losses within their respective settlements. However, some key benefits did arise from these ancient disaster management techniques and observations.

An early warning system in disaster risk management refers to ‘an integrated system of hazard monitoring, forecasting and prediction, disaster risk assessment, communication and preparedness activities, systems and processes that enables individuals, communities, governments, businesses and others to take timely action to reduce disaster risks in advance of hazardous events' (UNDRR, 2016). These systems allow societies to anticipate disasters and take action to protect lives and livelihoods pre-disaster. Mythology, folklore and other oral tradition provided the earliest forms of early warning systems against natural hazards, and have been shown to play this role even in recent times for indigenous societies (Lauer, 2012; Syahputra, 2019). During the 2004 Indian Ocean Tsunami, for example, the Moken, an indigenous people on the Andaman Islands in the Indian Ocean, who relied on the myth of the Laboon or the 'wave that eats people' to deduce that a tsunami was imminent evacuated to higher ground and survived, while those who had not heard these stories did not survive, leading to a skewed death toll (UNESCO, 2015).

Oral tradition, mythology and folklore have also provided a way for both past and present societies to identify, explain and understand historical disasters. The field of geo-mythology, which applies myths and legends to provide context for geological events, arose as a direct result. Geo-mythologists are defined as those who 'seek to find the real geological event underlying a myth or legend to which it has given rise' (Vitaliano, 1968; Vitaliano, 1973). They also served as a record of past natural disasters e.g., the South Pacific islands' origin myths detailed in (Nunn, 2003) that are believed to provide a record of previous volcanic eruptions (see also (Cashman and Cronin, 2008) for other myths explaining volcanic eruptions). Cosmic disasters can be deduced from ancient Aztec mythology and Hopi mythology; hurricanes from Taino and Mayan mythology; earthquakes from Tibetan folklore, Mayan mythology; and Polynesian tradition (Mendia-Landa, 2008). This is then supplemented with paleo-climatic data e.g., tree rings, ice cores, borehole data, corals, lake and ocean sediments, stalagmites, fire history data etc., to then provide a more comprehensive understanding of the evolution of the geological environment.

In addition, coping techniques for natural disasters have been an important consequence of these ancient practices. Natural disasters have been identified as one of the origins of religiosity (Bentzen, 2013), with disaster survivors using stories, rituals and ceremonies to reduce trauma, pain and guilt, and consequently restore hope for the future (Hirono and Blake, 2017). Psychological theories, including uncertainty hypothesis, supernatural punishment hypothesis, and religious coping hypothesis have all been identified as techniques for coping with disasters (Bentzen, 2013), with spirituality playing a central role in mental health improvement post-disaster.

Finally, mythology, legends and folklore provided the foundation for disaster risk management to develop and evolve over time, with occurrence of the disaster itself also providing the opportunity for study and improvement of disaster management (Mauch and Pfister, 2009). The next section details some of the key developments in disaster risk management over time.

2.3 Evolution of Disaster Risk Management

Early civilizations' shift from hunter-gathering to plant and animal domestication during the Neolithic revolution (Childe, 1936) provides the first formal manifestation of practices in natural hazard mitigation and disaster management. Earliest archaeological evidence of agriculture has been discovered from settlements of the Ayn Ghazal civilization (circa. 7200BCE - 5000BCE (Smit, 2019)), located in modern-day Jordan (Kafafi, 2014); and the Çatalhöyük civilization (circa. 7500BCE-5700BCE (Smit, 2019)) in central Turkey (Hodder, 2010). Furthermore, communal living which subsequently led to the rise of the first cities, developed in an effort to maximize agricultural capacity and boost food production within early civilizations, including in Ancient Sumer and Akkad in Mesopotamia (Kennett and Kennett, 2006). This surge in food production and storage then allowed the diversification of professions and services leading to the rise of craftsmen, traders, artisans, and the earliest forms of civil service and government. Initial natural hazard risk management further expanded in the form of flood management and irrigation practices, for example in the Tigris and Euphrates river valleys in Mesopotamia, and in the Nile river valley in ancient Egypt (circa. 3150BCE 30BCE) (Smit, 2019; Soroush and Mordechai, 2018).

Despite the developments that accompanied the rise of permanent settlements and agriculture, civilization also presented its challenges, especially with the rise of disease due to weakened immune systems from unsanitary living conditions and less varied diets compared to the hunter-gatherer diet (Hart-Davis, 2012). While religion and spirituality were applied extensively as an early method of surviving the worsening conditions that would be further exacerbated during times of natural disasters e.g., droughts and floods (Bentzen, 2013; Mauch and Pfister, 2009; Hughes, 2013), better systems of government were required for more effective decision-making. This led to improvements in decision analysis via establishment of social groups or councils of elders that were tasked with the role of risk analysis and management within the community (Coppola, 2006). Such groups ensured the resilience of societies (Leroy, 2022), and provided a foundation for the formal risk management departments present in many institutions today.

Evidence of risk transfer can be found as early as 1800BC, with the ancient Babylonian Code of Hammurabi (King, 2005; Harper, 1999), that included an early form of marine insurance, also known as 'bottomry', whereby merchants who sought loans to fund shipments would pay an additional sum to the lender who would then guarantee loan cancellation if the shipment was lost at sea (Smyth, 2013). These bottomry contracts have been shown to bear similarities to modern day catastrophe bonds (Holland, 2009). These same concepts were later applied by the Hindus, the Greeks, and the Romans. In addition, the Chinese, as far back as 3000BCE, would redistribute their goods over multiple ships to minimize catastrophic losses if one ship sunk on its river journey (Carter, 1983), giving rise to the earliest forms of diversification (Vaughan, 1997).

Risk sharing was formalised around 1000 BCE (Golding,1931 (cited in Holland (2009)); Prudential Insurance Company of America (1915)), with the advent of maritime laws including the Lex Rhodia, or the Rhodesian Sea Laws, that have been credited as a key propagator of the fundamental insurance principle of contribution (Prudential Insurance Company of America, 1915). According to Prudential Insurance Company of America (1915), part of the translation provided that 'If a ship is caught in a storm and makes jettison of its cargo, and breaks its sailyards and mast and tillers and anchors and rudders, let all these come into contribution together with the value of the ship and of the goods which are saved'. In this statement, it is evident that the loss of one was settled by all, through subdivision. The Babylonian Talmud, circa 586 BCE, also provided rules for loss sharing with regards to any cargo lost at sea, and included the provision for replacement of a lost ship (Rodkinson et al., 1903). In addition, it also provided for land travel protection for merchants and travellers in case of caravan robberies (Rodkinson et al., 1903). Marine risk management was still, however, the predominant form of disaster risk management due to the reliance on waterways for transport, trade and commerce. These forms of insurance had their limitations, however, as similar routes would result in a concentration of losses and thus risk overwhelming the insurer's capacity (Swiss Re, 2017).

Around 600BCE, the earliest forms of life and health insurance through risk sharing developed in Greek and Roman societies by the creation of guilds known as 'benevolent societies' (Swiss Re, 2017). These provided support to the bereaved families and paid members' funeral costs (Trenerry, 1926). These forms of societies are not limited to the past, as they have survived in different forms to the present, including as mutual aid societies (farmers in the Alps in the early 16th century) CE, mutual life insurance companies, co-operative societies, funding committees, and friendship groups (England's 'friendly societies' in the late 17th century) CE. Through to the Middle Ages in Flanders, other forms of insurance were then bundled up together with life and health insurance to include fire, shipwrecks, livestock loss, and imprisonment, among others (Trenerry, 1926). These organizations faced the same challenges of loss concentration and the additional limitations including lack of financial sophistication and poor fund management (Swiss Re, 2017).

The first stand-alone insurance transactions, especially in marine insurance, were developed later in the Middle Ages. These were motivated by developments within the church and with trends in disaster occurrence and loss management. A ban on sea loans by Pope Gregory IX in 1236 led to increased need for alternative forms of financing, with emphasis on the separation of marine insurance from other forms of insurance in order to avoid the label of usury that had led to their original ban. Stand-alone marine insurance thus developed consequently (Kohn, 1999; Sibbett, 2006), with the first authenticated record of marine insurance dating back to the year 1347 CE (Masci, 2011). Around this time, earliest forms of burglary insurance also developed, contracts which survived to the end of the 18th century CE (Manes, 1942; Masci, 2011). The ban on sea loans also provided the first formal separation of insurance from finance as forms of risk management (Masci, 2011). Modern insurance can also thus be traced back to this period.

Around this time, the roots of other forms of DRM, especially in relation to landscape management and optimization, were also taking shape within early North and South American civilizations. The Incan civilization occupied the Andes mountains of South America between the 13th and 15th centuries CE (Sassa et al., 2005). At first glance, the Incan settlements would seem a curious choice, especially given their locations. The Incas deliberately constructed their settlements on jagged mountain peaks located along fault lines (Sieczkowska et al., 2022). These sites were, and are still prone to landslides, earthquakes, and torrential rains (Hemphill, 2012). It would thus seem as if these societies deliberately ignored, or even actively sought, disaster warning signs in choosing their settlements. Despite what it may seem, however, the Incas' choices were quite logical, given all other considerations. The isolation and remoteness of such locations provided greater defence against attacks from enemies (Coppola, 2006). In fact, these locations proved so efficient that the Spanish conquistadors never found the Incan settlement of Machu Picchu (Hennings and Lynch, 2022). The fault lines provided protections against floods; the landslides soil for agriculture (Sassa et al., 2005); and the fractured rocks from the faults, reliable construction material for earthquake-proof architecture (Hennings and Lynch, 2022). In addition, the Incas pioneered comprehensive hydraulic water management systems that lasted for centuries, despite the dynamism of their environment, with some systems still functioning as recently as 2012 (Sieczkowska et al., 2022). The Incan case provides the first example of the transformation of a hazardous environment into and advantageous one for human settlement, proving that this is possible with a sufficient understanding of geological systems and processes.

Other forms of disaster protection also began taking shape from the 15th century onwards, chief among these being fire management practices. Although formal fire insurance took shape especially after major events like the Great Fire of London in 1666 (ICMIF, 2020) which destroyed 13,200 houses (Alagna, 2003), foundations of both fire management, firefighting and other emergency services had been set earlier in the 1st century CE by the Romans, during the reign of Emperor Augustus. The Romans had previously used slaves for fire management; but the use of slaves proved inefficient, due to a lack of training, tools, and motivation (Coppola, 2006). A dedicated firefighting unit was thus established in 6 AD by Emperor Augustus to prevent, detect, and extinguish fires, known as the *Cohortes Vigilum* (Daugherty, 1992). Modern firefighting departments and emergency services trace their roots back to these time. As fire often causes significant damage to property, property insurance (ICMIF, 2020) also developed as a result, to enable more comprehensive covers, and to insure property against all other non-fire related causes of property destruction. Formalised accident insurance also developed in turn to address all other risks, especially railway accidents (Hayter, 1949) etc., later in the 19th century.

Later developments include intercontinental expansions of disaster risk management practices, with emphasis on fire, property, and life insurance in the 18th, 19th and 20th centuries CE, including expansions to the US, Central and Eastern Europe, and Africa (ICMIF, 2020). World Wars in the 20th century CE and the rise in terrorist activities especially in the early 21st century CE, and technological developments and associated cyber risks (OECD, 2021), have also increased the need for protection against not only natural disasters, but also man-made, or anthropogenic disasters.

Though insurance has so far served as the main form of disaster management and protection, it is still limited in scope and impact, as these instruments have mostly been available only to rich nations (UNDRR, 2022; GRFF, 2021). Disaster losses, however, are felt to a larger degree by poorer and emerging nations, especially in terms of overall losses that include both human and economic losses, creating a mismatch between the instrument's role and its applicability. The table below displays, for example, the largest catastrophic overall mortality losses and their respective locations between the years 1900 and 2023. It is evident from Table 2.2 that the locations of significant mortality over the past seventy years have been greatly concentrated among poorer developing nations.

Table 2.2: *Top 10 Global Human Fatality Events in the Modern Era (1950-2022)*

Date(s)	Event	Location	Economic Loss (Nominal $ billion)	Fatalities
November 12, 1970	Cyclone Bhola	Bangladesh	0.7	300,000
July 27, 1976	Tangshan Earthquake	China	36	242,769
July 30, 1975	Super Typhoon Nina	Taiwan, China	6.6	230,029
December 26, 2004	Indian Ocean Earthquake/ Tsunami	Indian Ocean Basin	29	227,898
January 12, 2010	Port-au-Prince Earthquake	Haiti	11.0	160,000
April 1991	Cyclone Gorky	Bangladesh	3.9	139,000
May 2008	Cyclone Nargis	Myanmar	17.8	138, 366

Continued on next page

Table 2.2 – continued from previous page

Date(s)	Event	Location	Economic Loss (Nominal $ billion)	Fatalities
August 1971	Vietnam Floods	Vietnam	N/A	100,000
October 8, 2005	Kashmir Earthquake	Pakistan	10.0	88,000
May 12, 2008	Sichuan Earthquake	China	167	87,652

Source: Aon 2023 Catastrophe Insight

There is increasing need, therefore, for financial aid and tools to improve access to such tools for poorer nations that need it the most, in addition to better structured tools to address the needs of those at greater peril of natural disasters.

2.4 Recent Developments in Disaster Risk Management

As natural disaster losses have risen over the years (see figure 2.1 below) due to increases in both frequency and severity, the systematic study of disaster risk management acquired greater importance among both academics and practitioners.

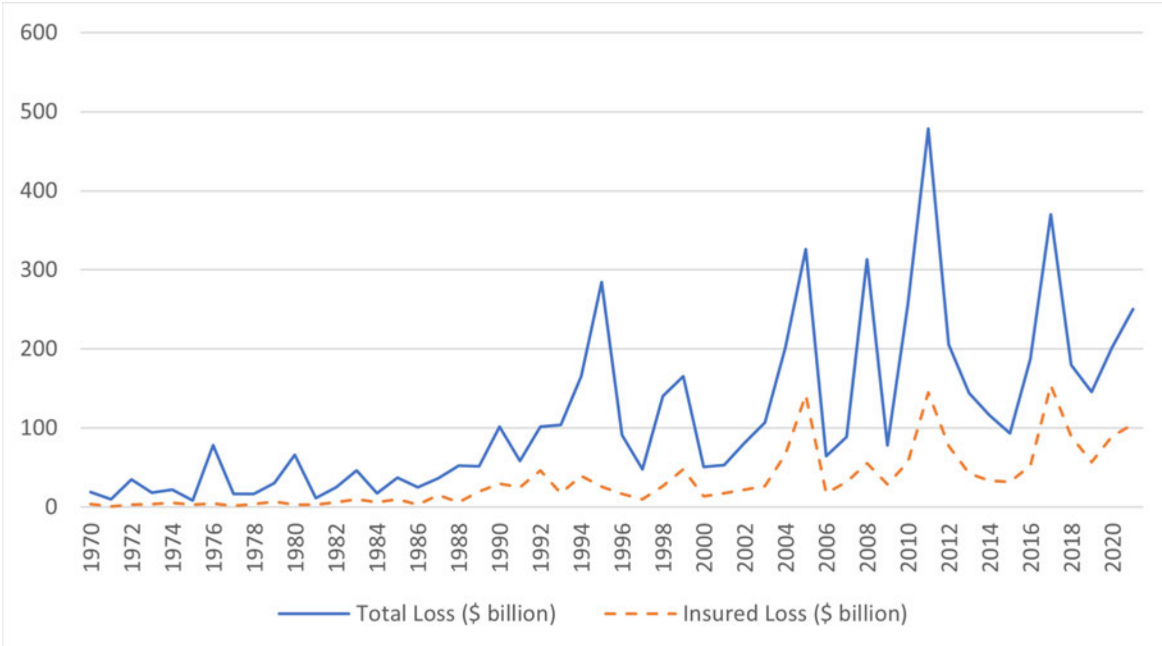

Figure 2.1: *1970-2020 Natural Catastrophe Losses*

Source: Compiled by author with data obtained from Swiss Re

Over the years of study, emphasis has slowly shifted to a more holistic approach that includes not only the hazards, but also the vulnerability, exposure, and capacity of populations to adapt to such events (Alexander, 2020). Due to this shift in view, recent developments in DRM have focused on ensuring that all pertinent factors determining a hazard's effect on the society have been incorporated into study models, and that proposed solutions account for all vulnerabilities. Some of the recent (20^{th} and 21^{st} century CE) developments are discussed below.

According to UNDRR, the 1960s saw some notable extreme events put the spotlight on the need for formalised disaster risk policies to address increasing losses. Notable events include the Iranian Buyin-Zara earthquake in September of 1962 that killed over 12000 people, injured over 2700, damaged over 21,300 houses and killed 35% of the local livestock (Ambraseys, 1963); the July 1963 Skopje earthquake in Yugoslavia that killed more than 1000 people, injured over 4000, displaced over 200,000, and destroyed 80 percent of the city (Sinadinovski and McCue, 2013); and the 1963 Caribbean hurricane disaster. These disasters led to creation of special reconstruction funds and the passing of resolutions for assistance by the UN; and improved solidarity towards humanitarian aid provision at a time when the world was divided by the cold war (Niebyl, 2021).

Assistance provision was then better formalised in the 1970s and the early 1980s. This period saw developments in pre-disaster planning at both national and international levels, and increased application of technology and scientific research for mitigation, prevention, and control of natural disasters. In 1971, the UN Disaster Relief Office (UNDRO) was created (UNDRR, 2023b; Lambert and Scott, 2019), with the coordinator authorized to 'promote the study, prevention, control, and prediction of natural disasters' and advise governments on disaster planning and early warning systems. UN resolutions passed as a result ensured improved humanitarian response to natural disasters after Afghanistan's (1971) (Muhammad et al., 2017) and Ethiopia's (1978, 1985) (Bayissa et al., 2015; Funk et al., 2019) heavy drought-related losses and led to establishment of Famine Early Warning Systems Network by USAID in Afghanistan (Brown, 2008) in 1985. In 1974, the United Nations Conference on Desertification was convened; and increased importance on disaster prevention and pre-disaster planning led to strengthening of the UNDRO and an overall strengthening of the UN's capacity to respond to natural and other disasters post 1981.

Multiple disasters around 1988, including floods, typhoons, hurricanes, and locust infestations motivated the UN to proclaims the 1990s as a decade of international cooperation in risk reduction, in an effort to motivate development of an action framework to handle natural disasters, especially for developing countries (UNDRR, 2023b). In 1989, the International Decade for Natural disaster Reduction (IDNDR) was proclaimed, to begin on the 1st of January 1990, with the second Wednesday of October designated as the International Day for Natural Disaster Reduction and observed annually. The Framework for Action for the International Decade for Natural Disaster Reduction (FAIDNDR) was consequently adopted with the international community being urged to adopt the framework.

In 1997, the Kyoto Protocol, the first greenhouse gas (GHG) emission reduction treaty was adopted. This agreement defined most of the 2000s, as it only entered into force on 16 Feb 2005 after 7 years. This process took a long time due to a complex ratification process, and it was Russia's ratification that finally brought treaty into force (SDDG, 2011). The agreement targeted to reduce six major greenhouse gas (GHG) emissions by 5.2% by 2012 relative to 1990 levels. These gases included carbon dioxide, methane, nitrous oxide, hydrofluorocarbons, perfluorocarbons, and sulphur hexafluoride. The treaty was subsequently amended in Doha in 2012 for a second period (2013-2020), but due to slow ratification, the amendment only came into force on 31 Dec 2020, thus reducing it to a mostly 'symbolic act' of closure of the Kyoto climate regime as the world moved on to the Paris Agreement (Farand, 2020). A key benefit of this agreement, however, is that is motivated carbon emissions and related financial instruments trading (Ünüvar, 2019).

The 2010s saw significant development in climate disaster risk management, as the world was increasingly becoming aware of climate change and its effects on the environment. The establishment of the Green Climate Fund in 2010 (Schalatek et al., 2019); and the Paris Agreement, Sustainable Development Goals (SDGs), and the Sendai Framework for Disaster Risk Reduction in 2015 are some of the key developments that brought climate protection to the forefront of disaster planning and management (UNDRR, 2022). These developments also improved the integration of climate disaster risk management with risk finance (GRFF, 2021). In addition, the launch of the InsuResilience Initiative by G7 countries in 2015 to provide insurance for 400 million poor by 2020 boosted disaster financing efforts (Golnaraghi and Khalil 2017; Hillier 2018 (cited in GRFF (2021))). Recently, the Covid 19 crisis demonstrated the important role of governments in ensuring efficient management of disaster risk to avoid negative disaster consequences, including the reversal of developmental gains; deceleration of poverty reduction; decreased hunger alleviation (UNDRR, 2023b).

Chapter 3

Financial Disaster Risk Management and Catastrophe Bonds

3.1 Financial Disaster Risk Management

As the frequency and severity of natural disasters increases with human-induced changes in climate, there is greater need for resources to support mitigation and adaptation efforts. This need for better investments and funding of climate change projects (Gamper, 2018) has led an increasing focus in financial disaster risk management (FDRM). According to the UNDRR, disaster events are projected to reach 560 a year, or 1.5 a day by 2030, with investments in disaster risk reduction yielding significant benefits. Multiple tools have thus been developed over the years to address disaster losses and any other arising needs. These can be classified into two broad categories: pre-disaster finance and post-disaster finance.

Risk transfer tools including insurance, reinsurance, and alternative risk transfer tools e.g., catastrophe bonds and other weather derivatives (UNISDR, 2004). Risk retention tools include government revenue and budget allocation, contingency and reserve funds, extrabudgetary funds, budget reallocations and alignment, and taxation (UNCDF, 2021; ADB, 2018; Cissé, 2021). External risk finance sources include grants loans and other funding sources, including traditional disaster risk reduction, development and climate finance; contingent credit/catastrophe deferred drawdown options; disaster response banking tools; disaster risk finance facilities; bonds including green and blue bonds; humanitarian assistance; forecast-based financing; and other private sector responses (UNCDF, 2021). All these tools then complement each other, and can thus be adopted together, each to address specific risks that they are better suited to, with risk retention being favoured for low severity high frequency events, and risk transfer and external finance being favoured for high-severity low frequency events that often impose the highest strain on economies and societies (ADB, 2018).

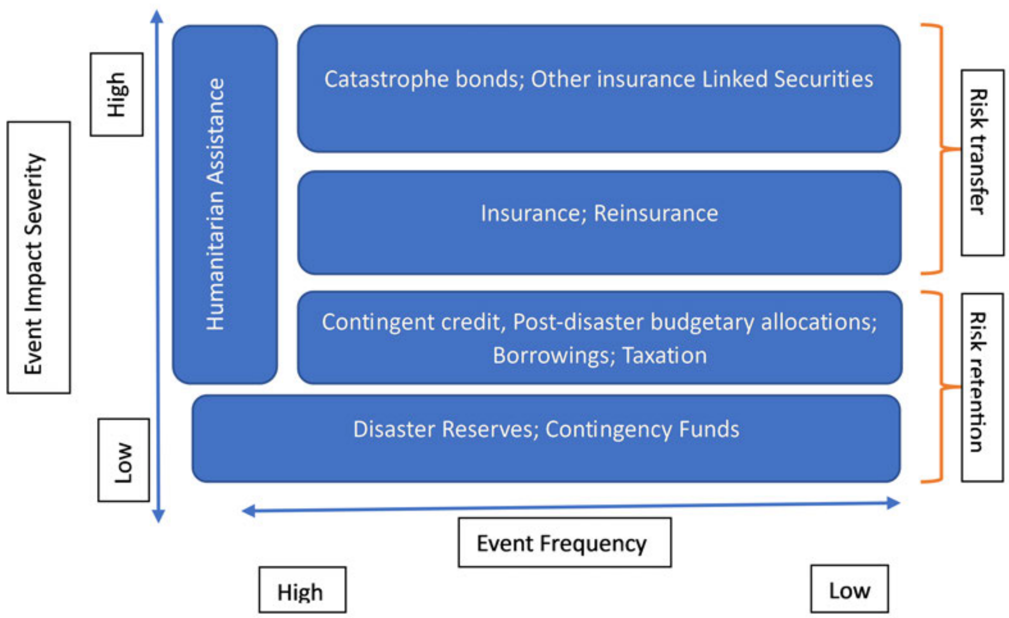

Figure 3.1: *Disaster Risk Financing Layers*

Source: Adapted from Asian Development Bank (2018, p.2)

Even though risk transfer instruments have seen increased uptake in the past decade, external finance, especially in the form of humanitarian assistance, still dominates as the main funding source for climate and disaster risk management (CDRF) (Stander, 2017). Progress in uptake and innovation has mainly been observed with risk transfer and external risk finance tools.

Of the sovereign risk insurance and regional insurance pools, the Caribbean Catastrophe Risk Insurance Facility (CCRIF) established in 2007 to reduce the financial costs of earthquakes and hurricanes by providing short-term liquidity to member countries (Ghesquiere et al., 2006) has seen the highest participation, attracting 19 Caribbean and 3 Central American members as of date. These high participation rates have enabled the facility to perform efficient risk pooling (GRFF, 2021), with 58 pay-outs totalling US$260 million so far. The Pacific Catastrophe Risk Insurance Company (PCRIC), established in 2016, performs the same function for Pacific island nations in the event of natural events including tropical cyclones, earthquakes, volcanic eruptions, and tsunamis. This facility has paid out approximately $US 11 million in four pay-outs, two under the Pacific Catastrophe Risk Assessment and Financing Initiative (PCRAFI) and two under the Pacific Catastrophe Risk Insurance Company (PCRIC). Other pools include the African Risk Capacity (ARC), established in 2012, and the Southeast Asia Disaster Risk Insurance Facility (SEADRIF), established in 2019. These facilities have all observed increased participation over time (GRFF, 2021), as nations increasingly begin to understand the key benefits of such insurance schemes. Another key source of immediate liquidity, the deferred catastrophe drawdown (CAT DDO), has provided the necessary funds to countries including Guatemala (2009), Kenya (2018), Colombia (2021) and the Dominican Republic (2018, 2022), among others, to fund immediate disaster-related costs, with many of the outstanding CAT DDO's taken within recent years (GRFF, 2021).

Of the disaster financing tools available, catastrophe bonds and other insurance-linked products are only sought in the most extreme of cases, when both insurance, reinsurance, and other financing capacity has been exhausted, or is unavailable for those in need. With recent observed environmental changes, however, these extreme loss instruments have seen growing popularity, which has then increased the need for better modelling and pricing to increase reach and capacity of such instruments. This study focuses on understanding such instruments in the context of all the interconnected fields driving climate change and climate finance in order to develop better tools that fit majority of the current and possible future climates. The next section thus discusses this financing tool in detail, including developments within the catastrophe bond and insurance-linked securities market over the years.

3.2 Catastrophe Bonds: History and Market Development

Catastrophe bonds were first introduced in the 1990s, following the loss in insurance capacity observed after the extreme loss events of Hurricane Andrew in 1992 and the Northridge earthquake in 1994. Hurricane Andrew was a Category 5 hurricane, based on the Saffir-Simpson Hurricane Scale (Zhang and Peacock, 2009), that struck north-western Bahamas, south of the Floridian peninsula, and south-central Louisiana (Rappaport, 1993) in August of 1992. Economic losses were estimated to reach US $30 billion (Muerman, 2008, cited in (Nowak and Romaniuk, 2016)), with homeowners in Florida alone estimated to receive US $ 11 billion in insurance settlements to fund reconstruction (Zhang and Peacock, 2009). Until Hurricane Katrina in 2005, Hurricane Andrew was the costliest storm in US history (Allen, 2012), and led to the insolvency of some insurers (Cummins et al., 2002).

This lack of capacity prompted protection-seekers to seek alternative sources of funding, in this case, securities markets. In an attempt to address this issue, the Chicago Board of Trade (CBOT) launched catastrophe futures in December of 1992 based on aggregate loss indices from the Property Claims Services (PCS) (Cummins, 2008; Cummins and Weiss, 2009), though these securities were later withdrawn due to lack of trading volume (Cummins, 2008). The lack of trading volume was a consequence of the scarcity of interest from insurers, which has been attributed to factors including thinness of the market, possible counterparty risk, threat of competition, and excessive basis risk (Cummins et al., 2004; Cummins, 2008; Cummins and Weiss, 2009; D'arcy and France, 1992).

The Northridge earthquake, which struck California in January 1994, compounded this effect. The magnitude 6.7 (Hauksson et al., 1995) earthquake was the most destructive and costly Californian earthquake since 1906 (Jones, 1994). The earthquake's economic losses were estimated at US \$ 49.3 billion, with US \$ 41.8 billion of this being direct economic losses (RMS, 2004). These two events' losses (Hurricane Andrew and the Northridge Earthquake) were in comparison to the previous decade's (1980-1992) losses of only about US \$25 billion in total, based on valuations by the Property Claims Services (Froot, 1999b). These two events thus motivated the modelling of new instruments that could better address the extreme risks within catastrophic events, including catastrophe bonds and other insurance-linked securities, weather, and other credit-risk derivatives (Froot and Posner, 2000). This section focuses on the most popular of the insurance-linked securities, i.e., the catastrophe bond.

Catastrophe bonds are debt securities sold in financial markets to provide insurance against catastrophic disasters. Like other bonds in the market, they pay regular coupons and principal at maturity. The principal repayment in a catastrophe bond, and sometimes the interest depending on the structure and conditional on the specified catastrophe not occurring, since the if the catastrophe occurs investors lose part or all their principal, and in some cases their interest. There are some similarities in structure between a catastrophe bond and a high yield/ junk bond (Cox and Pedersen, 2000). Both are priced based on the risk of default to the investor. While the default in high-yield or junk bond stems from the issuer defaulting on payments due to underlying issuer factors, or external factors affecting the issuer; a catastrophe bond's risk of default stems from the occurrence of a catastrophe, which occurs independent of the issuer's condition or financial market factors.

Due to this difference in the source of default between high-yield bonds and CAT bonds, catastrophe bonds are favoured by investors as instruments of diversification, as their returns are generally uncorrelated with the broader financial market (Cummins, 2008). Most catastrophe bonds are issued through a Special Purpose Vehicle (SPV). The SPV is a company created for the express purpose of providing reinsurance to the issuer if a catastrophe occurs. The company receives premiums from the issuer and in turn issues CAT bonds in the financial markets using the premiums as collateral. The proceeds from the bond issue, together with the premiums paid by the issuer, are invested in a collateral account consisting of high-quality assets. These investments are used to fund coupon and principal repayments to investors if the pre-specified catastrophe does not occur, and used to provide reinsurance to the issuer otherwise (PartnerRe, 2015). Figure 3.2 below conveys this general structure:

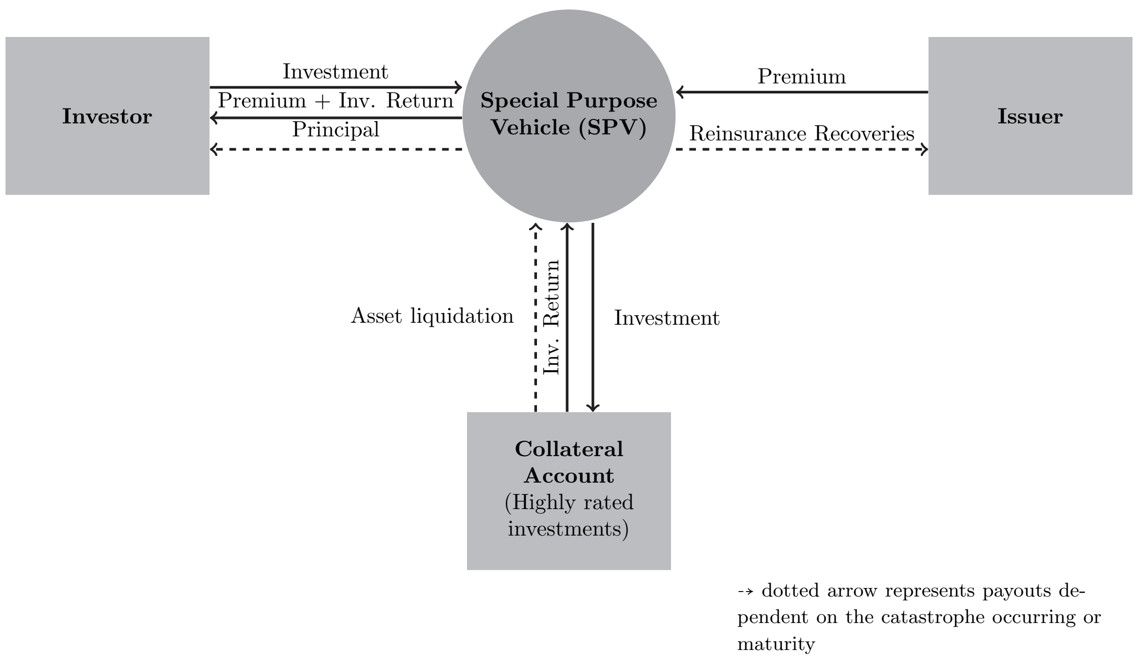

Figure 3.2: *Catastrophe Bond Structure*

Source: Created by author

The coupon paid to the investor consists of the premium and a baseline return in the market, which in the past, has generally been the London Interbank Offered Rate (LIBOR). The premium, also known as the spread, is composed of the expected loss on the underlying peril and a risk load (PartnerRe, 2015).

The Catastrophe and other Insurance Linked Securities (ILS) market has developed over time in key phases. The first phase, the market onset, is the direct result of

Hurricane Andrew and other major events observed around the early 1990s, lasting until the mid-1990s. This was a period of experimentation, marketing, and research into these new instruments. Academic literature also followed a similar trend, with early literature, according to Cummins and Weiss (2009), focused on explaining and analysing insurance derivatives (Cox and Schwebach, 1992; D'arcy and France, 1992), comparing derivatives to insurance (Niehaus and Mann, 1992), and discussing hedging strategies to insurers (Cox and Schwebach, 1992).

Following the Northridge earthquake in 1994, the first successful US $85 million catastrophe bond was issued by Hannover Re through its KOVER transaction (Zeller, 2007). Hannover Re, then a wholly owned subsidiary of a German mutual insurer, was heavily capital constrained at a time when insurance markets exhibited little capacity, and this proved a motivating factor to explore insurance securitization as a form of funding instead (Zeller, 2007). Securitization attempts continued through to 1995, since the CBOT futures had yet to generate much interest, these were replaced by CBOT options based on catastrophe loss indices by PCS, which were subsequently de-listed in 2000 due to a lack of trading (Cummins and Weiss, 2009; D'Agostino, 2002). Nationwide also issued contingent notes known as 'Act of God' bonds worth US $400m through the special trust, Nationwide Contingent Surplus Note (CSN) Trust (Cummins, 2008). This however, provided little solution due to, according to (Cummins, 2008), lack of segregation in liabilities and the inherent obligation for the issuer to eventually repay trust once funds have been withdrawn.

The period between the years 1996 and 2000 saw the first 'true, widely syndicated' catastrophe bond transactions being issued, starting with the GeorgeTown Re Ltd. Transaction in December 1996. This was a US $68.5 million bond issued by St Paul Re, and structured by Goldman Sachs, with AIR Worldwide as the risk modelling agents. The bond covered 'worldwide all perils, including marine and aviation', and included an indemnity trigger (Evans, 2021). The bond later suffered some losses due to events like Hurricane Floyd, Windstorms Anatol, Lothar and Martin, the 2000 UK Floods, and the 2001 attack on the World Trade Centre, subsequently paying out approximately US $0.5 million (Artemis, 2023). Regarding other securities, the Bermuda Commodities Exchange (BCE) attempted to develop a catastrophe options market in 1997, but this would be withdrawn two years later due to lack of trading (Cummins, 2008). The catastrophe bond market however thrived in 1997, with the United Services Automobile Association (USAA), one of the most consistent issuers in the catastrophe bond market to date (Artemis, 2023), issuing their first catastrophe bond, through the US $480 million SPV Residential Re Ltd. 1997 (Difiore et al., 2021). This transaction was so successful that it provided a model for later issues by Swiss Re and the Tokio Marine and Fire Insurance Company (Zolkos, 1997). The first catastrophe bond issue by a non-financial firm occurred in 1999, with the Concentric Ltd. Transaction, issued to insure against earthquake losses in Tokyo by Oriental Land Company, the owner of Tokyo Disneyland (Cummins, 2008).

According to Lane (2021), between 1996 and 2001, 36 deals were issued in total, with varied results. These deals were considered majorly experimental, with many being issued at a discount, and covering 5 or 6 perils including Space Launch, Oil Rig, Weather, Aviation, and Man-Made risks, according to Lane (2021). In addition, their risk assessment levels were non-comprehensive, with many having very high coupon rates (Lane, 2021). According to Cummins et al. (2004), for example, catastrophe bond premiums were nearly seven times the expected losses for bonds issued within this period. This phenomenon where prices were observed to be much higher than expected was analysed by several researchers, including, Canter et al. (1996) and Litzenberger et al. (1996). Possible explanations were proposed by Bantwal and Kunreuther (2000), who analysed the reluctance of investment managers to invest in catastrophe bonds, attributing it to behavioural factors, including ambiguity aversion, loss aversion, and uncertainty avoidance. Froot (2001), on the other hand, found that the most possible explanations were supply restrictions due to capital market imperfections and market power from traditional reinsurers.

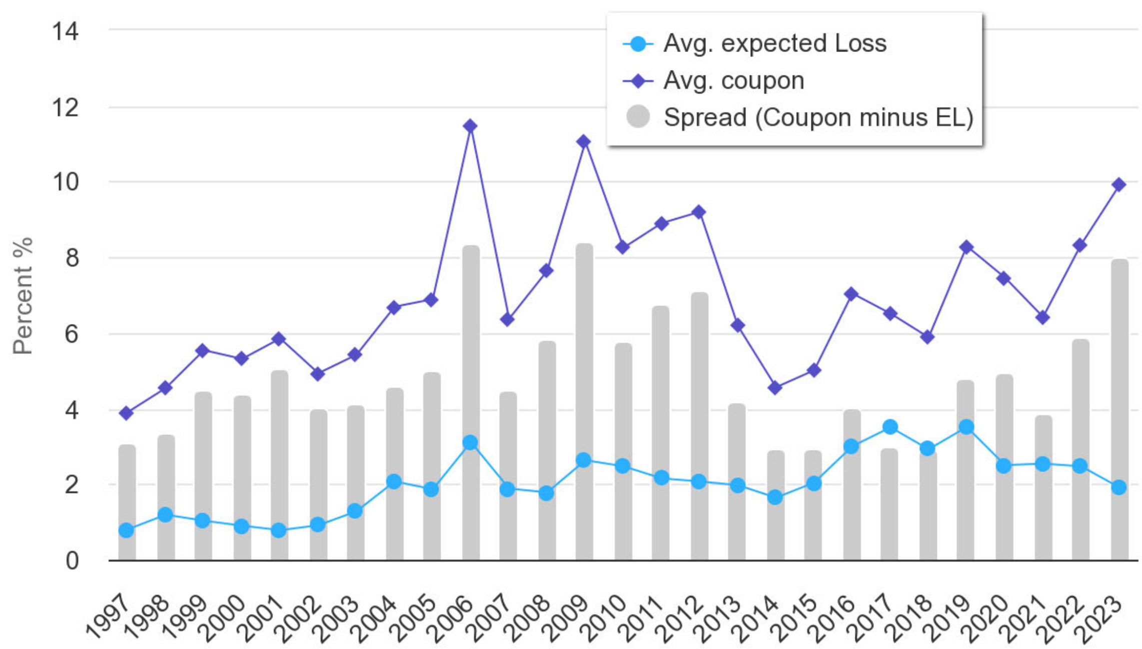

Figure 3.3: *Catastrophe Bonds and ILS Issuance's Average Expected Loss and Coupon (per Year)*

Source: www.Artemis.bm, Deal Directory, retrieved 15th June 2023

According to Figure 3.3, the market observed an increase in unique-risk catastrophe bonds in the period between 2001 and 2004 including bonds that covered against non-natural disaster risks including terrorism. This was in response to the rise of terrorist attacks including the September 2001 attacks on the USA. In 2003, for example, the Federation Internationale de Football Association (FIFA) issued the Golden Goal Ltd 2003 catastrophe bond to protect against the risk of event cancellations due to such man-made events. FIFA was compelled to issue this bond as a result of both the September 2001 attacks and the consequent withdrawal of insurers from the FIFA World Cup event cancellation insurance policy (Artemis, 2023). Researchers, on the other hand, focused on explaining catastrophe securities' pricing structures and determining their optimality. Focus was especially on addressing the basis risk (e.g., Harrington and Niehaus, 1999; Cummins et al., 2004) and moral hazard risks (e.g., Lee and Yu, 2002; Doherty, 1997; Doherty, 2000) that arose with index-based contracts and indemnity contracts respectively, with most researchers recommending hybrid covers incorporating both index and indemnity elements to address each of the risks comprehensively (Doherty and Richter, 2002).

Different theoretical frameworks for bond pricing were also explored around this time (Burnecki and Giuricich, 2017), following the pioneering works of Froot and O'Connell (1997) and Froot and O'Connell (1999), Froot and Posner (2000). Utility-based approaches were proposed by Cox and Pedersen (2000) and Egami and Young (2008); and arbitrage free approaches by Baryshnikov et al. (2001), Burnecki and Kukla (2003) and Vaugirard (2003a); in addition to standard actuarial pricing methodologies (e.g., Lane, 2000; Lane and Beckwith, 2008; Lane and Mahul, 2008) and equilibrium pricing transforms, including the Wang transform of Wang (1996), Wang (2000), and Wang (2002) and the Esscher transform (Gerber and Shiu, 1996; Kijima, 2006).

The year 2005 brought significant changes to the catastrophe risk insurance market, especially because of the multiple extreme loss events observed in the US, including Hurricanes Katrina, Rita, and Wilma. Hurricane Katrina, especially, deserves mention, as it was considered the costliest natural disaster in US history, with insured losses hitting US $62 billion, further depleting reinsurance capacity (Difiore et al., 2021). This was a category 5 hurricane, according to the Saffir Simpson hurricane wind scale (SSHWS), that hit the US Gulf Coast in August of 2005, especially devastating the city of New Orleans (Reid, 2019). The losses from these events refocused the spotlight back on the catastrophe bond and ILS market as a source of insurance protection, leading to record issuance in the two years following the events. Figure 3.4 below displays this increase in issuance levels. The year 2006 saw record issuance of $4.7 billion while 2007 saw issuance stand at a record $7.1 billion (Difiore et al., 2021).

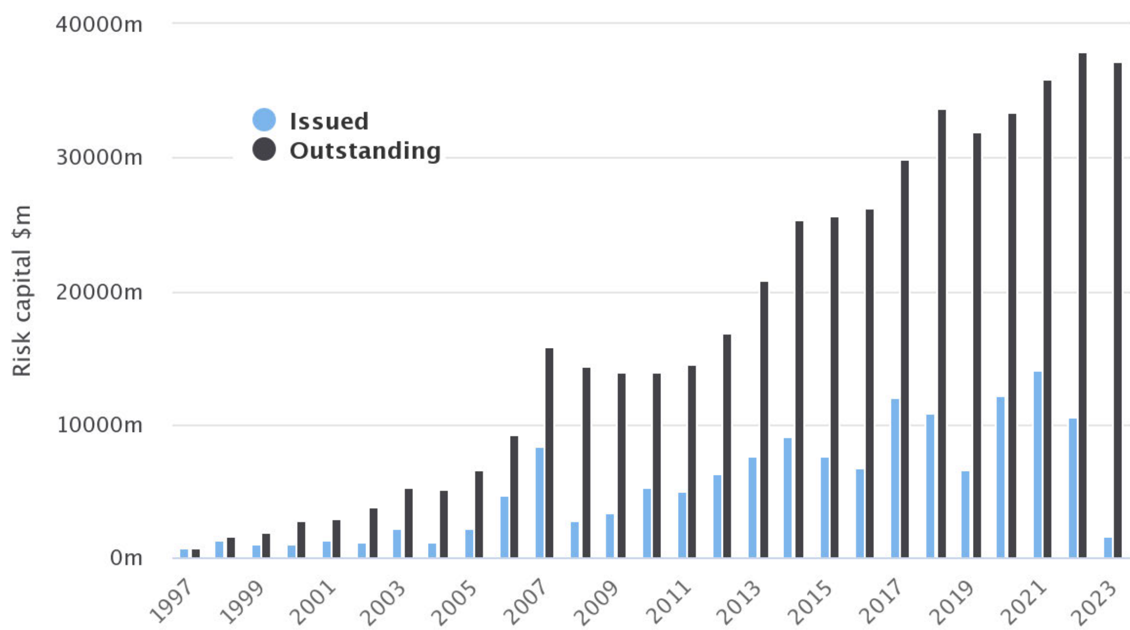

Figure 3.4: *Catastrophe bond and ILS risk capital issued and outstanding (by year)*

Source:www.Artemis.bm, Deal Directory, retrieved 15th June 2023

Dieckmann (2010) analysed these extreme catastrophic events, chiefly Hurricane Katrina, and finally addressed the high bond spread (Coupon rate minus Expected loss) question that had been brought up during the catastrophe bond market's early trading years by researchers including Froot (2001) etc. Dieckmann found that large consumption shocks similar to those of Hurricane Katrina were significant enough to affect bond spreads, implying that even though bond spreads had reduced overall, the existence of such shocks would always make it unlikely for such spreads to converge to the risk-free rate. Carayannopoulos et al. (2022) support this finding by studying market prices for the period 1999-2016 and find that despite an overall decrease in price of expected loss risk, large catastrophes increased this price by 34% on average. Herrmann and Hibbeln (2023), observing secondary trading activity in the catastrophe bond market, found that 21% of the observable yield spread on the catastrophe bond market was attributable to the liquidity premium, with high-risk bonds having the highest magnitudes of up to 141 basis points (bps) based on realized bid-ask spreads.

The year 2007 also saw further attempts at catastrophe derivatives market development in response to Hurricane Katrina. According to Cummins and Weiss (2009), futures and options on US Hurricane risk were introduced by two separate exchanges, the Chicago Mercantile Exchange (CME) and the New York Mercantile Exchange (NYMEX). The market continued adapting through this period, changing to better suit the needs arising due to not only the increasing frequency of extreme disaster, but also the possibility that warming sea surface temperatures could cause further extremes. Loss models were updated to include both normal sea surface temperatures and the option to use warm sea surface temperatures (WSST) (Lane, 2021), especially in times of higher uncertainty and rising risks.

In addition, the financial crisis led to an interesting phenomenon where a catastrophe bond made losses, not because of a natural event, but because of a financial event i.e., the bankruptcy of Lehman Brothers in 2008. Four bonds, Carillon A-1 Ltd, Ajax Ltd, Willow Re Ltd, and Newton Re 2008 A-1 Ltd, experienced losses due to their LIBOR arrangement with Lehman Brothers, who defaulted (Lane, 2021), leading to an instance of counterparty risk causing catastrophe bond losses. This prompted improvements in the catastrophe bond structure to avoid any future counterparty defaults, developments that were positively received by investors and thus helped keep catastrophe bonds as viable diversification instruments (Carayannopoulos and Perez, 2015).

In the 2010's there was an increase in research into factors affecting the price of catastrophic risk securities, and the impact of external factors unrelated to the catastrophic event or risk on the prices of such instruments. In particular, there was an increased exploration of econometric pricing techniques to explain cat prices, for example in research done by Braun (2016), Galeotti et al. (2013), and Gürtler et al. (2016). These techniques are further discussed in a later application chapter on the study of volatility of pricing among market issuers.

In addition, heavy loss events marking the start of the decade increased the need for disaster risk solutions, especially for developing countries that were poorer and could not access direct insurance. The Great Tohoku earthquake and the Thailand floods in 2011 wreaked havoc on the east Asian nations of Japan and Thailand. The magnitude 9.0 Tohoku earthquake, for example, was the most devastating earthquake in Japanese history, and the fourth most powerful earthquake ever recorded since 1900 (Lay et al., 2013; Stimpson, 2011). The earthquake's direct effects were much more limited than their indirect effects, which caused most of the damage (Stimpson, 2011). The tsunami that followed as a direct result of the earthquake, for example, is said to have caused 98% of the damage (NCEI, 2021), including nuclear meltdowns in Fukushima. This event also renewed interest in the coverage of unique risks in the catastrophe bond market, including nuclear risks (e.g., Kunreuther and Heal, 2012; Ayyub et al., 2016). The tsunami's economic losses were estimated at US$ 235 billion, according to the World Bank (Oskin, 2022), with losses experienced as far as Hawaii, California, French Polynesia, Galapagos Islands, Peru, and Chile (NCEI, 2021).

The final half of the decade also brought with it extreme events, marking the decade with the heaviest insured losses ever recorded. Hurricanes Harvey (17 Aug 2017 3 Sept 2017); Irma (30 Aug 2017 13 Sept 2017) and Maria (16 Sept 2017 2 Oct 2017) combined with wildfires and other catastrophes to make 2017 the most expensive year on record for US disasters, according to the National Oceanic and Atmospheric Administration. With extreme losses estimated at US$519 billion by Aon, it was inevitable that some of these losses would be borne by the catastrophe market. At least 25 SPVs were triggered by these combined events, according to recent statistics from Artemis, an ILS-dedicated service, marking the year with the largest number of triggered SPVs.

The World Bank pandemic bond, the IBRD CAR Series, was also issued during this time (Piantedosi, 2020), and later paid out due to Covid-related losses in 2020 (Artemis, 2023), an instance of a successful pandemic-cover catastrophe bond. The World Bank, through its disaster risk financing facilities, has continued to support governments and other disaster resilience efforts by issuing catastrophe bonds in conjunction with governments or sovereign risk pools to finance short-term liquidity needs of nations frequently affected by catastrophic events (World Bank Group, 2017; Sasaki and Ishiwatari, 2022).

In 2018, the California Camp Fire and Hurricane Michael contributed to heavy losses for the US, while Typhoon Jebi generated heavy losses for the Japanese insurance industry, the costliest since the 2011 Tohoku events (Simic, 2019).

The years 2019-2022 have seen even more extreme events, with 2021's US$ 329 billion total damage costs now holding the record for the third costliest inflation-adjusted year after 2005 (US$ 351 billion) and 2017 (the costliest at US$519 billion), according to Aon, and the second costliest together with 2005 and 2011, according to Munich Re. In 2022, Hurricane Ian, a category 5 hurricane based on the Saffir-Simpson Hurricane Wind Scale (SSHWS), was the most expensive single event, according to Munich Re, with total losses of US$100 billion and insured losses of US$60 billion. Other events that caused significant losses within the year include floods in Australia (US$6.6 billion total loss; US$4 billion insured) and winter storms in Europe (US$ 4.3 billion insured losses) (UNDRR, 2023a).

It is now widely accepted that the frequency and severity of catastrophic events has increased (MIS, 2023) either due to changes in climate or other geological factors like seasonality. The focus on climate change adaptation over the last few years, especially after the 2015 climate agreements like the Paris Agreement, the Sustainable Development Goals, and the Sendai Framework for Disaster Management (UNDRR, 2022), and the occurrence of pandemics like the Covid 19 crisis, have also made such disaster financing instruments more valuable (Schwarcz, 2020) to not only institutional issuers, but also local governments and supranational organizations like the World Bank. As the world finds ways to adapt to a changing climate, the role of these instruments in the recovery and reconstruction of lives and livelihoods will continue to increase in importance, further motivating the proposal of better and more comprehensive tools for current and future risks that may arise due to geological changes.

30 years since inception, the insurance linked securities (ILS) market, of which the catastrophe bond market dominates, has expanded to a capacity of US$39.66 billion, with 2023 issuance alone standing at US$6 billion as of May 2023. This is in comparison to the 1997 outstanding issuance levels of US$785.5 million, according to Artemis. Overall cumulative issuance as of May 2023 stands at US$151 billion. Even though these figures are still much lower than those of the reinsurance market (Cole, 2019), it is important to remember that catastrophe bonds were not developed to replace traditional tools like insurance and reinsurance, but rather to complement these products especially in times of exceptional strain to the reinsurance market. As their niche is different, there is always potential for growth within this market, now even more so due to effects of climate change.

Chapter 4

Mathematical Optimization and the EM Algorithm

4.1 A Brief History of Mathematical Optimization

"Nothing takes place in the world whose meaning is not that of some maximum or minimum." Leonhard Euler

Optimization is the formula of life. The concept of optimality is found in all of nature, though it acquires different names in different fields. Physicists and mathematicians use labels including the 'principle of least action'(e.g., Maupertuis, 1744; Maupertuis, 1746; Euler, 1744), economists the point of highest utility, evolutionary biologists have called it 'survival of the fittest', or 'natural selection' (e.g., Darwin, 1859; Spencer, 1872), and financial analysts use the 'highest return for a given risk', or 'optimal portfolios' (e.g., Markowitz, 1952; Tobin, 1958; Roy, 1952); to define their applied version of the concept. Despite being unaware of the formal concept of optimization, historical societies and civilizations including those of Ancient Egypt, Mesopotamia, Greece, Maya etc., found ways to express this optimality through whatever means were available to them at the time, including oral traditions, counting processes, and in their majestic constructions. Understanding the 'formulas' of optimality is therefore key to understanding nature and its changes over time, and subsequently building better solutions for life out of these observations, which can then be applied in any field of study.

While optimization as a concept exists and has always existed in all of nature's dynamism, Ancient Greek philosopher-mathematicians were among the earliest to turn these natural transformations into abstractions useful for the generalization of relationships. The earliest of these was Euclid, around 300 BCE (Fitzpatrick, 2008). Often regarded the 'Father of Geometry' (Campbell and Hayhurst, 2015; Sialaros, 2015), Euclid was among the first mathematicians to compile all the mathematical developments of the time in a sequential logically deductive way now known as the 'axiomatic method' (Hartshorne, 2013), in a book known as the 'Stoiecheion' or 'Elements' (Heath, 1956). Euclid considered problems of minimal distance between two points, and proved that this was a line; and showed that of all rectangle types with the same perimeter, the square possessed the greatest area of them all. These discoveries also led to further discoveries in geometry, catoptrics (the theory of mirrors and reflections), and spherical astronomy (Webster, 2014). Euclid's works were so influential that they inspired mathematical thought for centuries after his death, up until the 19th century and the formalization of non-Euclidian geometry (Bonola, 1955).

The next philosopher to actively consider optimization problems is reported in the works of Pappus of Alexandria, who lived around 300AD. The 'Synagoge' or 'Mathematical Collection' of Pappus (Simmons, 2007) is considered one of the most important references to mathematical works of Greek antiquity, as Pappus was among the last of the Greeks to compile the works of many Greek mathematicians in a time when philosophy and mathematics was undermined in favour of Christian religious views, thus retaining a reliable record of mathematical-philosophical thought of the time (Cuomo, 2007). Some of the mathematical developments mentioned in Pappus's collection include those of Euclid (325 BCE   265 BCE), Archimedes (287 BCE   212 BCE), and our current person of interest, Zenodorus (200 BCE   140 BCE) (Ferguson, 2004), among others.

Zenodorus is considered the first Greek mathematician to consider Dido's problem in his treatise 'On Isoperimetric figures', which though lost to time, can be found in excerpt form in the works of Pappus of Alexandria, Theon of Alexandria, and Proclus.

Dido’s problem, an isoperimetric problem, involves the finding of the greatest area that can be enclosed by a given perimeter or length. It is mentioned in the epic poem the Aeneid of Roman poet Publius Vergilius Maro (70 19 B.C.), more popularly known as Virgil. Here is the excerpt containing a description of Dido’s problem;

> "The Kingdom you see is Carthage, the Tyrians, the town of Agenor;
>
> But the country around is Libya, no folk to meet in war.
>
> Dido, who left the city of Tyre to escape her brother,
>
> Rules here--a long and labyrinthine tale of wrong
>
> Is hers, but I will touch on its salient points in order....
>
> Dido, in great disquiet, organised her friends for escape.
>
> They met together, all those who harshly hated the tyrant
>
> Or keenly feared him: they seized some ships which chanced to be ready...
>
> They came to this spot, where to-day you can behold the mighty
>
> Battlements and the rising citadel of New Carthage,
>
> And purchased a site, which was named 'Bull's Hide' after the bargain
>
> By which they should get as much land as they could enclose with a bull's hide."’

The maximum ‘land as they could enclose with a bull’s hide’ turned out to be a semicircle, with the shoreline as the starting point and the fixed border. Zenodorus analysed this problem and formalized it in an overall context, which, according to Nahin (2003), include these two important conclusions;

> ‘the area of a regular n-gon is greater than the area of any other n-gon with the same perimeter;’
>
> ‘given two regular n-gons with the same perimeter, one with $n = n1$, and the other with $n = n2 > n1$, then the regular $n2$-gon has the larger area.’

Which shows that the circle has the greatest area of any polygons with the same perimeter.

Zenodorus also made contributions to catoptrics, as mentioned in Diocles's work '*On Burning Mirrors*' (Toomer, 1976). Major contributions to catoptrics were however made by a different philosopher-mathematician around 100BCE, Heron or Hero of Alexandria (O'Connor and Roberston, 1999), who proved in his work, *Catoprica*, (Smith, 1999) that light reflected from a mirror travelled between two points through the path of shortest length. Though at the time Hero gave no proof of this deduction, the principle provided a key foundation for later developments, including in the 17th century mathematician Fermat's principle of least time, which is considered on of the building blocks to the calculus of variations (Ferguson, 2004). According to Grabiner (1983), Fermat had also read that 'a problem which has, in general, two solutions will have only one solution in the case of a maximum' in the works of Pappus of Alexandria, which then led him to discovering his concepts of maxima and minima.

After the Greek philosopher-mathematicians, a time gap exists in the development of optimization, with further discoveries only formalized beginning in the 16th and 17th centuries CE in Europe. At this time, according to Grabiner (1983), European mathematicians had familiarized themselves with both Greek mathematics and the Islamic world's algebraic developments enough to extend these concepts on their own.

A revolution thus began with the French mathematician Francois Vieta's invention of symbolic algebra in 1591, and the invention of analytic geometry in the 1630's independently by Descartes and Fermat (Grabiner, 1983). We will discuss some of the notable discoveries and inventions during this period in detail, starting with the German mathematician-astronomer Johannes Kepler (1571-1630) in 1615. Two major developments in applied optimization are attributed to Kepler, including the determination of the optimal dimensions of a wine barrel (Hellmann, 2019), a major contribution to later integral calculus. The story goes that Kepler purchased some wine for his second wedding, but the wine seller's technique of measuring the volume of the wine for pricing dissatisfied him. He then set out to determine the optimal dimensions of a wine barrel that would guarantee the most wine. Suffice it to say, Kepler proved that the wine seller's technique had been close to accurate all along! He later wrote a book regarding his experiments, known as *Nova stereometria doliorum vinariorum* (*New solid geometry of wine barrels*), a key contribution to Archimedes' works on solid geometry (Knobloch, 2017). The other major development was that of the 'secretary problem' or the 'marriage problem', which Kepler had earlier encountered when choosing said second wife. The problem is defined in Ferguson (1989) as 'a sequential observation and selection problem in which the payoff depends on the observations only through their relative ranks and not otherwise on their actual values.' This 'problem' and its subsequent solution have seen many applications in the field of optimal decision making to date.

A further development in applied optimization is seen later in 1638, when Italian astronomer Galileo Galilei (1564-1642) tried to determine the shape of a flexible hanging chain of uniform linear mass density, but erroneously concluded it to be a parabola (Kunkel, 2016; Renn and Damerow, 2003). Theoretical optimization also picked up around this time, beginning with the works of French mathematician Pierre de Fermat (1601-1665).

Together with French philosopher Rene Descartes (1596-1650), Fermat is considered one of the founders of the analytic geometry. According to Grabiner (1983), this meant that curves could be now represented by equations and that every equation determined a curve.

Fermat is said to have 'laid the technical foundations for differential and integral calculus'; together with French mathematician Blaise Pascal (1623-1662), was instrumental in establishing the foundations of probability theory; and established modern number theory Mahoney (1994). He proved that the necessary condition for a minima or maxima for a real-valued function on one variable is that the derivative must be zero (Neunzert and Siddiqi, 2000). Fermat also applied the concept of minima and maxima to optics, showing that light travelled between two points in minimal time, while slowing down in a denser medium. The latter deduction was a major point of contention between Fermat and Descartes, who believed that light travelled faster in denser mediums (Ferguson, 2004). Suffice it to say, Fermat was right. Subsequently, these studies of the concepts of extremes laid the foundation for the development of the techniques collectively labelled the ‘calculus of variations’.

The label ‘calculus of variations’ is a construct of Swiss mathematician Leonhard Euler (1707-1783), derived from his analysis of Italian-French mathematician Joseph-Louis Lagrange (1736-1813)’s works. This is a branch of mathematics that deals with optimizing, i.e., finding the maximum or minimums, of a function defined by an integral. In a way, this was the first attempt to formalize the concepts of optimization into mathematical formulas. The mathematical basis surrounding the calculus of variations were developed in the late 17th century, with the works of English mathematician Isaac Newton (1643[1]-1727) and German polymath Gottfried Wilhelm Leibniz (1646-1716).

Newton’s studies on the motion of bodies in resisting mediums, found in his book *Philosophae naturalis principia mathematica* (*Principia)* in 1685, is considered one of the first real problems in the calculus of variations (Ferguson, 2004; Dacorogna, 2007; Goldstine, 2012). In addition, the brachistochrone problem, which had been formulated by Galileo Galilei (1564-1642) in 1638, was finally solved by Swiss mathematician Johann Bernoulli (1667-1748) in 1696, and then by Leibniz, Newton, the French Mathematician Guillaume François Antoine, Marquis de l'Hôpital (1661-1704), and by Johann’s elder brother, Jacob Bernoulli (1655-1705). The brachistochrone problem, from Greek *brachistos*, shortest, and *chronos*, time, aims to determine the curve between two points for which an object would slide in the least time under gravity and neglecting friction (Johnson, 2004). In general, these mathematicians were able to formulate an integral representing the total slide time given the unknown curve and vary this unknown until a minimum slide time was established. The differential equation formed then solved to a curve known as the cycloid (Ferguson, 2004; Johnson, 2004).

The brachistochrone problem is one of the most famous problems in the calculus

[1]Different sources give different birth dates, with some placing it on the 25th December 1642 and others on the 4th of January 1643.

of variations (Dacorogna, 2007), and is also responsible for showing the connection between the least time principle of Fermat and the least time nature of the Brachistochrone (Ferguson, 2004). Leibniz and the Bernoulli brothers are also responsible for the solution of many problems in infinitesimal calculus i.e., the theory of differentiation and integration, and variational calculus using modern methods (Gårding, 1977).

The brachistochrone problem can be considered the birth of calculus of variations, but the field was generalised later in the 18th century by the Swiss mathematician Leonhard Euler (1707-1783), who had, for a time, had Johann Bernoulli for a mentor (Ferguson, 2004).

Applied optimization problems considered during this century include the honeycomb problem considered by German mathematician Johann Samuel König (1712-1757) around 1739, in reply to a question posed by French scientist René Antoine Ferchault de Réaumur that went as follows;

> "Of all possible hexagonal cells with pyramidal base composed of three equal and similar rhombs, to find the one whose construction would need the least material."

For which König's answer was 'the cell that had for its base three rhombs whose large angle was 109 deg 26', and the small 70 deg 34'', showing that the hexagonal structure of honeycombs is optimal. These results that were similar to earlier calculations by the Italian-French mathematician Giacomo Filippo Maraldi(or Jacques Philippe Maraldi) (1665-1729) (Maeterlinck, 1901). König is also more famously known for his dispute with French mathematician Pierre Louis Moreau de Maupertuis (1698-1759) regarding the true originator of the principle of least action.

In Euler's 1744 book on the calculus of variations titled *Methodus inveniendi lineas curvas maximi minimive proprietate gaudentes, sive solution problematis isoperimetrici latissimo sensu accepti*, or *A method for discovering curved lines that enjoy a maximum or minimum property; or the solution of the isoperimetric problem taken in the widest sense*, he extended the methods of calculus of variations, forming and solving differential equations for optimizing single-integral variables; showed how such equations could be used to represent equilibrium positions of elastic and flexible lines, and 'formulated the first rigorous dynamic variational principle' (Fraser, 2005). This book is considered by some to represent the birth of the theory behind the calculus of variations (Kreyszig, 1994a; Kreyszig, 1994b; Ferguson, 2004). The techniques were then later extended and simplified by Joseph-Louis Lagrange.

The principle of least action, heavily applied in mechanics, follows the general idea that nature follows the path of least action, or that 'nature is thrifty in all its actions', popularized by Maupertuis in 1744 (Maupertuis, 1744) and 1746 (Maupertuis, 1746). Euler also made an independent formulation of this principle at the same time as Maupertuis (Euler, 1744), but claimed no priority. This principle is important due to its applicability in the generation of equations of motions for mechanical systems, and its applications in the theory of relativity, quantum mechanics, quantum field theory, and Morse theory (CFGB, 2006). König's dispute with Maupertuis regarding this principle stemmed from the fact that König considered Leibniz as its originator, furnishing a copy of a letter supposedly written by Leibniz in 1707 that contained this principle. König, unfortunately, was labelled a forger (O'Connor and Robertson, 2003) as there was no way to prove the letter was actually written by Leibniz at the time, as it was not the original. Euler and the King of Prussia supported Maupertuis in refuting König's claim, while the French enlightenment writer Voltaire (François-Marie Arouet) (1694-1778) supported König.

Around 1760, the Plateau problem, named after Belgian physicist Joseph Plateau (1801-1883), was formulated by Joseph-Louis Lagrange. This is a problem of finding the surfaces of least area within a given boundary. Plateau's experimentations in 1849 proved that this surface could be found by immersing a wire frame into soapy water, with the wire frame representing the boundaries (Harrison, 2014). Later studies by American mathematician Jesse Douglas in 1931, Hungarian-American mathematician Tibor Radó (1895-1965), Russian mathematician Abram Samoilovitch Besicovitch (1891-1970), American mathematicians Herbert Federer (1920-2010) and Wendell

Helms Fleming (1928-2023) in the 1950s, and by Enrico Bombieri in the 1970s, extended and specialized the study of minimal surfaces, earning Douglas and Bombieri Field Medals for their work (Almgren Jr and Montgomery, 1974).

A further optimization development of note arising out of the 18$^{\text{th}}$ century is that of French mathematician Gaspard Monge, known as the transportation problem. This was a problem formulated by Monge in 1781 whereby he intended to find the optimal way of moving a pile of sand between military embankment sites at minimal cost (Monge, 1781; Peyré and Cuturi, 2019). This problem was later reformulated by Russian mathematician Leonid Kantorovich in 1942 (Kantorovich, 1942), who intended to solve practical concerns of optimal resource allocation (Peyré and Cuturi, 2019), and is now more popularly known as the Monge-Kantorovich problem (Chen et al., 2020). Other further formulations include those of Yann Brenier in 1987 (Brenier, 1987) that connected the problem with other fields including partial differential equations, fluid mechanics, geometry, probability theory, and functional analysis. This increased the concept's applicability, and it is now applied in image processing, cancer detection, and machine learning, among others.

In the 19$^{\text{th}}$ century optimization developed mainly as an abstract concept, and the first rigorous definitions of calculus were formulated, especially with the works of the 'father of modern analysis' (Baker, 1996), German mathematician Karl Theodor Wilhelm Weierstrass (1815-1897), and French mathematician Augustin-Louis Cauchy (1789-1857) (Grabiner, 1983; Borovik and Katz, 2012). It also saw some application, especially in the field of economics. Further improvements to previously defined theories and concepts were also developed at this time. The first optimization algorithms were also formulated during this period.

The major developments of this period began in 1805, when French mathematician Adrien-Marie Legendre's published his least squares method for algebraic fitting (Legendre, 1806), which was then later statistically backed by German mathematician Carl Friedrich Gauss (1777-1855) (who also claimed to have invented the least squares method much earlier (Stigler, 1981), to the ire of Legendre (Stigler, 1977)) and French mathematician Pierre-Simon, marquis de Laplace (1749-1827), among others.

Between the years, 1813-1815, the economic Law of Diminishing Returns, which is based on the (quasi) concave function began to take shape (Cannan, 1892), culminating in the works of Thomas Robert Malthus, Robert Torrens, Edward West, and David Ricardo, all published within a three-week period in 1815 (Brue, 1993). According to Brue (1993), this law was developed and applied to land rent, in an attempt to explain the fall in grain prices observed in England at the time. This fall was found to be caused by the end of the Napoleonic wars (1803-1815) (O'Rourke, 2006; Gates, 2011), and consequently, the reduced need to cultivate less fertile or inaccessible English land to supplement any grain shortages, as they had previously done when the Napoleonic wars had disrupted international trade. The end of the war and the restoration if imports had thus led to the observed decline in grain prices (Brue, 1993).

The year 1826 marks the beginning of the story of linear programming[2], when the linear programming problem was formulated by French mathematician and physicist Jean-Baptiste Joseph Fourier (1768-1830) (Fourier, 1826). Fourier is believed to have contributed in the following ways (Prékopa, 1980): first, he 'anticipated' the linear programming problem in 1824 (Grattan-Guinness, 1970); second, he formulated the inequality for the mechanical equilibrium in 1798 (Fourier, 1798); and third, he proposed a parametric solution of homogenous linear inequalities in 1826 (Fourier, 1826). 110 years later, in 1936, these methods were independently reinvented by American mathematician Theodore Motzkin (1908-1970) (Motzkin, 1936), leading to the current Fourier-Motzkin elimination (FME) method. Inspired by Fourier's work, Hungarian mathematician Gyula Farkas (1847-1930) formulated a fundamental theorem on linear inequalities towards the end of the 19$^{\text{th}}$ century and the beginning of the 20$^{\text{th}}$, culminating in a famous 1901 paper in which we find the Farkas lemma (Farkas, 1896;

[2]Some authors, e.g., Biggs (2021) attribute this beginning to a much earlier date, the 13$^{\text{th}}$ century, with Fibonacci's rules for mixtures using the Hindu-Arabic arithmetic system. As these were written in word form they did not gain much traction till the invention of algebraic symbols in the 17$^{\text{th}}$ century.

Farkas, 1901; Biggs, 2021). The Farkas lemma uses the fundamental linear inequality theorem to determine the necessary optimality conditions for non-linear programming, conditions that were later used to provide proof of the (Karush)-Kuhn-Tucker theorem in 1951 (Kuhn and Tucker, 1951; Prékopa, 1980), and to support further application of linear programming in optimization. Farkas's contributions to linear programming and optimization include (Prékopa, 1980): proving the basic theorem of linear inequalities in 1894 and 1898 (Farkas, 1894; Farkas, 1898); providing a rigorous proof for duality of Fourier's mechanical inequality principle in 1894 and 1895 (Farkas, 1894; Farkas, 1895); and providing an 'elegant parametric representation' for solutions to homogeneous linear inequalities beginning in 1898 (Farkas, 1898).

Renewed interest in linear programming and its applications was subsequently observed during the Second World War as the need for resource optimization increased (Chakraborty et al., 2020), but the application of linear programming for the optimal resource allocation began with the work of Russian mathematician Leonid Kantorovich (Boldyrev and Düppe, 2020) in 1939 when he published his Mathematical Methods of Organizing and Planning Production (Kantorovich, 1960; Koopmans, 1960), subsequently developing an algorithm for such applications.

During the Second World War, scientists focused on optimising linear functions over a set of linear inequalities as a way to ensure resource optimization (Chakraborty et al., 2020). This began with the 'simplex method' for solving US Airforce planning problems of American mathematician George Dantzig (1914-2005) and Dutch-American mathematician Tjalling Koopmans (1910-1985)'s application of linear programming models for analysis of classical economic theories in 1947 (Schrijver, 1998). Later developments include Hungarian-American mathematician John von Neumann (1903-1957)'s development of game theory and the duality theorem, later proven by Gale, Kuhn and Tucker (1951). In 1960, Zoutendijk (1960) developed the methods of feasible directions to enable the generalization of the simplex algorithm for non-linear problems. Linear programming then evolved to be solvable in polynomial time with the ellipsoid algorithm of Soviet-American mathematician Leonid Khachiyan (1952-2005) in 1979

(Khachiyan, 1979); and the introduction of interior point methods for solving linear programming problems by Indian mathematician Narendra Karmakar in 1984 (Karmarkar, 1984). Over time, linear programming and extensions have also evolved in application, moving beyond its original military and economic roots, to be applied in a broad range of fields, including in agriculture, manufacturing, healthcare, and in energy and transportation.

In the 19th century, after Fourier, optimization applications to forest economics were considered by German forester Martin Faustmann (1822-1876) in the mid-19$^{\text{th}}$ century (Scott, 2008). The optimum forest rotation problem involved attempting to maximize Faustmann's present value of the forest rotation income stream problem, which was later formally solved by Bertil Ohlin in 1924 (Findlay et al., 2002), though it is believed that this solution was known to researchers as early as the 1849 (Viitala, 2006).

Around this time, Augustin Louis Cauchy also presented the gradient descent (or steepest descent) method applied in nonlinear optimization in the 1847 publication *Méthode générale pour la résolution des systemes d'équations simultanées* (General method for solving systems of simultaneous equations) Cauchy (1847). This was an alternative to the model-based unconstrained nonlinear optimization techniques first developed by Newton (Nazareth, 1994). Cauchy developed this method to aid in solving complex quadratic problems in astronomy (Lemaréchal, 2012). Later, in 1907, French mathematician Jacques Hadarmard (1865-1963) also independently developed the technique (Hadamard, 1907; Courant, 1943). This technique has seen much application as an iterative machine learning algorithm for local minimization problems.

The early 20$^{\text{th}}$ century saw developments in convex analysis, through the works of Hermite (1883) and Hadamard (1896) (Krtinic and Mikic, 2018), Holder (1889), Jensen (1906), Minkowski (1910), and Minkowski (1911), among others, giving rise to famous probabilistic inequalities for convex functions, including the Jensen's inequality Burnside (1975) and the Hermite-Hadamard inequality (Sezer, 2021).

Optimization concepts were also applied in biology to explain the distribution of natural forms and the source of natural changes by Scottish biomathematician D'Arcy Wentworth Thompson (1860-1948) in 1917 (Thompson d'Arcy, 1917); and in finance for the determination of optimal portfolios by Markowitz in 1952 (Markowitz, 1952), Tobin (1958) and Marschak (1938).

Other notable 20th century contributions to optimization include the advent of combinatorial optimization techniques by Ford and Fulkerson (1956) and Ford and Fulkerson (1962), the development of optimal control theory in 1956 (Pontryagin, 1987) as a result of developments in dynamic programming concepts, especially due to the works of Bellman (1952) and Bellman (1956), the rise of computers, and the aerospace applications of initial programming ideas (Sargent, 2000). The sequential quadratic programming algorithms for constrained nonlinear optimization were also proposed by Wilson (1963), Han (1976), Han (1977), Powell (1978a), Powell (1978c), and Powell (1978b).

Even though there were further developments in other aspects of optimization as the subject area broadened in both theory and application, of interest to us are the mid-to-late 20th century developments in unconstrained optimization algorithms for both local and global optimization, including conjugate gradient methods, quasi-Newton methods, approximation methods, etc. It is these developments that motivated the search for specific-case algorithms to supplement their limitations. For purposes of parameter estimation, particularly maximum likelihood estimation, we study a class of special case application algorithms that have been used extensively for optimization purposes in cases of missing data or hidden variables, i.e., the Expectation-Maximization (EM) algorithms.

4.2 Background to the Expectation-Maximization (EM) Algorithm

"I felt like the old minstrel who has been singing his song for 18 years and now finds, with considerable satisfaction, that his folklore is the theme of an overpowering symphony" - Herman Hartley

When the Expectation-Maximization (EM) algorithm, an optimization technique for parameter estimation given missing or hidden data was formally proposed by Dempster et al. (1977) in 1977, it cemented this algorithm's place in the timeline of optimization. Dempster et al. (1977)'s paper was later supplemented by Boyles (1983), Wu (1983), and Redner and Walker (1984) (Bagozzi, 1994). The EM is a better-converging alternative to both general optimization methods like the Newton-Raphson methods and conjugate gradient methods; and methods of scoring (Titterington, 1984). To establish parameter estimates, the EM algorithm alternates between the Expectation step (E-step), which uses current or initial parameter estimates to create the log-likelihood expectation, and the Maximization step (M-step), which then maximizes the E-step's expected log-likelihood to determine new 'more likely' parameters, with are then used as the new initial parameters for the E-step (Meng and Dyk, 1997). The process then repeats until the local optimum parameter has been reached, signified by highest likelihood.

The intuition behind the EM algorithm, despite being formalized in 1977, however, was not a new concept, with Dempster et al. (1977) even noting that the algorithm had been "proposed many times in special circumstances". The next few paragraphs thus gives an overview of the 'roots' of the concepts driving the EM algorithm, and the historical developments that culminated in Dempster, Laird and Rubin's 1977 study.

The development of the EM algorithm can be traced back to the end of the 19th century, with the first EM-type algorithm being referenced by Newcomb (1886) and Pearson (1894) and applied to model parameter estimates for finite mixture models

(McLachlan and Krishnan, 2007; Bagozzi, 1994). This development has also been attributed to Fisher(1925)'s statistical identities (Meng and Dyk, 1997), and McKendrick (1926)'s 'Applications of mathematics to medical problems'(see e.g., Dietz, 1997).

The 1950s saw much improvement in the development of EM-type methods and their application. In 1955, these techniques were applied in gene-counting for the estimation of gene frequencies by Cedric Smith, Ruggero Ceppellini, and Marcello Siniscalco in 1955 (Ceppellini et al., 1955; Smith, 1957); reformulated for use in randomized block design by Healy and Westmacott (1956); and a version of the EM algorithm that provided the basis for the Dempster et al. (1977) formulation proposed by Herman Hartley in 1958 (Hartley, 1958).

In the 1960s, EM-type algorithms were formulated and applied, especially to Markov models with the works of Leonard Baum, Ted Petrie, and John Eagon (Baum and Petrie, 1966; Baum and Eagon, 1967), who introduced hidden Markov models (HMMs) to the world. These HMM models have been popular in applications including speech recognition (Juang and Rabiner, 1991), signal processing, and gene sequencing, etc.

Baum and Petrie extended their studies and provided a more comprehensive results of their model in their 1970 paper, together with George Soules and Norman Weiss (Baum et al., 1970). Orchard and Woodbury (1972) define their contribution in their paper 'A missing information principle: theory and applications' as follows 'present a general philosophy for dealing with the problem of missing information, and to give a method which will lead quite easily to maximum likelihood estimates of the parameters obtained from the incomplete data using as nearly as possible the same techniques as if the data were all present.'. This is identical to the process followed by EM algorithms to arrive at parameter estimates.

The Richardson-Lucy algorithm, a nonlinear iterative technique for image deblurring and restoration developed independently by William Richardson in 1972 and Leon Lucy in 1974 is also a type of EM algorithm (McLachlan and Krishnan, 2007). Carter and Myers (1973) show how the maximum likelihood parameter estimation problem for a linear combination of probability functions can be solved through an iterative algorithm that reduces the problem to a complete data problem, which is the EM algorithm.

Other key sources cited in Dempster et al. (1977) include the 'self-consistency principle' of Efron (1967) and a later extension of Efron (1967)'s idea by Turnbull (1976) to incorporate not only single-censored data, but also other grouped and truncated data; and Sundberg (1974), Sundberg (1976), and Orchard and Woodbury (1972) for the theory behind the EM algorithm, among others.

The EM algorithm has gained much popularity over the years especially due to its attractive convergence properties and computational efficiency (McLachlan and Krishnan, 2007). In addition, it provides a simple and straightforward class of algorithms that can be modified for multiple applications and extended or improved by merging it with other general optimization algorithms like the Newton-Raphson algorithms to further improve its efficiency. Because of this, EM algorithms have seen broad applicability, including finite mixture modelling, variance components, hyperparameter estimation, hidden Markov models, iteratively reweighted least squares, and factor analysis, etc. (Dempster et al., 1977).

Catastrophic loss modelling, on the other hand, can be complicated to accomplish, especially due to the intractable nature of most of the modelling and subsequent pricing equations. Because of this, many techniques used to accomplish the modelling process tend to be computationally expensive, especially due to the simulations required for each of the equations involved (see e.g., Ma and Ma, 2013; Burnecki and Giuricich, 2017). The techniques underlying the EM algorithm can bypass this problem, as the losses are formulated in accessible distribution-forms that are then combined to ensure a complete loss structure, especially in the tails (Dempster et al., 1977; Raudenbush and Bryk, 2010; McLachlan and Krishnan, 2007). The final 'mixed' distribution is then used as a model for overall losses, and the distribution then applied as the underlying distribution in pricing models. This process increases not only the computational efficiency of the modelling process (McLachlan, 2008), but also provides the opportunity to incorporate many different elements of loss observations that would otherwise be difficult to incorporate into normal models (Dempster et al., 1977; Baum and Petrie, 1966; Rabiner, 1989), including elements like dependency and heavy tail modelling. It is for these reasons that this study applies the EM algorithm to climate risk modelling, as it provides more comprehensive modelling options for not only the observed catastrophic losses, but also for catastrophe bond price analysis.

The following sections will thus focus on the application of the EM algorithm to catastrophic loss modelling and catastrophe bond pricing and analysis, with the aim of ensuring more robust and comprehensive models and thus 'fair' pricing for catastrophic risk finance instruments that then provide protection against the risks of such catastrophes. The first application involves an application of the EM algorithm for variance component analysis, with the goal of determining whether internal issuer factors have the potential to affect their issuer-specific catastrophe bond prices, even though this should not be the case as catastrophic risks are independent of and external to issuer company-specific risks. The second application intends to propose a model that better incorporates the heavy tails of catastrophic loss processes, through finite mixture modelling; while the third application proposes a model that can better incorporate the dependence structure of single-peril catastrophic losses over time and location.

Chapter 5

Exploring Inefficiencies in the Primary Catastrophe Bond Market with a Focus on the 'Issuer Effect'[1]

The COVID pandemic has highlighted the importance of hedging against catastrophic events, for which the catastrophe bond market plays a critical role. Most catastrophe bonds issued in the primary catastrophe bond market are sold by the same issuers every year, and within each year. Significant similarities in the bond characteristics are therefore anticipated, which ultimately leads to similarities in pricing for these bond issuers over time. Using a very rich database with primary catastrophe bond data from 1997 to 2020, and proposing a novel random intercept model, the variations in catastrophe bond premiums introduced by the differences between issuers are captured, analysed and found to be significant. To accomplish this, we develop a two-level model based on the Expectation-Maximisation (EM) algorithms' variance components analysis. We then apply this to a unique, hand-collected dataset, which is one of the largest and most detailed datasets to date containing: 101 different issuers, 794 different bonds, spanning from 1997-2020, to identify issuer effects robustly, isolating them from bond specific

[1]This section of the study has already been published in the International review of Financial Analysis, as Chatoro, M., Mitra, S., Pantelous, A. A., & Shao, J. (2023). Catastrophe bond pricing in the primary market: The issuer effect and pricing factors. International Review of Financial Analysis, 85, 102431. `https://doi.org/10.1016/j.irfa.2022.102431`

pricing effects, therefore providing more credible pricing factor results. We find that bond pricing and volatility are heavily impacted by the issuer, causing 26% of total price variation. We also identify specific issuer characteristics significantly impact bond pricing and volatility, and can account for up-to 36% of total price variation. We further find that issuer effects are significant over different market cycles and time periods, causing substantial price variation. The size and content of our data also enables us to identify the counter-intuitive relation between bond premiums and maturity, and bond premiums and hybrid bond triggers. Our results give strong evidence that the primary catastrophe market remains inefficient. *Keywords:* Catastrophe risk bonds; Primary market; Multilevel modelling techniques; Issuer effect; Hedging

5.1 Introduction

The COVID-19 pandemic was catastrophic for many economies and societies. Previously, and despite the constant depiction of contagious disease outbreaks in popular entertainment, a real-life global pandemic of this scale was never truly considered. Although some previous events have been insured e.g. the Wimbledon tennis tournament, which had been insured against the SARS outbreak since 2003, leading the organisation's policy to pay out US$142 million to cover the cost of cancelling the 2020 tennis tournament, [2] these types of coverage are not always guaranteed in each year e.g. in the Wimbledon case, the coverage was not renewed in 2021 due to an increase in premiums [3]. The rarity of such events, in addition to their high insurance costs, implies that in most cases, these high cost disasters go uninsured. Alternative tools that provide protection against possible disaster in the form of high-yield debt instruments, such as the catastrophe (CAT) bond, were therefore introduced to tackle such issues.

The CAT bond market developed largely in response to the reduction in reinsurance capacity observed after Hurricane Andrew in 1992. It was established as an alternative platform for companies to acquire reinsurance protection as reinsurance companies were overwhelmed by increasing losses due to catastrophic events (Swiss Re, 2012). Similar to other debt securities, CAT bonds pay regular coupons and the principal value at maturity. However, the coupon paid to the investor consists of a baseline return and a premium.[4] The former is determined based on market conditions at the time, and the latter, also known as the spread, is composed of the expected loss on the underlying peril and a risk load (Patel, 2015).[5] Further, the risk load is determined based on

[2]https://www.insurancetimes.co.uk/news/wimbledon-set-for-coronavirus-windfall-in-huge-pay-out-from-pandemic-insurance/1433146.article

[3]https://www.insurancetimes.co.uk/news/wimbledon-boss-confirms-the-championship-will-not-have-pandemic-insurance-in-2021/1433726.article

[4]In the past, it has generally been based on the London Interbank Offered Rate (LIBOR), or a similar well-known index (Cummins, 2008).

[5]The mathematical expression is given by $Premium(P) = \textit{Expected Loss (EL)} + \textit{Risk Load (RL)}$.

the bond characteristics and other external factors including the bond's underlying peril, the trigger, the bond rating, the bond issuer, the time of issue, the reinsurance cycle and the state of the competing financial market, among others (e.g., Lane and Beckwith, 2008; Bodoff and Gan, 2009; Papachristou, 2009; Braun, 2016; Gürtler et al., 2016). The principal repayment (and sometimes the coupons, depending on the structure) is conditional on the specified catastrophe not occurring. If the catastrophe occurs, investors lose either part or all of their coupon and/or principal.[6]

To date, over $123 billion worth of CAT bonds have been issued. Figure 5.1 shows the development of CAT bond issues in US$ and the number of deals over the years in the primary market.[7]

[6]There are some similarities in structure between a CAT bond and a high-yield or junk bond (Cox and Pedersen, 2000). Both are priced based on the risk of default to the investor. For high-yield or junk bond the default stems from the issuer defaulting on payments due to underlying issuer factors, or external factors affecting the issuer. For a CAT bond, however, the risk of default stems from the occurrence of a catastrophe, which in most cases occurs independently of the issuer's condition or financial market factors. Due to this difference in the source of default between high-yield bonds and CAT bonds, CAT bonds are favoured by investors as instruments of diversification, since their returns are generally uncorrelated with broader financial market factors that normally affect other financial instruments (e.g., Cox and Pedersen, 2000; Zimbidis et al., 2007; Carayannopoulos and Perez, 2015). Investors also choose to invest in these bonds because of their attractive risk-adjusted returns, when compared to other financial market instruments (Swiss Re, 2012).

[7]Data provided by https://www.artemis.bm/deal-directory/ (Retrieved on 22nd June 2020)

Figure 5.1: *Catastrophe Bond Issuance by Year*

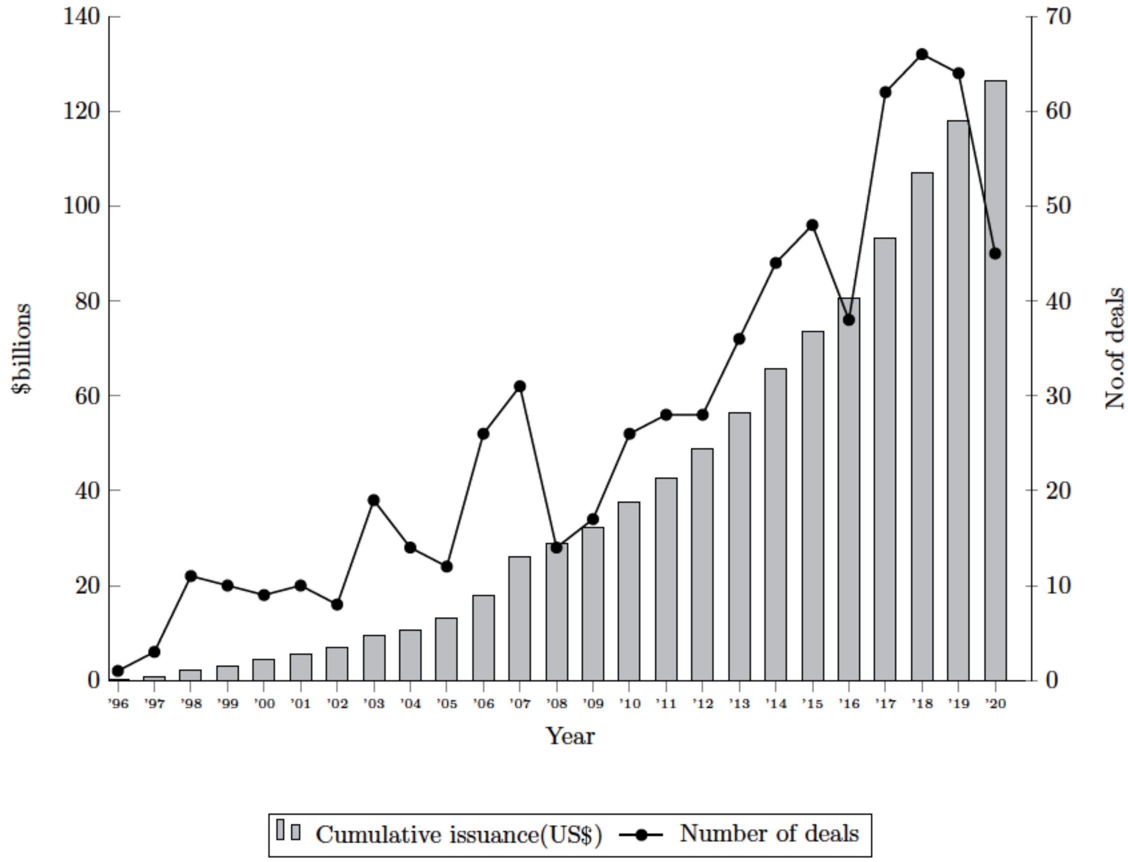

Note: The figure above shows the development of CAT bond issues over time since the inception of the CAT bond market in 1996. To date (22nd June 2020), over US$123 billion worth of these bonds have been issued. The bar graph displays the total cumulative issuance while the line graph displays the number of CAT bond issues within the respective year. This data was retrieved from the Insurance Linked Securities' website Artemis.bm (Retrieved 22nd June 2020).

The catastrophe bond market is still in its expansion stage, only having been formally in existence for approximately 20 years. To ensure its successful growth and wider investor participation, it is important that inefficiencies are identified and solutions proposed to improve participation rates. One of the most common characteristic of primary CAT bond issues is that they are issued by the same issuers every year, or even within the year (Major, 2019). These issues usually have similar characteristics, since most new bonds are renewals of older expiring bonds, which are issued by the same issuers to cover the same catastrophic events. Despite these similarities, the risk factors of a CAT bond relate to the catastrophe itself, and not to the issuer. Further, the Special Purpose Vehicle (SPV)[8] that issues the CAT bond ensures bankruptcy remoteness (Pearce II and Lipin, 2011), effectively separating the risks faced by the issuing company from those of the CAT bond.[9] In principle, issuers' characteristics should not, therefore, have any impact on premium determination.

This is not always the case in practice, however, as frequent issuers may receive better deal terms and pricing over time than infrequent issuers due to the relationships developed with investors (Spry, 2009). The Covid-19 pandemic has also further attracted new issuers to the market looking to benefit from both the protection and diversification potential offered by ILS instruments. These issuers would be interested in understanding the specific risks faced by newer entrants before formally participating in the CAT market. Furthermore, new types of ILS investments that the market

[8] The SPV is a company created for the express purpose of providing reinsurance to the issuer if a catastrophe occurs (e.g., Cox and Pedersen, 2000; Zimbidis et al., 2007; Pearce II and Lipin, 2011). The company receives premiums from the issuer and in turn issues CAT bonds in the financial markets using the premiums as collateral. The proceeds from the bond issue, together with the premiums paid by the issuer, are invested in a collateral account consisting of high-quality assets. These investments are used to fund coupon and principal repayments to investors if a pre-specified catastrophe does not occur, and used to provide reinsurance to the issuer otherwise.

[9] Once the issuing company has transferred the premiums, which serve as collateral for the CAT bond, the SPV takes up the responsibility for ensuring full and timely cash flow payments are provided to investors.

seems keen on introducing[10] can only be successful if the necessary issuer screening and market efficiency analysis is conducted to determine suitability. Issuer considerations will therefore need to be incorporated into pricing models to ensure that the models are exhaustive and complete.

Research analysing the effect of the issuer on CAT bond premiums is scarce. Of the major studies assessing factors that affect CAT bond premiums, only Major and Kreps (2002), Braun (2016) and most recently, Goetze and Gürtler (2020) explicitly study the impact of the issuer. These studies, however, are either limited by their small sample size (Major and Kreps, 2002), or number of issuers analysed (Braun, 2016), or are focused only on the secondary market (Goetze and Gürtler, 2020). Distinctly to Goetze and Gürtler (2020), this paper focuses on the effect of the issuer on initial premiums charged for CAT bonds issued in the primary market. Other stylised factors relating to the issuer, the market, and the time period are further analysed to establish the characteristics that introduce the greatest variability in the bond premiums charged to specific issuers. These include the effect of the total CAT bond issue size since inception, the number of years the issuer has returned to the primary CAT market to issue bonds, the issuer's line of business, the state of the market cycle at the time of the bond issue, and the effect of the time of issue. Further, we incorporate the effect of all the issuers that have issued bonds in the primary market since inception, instead of focusing on only one issuer. This effect is then tested on a much larger sample of all CAT bonds issued in the primary market between June 1997 and March 2020.

The present paper assumes that, even after controlling for all the other factors that affect CAT bond prices, base premiums still vary based on who sponsors the bond. To determine the significance of this observation on CAT bond pricing, this study applies multilevel modelling techniques to estimate the level of variation in bond premiums as a result of pricing differences between issuers in the primary market. Multilevel analysis allows us to separate the effects of the issuer from those of the other explanatory

[10]https://www.artemis.bm/news/cat-bond-market-can-grow-to-50bn-pandemic-risk-esg-are-drivers-swiss-re/

variables believed to impact premiums, in addition to quantifying the level of variation in premiums between issuers arising as a result of their inherent differences. We find this issuer effect to be significant, implying that variations in base premiums due to the issuer exist. Around 11% of the variation in premiums appears to be as a result of between issuer differences. Furthermore, this variation is reported to be much larger for smaller issuers based on issue size, for issuers that have issued less in the primary CAT bond market (i.e., less consistent issuers), and for companies in the primary business of conducting insurance as opposed to reinsurance or other multi-line businesses. We also identify the three independent factors that have the largest impact on premiums as the expected loss, the peril and the reinsurance cycle. Finally, the robustness of our results is established across the major stages of the market cycle and for different time periods.

The contribution of this research is therefore as follows. First, we develop a two-level model on the largest sample size to date to determine the effect of issuer variations on issuer premiums. We also quantify the magnitude of this issuer effect to better establish the amount of volatility introduced by the differences between issuers. The magnitude of the effect of the other major explanatory variables (those whose effect on premiums does not change as the issuer changes) is also calculated to enable identification of the key fixed factors. Second, we extend the issuer analysis to identify the specific characteristics of the issuer that impact this volatility the most. This involves splitting the sample into smaller sub-samples based on specific characteristics of the issuers, including the effect of the issuer's line of business, the issuer's total CAT bond issue size in the primary market since inception, and the number of years for which the issuer has been issuing bonds in the primary market. Finally, we extend the analysis of these factors to determine the level of issuer variation that influences premiums in different stages of the market cycle and over different time periods. In aggregate, by testing for the existence of the issuer effect and the main characteristics determining the magnitude of this effect, we effectively determine the extent to which the primary CAT bond market exhibits inefficiencies. As an important impact, these inefficiencies considered here can be exploited by future first-time issuers, who can use them to pick the optimal avenue through which to issue new bonds. These results can also provide an understanding of the factors to consider before introducing a new product to the ILS market, especially when conducting issuer screenings. This will further lead to increased participation and growth of the ILS markets.

The rest of this article is structured as follows: Section 5.2 introduces the hypotheses to be assessed in determining the factors that affect CAT bond pricing. Section 5.3 describes the sample selection and data characteristics. Section 5.4 gives the methodology and empirical analysis, while Section 5.5 discusses potential implications for CAT market participants. Section 5.6 concludes the article and an appendix follows thereafter.

5.2 Development of Hypotheses

To assess the effect of issuer differences on bond premiums, we incorporate both the effect of the issuer (i.e., random effect) and that of other explanatory factors (i.e., fixed effects). *Random effects* represent the factors that lead to variable premiums as we move between the groupings created by the previously mentioned factors. They introduce an additional source of variation to the model, in addition to the error term that represents the unexplained variation (Raudenbush and Bryk, 2010). Fixed effects, which represent those factors whose effect on premiums does not change as the grouping changes, will therefore explain the premiums to a large extent before the remaining variation is allocated between the issuers and the unexplained variation (Major, 2019). This section identifies and justifies both the fixed and random effects that will be tested for inclusion into the final model, following previous research and other observations.

Based on Lane (2018), we establish our hypotheses using common factors affecting CAT bond pricing, such as (1) the expected loss, (2) the CAT bond deal structure, (3) the reinsurance cycle, (4) the bond issue or sponsor and (5) the competitive fixed income financial markets. In addition, other factors, including maturity, issue date and bond rating, are assessed. Hypotheses are generated for each of these explanatory factors as follows.

5.2.1 Issuer

Issuer characteristics are assumed to affect the impact of the issuer on the premium, with higher or lower premiums charged depending on underlying characteristics. In previous treatments, the issuer effects are either included as dummy variables (Braun, 2016) or not included at all (Lane, 2018). However, there are challenges that arise with the use of dummy variables to incorporate issuer effects. Observing our dataset, over 100 issuers have participated in the CAT bond market since inception, and unless these issuers are aggregated into smaller classifications, testing the issuer effect will be impossible. Aggregation, which involves averaging across issuers, may however lead to the loss of key issuer information that could be relevant to the analysis.

In a single-level model with only one error term that represents the fixed effects, the issuer-specific differences are not sufficiently considered. This leads to under-estimation of standard errors and over-estimation of the significance of explanatory variables, and thus, to incorrect inferences. As a result, a multilevel model is recommended instead (see, e.g., Raudenbush and Bryk, 2010; Nezlek, 2012).

In the corresponding pricing literature, very few of the CAT bond studies actually apply a multilevel model for their analysis. Major and Kreps (2002) are among the first to consider it to assess the impact of "client-specific factors" on pricing, which they find to be significant. It should be noted, however, that their dataset was much smaller, and with a much smaller number of issuers compared to the present study's dataset. In addition, the "client-specific factors" are not subsequently broken down to identify which specific factors have the greatest impact on pricing. Gürtler et al. (2016) apply a multilevel model to incorporate the effects of time in secondary market data. Recently, Goetze and Gürtler (2020) consider something similar to test the effect of sponsor-specific variables on premiums in the secondary market. Distinctly to them, we test for the existence of the issuer effect in the primary market issues to assess the penalty "at issue".

In a multilevel structure, units belonging to a lower level would be grouped into units at a higher level (Wang et al., 2011). If the individual data points can be clustered based on an identifying characteristic of each group, then the individual data points will comprise the lower (micro) level, while the grouping characteristic will form the units for the higher (macro) level. In our case, most of the bonds are issued by the same issuers every year, or even within the year. Since most of these issuers cover similar risks to every other issuer, it is possible that investors base their pricing decisions for future bonds on the same company on the past premiums. This implies that, when all other factors affecting premiums are held constant, the identity of the issuer, or their total number of issues, might lead to differences in premiums charged for different issuers. Seasoned issuers may receive lower rates based on their standing as frequent issuers, while new issuers may receive higher rates. This deduction is in line with Spry (2009), who explains that an issuer with a strong track record has the ability to issue even more bonds at better pricing terms over time. The similarities in bonds issued by the same issuer also lead to higher correlation in premiums for a given issuer. This means that the individual observations will no longer be independent, but dependent based on the issuer of the bond. The following hypothesis assesses whether the issuer's characteristics, reputation or track record have any influence on their premiums.

Hypothesis 1a: *After controlling for all other independent variables, premiums will still differ depending on the bond issuer.*

In addition, other supporting hypotheses are tested to identify the characteristics of the issuers that introduce the greatest volatility into premiums. These supporting hypotheses include:

Hypothesis 1b: *Issuers with a higher total issue volume will have lower volatility in premiums arising as a result of the issuer effect compared to those with a lower total issue volume.*

Hypothesis 1c: *The longer the issuer has participated in the primary CAT bond market, the lower their premium volatility will be due to the issuer's characteristics.*
Hypothesis 1d: *Issuers in the insurance industry will have higher volatility than issuers in other lines of business such as reinsurance or multi-line.*

5.2.2 Additional factors

Peril

Following Cummins and Mahul (2009), we break down our perils into four major categories: *Peak* are US-based perils including US hurricanes and earthquakes, *non-peak* includes European wind storms and Japanese earthquakes, *diversifying* includes all other non-US perils, e.g., Mexican earthquakes, Australian earthquakes and hurricanes, and *multi-perils* combines peak and non-peak perils in the same transaction.

It is assumed that peak CAT bonds will normally have higher premiums than non-peak (non-US) bonds (Cummins, 2008). This is because the peak regions are more prone to natural disasters such as hurricanes, typhoons, earthquakes, tornadoes etc. In addition, peak bonds do not offer as much diversification benefit as non-peak bonds, due to the concentration of investor portfolios in peak regions. Multi-peril bonds are also assumed to have higher spreads due to the complexity of the deal structure (Gürtler et al., 2016; Patel, 2015). Our hypothesis is therefore as follows:
Hypothesis 2: *Peak or multi-peril bonds will have higher risk premiums than non-peak or single-peril bonds respectively.*

Trigger

There are five major trigger types in the CAT bond market: *indemnity*, *parametric*, *industry loss*, *modelled loss* and a *hybrid trigger* - representing a combination of any of the other four. Indemnity triggers provide a perfect hedge, where pay-outs are based on the issuer's actual losses. All the other triggers are non-indemnity triggers based on a specified index. Industry loss triggers pay out if the value of industry losses exceeds a specified level. Parametric triggers pay out based on the CAT bond meeting pre-defined physical parameters, e.g., wind speed and location of a hurricane or magnitude and location of an earthquake, while a modelled loss is determined by running the catastrophe's physical parameters on the modelling firm's database of industry exposures (MMC Securities, 2007). Non-indemnity triggers are an imperfect hedge and do not always fully cover the issuer's actual losses.

Indemnity-triggered bonds would be expected to have higher spreads because of the reduced basis risk to the sponsor and the increased moral hazard risk to the investor (Doherty and Richter, 2002). There are also increased transaction costs because of the more extensive due diligence that would need to be carried out compared to a non-indemnity bond (Cummins and Weiss, 2009). Empirical studies on the effects of the trigger on a CAT bond's price have derived mixed results. Gürtler et al. (2016) report no significant effect of the trigger on the premiums. Braun (2016) and Papachristou (2009) also find that the trigger term is much less influential in pricing. Dieckmann (2010), however, reports that the trigger is significant. It is worth noting, however, that Dieckmann's sample size was much smaller, with only 61 CAT bonds considered. Similar to previous studies, we test the effect of the indemnity trigger on risk premiums through the following hypothesis.

Hypothesis 3: *Indemnity-triggered bonds have higher premiums than non-indemnity triggered bonds.*

We also assume that bonds with hybrid triggers will have higher risk premiums due to the complex nature of the bonds. An additional hypothesis then becomes:

Hypothesis 4: *Bonds with multiple triggers have higher risk premiums than bonds with a single trigger.*

Rating

Ratings give investors an indication of what the bond's risk of default might be and help companies reduce their cost of capital by providing credit enhancements (White, 2013). In analysing CAT bond ratings, we focus on two aspects: the impact of the lack of a bond rating, and the impact of a specific rating, on the bond premium. In the first case, we seek to determine whether the lack of a rating on CAT bonds impacts the premiums compared to similar bonds with a rating. The majority of CAT bonds issued within the past eight years do not have a rating. This either means that investors are capable of conducting their own due diligence, or that ratings would not add any other significant information to what investors already know. Cummins (2008) states that the modelling firm's analysis is a more important driver of price than ratings, and for Krutov (2010), investors do not rely on bond ratings, in general.

We also analyse whether specific types of ratings still influence the bond premium. Past literature supports the view that stronger ratings lead to lower premiums. Gürtler et al. (2016) find that, as the rating declines, premium increases, and this result is similar to those of Galeotti et al. (2013) and Braun (2016). As CAT bonds drop ratings, though, this effect might not be observable in the long term. We test two hypotheses, one for the impact of a given rating and the other for the impact of no ratings, on prices. Assuming all other factors affecting premiums are controlled for, the hypotheses then become:

Hypothesis 5: *Bonds with a higher rating have a lower risk premium.*

Hypothesis 6: *Non-rated bonds have higher risk premiums than rated bonds.*

Issue date/quarter

This will be used to test for the significance of the issuance season, especially the pre- versus post-hurricane seasons. Most issues occur in the second (Q2) or fourth (Q4) quarter, and Q2 precedes the hurricane season; therefore, it is assumed that there will be higher spreads allocated to this period compared to the other quarters due to an increase in perceived risk (e.g., Patel, 2015). Seasonal effects are tested in Galeotti et al. (2013) using the seasonal index proposed in Lane and Beckwith (2009). The authors report no significant seasonal effect, which they attribute to either no effect or a misspecified index. We specify the hypothesis below:

Hypothesis 7: *Issues in Q2 have a higher risk premium than issues in the other quarters.*

Maturity

On average, CAT bonds have a maturity period of about three years, but maturity has been observed to be as short as five months and as long as six years. Investment literature suggests that longer-term bonds should have higher risk due to the increased sensitivity of their prices to fluctuations in interest rates (e.g., Bodie et al., 2014). They would therefore be expected to have higher premiums. To determine whether this assumption holds, we specify the following hypothesis:

Hypothesis 8: *Longer-maturity bonds have higher spreads than shorter-maturity bonds.*

Cyclic index

The insurance market faces cycles; prices have been observed to increase after significant catastrophic events or capital outflows due to other economic events, and they decrease due to capital inflows and stability in the catastrophe losses (see, Lane and Mahul, 2008; Cummins and Weiss, 2009; Lane, 2018; Swiss Re, 2019). There can be hard, soft and neutral markets representing, respectively, increasing, decreasing and stable prices. [11] Whether the bond is issued in a hard, soft or neutral market will affect its observed spreads due to the overall market's conditions and investor sentiment at the time of issue. Bonds issued in hard markets tend to have higher premiums than comparable bonds issued in soft markets due to a higher cost of coverage and changes

[11] According to Lane and Beckwith (2020), a hard market represents a period of more 'more aggressive demand for protection from issuers than the appetite for assuming risk among investors (pg.8)' and therefore premiums rise in turn, while a soft market represents a period of less demand from issuers compared to investor risk appetite and thus premiums fall. Neutral markets exist in times when the demand for protection balances out with investor risk appetites.

in risk perception (Patel, 2015; Lane and Beckwith, 2007).

Similar to Gürtler et al. (2016), we apply a property catastrophe cyclic index by Guy Carpenter[12] to test the effect of these cycles on premiums.

Hypothesis 9: *CAT bond premiums increase in line with the cyclic index.*

Competing financial environment

Since CAT bonds are similar to defaultable bonds with an equal rating (Cox and Pedersen, 2000), investors have a choice of either investing in the corporate or the CAT bonds (or both). If the CAT bond market intends to attract investors, it has to price these bonds with reference to the prices in the competing market. The premiums can be slightly lower or higher depending on the diversification benefit provided by each bond, but premiums on corporate bonds still provide a benchmark for assessing premiums in the CAT bond market.

Hypothesis 10: *CAT bond premiums move proportionally to the spreads in similar high-yield corporate bonds.*

5.3 Data

5.3.1 Sample selection

Our sample is an original dataset of 724 CAT bonds issued in the primary CAT bond market between June 1997 and March 2020. For each bond, we have information on the issuer, underwriters, size of issue (in millions of US dollars), issue rating[13], term, issue and maturity month, spread per annum, expected loss, peril and geographical location, trigger, probability of first loss and the conditional expected loss. The data is acquired from Lane Financial LLC's trade notes and cross-checked with other sources

[12] The Catastrophe Bond Market at Year-End: The Market Goes Mainstream (Retrieved 11 September 2020) https://www.gccapitalideas.com/2008/02/28/the-catastrophe-bond-market-at-year-end-the-market-goes-mainstream/

[13] For bonds with multiple ratings, we picked the lowest rating.

to include missing information. Some of these other sources include the Insurance Linked Securities' (ILS) portal Artemis.bm, Aon's Annual ILS Reports, Swiss Re's ILS Market Updates, Munich Re and Guy Carpenter reports, the Institute and Faculty of Actuaries' publications and Froot (1999a). The raw dataset is made up of 749 bonds, but 25 observations are excluded, either due to missing values of key variables or different payment structures from those of a typical CAT bond.[14] We also exclude all life and health bonds as they have different underlying variables that determine their pricing.

5.3.2 Issuers

The data, once grouped based on issuers, consists of 101 individual issuers, with Swiss Re (173 bonds), USAA (74 bonds), Munich Re (30 bonds), Hannover Re (26 bonds) and SCOR (21 bonds) representing the top five issuers by number of tranches. Swiss Re (11.22%), USAA (8.46%), Hannover Re (5.25%), Everest Re (4.34%) and Munich Re (4.18%) are the top five issuers by size of issues. The individual issuer data for all 101 issuers is given in Appendix A. Table 5.1 gives an example of the similarities and developments in issues over time, with a focus on one of the pioneer issuers, USAA.

USAA's CAT bonds, known as Residential Re, are among the first bonds to have been issued in the market in 1997. Over the years, USAA has issued a minimum of one CAT bond every year, and is one of the most consistent issuers in the market. USAA's issue characteristics over time show an increase in bond term from one to four years, a decrease in issue ratings (from AAA to B- following the S&P scale), an increase in the number of classes per issue, and an extension of coverage regions and perils. Later deals cover unique risks such as volcanic eruption, meteorite impact, and even operational risks. This implies that market participants either trust the company more, or that a better understanding of USAA's CAT bonds has increased their willingness to take on

[14] They include bonds triggered by multiple losses, e.g., Bay Haven Ltd which covered six events occurring only after the first three events had occurred, effectively covering frequency instead of severity of losses (Lane and Beckwith, 2007).

Table 5.1: *Changes in structure and key terms of USAA issues*

Year	No.	Size($m)	Term	Month	S&P Global Rating	Peril
1997	2	477	1	June	AAA, BB	US Hurricane
1998	1	450	1	June	BB	US Hurricane
1999	1	200	1	June	BB	US Hurricane
2000	1	200	1	May	BB+	US Hurricane
2001	1	150	3	May	BB+	US Hurricane
2002	1	125	3	May	BB+	US Hurricane
2003	1	160	3	May	BB+	US Hurricane; Earthquake
2004	2	227.5	3	May	BB,B	US Hurricane; Earthquake
2005	2	176	3	May	BB,B	US Hurricane; Earthquake
2006	2	122.5	3	June	B,BB+	US Hurricane; Earthquake
2007	5	600	3	June	BB,B,B,BB+,BB+	US Hurricane; Earthquake
2008	3	350	3	May	BB,B,BB+	US Hurricane; Earthquake; Thunderstorm; Winter storm; Wildfire
2009	2	250	3	May	BB-,B-,BB-	US Hurricane; Earthquake; Thunderstorm; Winter storm; Wildfire
2010-1	4	405	3	May	BB,B+,B-,NR	US Hurricane; Earthquake; Thunderstorm; Winter storm; Wildfire
2010-2	3	300	2.5	Dec	BB,NR,NR	US Hurricane; Earthquake; Thunderstorm; Winter storm; Wildfire
2011-1	3	250	4	May	B+,B-,B	US Hurricane; Earthquake; Thunderstorm; Winter storm; Wildfire
2011-2	2	150	4	Nov	NR,NR	US Hurricane; Earthquake; Thunderstorm; Winter storm; Wildfire
2012-1	3	200	4	May	BB-,BB,NR	US Hurricane; Earthquake; Thunderstorm; Winter storm; Wildfire
2012-2	4	400	4	Nov	BB+,BB,NR,NR	US Hurricane; Earthquake; Thunderstorm; Winter storm; Wildfire
2013-1	2	300	4	May	B-,NR	US Hurricane; Earthquake; Thunderstorm; Winter storm; Wildfire
2013-2	2	150	4	Dec	NR,BB-	US Hurricane; Earthquake; Thunderstorm; Winter storm; Wildfire
2014-1	2	130	4	May	NR,NR	US Hurricane; Earthquake; Thunderstorm; Winter storm; Wildfire; Volcanic and Meteorite
2014-2	1	100	4	Dec	NR	US Hurricane; Earthquake; Thunderstorm; Winter storm; Wildfire; Volcanic and Meteorite
2015-1	2	150	4	May	NR,NR	US Hurricane; Earthquake; Thunderstorm; Winter storm; Wildfire; Volcanic and Meteorite
2015-2	1	125	4	Dec	B-,NR	US Hurricane; Earthquake; Thunderstorm; Winter storm; Wildfire; Volcanic and Meteorite
2016-0	1	50	4.5	March	NR	US Hurricane; Earthquake; Thunderstorm; Winter storm; Wildfire; Volcanic and Meteorite; ONP
2016-1	3	250	4	May	NR,NR,BB-	US Hurricane; Earthquake; Thunderstorm; Winter storm; Wildfire; Volcanic and Meteorite; ONP
2016-2	3	400	1,4,4	Nov	NR,B-,B-	US Hurricane; Earthquake; Thunderstorm; Winter storm; Wildfire; Volcanic and Meteorite; ONP
2017-1	3	425	1,4,4	May	NR,NR,BB-	US Hurricane; Earthquake; Thunderstorm; Winter storm; Wildfire; Volcanic and Meteorite; ONP
2017-2	3	295	1,4,4	Nov	NR,NR,B-	US Hurricane; Earthquake; Thunderstorm; Winter storm; Wildfire; Volcanic and Meteorite; ONP
2018-1	2	350	1,4	May	NR	US Hurricane; Earthquake; Thunderstorm; Winter storm; Wildfire; Volcanic and Meteorite; ONP
2018-2	2	200	1,4	Nov	NR	US Hurricane; Earthquake; Thunderstorm; Winter storm; Wildfire; Volcanic and Meteorite; ONP
2019-1	2	135	4	May	NR	US Hurricane; Earthquake; Thunderstorm; Winter storm; Wildfire; Volcanic and Meteorite; ONP
2019-2	2	160	1,4	Nov	NR	US Hurricane; Earthquake; Thunderstorm; Winter storm; Wildfire; Volcanic and Meteorite; ONP

Note: This table shows the development of USAA's CAT bond issues over time. Changes in the number of bond issues per year (No.), the issue sizes (in $m), the terms of the issued bonds (in years), the issue month, the rating expressed in the S&P scale at issue and the covered peril can be deduced from the respective columns of the table. The rating abbreviation NR represents bonds that were Non-Rated, while the peril abbreviation ONP represents Other Natural Perils identified as catastrophes by reporting agency PCS.

more risk.

USAA has developed a reputation for consistency that has accorded the company more leeway in product structuring, leading to more complex products over time. We want to determine whether some issuers are charged higher premiums based purely on their company characteristics or their reputation in the market. If the pricing is similar, then all companies should face a similar trajectory to that of USAA, with earlier deals including more stringent requirements than later deals. Premiums should also be similar for bonds with the same characteristics, but different issuers.

To determine whether variations in premiums exist by issuer, we run a two-level model, with issuers as our second-level variables, or *random effects*. The remaining independent variables are taken as first-level variables, or *fixed effects*, since their effect on premiums is independent of the issuer characteristics. These concepts are elaborated upon in Section 5.4.

5.3.3 Other predictors

Table 5.2 presents the remaining characteristics of the data, excluding issuer characteristics. It breaks down key characteristics of CAT bond issues over the observation period. The *Size* column gives the total issue size of all CAT bonds issued under each classification in millions of US dollars. *Obs* stands for the *total number of observations* within each classification, while *P* is the *average CAT bond premium* and *EL* the *average expected loss*. *P/EL* is a *multiple*, derived by dividing the premium by the expected loss value. This multiple gives the number of times the premium is higher than the expected loss, and is normally higher during hard markets or for complex CAT bonds, e.g., multi-peril bonds or bonds with hybrid triggers. *EER* is the *expected excess return*, given by the premium minus the expected loss. It represents how much investors demand for taking on the risk associated with bonds of a given characteristic. The *Term* variable, which is given in months, is the *average length of time* the bonds within each classification are issued for. A discussion of each of the characteristics is given below.

Table 5.2: *Summary data characteristics*

	Size ($m)	Obs. (No)	P(%)	EL (%)	P/EL	EER (%)	Term
Peril							
Peak	65,718.53	460	7.89	2.60	6.54	5.29	36.00
Multiperil	12,927.30	127	9.65	3.41	7.80	6.24	36.53
Non-Peak	12,111.42	91	4.85	1.54	5.24	3.31	42.59
Diversifying	6,114.11	46	5.13	2.45	2.69	2.69	37.67
Trigger							
Hybrid	2,145.50	33	13.96	5.21	3.33	8.75	33.33
Indemnity	47,801.66	307	6.71	2.37	8.11	4.34	38.19
Industry loss	29,545.90	200	8.98	3.08	4.07	5.89	37.43
Modelled loss	3,951.10	40	7.18	1.62	6.36	5.57	36.20
Parametric	13,427.20	144	6.46	2.10	6.45	4.36	35.06
Rating							
High yield	49,571.41	396	7.47	1.86	5.04	5.60	35.34
Investment grade	3,199.60	33	2.34	0.15	49.46	2.19	35.76
Not Rated	44,100.35	295	8.47	3.87	3.29	4.60	39.43
Issue Quarter							
Quarter 1	20,443.26	149	7.22	2.40	7.76	4.81	38.30
Quarter 2	41,865.46	304	7.38	2.42	6.43	4.96	36.78
Quarter 3	8,678.50	63	7.33	2.24	7.58	5.09	35.73
Quarter 4	25,884.14	208	8.42	3.12	4.85	5.30	36.86
Grand Total	96,871.36	724	7.64	2.60	6.35	5.04	37.02

Note: This table summarises the main characteristics of the categorical variables included in our sample. These include the bond peril, the bond trigger, the bond rating at issue, and the issue quarter. For each of these variables, the size of issue (in millions of US dollars), the number of bonds/observations (Obs.No), the expected loss (EL), the premium (P), the multiple of the premium given the expected loss (P/EL), the expected excess return (EER), and the bond term (in months) are given. These values are calculated for the full dataset of 724 CAT bonds issued in the primary market between June 1997 and March 2020.

Categorical predictors

Peak perils, i.e., US-based earthquakes and hurricanes, represent a major portion of the bonds issued in the market at 63% of the total observations. These are followed by multi-peril bonds, which are bonds covering both US perils and other non-US perils, at 18%. In total, these two classifications alone represent 81% of the market, showing that US-based issues still dominate the market for catastrophe bonds. The non-peak perils of EU wind and Japanese earthquakes represent 13% of the market, while diversifying perils, i.e., all non-US perils excluding EU wind and Japanese earthquakes, compose the remaining 6% of the market. Diversifying and non-peak perils, which together make up 19% of the market, represent a great opportunity for investors to diversify away from the US market. Due to this, their spreads are generally much lower than those of the peak and multi-peril bonds in the primary market. To confirm this relationship, we build our dummy variable *Peril* (see Hypothesis 2) as follows:

$$Peril = \begin{cases} 1, & \text{if peak or multiperil.} \\ 0, & \text{if non-peak or diversifying.} \end{cases} \tag{5.1}$$

Indemnity bonds are a significant proportion of the CAT bond market at 42%, followed by industry loss index bonds (28%) and parametric bonds (20%). Modelled loss and hybrid bonds bring up the rear at 6% and 5%, respectively. It seems that investors still buy indemnity bonds despite some of their previously discussed risks. In fact, since 2013, indemnity bonds have consistently made up over 50% of the total bonds issued (Lane and Beckwith, 2020). On average, the spreads for the hybrid bonds, at 14%, are much larger than the spreads for any of the other triggers. This, however, is due to the fact that bonds using hybrid triggers are mainly complex multi-peril bonds, represented by the high expected loss figure of 5.21%. The multiple of hybrid-triggered bonds is also much lower than that of other bonds, further reinforcing this deduction. All other triggers have average spreads ranging between 6% and 9%, and EER between 4% and 6%. This also means that, on average, there is not much difference in pricing based on trigger. To determine whether the hybrid trigger affects bond premiums (see Hypothesis 4), we use the dummy variable *Trigger* as follows:

$$Trigger = \begin{cases} 1, & \text{if hybrid.} \\ 0, & \text{otherwise.} \end{cases} \tag{5.2}$$

The indemnity trigger hypothesis (see Hypothesis 3) is tested by replacing hybrid with indemnity in the above equation.

In recent years non-rated bonds have dominated the market, while the number of rated bonds has fallen significantly. Non-rated bonds comprise 41% of our sample, and this number is expected to increase for future issues. Rated bonds make up the remaining 59%, with high-yield bonds representing 55% and investment-grade bonds the other 4%. Investment-grade bonds have the lowest spreads due to their very low expected loss values, while both the non-rated and high-yield bonds have similar spreads. Table 5.3 gives a further breakdown of the main ratings.

Table 5.3: *Catastrophe bond ratings*

Lowest Rating	Size ($m)	Obs. (No)	P(%)	EL (%)	P/EL	EER (%)	Term
AA	256.00	1	0.66	0.01	66.00	0.65	36.00
A+	26.50	1	1.01	0.01	144.29	1.00	36.00
A	647.60	1	1.77	0.01	177.00	1.76	36.00
A-	225.50	4	2.03	0.04	64.58	2.00	29.00
BBB+	509.50	5	2.45	0.08	119.51	2.37	43.20
BBB	225.00	2	2.77	0.07	82.20	2.70	36.00
BBB-	1,599.50	20	2.49	0.22	11.77	2.28	35.80
BB+	13,145.28	81	4.73	0.82	6.51	3.90	39.73
BB	12,038.68	77	5.96	1.06	6.26	4.89	33.45
BB-	9,244.05	103	6.67	1.43	4.98	5.25	36.01
B+	5,226.00	35	9.01	2.22	4.18	6.79	35.14
B	6,906.00	60	10.57	3.44	3.28	7.14	30.97
B-	2,721.40	39	12.23	4.07	3.04	8.16	34.72
NR	44,100.35	295	8.47	3.87	3.29	4.60	39.43
Grand Total	96,871.36	724	7.64	2.60	6.35	5.04	37.02

Note: This table summarises the CAT bond ratings (at issue) for the bonds included in the sample. The ratings are standardised to the Standard & Poors (S&P) scale, and can be split into three main groups. These are the investment-grade bonds (those with a BBB- rating and above); high-yield bonds (those with a B- rating and above, up to BB+); and the non-rated (NR) bonds. For each of the ratings displayed, the size of issue (in millions of US dollars), the number of bonds/observations (Obs.No), the expected loss (EL), the premium (P), the multiple of the premium given the expected loss (P/EL), the expected excess return (EER), and the bond term (in months) are given. These values are calculated for the full dataset of 724 CAT bonds issued in the primary market between June 1997 and March 2020.

For the rating variable we test the effect of having either an investment-grade rating or having no rating on the premium as given by Hypotheses 5 and 6, respectively.

Q2 is the most dominant issue period, with 42% of all the bonds issued in this quarter, followed by Q4 at 29% and the first quarter(Q1) at 20%. The third quarter(Q3), which represents the hurricane season, has the least number of issues at approximately 9%. Average spreads, however, seem to be within a similar range. This introduces the possibility that the issues might not be affected by the issue date. The suggestion from the literature is that Q2 has higher spreads because it falls before the hurricane season (Braun, 2016). This will be tested in the regression models using the dummy variable *Quarter*, as defined in Eq. (5.3) (see Hypothesis 7).

$$Quarter = \begin{cases} 1, & \text{if issued in the second quarter.} \\ 0, & \text{otherwise.} \end{cases} \tag{5.3}$$

Continuous predictors

The Guy Carpenter Global Property Catastrophe Rate on Line Index (GC RoL Index) is used as a representative of the reinsurance cycle (see Hypothesis 9). This is an index of global property catastrophe reinsurance rate-on-line movements covering all major global catastrophe reinsurance markets. Since most CAT bonds cover property-related risks, this index is assumed to be a good representative of the state of the property reinsurance market. The state of the competing financial environment (see Hypothesis 10) is proxied by the ICE Bank of America Merrill Lynch BB US High Yield Option-Adjusted Spread Index (BB Spread Index). This index tracks the performance of US-dollar-denominated BB-rated corporate debt, publicly issued in the US domestic market. A majority of the rated CAT bonds carry a BB rating. Therefore, this index contains securities that compete with the CAT bond market for investments.

Figure 5.2 summarises the GC RoL Index and the Corporate BB Spread Index, respectively. From the GC Rol Index graph, we can pick out the key hard market periods due to their increased spreads. Spikes in the index are observed after the

9/11 attacks in 2001, after Hurricane Katrina in 2005, during the financial crisis, and after the 2017 Atlantic hurricane season that saw Hurricanes Irma, Harvey and Maria, among others, cause widespread losses.[15] This shows that premiums increase following major catastrophes or in periods of extreme economic turmoil. The BB Spread chart further reinforces this point, with notable spikes in the index after 9/11 and during the financial crisis. One of the most notable differences between the two graphs is the effect of natural catastrophes, which did not seem to affect corporate spreads as much as it did the reinsurance cycle. The financial crisis also seems to have affected the corporate spreads more than the property catastrophe reinsurance market.

Table 5.4 gives a summary of the characteristics of the remaining continuous variables.

[15]According to Swiss Re (2018), global insured losses from catastrophes in 2017 were estimated at US$136bn.

Figure 5.2: *The Reinsurance cycle and State of the Financial Market*

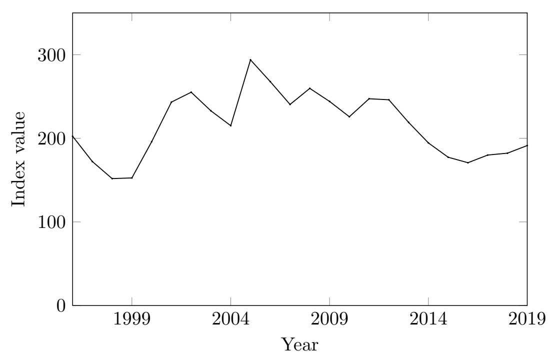

(a) *the reinsurance cycle*

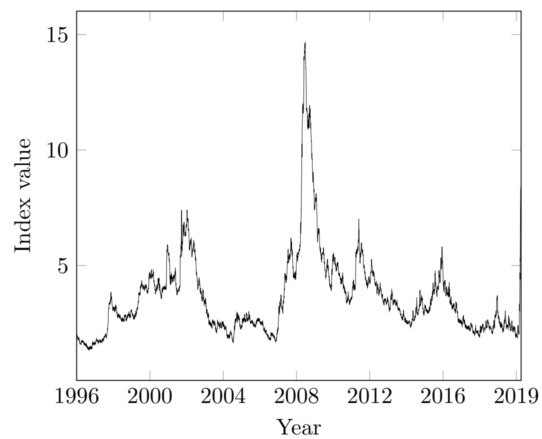

(b) *state of financial market*

Note: The line graphs above display developments in the reinsurance cycle and the competing financial environment over the period of analysis. The reinsurance cycle is represented by the Guy Carpenter Global Property Catastrophe Rate on Line Index (GC Rate-on-Line Index), and is given annually for the period beginning January 1997 (for 1996) and ending January 2020 (for 2019). The competing financial environment is represented by the ICE Bank of America Merrill Lynch BB US High-Yield Option Adjusted Spread Index (BB Spread Index), and is given daily for the period beginning 31st December 1996 and ending 31st March 2020.

Table 5.4: *Summary descriptive statistics*

Variable	Mean	Median	Std.Dev.	Minimum	Maximum
Size ($m)	133.800	100.000	117.371	1.800	1500.000
EER (%)	5.000	4.100	3.500	0.650	41.100
EL (%)	2.600	1.600	2.600	0.007	17.400
Premium(%)	7.600	6.100	5.100	0.660	49.900
Term (months)	37.025	36.000	12.067	5.000	69.000

Note: This table summarises descriptive statistics of the continuous variables in our sample, excluding the reinsurance cycle and the competing financial environment, which are separately displayed. These variables include the bond issue size (in millions of US dollars), the expected loss (EL), the bond premium (P), the expected excess return (EER) (calculated as the difference between the premium and the expected loss), and the bond term (in months). The mean, median, standard deviation, and minimum and maximum values are displayed for each variable, for the full dataset of 724 CAT bonds issued in the primary market between June 1997 and March 2020.

The average spread in the CAT bond market is 7.6% while the median spread is 6.1%, showing that there might be outliers in the dataset that are weighted more heavily in determining the mean spreads. This is against an average expected loss of 2.6%, representing the low probability of most catastrophic events. In fact, the minimum expected loss of 0.007% is so low it is close to zero. This would be the expected loss allocated to a very remote event, or a covered loss layer that is highly unlikely to be hit. The CAT bonds have an average term of three years and an average size of US$133 million.

The linear relationship between the above variables is displayed in the correlation matrix of Table 5.5.

Table 5.5: *Correlation matrix of continuous variables*

Variable	Premium	EL	GCIndex	BBSpread	Term	Size
Premium	1.0000					
EL	0.7792***	1.0000				
GCIndex	0.2585***	-0.0822**	1.0000			
BBSpread	0.1387***	0.0770**	0.2477***	1.0000		
Term	-0.2563***	-0.1361***	-0.2123***	0.0494	1.0000	
Size	-0.2454***	-0.1968***	-0.2329***	-0.1299***	0.1746***	1.0000

Note: This table displays the pairwise correlations of the continuous variables included in our sample. These include the CAT bond premium, the expected loss (EL), the reinsurance cycle (represented by the Guy Carpenter Index, GCIndex), the competing financial environment (represented by the BB Corporate Bond Index, BBSpread), the bond term (in months) and the bond size (in millions of US dollars). The significance of each of these values is also indicated. Significance at 90%, 95%, and 99% confidence levels are indicated by *, **, and ***, respectively.

The bond premium is significantly correlated with all the other continuous variables. It is positively correlated with the expected loss, the reinsurance cycle and the competing financial market, and negatively correlated with the bond term and issue size. The largest positive linear relationship is between the expected loss and the premium, providing support for the deduction from the literature that the expected loss is the main factor applied in the determination of CAT bond premiums. Term and size have a negative correlation with the premiums, implying that premiums actually decrease as we increase both the term and size of a CAT bond issue. The term and size variables also have a significant negative correlation with the expected loss, the reinsurance cycle and the competing financial market. When the term and size variables are compared to each other, however, the relationship is significantly positive, with an increase in size corresponding to an increase in term and vice versa. Each of these factors will be analysed in more detail in a multilevel model to determine causality.

5.4 Empirical Analysis

5.4.1 Model specification

Our issuance data[16] has shown that most CAT bonds are sold by the same issuers year-on-year, and multiple bonds can be sold by a given issuer within a given year. The bonds are therefore nested within groups, which in this case represent the issuers. Table 5.1 also shows that there are major similarities in characteristics for bonds issued by the same issuer over time. The question of the issuer effect, arising from this hierarchical structure and the similarities in bond characteristics, on pricing, is the focus of this research. For this purpose, we will be applying multilevel modelling techniques,[17] in particular, a two-level random intercept model, since we will be assuming that only the intercept varies for the issuers, while the slope remains the same for all issuers. This implies that the minimum premium charged for each company changes based on the issuer, but the manner in which the other predictors, e.g., peril, trigger, cycle, affect the premiums does not change based on the issuer. The assumption here is that investors determine premiums based on the characteristics of the CAT bond itself first, before reviewing these expectations based on the issuer characteristics.

Furthermore, before running the regression models, we first determine the independent variables to be included. We analyse all the factors included in the hypotheses in initial multi-level regressions. To test the model's fit and determine its suitabil-

[16]See Appendix .1 for more details on the summary of all analysed issuer characteristics.

[17]Multilevel modelling techniques have mainly been used in educational and psychological research in the past, to model hierarchical structures (see, e.g., Nezlek (2012), Bryk and Raudenbush (1987), Kreft and Leeuw (1998), and Raudenbush and Bryk (2010)). However, their application is not only limited to the aforementioned fields, as researchers studying CAT bond pricing, e.g. Major (2019), have proposed that the CAT bond hierarchical structure be taken into account through multi-level models. Appendix .2 presents the structure of a multilevel model.

ity for the data, goodness-of-fit tests based on the log-likelihood ratio (LLR) and the Akaike Information Criterion (AIC) (Akaike, 1974) are conducted.[18] We will therefore be comparing the more complex model, the one with the random effects, against the simpler model without random effects. A lower AIC value will support the two-level model's superiority over the single-level model.

The final factors are chosen based on their significance, with the requirement being at least a 90% confidence level. The final model includes the following eight factors: *expected loss, peril, reinsurance cycle*, *competing financial environment*, *term*, *investment-grade rating*, *hybrid trigger* and *issuer*. The indemnity trigger, the impact of a lack of credit rating, and the issue quarter representing Hypotheses 3, 6 and 7 respectively, are all insignificant and therefore excluded from the model. Table 5.6 summarises a comparison between the final specified model and alternative models that include those excluded (insignificant) factors. Further, since the likelihood ratio test statistic (LRT) is also significant for all the models, it further supports the deduction that a multi-level model offers the best fit for our data. The conditional and marginal R-squared values, which are calculated based on Nakagawa and Schielzeth (2012), represent the amount of variation explained by the total of the fixed and random effects, and the variation explained by the fixed effects only, respectively. The intra-class correlation coefficient (ICC) gives the variation explained by the random effects only. Of the three excluded factors, the "indemnity trigger" model displays the closest similarity to our final model, but is subsequently not chosen because the hybrid trigger is significant

[18]Likelihood ratio tests provide a way to compare the model with the random effect term (the two-level model) against one without the random effect term based on their likelihoods and determine whether the two are significantly different. The AIC, on the other hand, gives a measure of the information lost as the model's complexity increases by considering the estimated residual variance and the complexity of the model as additive terms (Chen and Li, 2017). The AIC equation is represented below (Akaike, 1974):

$$AIC = -2 * ln(L) + 2k$$

where L represents the maximum likelihood and k represents the number of estimated model parameters.

when compared to the indemnity trigger. The proposed novel two-level model displays superior performance in goodness-of-fit tests, i.e., a lower AIC and significant LRT.

Table 5.6: *Model factor specification*

	Final model	Hypothesis 3 (Indemnity)	Hypothesis 6 (Not Rated)	Hypothesis 7 (Issue Quarter 2)
Marginal R^2	0.8172	0.8135	0.8040	0.817
Conditional R^2	0.8369	0.8377	0.8182	0.8368
ICC	0.1078	0.1297	0.0725	0.1082
AIC	2837.5	2840.9	2899.1	2841.5
LRT	12.71***	14.58***	7.90***	12.75***

Note: This table summarises the explanatory and fit properties of the final model in comparison to models that include the excluded (insignificant) factors from the hypotheses. The respective models' equations are given below:

Final model

$$P = \beta_0 + \beta_1 EL + \beta_2 PeakMultiperil + \beta_3 GCIndex + \beta_4 BBSpread + \beta_5 Term + \beta_6 IG \\ + \beta_7 Hybrid + u_{ij} + \varepsilon_{ij} \tag{5.4}$$

Hypothesis 3 (Indemnity trigger)

$$P = \beta_0 + \beta_1 EL + \beta_2 PeakMultiperil + \beta_3 GCIndex + \beta_4 BBSpread + \beta_5 Term + \beta_6 IG \\ + \beta_7 Indemnity + u_{ij} + \varepsilon_{ij} \tag{5.5}$$

Hypothesis 6 (Lack of a Credit Rating)

$$P = \beta_0 + \beta_1 EL + \beta_2 PeakMultiperil + \beta_3 GCIndex + \beta_4 BBSpread + \beta_5 Term + \beta_6 Non - Rated \\ + \beta_7 Hybrid + u_{ij} + \varepsilon_{ij} \tag{5.6}$$

Hypothesis 7 (Issue Quarter 2)

$$P = \beta_0 + \beta_1 EL + \beta_2 PeakMultiperil + \beta_3 GCIndex + \beta_4 BBSpread + \beta_5 Term + \beta_6 IG \\ + \beta_7 Hybrid + \beta_8 Quarter + u_{ij} + \varepsilon_{ij} \tag{5.7}$$

In the equations above, *EL* represents the expected loss, *PeakMultiperil* represents all peak and multiperil bonds, *Term* represents the bond term in months, *IG* represents an investment-grade rating, while *Non-Rated* represents bonds without a credit rating, *Hybrid* represents the hybrid trigger, *Indemnity* denotes the indemnity trigger, *Quarter* is the second quarter of the year, *BBSpread* is the high yield corporate bond index and *GCIndex* represents the reinsurance cycle index. The conditional and marginal R-squared values are calculated based on Nakagawa and Schielzeth (2012), with the conditional R-squared representing the amount of variation explained by the total of the fixed and random effects, and the marginal R-squared representing the variation explained only by the fixed effects. The intra-class correlation coefficient (ICC) gives the variation explained only by the random effects. In addition, the Akaike information criterion (AIC) and the likelihood ratio test (LRT) statistic are given. The significance of each of these values is also indicated. Significance at 90%, 95%, and 99% confidence levels are indicated by *, **, and ***, respectively. These values are calculated for the full dataset of 704 CAT bonds (after exclusion of outliers) issued in the primary market between June 1997 and March 2020.

The proposed two-level model is given by Eq. (5.8), where *EL* represents the expected loss, *PeakMultiperil* represents all peak and multiperil bonds, *Term* represents the bond term in months, *IG* represents an investment-grade rating, *Hybrid* represents the trigger, *BBSpread* is the high yield corporate bond index and *GCIndex* represents the reinsurance cycle index. The random intercept accounts for the issuer effect. u_j is the variation due to the issuer (level 2) while ε_{ij} is the level 1 unexplained variation.

$$P = \beta_0 + \beta_1 EL + \beta_2 PeakMultiperil + \beta_3 GCIndex + \beta_4 BBSpread + \beta_5 Term + \beta_6 IG + \beta_7 Hybrid + u_{ij} + \varepsilon_{ij} \tag{5.8}$$

Note that Eq.(5.8) also includes an intercept term. Some researchers propose the inclusion of the intercept term to account for very low expected-loss bonds (Lane, 2018), while others propose exclusion, since a bond with an expected loss of zero would probably not be issued (see, e.g., Braun, 2016). We include the intercept term to avoid creating artificial steepness or flatness of the slope arising as a result of forcing the intercept to begin at zero. For this intercept to make logical sense though, we centre the data based on the minimum values of the respective independent variables in the dataset. The intercept therefore represents the bond with the lowest value of each of the continuous variables and that has the characteristics included in a dummy variable of zero.[19]

The final sample excludes outliers, identified by using studentised deleted residual plots and Cook (1977)'s distance. To generate studentised deleted residuals, the observations are deleted one at a time, and the regression model fitted to the remaining $n-1$ observations. The observed response values are then compared to the values from the refitted model to generate the deleted residuals. Thereafter, these deleted residuals are standardised to generate studentised residuals (Aguinis et al., 2013). Cook

[19] This would be a 6 month USD 1.8m non-US, non-indemnity, non-Swiss Re, high yield catastrophe bond with expected loss of 0.007% issued when both the GC Index and the BB Spread Index were at their lowest over the estimation period (i.e., at 151.8 and 1.4783 respectively) and issued before the month of April or after the month of June in a given year.

(1977)'s distance follows a similar process, and considers both residuals and leverage, i.e., both the independent and dependent variables. We only exclude those bonds that were identified as outliers by both the studentized residual plots and Cook (1977)'s distance. 20 bonds are therefore excluded from the original sample of 724, leaving 704 bonds in the dataset.[20]

5.4.2 Assumptions

The goodness-of-fit test results (see Table 5.7) show that the model with random effects (i.e., our two-level model) is a better fit for the data than a model without the random effects. In addition, the LRT is significant at the 99.9% confidence level, favouring the 10-parameter (i.e., two-level) over the 9-parameter (i.e., the single-level) model.

[20]Most of the excluded issues covered bonds with unique underlying structures or covering unique property. The Swiss Re Successor Series, for example, from which six of the excluded bonds originated, were priced at extremely high premiums, different from any other bond ever issued. This was a shelf programme that allowed flexibility of model structure and had unique pay-out characteristics (MMC Securities, 2007; Lane and Beckwith, 2007).

Table 5.7: *ANOVA-like Table for Random Effects : Single term deletions*

Deleted Variable	Parameters (No.)	logLik	AIC	LRT	Dof	Pr(>Chisq)
None	10	-1408.7	2837.5			
Random effect (issuer)	9	-1415.1	2848.2	12.71	1	0.0004***

Note: This table displays the goodness-of-fit test results for our two-level model when compared to a single-level model for our data. The random effect term (the issuer effect) is removed in the second model, and the two models then compared to determine which of the two provides the best fit for the distribution of the data. The model with a superior fit will have a lower Akaike information criterion (AIC) and a significant likelihood ratio test (LRT) statistic. The table also displays the number of parameters in each model (Parameters (No.)), the log-likelihood ratio (logLik) for each of the models, the degrees of freedom for the likelihood ratio test, i.e. the difference in the number of parameters between the two models, and the p-value based on the Chi-square distribution (Pr(>Chisq))(Kuznetsova et al., 2017). The significance of the LRT is also indicated. The significance of each of these values is also indicated. Significance at 90%, 95%, and 99% confidence levels are indicated by *, **, and ***, respectively.

A multilevel model applies maximum likelihood to estimate its parameters. This technique assumes a large sample size and that the standard errors are normally distributed (Wang et al., 2011). For the sample to be considered large, both the number of groups and number of observations should be large. Our sample size of 704 CAT bonds and 101 issuers is assumed large enough to meet the first assumption, based on sample size recommendations by Maas and Hox (2005). To test for normality in standard errors, we generate a QQ plot of residuals (see Figure 5.3).

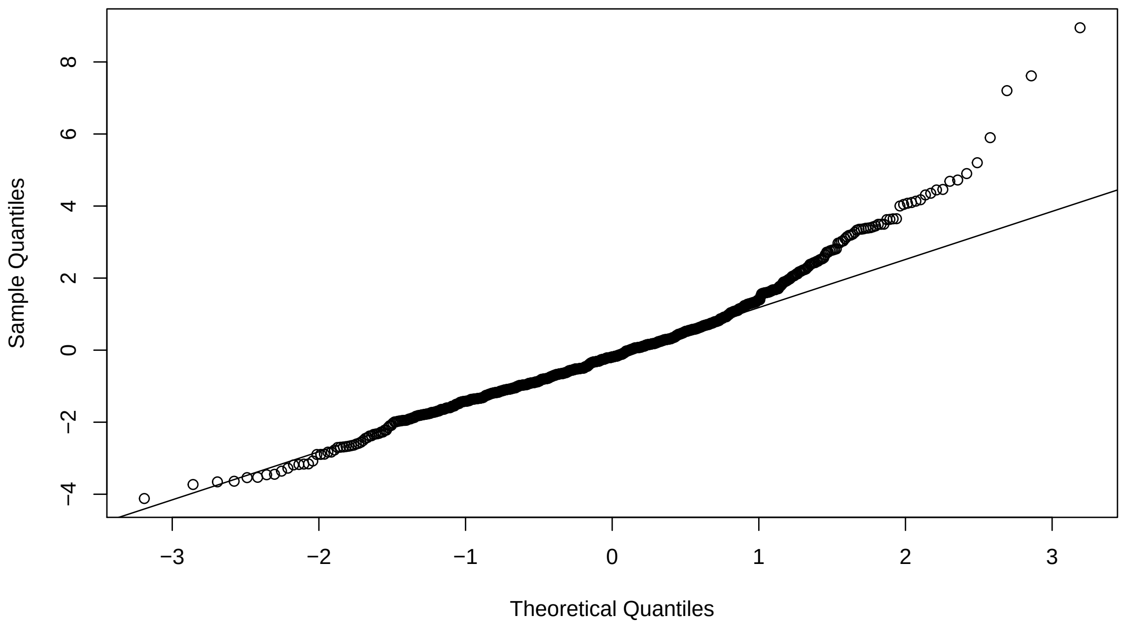

Note: The figure above displays the distribution of residuals (sample quantiles) against theoretical normal residuals for our sample. For the normality of residuals assumption to hold, the plotted residuals should lie close to the diagonal line.

For the normality assumption to hold, the majority of the data points should lie close to the straight line in the QQ plot. Even though most of our data points do lie on the straight line, they are still skewed to the right. If maximum likelihood were applied, the fixed effects (level 1 estimates) would not necessarily be biased, but standard errors and other variance components would be biased downward (Leeden et al., 2007; Busing, 1993). For this reason, we apply the restricted maximum likelihood (REML) estimation technique instead of maximum likelihood (ML) estimation, since the REML has been shown to yield more accurate results in such cases (Forman, 2019).

Other assumptions include linearity (Galeotti et al., 2013), and homogeneity of the variance for individual observations, which is assumed to hold based on the figure below, and confirmed by an Analysis of Variance (ANOVA) test.[21]

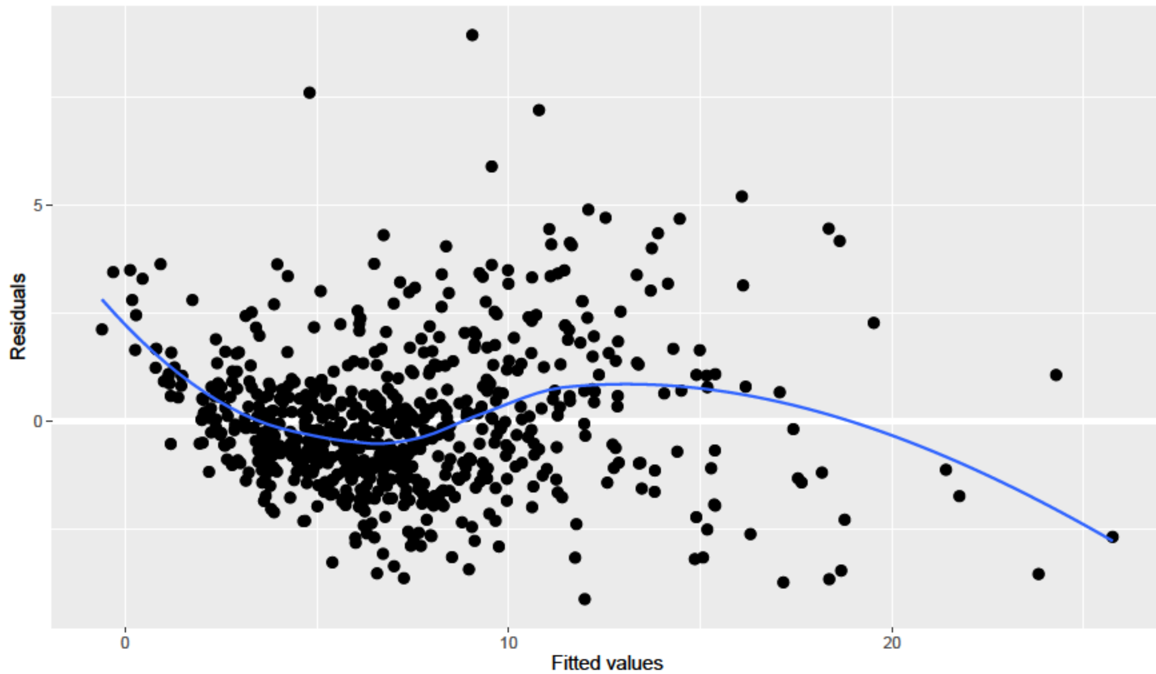

Note: The figure above displays the distribution of level 1 residual variance. For the homoscedasticity assumption to hold, the plotted residuals should be distributed equally above and below the blue line. The assumption is also confirmed through a separate ANOVA test in Appendix .4.

The collinearity diagnostics for the fixed effects also give low variance inflation factors (VIF)(VIF < 1.1) for all fixed effects, thus allowing us to assume that the "no-collinearity" assumption is met. The next three sections detail the results of the multilevel tests, for both fixed effects and random effects.

[21]The results of this test are given in Appendix .4.

5.4.3 EM Algorithm for Variance Components Analysis

The following algorithmic steps are taken in order to arrive at the within issuer variation estimates, via the Expectation-Maximization algorithm. The underlying mathematical derivations can be found in the Appendices section (see Appendix .3)

1. Initialization: Assign some initial values for $\gamma_{00}, \gamma_{k0}, {\sigma^2}_e$, and ${\sigma^2}_{u0}$.

2. The Expectation Step: Evaluate the expected log-likelihood for complete data given observed data in the final iteration, i.e.,

$$Q(\delta, \delta^{(k-1)}) = E[l(\delta; y, u)|y; \delta^{(k-1)}] \tag{5.9}$$

3. The Maximization Step: Update δ through

$$\hat{\delta} = \underset{\delta}{\operatorname{argmax}} \quad Q(\delta, \delta^{(k-1)}) \tag{5.10}$$

4. Repeat the Expectation and Maximization steps above until convergence is achieved.

5.4.4 Fixed effects

All of the fixed effects are significant based on Table 5.8. In addition to the expected loss, the peril hypothesis (see Hypothesis 2) is supported. The results summarised in Table 5.8 show that, on average, premiums on peak and multi-peril bonds are about 2.25% higher than those on non-peak or diversifying bonds. This could be a result of the frequency of occurrence of the peak perils in the specified regions, which generates more volatility in expected loss estimates over time.

Of the two trigger hypotheses analysed, the hybrid trigger is included in the final model while the indemnity trigger is excluded. This is because we cannot confirm the indemnity hypothesis based on the evidence, while the hybrid trigger is significant at the 95% confidence level. In support of Hypothesis 5, hybrid triggered bonds seem to demand 0.71% more in premiums at the 95% confidence level. The findings on the indemnity trigger are in line with findings from previous studies (see, e.g., Braun, 2016; Gürtler et al., 2016), while those on the hybrid trigger are not. In fact, none of the existing studies identifies the hybrid trigger as a factor to be considered. This might be due to the smaller sample sizes that limit analysis of the hybrid trigger.

The bond rating hypotheses lead to different conclusions. Only the investment grade rating seems to have a major impact on premiums, while the effect of a lack of rating cannot be confirmed as this factor is not significant. Highly rated bonds receive lower premiums when compared to either lower or non-rated bonds. With a difference of about 2.67% on average, these results confirm Hypothesis 5. In addition to the rating, both the reinsurance cycle (see Hypothesis 9) and the state of the competing financial market (see Hypothesis 10) have an effect on premiums. As the values of both these indexes increase, the CAT bond premiums also increase. Hypothesis 7, regarding the issue quarter, is not supported by the evidence and is therefore also excluded from the final model. These results are in line with the findings of previous studies (e.g., Lane, 2018; Gürtler et al., 2016).

The maturity factor (see Hypothesis 6) leads to some unexpected results; the bond term is significant, but this term is inversely related to the premiums. We hypothesised that the longer-term bonds might lead to higher premiums, but we get the opposite result instead. Increasing the bond term by one more month leads to a 0.02% decrease in premiums on average. This might be because the longer term allows investors to earn interest for a longer period than the shorter term. It is also worth noting that the term variable is not significant in previous studies, an effect we attribute to smaller sample sizes that failed to pick up developments in the CAT bond market.

To analyse effect size, we use a variation of the Cohen (1992)'s f^2 included in Selya et al. (2012) that measures the local effect size, i.e., the magnitude of the effect of each independent variable on the variation in the dependent variable. According to Cohen (1992), the effect size is considered large at 0.35, medium at 0.15 and small at 0.02. From the results in Table 5.8, it is evident that the expected loss, peril and the reinsurance cycle have the greatest effect on the variation in the premiums. The state of the competing financial environment has a small-to-medium effect, and the term and bond rating have a small effect. Finally, the bond trigger has a very small effect. The effect of the expected loss is exceedingly large, in line with theoretical deductions that the expected loss is the main factor driving CAT bond premiums (see, e.g., Lane, 2018). The reinsurance cycle and peril are the second- and third-largest factors, respectively. These factors are all identified in initial studies by Lane and Beckwith (2008) as key factors that determine premiums.

5.4.5 Random effects

In Table 5.9, the random effect term represented by σ_u, the variability introduced by the issuers, is significant at the 95% confidence level. This implies that an issuer effect exists, confirming Hypothesis 1a, i.e., that there are similarities in premiums on bonds issued by the same issuer, and differences in premiums on bonds issued by different issuers with similar characteristics. To determine the size of this effect, we use the ICC. This can be interpreted as the amount of variation arising due to the random effects as a proportion of the total variation in the model (Lorah, 2018). The ICC displayed in Table 5.9 indicates that around 11% of the variation in the regression model can be explained by issuer differences.

We also assess whether the two-level model is a better fit for the data than a single-level model through the LRT. A significant LRT would indicate that the model with random effects (the issuer effect, in this case) was a better model for this type of data than a model without random effects. Our LRT is significant, proving that the multilevel model is a better model for this data type than a single-level model. A comparison of the largest and smallest issuers by total issue size gives the results reported in Table 5.9.

Table 5.8: *Fixed effect estimates*

	Estimate	Standard error	Effect size
Fixed effects			
Intercept	-0.5907*	0.3440	
Expected Loss	1.3986***	0.0314	3.0141
PeakandMultiperil	2.2520***	0.1932	0.1984
GCIndex	0.0377***	0.0023	0.3845
BBSpread	0.4613***	0.0471	0.1283
Term	-0.0239***	0.0064	0.0166
IG	-2.6742***	0.3312	0.0994
Hybrid	0.7057**	0.3415	0.0035
Issuers	101		
Observations	704		

Note: This table provides estimates of the relationship between CAT bond premiums and factors believed to affect those premiums, excluding the effect of the bond issuer. The factors include the expected loss, the underlying peril, the reinsurance cycle (represented by the Guy Carpenter Index), the competing financial market environment (represented by the BB Spread Index), the bond term, the bond rating (Investment-Grade), and the bond trigger (Hybrid). The data covers all CAT bonds issued in the primary market between June 1997 and March 2020, and consists of 704 CAT bonds issued by 101 issuers after excluding outliers. Estimates are annualised percentage changes in premiums given a unit change in the covariates, and the effect size measure is derived through the Cohen's f^2 measure. The significance of each of these values is also indicated. Significance at 90%, 95%, and 99% confidence levels are indicated by *, **, and ***, respectively.

Table 5.9: *Hypothesis 1a: Random (issuer) effect estimates*

	Estimate	Standard error
Random effects		
σ_u	0.5922**	0.1593
σ_e	1.7042***	0.1663
LRT	12.7100***	
ICC	0.1087	
Issuers	101	
Observations	704	

Note: This table summarises the effect of issuer variability on CAT bond premiums for all 101 issuers. The σ_u estimate gives the volatility introduced due to differences in pricing between issuers, while the σ_e term represents the level of unexplained volatility. To determine whether the multi-level model provides a better fit for the data than a single-level model, we use the likelihood ratio test (LRT). A significant LRT would indicate that the multi-level model was indeed better than the single-level model. The intra-class correlation (ICC) indicates the proportion of the total variability in the premiums that arises due to issuer pricing differences (around 11% in this case). The significance of each of these values is also indicated. Significance at 90%, 95%, and 99% confidence levels are indicated by *, **, and ***, respectively.

5.4.6 Extended random effect analysis

After establishing the significance of the issuer effect for the full sample, we now focus on specific issuer characteristics. To establish issuer-specific characteristics with the greatest impact on the issuer effect, we analyse three main characteristics. These include the number of years for which the issuer has issued bonds in the primary CAT bond market, the issuer's total issue size since the inception of the CAT bond market, and the issuer's line of business.

In each of the tables below, the full dataset consisting of 704 CAT bonds issued by 101 issuers is split into sub-samples that represent a classification of each issuer characteristic being tested. The explanatory variables, in addition to the issuer, include the expected loss, the underlying peril, the reinsurance cycle (represented by the Guy Carpenter Index), the competing financial market environment (represented by the BB Spread Index), the bond term, the bond rating (Investment-Grade), and the bond trigger (Hybrid). The results of each analysis are summarised below.

By issue size

To generate the results in Table 5.10, issuers are classified based on the total size of their bond issues in the CAT bond market since inception. The issuer sample is then split into three equal sub-samples based on the number of issuers, resulting in three sub-samples, each with approximately one-third of the total issuer population. The results displayed in Table 5.10 show that the effect of issuer differences on premiums is larger for those issuers with a smaller issue size than for those with a larger issue size, confirming Hypothesis 1b. The ICC is therefore considerably higher for smaller issuers than for larger ones, signifying the larger amount of variability that results from this sub-group's smaller issues.

Most of the fixed effects, excluding the term and the trigger (Hybrid), remain significant, with the confidence levels increasing for larger and medium issuers. This might signify the decreasing effect of the issuer differences and the increasing effect of other variables in explaining premiums as the issue size increases. The term variable is insignificant for medium issuers, while the trigger is insignificant for both large and small issuers, implying that these factors' influence on premiums is yet to stabilise enough to enable any long-term inferences to be made about them.

Table 5.10: *Hypothesis 1b: Random effects by total issue size*

	Larger issuers		Medium issuers		Smaller issuers	
	Estimate	Standard error	Estimate	Standard error	Estimate	Standard error
Fixed effects						
Intercept	-1.3757***	0.4447	-1.8549**	0.8143	2.2975**	0.9146
Expected loss	1.4175***	0.0352	1.3171***	0.0861	1.2636***	0.0617
PeakandMultiperil	2.5655***	0.2277	1.8337***	0.4001	1.2350*	0.6079
GCIndex	0.0428***	0.0029	0.0310***	0.0049	0.0135**	0.0048
BBSpread	0.4211***	0.0508	1.1445***	0.1847	0.3892*	0.1868
Term	-0.0151**	0.0075	0.0043	0.0180	-0.0378*	0.0179
IG	-2.8340***	0.3952	-1.9867***	0.7303	-2.8524***	0.4926
Hybrid	0.6058	0.4010	1.7397***	0.6234	-0.3627	1.5218
Random effects						
σ_u	0.6200**	0.1914	$0.0000^{\dagger}$	0.4115	1.3408***	0.5374
σ_e	1.7440***	0.1896	1.4799***	0.5058	0.5803***	0.1140
ICC	0.1122		0.0000		0.8423	
Issuers	34		33		34	
Observations	558		92		54	

† In this instance, the variation associated with the issuer effect is so small compared to the background noise that this volatility is assumed to be zero.

Note: This table displays estimates of the factors affecting CAT bond premiums for different total issue sizes. The bond issue size is aggregated for all the bonds sold by the respective issuer to determine the issuer's sub-group. The data are then split equally over the three main sub-samples to ensure each sub-sample contains an equal number of issuers. Larger issuers represent the top one-third of all issuers, while the smaller issuers represent the bottom one-third of all issuers based on total issue size. All other issuers are included in the medium sub-sample. Finally, estimates and standard errors are calculated for both fixed and random effects. The significance of each of these values is also indicated. Significance at 90%, 95%, and 99% confidence levels are indicated by *, **, and ***, respectively.

By number of years in the primary market

The number of years for which the issuer has been issuing bonds in the primary CAT bond market is used here as a proxy for the issuer's reputation in the market. We assume that the longer the issuer stays in the market, the better their terms of issue (see Hypothesis 1c). This follows from deductions from Spry (2009) that major issuers could be rewarded with better pricing terms, since multiple issues over a longer period display their consistency to the bond market investors. Table 5.11 supports Hypothesis 1c, showing that the issuer's impact on premiums is greatest for those bonds issued by companies that have been issuing CAT bonds for one year or less, while this impact is smallest for those companies that have been issuing bonds over a longer time period. This might be because first-time issuers do not have the required time to establish a trusted investor base for themselves when compared to those companies that have been in the market for a longer period. As the company issues more and more bonds therefore, its terms of issue should also improve, and the effects of issuer characteristics on pricing should diminish. This is evidenced by the decreasing ICC value in Table 5.11 as the number of years in the market increases. Though the random effects are significant in each instance, they are significant at a a higher confidence level (99%) for one-time issuers than for those issuers that have been in the market for longer (90%).

In addition, fixed effects are stronger for those companies that have established a reputation than for those that have not, further supporting the deduction that issuer characteristics tend to have less of an impact over time, as other factors take precedence. The effect of the hybrid trigger is insignificant in all sub-samples, indicating that this might not be a very stable covariate, while the effect of the bond term and the competing financial environment is only insignificant for the shorter-period issuers. This might be because the effect of these factors is better established over a broader time period than that allowed for by these issues.

Table 5.11: *Hypothesis 1c: Random effects by years in primary CAT market (reputation)*

	One year		Two to three Years		Four years or more	
	Estimate	Standard error	Estimate	Standard error	Estimate	Standard error
Fixed effects						
Intercept	1.0147	0.7524	0.0741	0.7033	-1.4230***	0.4893
Expected Loss	1.2545***	0.0671	1.3221***	0.0705	1.4303***	0.0377
PeakandMultiperil	1.4077***	0.4615	2.1600***	0.4992	2.4751***	0.2448
GCIndex	0.0200***	0.0048	0.0450***	0.0074	0.0431***	0.0030
BBSpread	0.2167	0.1898	0.2616*	0.1549	0.4542***	0.0534
Term	-0.0093	0.0155	-0.0309**	0.0141	-0.0155*	0.0081
IG	-2.1645***	0.4203	-4.6744***	1.0843	-2.7844***	0.4069
Hybrid	-0.4610	1.3704	0.3734	0.6783	0.5959	0.4121
Random effects						
σ_u	1.0964***	0.3836	1.0150*	0.5393	0.6139*	0.0140
σ_e	0.7387***	0.1527	1.3154***	0.2801	1.7906***	0.2086
ICC	0.6878		0.3732		0.1052	
Issuers	44		30		27	
Observations	72		121		511	

Note: This table provides estimates of the relationship between CAT bond premiums and factors believed to affect these premiums based on the issuer's longevity in the CAT bond market. The number of years for which the respective issuer has been issuing bonds in the primary CAT bond market is aggregated and each issuer allocated according to this length of time. Issuers who have only issued bonds in one year fall within the first class, those who have been issuing for two or three years fall into the second class, and those who have been issuing bonds for four years or more fall into the third class. The time splits are chosen to ensure that each sample includes an adequate number of issuer observations (level two variables) to aid analysis. Estimates and standard errors are then calculated for both fixed and random effects in each sub-group. The significance of each of these values is also indicated. Significance at 90%, 95%, and 99% confidence levels are indicated by *, **, and ***, respectively.

By issuer's line of business

To estimate the effect of the issuer's line of business on issuer premium volatility, the data are split into three sets of observations based on each specific issuer's main line of business. Table 5.12 provides the estimates and standard errors of the multilevel regressions on the three sub-samples. From this table, we can see that the random effects are significant only for those issuers operating mainly as insurers, and insignificant for both reinsurers and multi-line businesses, in line with Hypothesis 1d. This might be a consequence of the sizes of the companies that fall into each of these classifications, with reinsurers and multi-line companies being significantly larger in size than most insurers, especially since they need to be able to take on insurer losses. This ability can afford such companies a better reputation than smaller insurance companies. In addition, and similar to the observation regarding Table 5.10, fixed effects continue to be significant, with confidence levels increasing as the issuer effect decreases. The hybrid trigger is also insignificant in each sub-sample, while the bond term is insignificant for insurers.

Table 5.12: *Hypothesis 1d: Random effects by issuer's line of business*

	Insurers		Reinsurers		Multiline/Others	
	Estimate	Standard error	Estimate	Standard error	Estimate	Standard error
Fixed effects						
Intercept	0.2833	0.7799	-0.4213	0.7526	1.3377**	0.4616
Expected Loss	1.3330***	0.0747	1.3549***	0.0619	1.4195***	0.0427
PeakandMultiperil	1.3725***	0.4660	2.5580***	0.4546	2.6479***	0.2332
GCIndex	0.0258***	0.0041	0.0377***	0.0049	0.0408***	0.0031
BBSpread	0.5643***	0.0890	0.6000***	0.1023	0.3638***	0.0662
Term	-0.0209	0.0146	-0.0316**	0.0151	-0.0137*	0.0079
IG	-1.4306**	0.6087	-1.9646***	0.7060	-3.4174***	0.4575
Hybrid	0.2551	1.6248	0.8084	0.7004	0.4566	0.4100
Random effects						
σ_u	0.7892**	0.2538	0.6116	0.3981	$0.0000^{\dagger}$	0.0293
σ_e	1.3947***	0.2243	1.5628***	0.3371	1.8432***	0.2253
ICC	0.2425		0.1328		0.0000	
Issuers	47		27		27	
Observations	194		144		366	

† In this instance, the variation associated with the issuer effect is so small compared to the background noise that this volatility is assumed to be zero.

Note: This table displays estimates of the factors affecting CAT bond premiums based on the issuer's main line of business. 'Insurers' include those businesses that primarily conduct insurance business; 'Reinsurers' include those businesses that primarily conduct reinsurance business or are syndicates; and 'Multiline/Others' includes all other companies, including those that conduct both insurance and reinsurance business, investment managers, or insurance agents. Companies not operating in the financial services sector are also included within this classification, including supranational organisations and utility companies. Each issuer is then allocated into their respective sub-groups and estimates and standard errors calculated for both fixed and random effects. The significance of each of these values is also indicated. Significance at 90%, 95%, and 99% confidence levels are indicated by *, **, and ***, respectively.

By market cycle

The CAT bond market has been shown to follow reinsurance cycles (Lane and Mahul, 2008; Lane and Beckwith, 2008), with rising premiums during periods of high losses, and lower premiums in periods of low losses and capital inflows. Hard markets are observed in periods of increasing losses, especially following major catastrophic events, and are characterised by higher-than-expected premiums. Soft markets, on the other hand, represent periods of low losses and capital inflows, and are characterised by lower-than-expected premiums. Neutral markets are characterised by premiums close to their expected values.

Table 5.13 displays the results of the multilevel regressions on each of the sub-samples. The results show that random effects are significant only in the soft or neutral market periods, but not in the hard market. This could be because other factors, particularly the fixed effects, have a larger impact on premium variability in hard market periods than the issuer, evidenced by higher estimates for the fixed effects in hard markets. The proportion of variability based on the ICC is therefore higher in soft or neutral markets due to the higher impact of issuer differences and lower impact of fixed effects on premiums. The term variable is also only significant in hard markets, while the trigger variable representing the hybrid trigger is only significant in soft or neutral markets.

Table 5.13: *Robustness by state of market cycle at issue*

	Hard market		Soft or neutral market	
	Estimate	Standard error	Estimate	Standard error
Fixed effects				
Intercept	-0.2640	0.4936	-1.5230***	0.4011
Expected Loss	1.4192***	0.0506	1.3858***	0.0314
PeakandMultiperil	2.7479***	0.2793	1.9092***	0.2126
GCIndex	0.0337***	0.0032	0.0395***	0.0027
BBSpread	0.5808***	0.0604	0.3760***	0.0725
Term	-0.0297***	0.0097	0.0034	0.0069
IG	-2.2472***	0.5815	-2.7234***	0.3213
Hybrid	0.7559	0.5834	0.7356**	0.3392
Random effects				
σ_u	0.4780	0.2797	0.5751**	0.1439
σ_e	1.8942***	0.3268	1.2406***	0.1235
ICC	0.0603		0.1769	
Issuers	78		65	
Observations	329		375	

Note: This table provides estimates of the extent to which the chosen independent variables impact CAT bond premiums over the state of the market cycle. The data are split according to the state of the cycle prevailing at issue. This results in two sub-samples, one representing hard market issues where premiums are assumed to be higher than expected and the other representing soft or neutral market issues where premiums are assumed to be lower or stable respectively (According to Lane and Beckwith (2020), a hard market represents a period of more 'more aggressive demand for protection from issuers than the appetite for assuming risk among investors (pg.8)' and therefore premiums rise in turn, while a soft market represents a period of less demand from issuers compared to investor risk appetite and thus premiums fall. Neutral markets exist in times when the demand for protection balances out with investor risk appetites). Both the fixed effects and the random effects are displayed, with their respective estimates and standard errors. The significance of each of these values is also indicated. Significance at 90%, 95%, and 99% confidence levels are indicated by *, **, and ***, respectively.

By time

Based on Table 5.14, in both samples, the random effects and most of the fixed effects are significant, at least at a 90% confidence level. Random effects are significant at 90% confidence, with around 12% of the total variation in premiums being explained by issuer differences. Fixed effects including the expected loss, the underlying bond peril, the reinsurance cycle and the competing financial environment are significant at a 99% confidence level in both time periods, while the term and trigger variables are insignificant. The rating variable, representing investment-grade bonds, is significant only in the pre-2010 sample (1997-2010), and insignificant in the post-2010 sample (2011-2020). This can be explained by the fact that most bonds issued after 2010 do not have a rating, and those that do are mainly non-investment grade bonds. The effect of the investment-grade rating is therefore mainly observed in the first sub-sample.

Table 5.14: *Robustness by time period*

	1997-2010		2011-2020	
	Estimate	Standard error	Estimate	Standard error
Fixed effects				
Intercept	0.9287**	0.4548	-1.9594***	0.4514
Expected Loss	1.8603***	0.0581	1.3127***	0.0329
PeakandMultiperil	2.1222***	0.2409	2.2988***	0.2560
GCIndex	0.0156***	0.0032	0.0530***	0.0037
BBSpread	0.3416***	0.0522	0.3727***	0.0941
Term	-0.0125	0.0084	-0.0003	0.0089
IG	-2.1723***	0.3434	-2.0310	1.4696
Hybrid	-0.1225	0.3991	-0.1759	0.5796
Random effects				
σ_u	0.5822*	0.1969	0.5281*	0.1469
σ_e	1.6237***	0.2206	1.4415***	0.1672
ICC	0.1139		0.1183	
Issuers	53		72	
Observations	323		381	

Note: This table provides estimates of the extent to which the chosen independent variables impact CAT bond premiums over two (almost) equal time periods. The data are divided into two sub-samples: one representing the early CAT bond issues (1997-2010), and the other representing more recent CAT bond issues (2011-2020). The data is split almost exactly in half to ensure the retention of a sufficient number of issuers (the level two variable) in each sample to aid comparison. Both the fixed effects and the random effects are displayed, with their respective estimates and standard errors. The significance of each of these values is also indicated. Significance at 90%, 95%, and 99% confidence levels are indicated by *, **, and ***, respectively.

5.5 Implications for Issuers and CAT Market Participants

This study confirms that premium variability introduced by issuer differences does indeed exist, despite the risk of a CAT bond arising from the underlying catastrophe, which occurs independently of the state of the issuer (Cummins, 2008). In addition, the bankruptcy-remote SPV that issues the bond ensures that bond payouts are not related to the issuer. Despite these indicators of the independence of risks, investors, it seems, still take into account issuer-specific factors when pricing CAT bonds. In particular, it has been established that investors consider the reputation of the issuer in the CAT bond market, based on the total size of issue since inception and the length of time spent as issuers in the primary market, when pricing. In addition, insurers tend to experience more variability than other types of issuers such as reinsurers and multi-line businesses. This raises the possibility of issuance through a more established company, especially for those less established in the markets, or those conducting mainly insurance business. Indeed, this practice of "balance sheet lending" (Lane, 2018) has been practised by more established companies such as Swiss Re in the past. According to Lane (2018) however, Swiss Re has since ceased this practice. Despite this, issuers can still issue bonds for other companies if they choose to, so newer issuers and insurers could still have the option of issuing through a more established company if their pricing terms prove too expensive or inefficient.

Other options include issuance through other types of markets that could prove to have better terms, e.g., reinsurance markets, the corporate bond markets, derivatives markets, or through private issues of insurance-linked securities. These avenues all have their disadvantages though, since most do not price catastrophic risks as their main risks. Their pricing terms could prove even more expensive and standardised for the issuer than the CAT market. Creating a customised disaster-risk-financing instrument might incur higher transaction costs than using already-established instruments like

CAT bonds, which are better customised for catastrophic risks (Cummins, 2008). The less established issuer could also set aside reserve funds, effectively retaining the risk instead of transferring it. In addition to the uncertainty in estimating such reserves, this could prove to be an inefficient use of funds, since the same funds could be assigned to more productive uses and better risk management options applied. Issuers will therefore have to establish the opportunity cost of issuing through the CAT bond market and receiving a potentially inefficient price versus using alternative sources of disaster-risk-financing that could still prove more expensive. As the cheapest choice might still be the CAT bond market, these issuers can then look into available avenues of issue in the CAT market and choose the most efficient.

Existing issuers, on the other hand, seek to renew their deals. Our results show that they could receive better terms over time, as the variability introduced by their characteristics reduces over time. This could motivate existing issuers to continue using the primary CAT market as their source of funding, and increase market liquidity. Existing issuers could also gain access to more unique instruments, including better terms through private placements, as their issues increase. This could further increase participation and encourage expansion of the CAT bond market by volume.

Whether the increase in issues for existing issuers is enough to offset the potential decrease from the loss of new issuers can only be determined over time based on how the CAT market develops. The Covid-19 pandemic could have motivated new issuers to acquire protection from the CAT market, but this may not be sustainable, especially if a pandemic of this magnitude is viewed as a short-lived one-time event. The types of new issuers could also be limited to those exposed to pandemic risks. To attract a diverse range of issuers and investors, therefore, market inefficiencies will need to be recognized and addressed. This inefficiency also impacts the overall operational and allocative efficiency of the CAT bond market, and could affect returning investor participation in the long run, further hindering the development of this market.

5.6 Conclusion

This study set out to establish the existence and significance of the issuer effect in the primary catastrophe (CAT) bond market by applying two-level analysis techniques to the data. The novel random intercept model produces reliable estimates and more robust standard errors for the fixed effects due to its ability to pick out the second level of variability arising from issuer-specific variables, as it incorporates the premium variations by issuer at the second level and the remaining independent variables (fixed effects) at the first level.

The key explanatory variables included, in addition to the issuers, are the expected loss, peril, term, trigger, rating, reinsurance cycle and state of the competing financial environment. These factors are similar to those identified in previous studies (e.g., Braun, 2016; Gürtler et al., 2016; Lane, 2018) on CAT bond pricing, with the exception of the term and trigger variables. These two factors are included due to their significant effect on the premium, an effect attributed to the larger sample size that allows factor developments over time to be picked out.

From the results, we establish that the issuer effect exists, and that the variation introduced by issuers is significant. We report that around 11% of the total variation in CAT bond premiums is due to differences between issuers, based on the intra-class correlation coefficient (ICC). Classifications of issuers based on length of time in the primary market, total issue size and line of business further enable us to determine that the issuers introducing the greatest variability are those with a smaller total issue size, those which have been issuing bonds in the primary market over a shorter period, and those issuers whose primary business is insurance as opposed to reinsurance or a multi-line business. We also identify the fixed effects with the largest impact on premiums by magnitude to be the expected loss, the peril and the reinsurance cycle.

These results support deductions that, all else constant, within-issuer CAT bond similarities introduce between-issuer differences in premiums. These differences are attributable to issuer reputation, issuer characteristics and total size of issues. Issuers with smaller total issue sizes and a shorter period (lower consistency) in the primary market tend to exhibit more variability, with stability in pricing increasing as the issuer's presence within the CAT bond market increases. Issuers conducting mainly insurance business also experience higher volatility in premiums than those in reinsurance or multi-line businesses, an observation that could be attributed to the reputations of these respective companies in the market.

Even though the issuer effect has been established to have an impact on variability in the baseline premium, and the main issuer characteristics impacting this volatility identified, the nature of the data limited further analysis into more issuer-specific factors. CAT bond data are unbalanced with regards to the number of observations per issuer. Some issuers have as many as 173 observations while others have only 1 or 2 observations. This is controlled for by the use of a shrinkage estimator in the multi-level model, but a challenge still arises when conducting further tests that require splitting the data into smaller groups, e.g. tests looking into issuer characteristics and robustness of estimates. Most of these tests risk losing either a number of issuers from the sample or observations from the groups, thereby reducing the reliability of the multilevel model estimates of the random effects. In addition, data related to other issuer-specific characteristics such as the bond rating at the time of a bond issue in the primary market are scarce, and also raises a challenge for those issuers that have issued over multiple periods as these factors are not constant. Despite this, future research could still expand the scale of the tests and establish more relationships as more data becomes available. In addition, other techniques that do not rely on the assumptions of maximum likelihood estimation, e.g., non-parametric bootstrap techniques, could be used to further test for these relationships.

Finally, this study is able to identify that variations in CAT bond premiums as a result of issuer differences do, in fact, exist. This implies that the primary CAT bond market is still inefficient, and might provide an opportunity for issuers to exploit these inefficiencies by using the platform with the least amount of volatility. Based on issue size and consistency of issues in the primary market, larger and more seasoned issuers experience less volatility in premiums than smaller, less consistent issuers. In addition, insurers experience more volatility than reinsurers or multi-line companies. New issuers and insurers may therefore need to take into consideration the fact that direct issuance may cost them more than indirect issuance. The opportunity cost of direct versus indirect issuance will therefore need to be established when assessing the available funding options. For those looking to introduce new ILS instruments, the study also provides an understanding of key risks that might impact market efficiency and identifies factors that may need to be considered during product development to ensure the success of these new securities.

Chapter 6

A Compound Poisson Flexible Mixture Model (CPFMM) for Catastrophic Loss Modelling and Valuation using Expectation Maximization(EM) Algorithms

Catastrophe bonds are financial securities that provide insurance against the risk of extreme events. Since these bonds functions as both financial securities and an insurance products, valuation techniques usually involve the determination of expected losses and the frequency of such losses through insurance pricing techniques and thereafter incorporating this information into a bond pay-off function derived through financial modelling assumptions. Each stage of the valuation process includes multiple assumptions with regards to loss distributions, interest rate processes and bond pricing functions. The final pricing functions are therefore often complex and non-smooth. This creates a challenge in the numerical integration process, as most of these functions are analytically intractable. Previous catastrophe bond valuation literature has applied either adaptive Monte Carlo techniques or approximation methods to optimise their functions. Despite this, few approximation techniques exist for heavy-tailed data. This study proposes an alternative numerical approximation technique for heavy-tailed

data based on Expectation-Maximization (EM) optimization techniques. Individual loss models, optimised as flexible mixture models through EM algorithms, are fitted to both loss frequency and loss severity data from the US's Property Claims Services to establish the most optimal models. Thereafter, the optimal loss models' performance and fit are compared with that of similar mixture-type models optimized via the more popular Newton-Raphson algorithms, as opposed to Expectation Maximisation (EM) algorithms, including General Composite Models (GCMs) and Composite Mixture Models(CMMs). Results indicate that the EM-based finite mixture model provides the most optimal fit for such heavy-tailed data, while retaining computational efficiency and robustness when compared to the Newton-Raphson (NR)-based models. A Compound Poisson Flexible Mixture Model (CPFMM) for heavy-tailed catastrophic aggregate loss processes is then formulated using the most optimal loss frequency and loss severity flexible mixture models. Subsequently, this model is employed in the valuation of two catastrophe bond instruments with different payoff functions to prove its applicability and efficiency.

6.1 Introduction

For the past twenty years, the catastrophe (CAT) bond market has provided funding for extreme events that had previously proved difficult to insure through traditional means. It has therefore been a useful source of alternative financing and investing, especially when traditional financing tools have been unattractive due to their correlations with financial market risks. The market continues growing and expanding each year, with total cumulative issuance of about US $145 billion [1] since inception. Improvements in valuation techniques and loss modelling have also attracted new investors and contributed to the expansion. As the catastrophic risk landscape is constantly changing, however, there is always a need to update available techniques to account for these changes and retain valuation reliability. Due to this, researchers have over the years

[1]This figure is retrieved from the Insurance Linked Securities'(ILS) website Artemis.bm on the 14th of June 2021

dedicated their studies to proposing new valuation techniques that could improve the efficiency of this system and enable valuers determine fair prices as the market evolved.

The catastrophe bond valuation process in the past has involved the merging of financial and actuarial modelling assumptions to determine price estimates; including interest rate assumptions, bond valuation assumptions, and aggregate claims modelling assumptions. As the catastrophe bond market is incomplete, the probability distribution of the expected losses has to be incorporated into the pay-off function to establish the final expected pay-offs under all available loss possibilities (Cox and Pedersen, 2000). The multiple pricing assumptions also imply that, in most cases, researchers can only focus on improving one aspect of the valuation process at a time, or risk losing model tractability and efficiency. Some of the studies dedicated to improving these key aspects of the pricing process are summarized below, based on their research focus.

Early studies in catastrophe bond valuation aimed at introducing the catastrophe bond structure and the financial and insurance theories underlying this instrument. Most of the theoretical foundations underlying catastrophe bond valuation were developed at this stage, including the incomplete markets framework and equilibrium pricing techniques of Cox and Pedersen (2000) and the arbitrage pricing framework of Vaugirard (2003b). Insurance pricing techniques were also formalized for extreme events through the extreme value theory (see e.g. Embrechts et al. (1999) and other suitable machine learning techniques e.g. Monte Carlo (MC) methods applied (see e.g. Ermoliev et al. (2000) , Vaugirard (2003a). Once these theoretical foundations were established, the next set of studies developed pricing models based on these aforementioned models and assumptions. Each of these studies also improved a specific aspect of the valuation process, further discussed below.

Among the first areas of improvement after the establishment of theoretical foundations was the modelling the aggregate claims process. Studies focused on developing the claim distribution process, especially through Poisson processes and its extensions. These include the compound doubly stochastic Poisson process (e.g., Burnecki and Kukla, 2003; Burnecki et al., 2005) and the Poisson shot noise process (e.g., Albrecher et al., 2004). The non-homogenous Poisson process for claim arrivals was also proposed to model claim frequency distributions. These processes continue to be applied over time to model aggregate loss distributions for catastrophic events (e.g., Härdle and Cabrera, 2010; Ma and Ma, 2013; Shao et al., 2017; Burnecki et al., 2019). In addition, alternative valuation methods e.g. transformation techniques of Wang (2000) were developed to further improve the claim modelling process.

Other valuation-based studies focused on modelling the financial processes underlying valuations, especially the interest rate process and the equilibrium pricing techniques. Nowak and Romaniuk (2013), in developing their valuation framework, compared the different interest rate processes to establish their applicability and suitability for CAT bond modelling. Their work was an extension of the arbitrage pricing framework developed by Vaugirard (2003b), and has subsequently been expanded upon in Nowak and Romaniuk (2016) to incorporate the effects on correlations in the underlying random processes and a multi-factor interest rate model. In addition, and contrary to previous studies that considered overall catastrophe losses without regard to the source of the loss, recent studies have tried to price specific types of losses and events (e.g. Deng et al. (2020) for global drought CATs,); or value bonds with specific unique structures (e.g. Burnecki et al. (2019) for index-linked convertible CATs). Other extensions include incorporating the effect of dependencies between risks through Markov chains (Shao et al., 2017) and copulas (Chao and Zou, 2018), among others.

Having established the state of current valuation research, and its key developments and contributions, we now focus on one specific element of these valuation frameworks, that is, the solution-seeking processes of the proposed models and their valuation equations. More specifically, we look at the process of numerical integration of the catastrophe bond valuation equations. Numerical integration techniques for catastrophe bond valuation were also developed in line with other model assumptions, with an emphasis on Monte Carlo (MC) integration (see e.g. Ermoliev et al. (2000). Monte Carlo integration methods have been favoured in the past as they are robust and independent of the dimensionality of the valuation integral, which can often be multi-dimensionally complex. Despite its advantages, the integration process can still be computationally expensive, especially as the number of dimensions is increased (Caflisch, 1998). Given the complex nature of the CAT valuation equations due to the multiple assumptions taken into account when pricing catastrophic risks, this could limit the exploration of more complex valuation techniques that might be better representations of the catastrophe bond market, especially as climate change and demographic trends continue to change catastrophic loss structures (Swiss Re, 2023). Incorporation of these structural complexities can, however, still be a challenge (see e.g., Davison and Smith, 1990; McNeil, 1997). This is because any small or minimal change in valuation equations further complicates already-complex models, thereby increasing the models' associated computational costs. To address this, it is crucial that the numerical integration element of the modelling process be made efficient, and the process optimized to allow ease of trend or change incorporation. It is also important that the proposed models be easy to understand and replicate, if there is any intention of their practical application.

To this effect, this chapter proposes a valuation model that optimizes functions through the Expectation Maximisation (EM)'s (Dempster et al., 1977) flexible-mixture class of algorithms, for both catastrophe loss frequency and catastrophe loss severity modelling. These techniques have the advantage of creating both analytically tractable distribution functions (Miljkovic and Grün, 2016), limiting over-smoothing of the tails of the distribution which are the focus of extreme event modelling (Embrechts et al., 1997), and most importantly, retaining computational efficiency while accomplishing all these tasks. These characteristics are important especially due to the nature of recent catastrophic loss trends, which have been reflecting heavier tails due to significant increases in loss severities (see e.g., Swiss Re, 2023).

To accomplish this, we fit individual loss models optimised through the EM algorithms to both the loss frequency and loss severity data from the US's Property Claims Services' catastrophe industry loss data. Thereafter, we compare the loss severity's individual loss model's performance and fit with that of similar mixture-type models created via the use of a more common and popular optimization method, the Newton-

Raphson algorithm, as opposed to the Expectation Maximisation (EM) algorithms, including General Composite Models (GCMs) and Composite Mixture Models(CMMs). The results indicate that the EM-based finite mixture model provides the most optimal fit for such heavy-tailed data, while retaining computational efficiency and robustness when compared to the Newton-Raphson (NR)-based models. We then create an aggregate loss model, the Compound Poisson Flexible Mixture Model (CPFMM) for heavy-tailed catastrophic loss processes using the most optimal loss frequency and loss severity flexible mixture models. Subsequently, we apply this model to the valuation of two catastrophe bond instruments with different payoff functions, one with its principal-at-risk and the other with its coupon-at-risk, and assuming interest rates follow the Cox-Ingersoll-Ross (CIR) process, in order to prove applicability and efficiency.

The results of the proposed Compound Poisson Flexible Mixture Model (CPFMM), optimized through the Expectation-Maximisation (EM) algorithm, and applied in this chapter, prove the efficiency and applicability of EM-type algorithms to heavy-tailed problems, with improved fit statistics and stability of estimates when compared to similar Newton-Raphson based models. These results are of particular impact to extreme loss risk modellers and other market pricing experts who generate the required models underlying such disaster financing instruments. In addition, the risk modelling and pricing improvements will benefit protection seekers, assuring them of fair pricing for their instruments and investor uptake of their products due to reduced information asymmetries. This will also in turn expand the insurance linked securities (ILS) market's capacity to provide more adapted catastrophe risk management instruments better suited for larger scale financing applications, subsequently allowing all stakeholders to benefit from the increased capacity. Vulnerable communities will also gain more efficient disaster recovery tools, especially to cover the increasing risks of climate change.

The rest of this article is structured as follows: Section 6.2 introduces the valuation framework, the problem set-up, and the methodology. Section 6.3 describes the sample selection, empirical analysis and results, while Section 6.5 concludes the article.

6.2 Valuation Framework

6.2.1 Assumptions

Similar to previous literature (e.g., Cox and Pedersen, 2000; Ma and Ma, 2013; Shao et al., 2017; Burnecki et al., 2019) we assume the following modelling assumptions: 1) financial market events are independent of catastrophic events; 2) it is possible to diversify risks posed by catastrophic events by diversifying the insured locations and perils; and 3) the financial market is arbitrage free with equivalent martingale measure.

6.2.2 General pricing formula

Suppose we have the probability space $(\Omega, \mathcal{F}, \mathcal{P})$, where Ω is the sample space, $\mathcal{F}$ is a σ-algebra representing a set of all possible events while $\mathcal{P}$ is a probability measure. Following from Burnecki and Giuricich (2017), and assuming an arbitrage free financial market, the value V_t of a contingent claim C_T at time $t \geq 0$ is given by the following equation

$$V_t = e^{-r(T-t)}\mathbb{E}^{\mathcal{P}}[C_T|\mathcal{F}_t] \tag{6.1}$$

under the real-world probability measure $\mathcal{P}$. In equation (6.1), r represents a constant rate of interest,$\mathcal{F}_t$ the number of events till time t, and $\mathbb{E}^{\mathcal{P}}$ denotes the expectation under the real world probability measure $\mathcal{P}$.

6.2.3 Interest rate process

To model the interest rate process for the short rate $\{r(t) : t \in [0, T]\}$, we apply the equilibrium interest rate model of Cox, Ingersoll and Ross (CIR) (Cox et al., 1985). In the CIR model, interest rates are assumed to display mean-reversion, with a standard deviation proportional to $\sqrt{r}$ (Hull, 2017). This model ensures that the possibility of negative interest rates is eliminated. The interest rate process under the risk-neutral measure $\mathcal{Q}$ is then given as;

$$dr(t) = a(b - r_t)dt + \sigma\sqrt{r_t}dW_t \tag{6.2}$$

where a, b and σ are non-negative constants; and $2ab > \sigma^2$. $(W_t)_{t\in[0,T]}$ denotes a Brownian motion.

Under the real-world measure $\mathcal{P}$, we assume the spot interest rate follows the form;

$$dr(t) = [ab - (a + \lambda_r)r(t)]dt + \sigma\sqrt{r_t}dW_t^* \tag{6.3}$$

where $W_t^* = W_t + \int_0^t \frac{\lambda_r\sqrt{r_s}}{\sigma}ds$ denotes a Brownian motion under the real world measure $\mathcal{P}$ and λ_r is a constant (Ma and Ma, 2013). Assuming $\mathcal{P}$ and $\mathcal{Q}$ are equivalent measures, we can obtain the Radon-Nikodym derivative of $\mathcal{Q}$ with respect to $\mathcal{P}$ i.e.

$$\frac{d\mathcal{Q}}{d\mathcal{P}}_{\mathcal{F}_t} = exp(-\frac{1}{2}\int_0^t \frac{\lambda_r^2 r_s}{\sigma^2}ds + \int_0^t \frac{\lambda_r\sqrt{r_s}}{\sigma}dW_s^* \tag{6.4}$$

The stochastic form of the market price of risk process $\lambda_r^*(t)$ is given by

$$\lambda_r^*(t) = \frac{\lambda_r}{\sigma}\sqrt{r_t} \tag{6.5}$$

The price of a principal-at-risk bond at time t can be determined from the following equalities (Brigo and Mercurio, 2007);

$$B_{CIR}(t,T) = A(t,T)e^{-B(t,T)r_t}, \tag{6.6}$$

where

$$A(t,T) = \left[\frac{2he^{(a+\lambda_r+h)(T-t)/2}}{2h + (a+\lambda_r+h)(e^{(T-t)h} - 1}\right]^{\frac{2ab}{\sigma^2}}, \tag{6.7}$$

$$B(t,T) = \left[\frac{2e^{(T-t)h} - 1}{2h + (a+\lambda_r+h)(e^{(T-t)h} - 1}\right], \tag{6.8}$$

$$h = \sqrt{(a+\lambda_r)^2 + 2\sigma^2} \tag{6.9}$$

6.2.4 Aggregate claims process

In the collective risk model (Cramer-Lundberg model), the stochastic process N_t represents the number of claims occurring until time t. This is modelled as a Poisson process with intensity $\lambda > 0$ (Korn et al., 2010). The size of the individual claims is denoted by the non-negative random variables $X_i, i = 1, ..., N_t$ with the distribution function $F(x) = P\{X_i < x\}$.

In this model, we assume 1) the number of claims is independent of the claim sizes; and 2) the individual claims are independent and identically distributed. We also assume the aggregate loss process $\{L_t : t \in [0, T]\}$ follows a compound Poisson process and is defined as;

$$L_t = \sum_{i=1}^{N_t} X_i \tag{6.10}$$

and L_t=0 when $N_t = 0$.

6.2.5 CAT Bond Pricing Model

Consider two index-linked CAT bonds[2]; a principal-at-risk CAT bond and a principal-and-coupon-at-risk CAT with both the coupons and principal at risk if a catastrophe occurs. First consider the principal-at-risk CAT bond with pay-off (${P_{CAT}}^{(1)}$) and maturity $T > 0$. The payoff structure can be defined as;

$${P_{CAT}}^{(1)} = \begin{cases} 1, & \text{if } L_T < D. \\ \rho, & \text{if } L_T \geq D. \end{cases} \tag{6.11}$$

where L_T represents the aggregate claims at time T, D is the threshold level that triggers a payout, and $\rho(0 \leq \rho < 1)$ represents the proportion of principal recovered by the investor at time T if the bond is triggered. The value of this bond at time t given the catastrophe loss distribution $F(x)$ and the claim arrival process N_t is then given by (see e.g., Ma and Ma (2013) and Burnecki and Giuricich (2017));

$$\begin{aligned} V_t &= e^{-\int_t^T r_s ds} \mathbb{E}^{\mathcal{Q}}[{P_{CAT}}^{(1)} | \mathcal{F}_t] \\ &= B_{CIR}(t, T) \;\; \rho + (1 - \rho) \times \sum_{n=0}^{\infty} e^{-\lambda_t (T-t)} \frac{(\lambda_t (T - t))^n}{n!} F^{*n}(D) \end{aligned} \tag{6.12}$$

[2]an index linked CAT pays out to the issuer if the losses from the pre-specified event exceed losses on a certain catastrophe loss index

under the risk-neutral probability measure $\mathcal{Q}.F^{*n}(D) = Pr(X_1 + X_2 + ... + X_n \leq D$ is the n-fold convolution of F and

$$\begin{aligned}
B_{CIR}(t,T) &= A(t,T)e^{-B(t,T)r_t}, \\
A(t,T) &= \left[\frac{2he^{(a+\lambda_r+h)(T-t)/2}}{2h + (a+\lambda_r+h)(e^{(T-t)h} - 1}\right]^{\frac{2ab}{\sigma^2}}, \\
B(t,T) &= \left[\frac{2e^{(T-t)h} - 1}{2h + (a+\lambda_r+h)(e^{(T-t)h} - 1}\right], \\
h &= \sqrt{(a+\lambda_r)^2 + 2\sigma^2}
\end{aligned} \tag{6.13}$$

Now consider the principal-and-coupon-at-risk CAT bond with a constant coupon $c > 0$ and the payoff structure;

$$P_{CAT}{}^{(2)} = \begin{cases} c+1, & \text{if } L_T < D. \\ \rho(c+1), & \text{if } L_T \geq D. \end{cases} \tag{6.14}$$

where L_T represents the aggregate claims at time T, D is the threshold level that triggers a payout, and $\rho(0 \leq \rho < 1)$ represents the proportion of coupon and principal recovered by the investor at time T if the CAT bond is triggered. Similarly, the value of this bond at time t given the catastrophe loss distribution $F(x)$ and the claim arrival process N_t is then given by;

$$\begin{aligned}
V_t &= e^{-\int_t^T r_s ds}\mathbb{E}^{\mathcal{Q}}[P_{CAT}{}^{(2)}|\mathcal{F}_t] \\
&= B_{CIR}(t,T) \left[\rho(c+1) + (1-\rho(c+1)) \times \sum_{n=0}^{\infty} e^{-\lambda_t(T-t)} \frac{(\lambda_t(T-t))^n}{n!} F^{*n}(D)\right]
\end{aligned} \tag{6.15}$$

where $F^{*n}(D) = Pr(X_1 + X_2 + ... + X_n \leq D$ is the n-fold convolution of F and

$$\begin{aligned}
B_{CIR}(t,T) &= A(t,T)e^{-B(t,T)r_t}, \\
A(t,T) &= \left[\frac{2he^{(a+\lambda_r+h)(T-t)/2}}{2h + (a+\lambda_r+h)(e^{(T-t)h} - 1}\right]^{\frac{2ab}{\sigma^2}}, \\
B(t,T) &= \left[\frac{2e^{(T-t)h} - 1}{2h + (a+\lambda_r+h)(e^{(T-t)h} - 1}\right], \\
h &= \sqrt{(a+\lambda_r)^2 + 2\sigma^2}
\end{aligned} \tag{6.16}$$

6.2.6 The EM Algorithm and Flexible Mixtures

Assuming claim arrivals N_t follow a time-inhomogeneous Poisson process and a claim severity variable $X_i \geq 0$ with distribution $F(x) = P(X_i < x)$, the aggregate loss (L_t) distribution is given as (see e.g., Ma and Ma (2013));

$$
\begin{aligned}
F(x,t) &= \sum_{n=0}^{\infty} exp\{-\lambda_t t\} \frac{(\lambda_t t)^n}{n!} F^{*n}(x), && x > 0 \qquad (6.17) \\
&= exp\{-\lambda_t t\}, && x = 0
\end{aligned}
$$

since the convolution function $F^{*n}(x)$ is analytically intractable, approximation methods including the normal approximation, the inverse gaussian approximation and the gamma approximation have been applied instead (Burnecki and Giuricich, 2017). Burnecki and Giuricich (2017) also show that few approximations exist for very heavy-tailed distributional assumptions. Since we assume catastrophe loss data is assumed to be heavy-tailed, heavy-tailed probability distributions are often applied to fit the data and explain the loss structure (Miljkovic and Grün, 2016). It is therefore necessary that approximation methods proposed are applicable to the heavy-tailed structure of extreme events data.

In this study, we propose an approximation method based on the Expectation Maximization (EM) Algorithm (the EM Approximation). The EM Algorithm is used to generate maximum likelihood estimates for incomplete data or latent/hidden variables. We will therefore be artificially formulating our problem as an incomplete data problem to facilitate maximum likelihood estimation (Ng et al., 2011).

Problem Set-up

Assume $X = \{X_1, X_2, ..., X_n\}$ is a sample of independently and identically distributed random variables derived from an M-component finite mixture of probability distributions. The density function f of the mixture distribution is the weighted average of the M-component densities with mixing weights ω_m ($\omega_m \geq 0$, $m = 1, ..., M$, and ${}_{m=1}^{M}\omega_m = 1$) (Sitek, 2016)

$$f(x|\vartheta) = \sum_{m=1}^{M} \omega_m f_m(x|\theta_m), \tag{6.18}$$

where $\vartheta = (\omega', \theta')' = (\omega_1, \omega_2, ..., \omega_m, ..., \omega_{m-1}, \theta'_1, \theta'_2, ..., \theta'_m, ..., \theta'_M)$ is the vector of unknown parameters .The density functions f_m are assumed to be absolutely continuous with respect to the Lesbegue measure and to be derived from the same univariate parametric family with d-dimensional parameter vector θ_m, $\mathfrak{F} = \{f_m(.|\theta_m), \theta_m \in \Theta \subset \mathbb{R}^d\}$ (Miljkovic and Grün, 2016; Sitek, 2016)). For purposes of analysis, we consider five heavy-tailed distributions; Gamma, Burr, Weibull, Lognormal and Birnbaum-Saunders. Most of these distributions have been tested for extreme event modelling in previous literature (see e.g Miljkovic and Grün (2016)) and shown to provide a good fit.

The Classical EM Algorithm

Assume the complete data is given by $Z = (X, Y)$ where X is observed but Y is hidden (or unobserved). The log-likelihood for this complete data can then be represented by $l(\vartheta; X, Y)$, where ϑ represents an unknown parameter vector for which we would like to find the maximum likelihood estimate. The EM Algorithm accomplishes this through two steps. The Expectation Step (E-step) computes the expected value of $l(\vartheta; X, Y)$ given the observed data X and an initial estimate for the parameter vector ϑ i.e. $\vartheta_{initial}$.

The E-Step

$$\begin{aligned} Q(\vartheta, \vartheta_{initial}) &\coloneqq E[l(\vartheta; X, Y)|X, \vartheta_{initial}] \\ &= \int l(\vartheta; X, y) p(y|X, \vartheta_{initial}) dy \end{aligned} \tag{6.19}$$

where $p(.|X, \vartheta_{initial})$ represents the conditional density of Y given X, assuming $\vartheta = \vartheta_{initial}$.

The Maximization step (M-step) then maximizes the expectation derived in the E-step over ϑ.

The M-Step

We therefore set

$$\vartheta_{new} := \max_{\vartheta} Q(\vartheta, \vartheta_{initial}) \tag{6.20}$$

The new $\vartheta_{initial}$ is then set to equal ϑ_{new}, and the process repeated until convergence.

The EM Algorithm and Flexible Mixtures

For the complete data $Z = (X, Y)$ defined above, $Y = (Y_{im} \in \{0, 1\}, i = 1, ..., n, m = 1, ..., M)$ is the hidden variable that allocates each observation to their specific component. Y is assumed to consist of M vectors $y = (y_1, y_2, ..., y_n)$ for $m = 1, ..., M$, where

$$y_{im} = \begin{cases} 1 & \text{if observation } x_i \text{ originates from component } m \\ 0 & \text{otherwise} \end{cases} \tag{6.21}$$

The complete data likelihood function for the finite mixture is then defined as;

$$L(x_1, x_2, ..., x_n|\vartheta, \omega) = \prod_{i=1}^{n} \prod_{m=1}^{M} (\omega_m f_m(x_i|\theta_m))^{y_{im}} \tag{6.22}$$

The complete data log-likelihood can then be expressed as

$$l(x_1, x_2, ..., x_n|\vartheta, \omega) = \sum_{i=1}^{n} \sum_{m=1}^{M} y_{im}[log(\omega_m) + log(f_m(x_i|\theta_m))] \tag{6.23}$$

In numerical simulation, the expected complete data log-likelihood (E-step) is determined by replacing hidden values with their expected values given the observed values X and the parameter estimates from the most recent iteration i.e. the $k-1$'th iteration for the k'th simulation. This expected value is then given by;

$$\omega_{im}^{(k)} = E[y_{im}|x_i, \vartheta^{(k-1)}] = \frac{\omega_m^{(k-1)} f_m(x_i|\theta_m^{(k-1)})}{{}_{m'=1}^{M} \omega_{m'}^{(k-1)} f_{m'}(x_i|\theta_{m'}^{(k-1)})} \tag{6.24}$$

where $\omega_{im}^{(k)}$ is the posterior probability that x_i originates from the m'th mixture for the kth iteration of the EM Algorithm (Ng et al., 2011). The EM Algorithm then iteratively maximizes the following operator;

$$Q(\vartheta|\vartheta^{(k-1)}) = \sum_{i=1}^{n}\sum_{m=1}^{M}\omega_{im}^{(s)}[[log(\omega_m) + log(f_m(x_i|\theta_m))] \tag{6.25}$$

The E-step is the same for all distributions considered as it is independent of parametric form in $\mathfrak{F}$.

The M-step generates new estimates for the unknown parameters ω and θ by maximization of the Q-operator. The ω estimates are updated in the kth iteration by

$$\widehat{\omega_m}^{(k)} = \frac{1}{n}\sum_{i=1}^{n}\omega_{im}^{(k)} \tag{6.26}$$

By solving a weighted maximum likelihood estimation problem for each of the component distributions with the posterior probabilities as weights, we can generate new estimates for θ_m. This can be solved analytically if possible, or by numerical optimization. In the distributions that follow, θ_k is obtained in the M-step as follows (Miljkovic and Grün, 2016);

Gamma: X $\sim$ G(λ, θ)

The Gamma distribution has the form

$$f(x;\lambda,\theta) = \frac{1}{\Gamma(\lambda)\theta^{\lambda}}x^{\lambda-1}e^{-x/\theta} \tag{6.27}$$

where $\lambda > 0$ denotes the shape parameter, $\theta > 0$ the scale parameter, and $\Gamma(\lambda) = (\lambda-1)!$.

M-step maximization of the Q-operator with respect to θ given λ gives the following closed form solution

$$\widehat{\theta}_m^{(k)} = \frac{\widehat{\lambda}_m^{(k)}\widehat{\omega}_m^{(k)}n}{{}_{i=1}^{n}\,\omega_{im}^{(k)}x_i} \tag{6.28}$$

Marginal weighted log-likelihood, with $\widehat{\theta}_m$ as a function of $\widehat{\lambda_m}$; and numerical optimization are used to generate an estimate for λ.

Burr: X $\sim$ Burr $(\lambda, \theta, \gamma)$

The Burr distribution has the form;

$$f(x;\lambda,\theta,\gamma) = \frac{\lambda\gamma(x/\theta)^{\gamma}}{x(1+(x/\theta)^{\gamma})^{\lambda+1}}, \tag{6.29}$$

where $\lambda > 0, \gamma > 0$ denote the shape parameters while $\theta > 0$ denotes the scale parameter. The M-step maximization the Q-operator with respect to λ given θ and γ gives the closed form solution;

$$\widehat{\lambda} = \frac{n\widehat{\omega}_m^{(k)}}{\sum_{i=1}^{n} \omega_{im}^{(k)} log\left(1 + \left(\frac{x_i}{\widehat{\theta}_m^{(k)}}\right)^{\widehat{\gamma}_m^{(k)}}\right)} \tag{6.30}$$

Marginal weighted log-likelihood, with $\widehat{\lambda}_m$ as a function of $\widehat{\theta_m}$ and $\widehat{\gamma}_m$; and numerical optimization are used to generate estimates for θ and γ.

Weibull: X $\sim$ W(λ, α)

The Weibull distribution with shape parameter $\alpha > 0$ and scale parameter $\lambda > 0$ has a density function of the form

$$f(x;\lambda,\alpha) = \frac{\alpha}{\lambda}(\frac{x}{\lambda})^{\alpha-1}e^{-(x/\lambda)^{\alpha}} \tag{6.31}$$

Weighted log-likelihoods and numerical optimization are used to obtain estimates for α and θ.

Log-normal: X $\sim$ W(μ, σ^2)

The log-normal density function is given as

$$f(x;\mu,\sigma^2) = \frac{1}{x\sigma\sqrt{2\pi}}exp(-\frac{(logx-\mu)^2}{2\sigma^2} \tag{6.32}$$

where μ denotes the location parameter, $\sigma > 0$ denotes the scale parameter, and $x > 0$. M-step maximization the Q-operator with respect to μ and σ given μ gives the closed form solutions;

$$\widehat{\mu}_m^{(k)} = \frac{\sum_{i=1}^{n} \omega_{im}^{(k)} log(x_i)}{\sum_{i=1}^{n} \omega_{im}^{(k)}} \tag{6.33}$$

and

$$(\widehat{\sigma}_m^2)^{(k)} = \frac{\sum_{i=1}^{n} \omega_{im}^{(k)} (log(x_i) - \widehat{\mu}_m^{(k)})^2}{\sum_{i=1}^{n} \omega_{im}^{(k)}} \tag{6.34}$$

Birnbaum-Saunders: X $\sim$ B-S(γ, μ, β)

The Birnbaum-Saunders distribution with shape parameter $\gamma > 0$, location parameter μ, and scale parameter $\beta > 0$ has the form

$$f(x;\gamma,\mu,\beta) = \frac{\sqrt{\frac{x-\mu}{\beta}} + \sqrt{\frac{\beta}{x-\mu}}}{2\gamma(x-\mu)} \phi \left(\frac{\sqrt{\frac{x-\mu}{\beta}} - \sqrt{\frac{\beta}{x-\mu}}}{\gamma} \right) \tag{6.35}$$

where $x > \mu$.

Weighted log-likelihoods and numerical optimization are used to obtain estimates for γ, μ and β.

Model selection and goodness-of-fit

To identify the optimal m-component mixture for a given dataset under each of the considered distributions, goodness-of-fit tests based on the Akaike Information Criterion (AIC) and the Bayesian Information Criterion(BIC) are conducted.

The Akaike Information Criterion (AIC) (Akaike, 1974) provides a measure of the information lost when the specified model if fitted to a given dataset. It is calculated as follows;

$$AIC = -2ln(L) + 2k \tag{6.36}$$

where L is the maximum likelihood while k denotes the number of estimated model parameters.

The Bayesian Information Criterion (BIC) (Schwarz, 1978) performs the same function as the AIC, and considers both the parameters and the number of observations in determining the information lost. The BIC is calculated as;

$$BIC = -2ln(L) + kln(n) \tag{6.37}$$

where L is the maximum likelihood, k is the number of parameters, and n represents the total number of observations. The lower the value of either the AIC or BIC, therefore, the better the model. However, since the BIC penalizes model complexity more heavily than the AIC, it is prioritized in cases where the two values lead to inconsistent conclusions on the choice of distribution.

6.3 Model Application

6.3.1 Data

Pricing an index-linked catastrophe bond requires specification of the respective loss index, since these bonds' payoff are determined by the losses recorded by the underlying index. One of the most popular underlying indices is created by the US's Property Claims Services (PCS), which records property losses from natural catastrophes in the USA and its associated territories. This data is used by industry catastrophe risk modellers and valuers to represent the underlying catastrophic loss processes. For this reason, we also use PCS data for purposes of application. Our specific dataset spans the period beginning January 1985 and ending March 2014[3]; and includes loss estimates from majority natural perils, including, for example, hurricanes, tornadoes, earthquakes, tropical storms, wildfires and winter storms. The gross loss figures are

[3]The data is only used for application purposes. The timeline from January 1985 to March 2014 is a result of data unavailability due to extreme data costs for individual researchers after this period. The data was deemed acceptable to use as it was only used to fit the model and prove that the model could efficiently be applied to heavy-tailed data. Other recent studies have applied even older datasets, for example the Danish Fire data that spans the period beginning January 1980 and ending December 1990 for similar purposes (see e.g Miljkovic and Grün (2016)).

then adjusted for inflation to their 2014 values using the US Consumer Price Index. A time series plot of the data is displayed below;

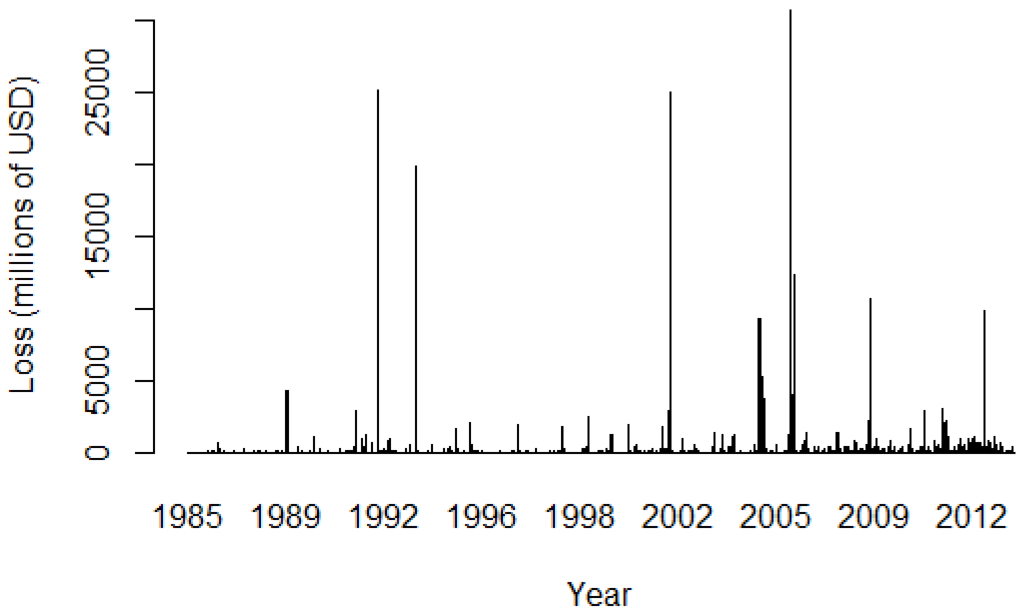

Figure 6.1: *Full PCS Data Histogram*

Note: This figure displays a summary of catastrophe industry loss estimates from the Property Claims Services (PCS). The data covers the periods beginning January 1985 and ending March 2014, and comprises loss estimates from a majority natural perils, including hurricanes, earthquakes, tornadoes, wildfires, and winter storms. The displayed figures are inflation-adjusted estimates to 2014, using the US consumer price index. The losses are displayed in millions of US dollars, with the y-axis displaying loss estimates, and the x-axis displaying the respective dates.

From the time series plot, key periods with the most severe losses can be identified. The year 1989 saw the occurrence of Hurricane Hugo; and the interval between the years 1992 and 1994 the occurrence of Hurricane Andrew and the Northridge Earthquake respectively. The year 2001 coincides with Tropical Storm Allison, while the time interval between 2004 and 2006 coincides with Hurricanes Frances, Jeanne, Katrina and Wilma. Hurricane Ike led to increased losses in 2008; while several extreme Wind and Thunderstorm events caused significant damage in 2011. Hurricane Sandy's 2012 losses complete these key 'spike periods' for this dataset.[4] The annual loss frequencies and loss severities are further summarised in the following figures;

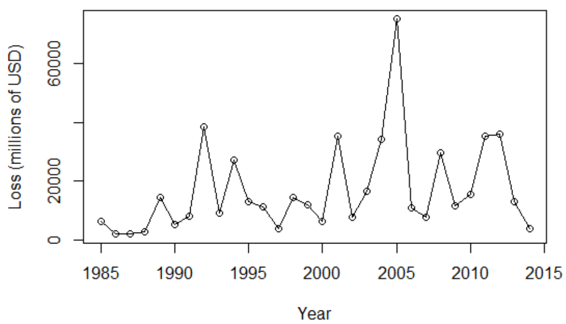

(a) *Catastrophic Loss Severity*

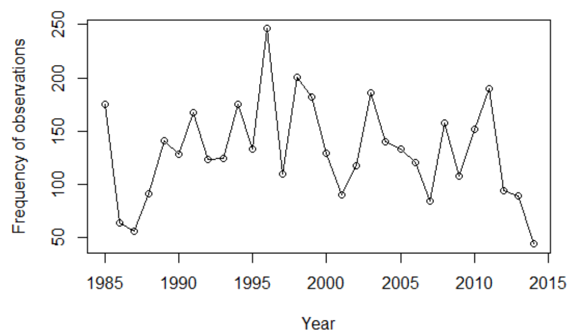

(b) *Catastrophic Loss Frequency*

Note: The two plots above summarize the catastrophic loss severity values (left), and the catastrophic loss frequency (right) values for the PCS data spanning the period beginning January 1985 and ending March 2014. The Loss Severity plot displays aggregate loss estimates in millions of US dollars per year, while the Loss Frequency plot displays the annual loss frequencies per year.

The data's summary descriptive statistics are given in the following table

[4]This PCS data is focused on the US and its associated territories, but this is not an issue for CAT bond valuation, as most of these bonds are currently issued with US-based underlying perils.

Table 6.1: *Summary Statistics for PCS Catastrophe Industry Loss Data*

Statistic	Value (USDm)
Minimum	1.07
Maximum	30630.28
Mean	128.46
Median	28.90
Skewness	22.45
Kurtosis	581.61

Note: The table gives a summary of the PCS data descriptive statistics. These descriptive statistics relate to data spanning the period beginning January 1985 and ending March 2014, with the specific statistic displayed in the 'Statistic' column and its exact value displayed in the 'Value' column in millions of US dollars. The statistics assessed include the data's range, given by the minimum and maximum values, its measures of location, including its mean and median, and finally the data's measures of shape, given by the skewness and kurtosis values. The table provides a good reference for an initial deduction of the heavy-tailed characteristics of the data.

From the table above, we can infer that the mean is approximately 4 times the median, suggesting that PCS data is right skewed, with a longer tail on the right. This assumption is justified by a maximum loss value that is about 239 times the mean, and skewness and kurtosis values of 22.45 and 581.61 respectively. These statistics suggest that the data is heavy-tailed, and this will be further confirmed by the following diagnostic tests, which are based on extreme value theory.

6.3.2 Further Heavy Tail Diagnostics based on Extreme Value Theory (EVT)

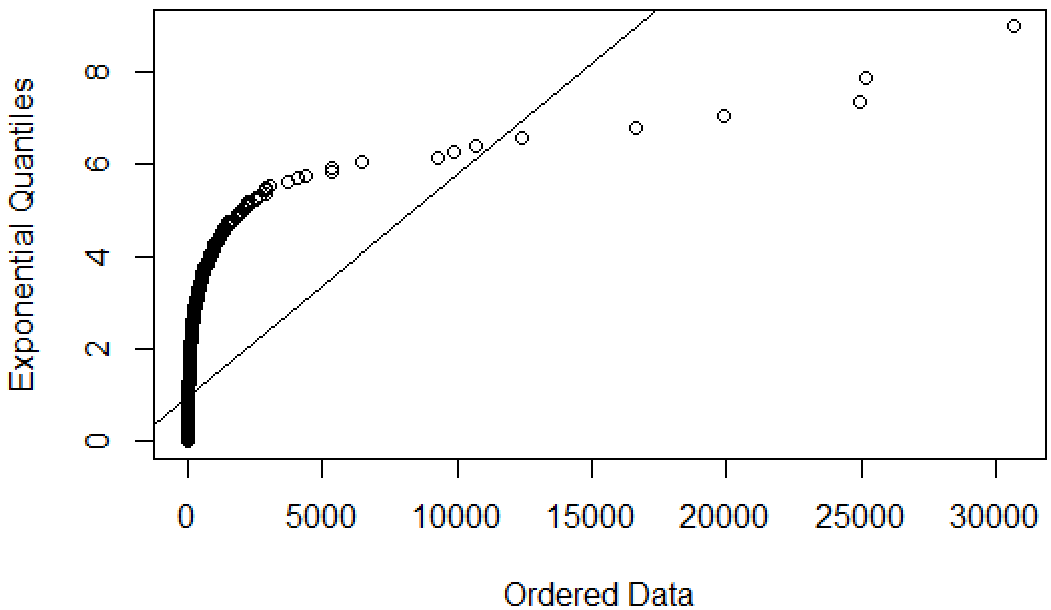

Figure 6.3: *Exploratory QQ plot of PCS data for extreme value analysis*

Note: The figure displays an exploratory quantile-quantile plot, used to test and further confirm the heavy-tailed characteristics of the PCS data. Departures from the medium-tailed distribution, which in this case is the exponential distribution, indicate either heavy-tailed data for convex departures, or lighter-tailed data for concave departures.

The exploratory QQ plot is used for the identification of any departures from a medium-tailed distribution, with the medium-tailed distribution in this case being the exponential distribution. Convex departures are an indication of thinner-tailed data, while concave departures, similar to our case, serve as proof of the heavy-tailed nature of the data. This heavy-tailed observation is further supported by the sample mean excess plot, whose upward trend is an indication of heavy-tailed behaviour. It is therefore evident from the Figure 6.3 and Figure 6.4 that the PCS data displays heavy-tailed behaviour.

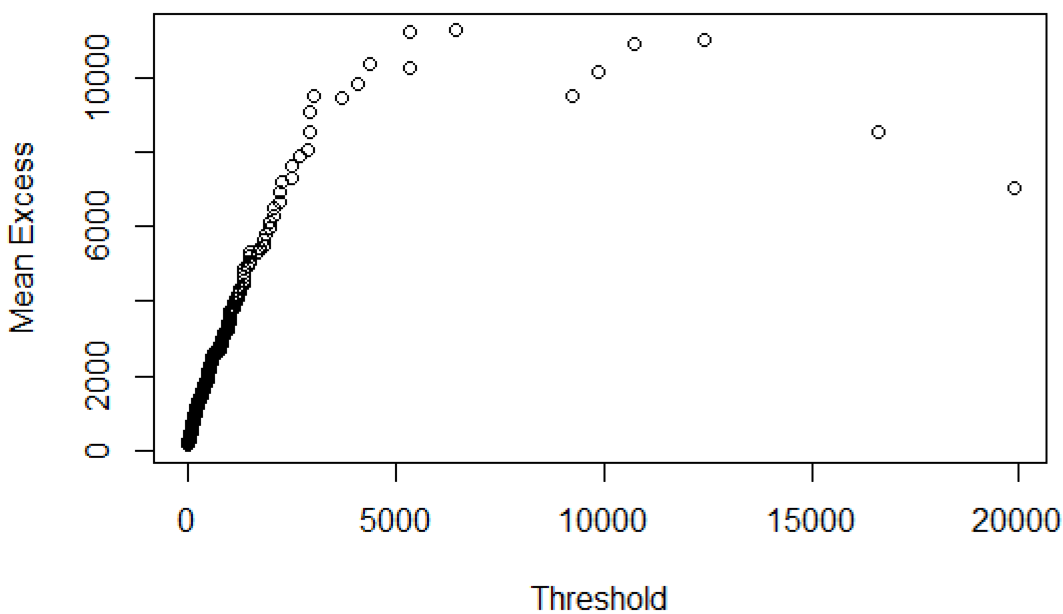

Figure 6.4: *Sample Mean Excess plot of PCS data*

Note: This plot represents the sample mean excess plot for the PCS data, used to further assess the heavy tail characteristics of the data. An approximately straight line indicates Pareto heavy-tailed behaviour, while a flat line indicates medium-tailed behaviour like that of the exponential distribution.

6.4 Finite Mixture Model Fitting

Once the heavy-tailed nature of the data has been established, we now turn our attention to the fitting of the previously defined (see Sub-section 6.2.6) flexible mixture distributions to the data. These include the gamma, burr, weibull, lognormal, and the birnbaum-saunders distributions for the loss severity, and the poisson distribution for the loss frequency. The optimal mixture model under each distribution is chosen based on a low BIC value, and then compared with the other previously defined distributions to pick the overall best fitting mixture model. We use the R software and packages **ForestFit** (Teimouri et al., 2020), **flexmix** (Leisch, 2004; Grün and Leisch, 2008), and **gendist** (Bakar et al., 2016) for these purposes. Results of these tests are given in the following tables, for both the loss frequencies and the loss severity, with *M* representing the number of components making up the mixture; *NLL* the Negative Log-Likelihood value; and *AIC* and *BIC* the Akaike Information Criterion and the Bayesian Information Criterion respectively;

6.4.1 Loss Frequency Model

For the loss frequency model we consider the Poisson distribution, a popular distribution for claim frequency modelling in actuarial applications (see e.g., Burnecki and Kukla (2003), Burnecki et al. (2005), and Albrecher et al. (2004)).

Poisson: X $\sim$ G(λ)

The Poisson distribution function is

$$f(x;\lambda) = \frac{\lambda^x}{x!}e^{-\lambda} \tag{6.38}$$

where $\lambda > 0$ denotes the rate parameter.

M-step maximization of the Q-operator with respect to λ gives the closed form solution

$$\widehat{\lambda}_m^{(k)} = \frac{{}^{n}_{i=1}\,\omega_{im}^{(k)} x_i}{{}^{n}_{i=1}\,\omega_{im}^{(k)}} \tag{6.39}$$

Table 6.2: *EM-based Flexible Mixture Modelling: Loss Frequency*

Distribution	M	NLL	AIC	BIC
Poisson	1	2688.82	5379.64	5384.4
	2	2221.83	4449.66	4463.95
	3	**2159.40**	**4328.8**	**4352.61**
	4	2159.40	4332.8	4366.13

Note: The table provides results of the flexible mixture model fits to the loss frequency data, via the R packages flexmix, ForestFit, and gendist. In the table, M represents the number of components of the distribution that make up the mixture; NLL represents the Negative Log-Likelihood value; and AIC and BIC display the Akaike Information Criterion and the Bayesian Information Criterion respectively, which are used to identify the distribution and components that provide the most optimal fit for the data. The components with the lowest BIC value are highlighted in bold font and represent the mixture model under each distribution with the best fit characteristics.

6.4.2 Loss Severity Model

For the loss severity model, we use the distributions previously defined in section 6.2.

Table 6.3: *EM-based Flexible Mixture Modelling: Loss Severity*

Distribution	M	NLL	AIC	BIC
Lognormal	1	74881.06	149766.1	149778.7
	2	**74745.59**	**149501.2**	**149532.6**
	3	74738.78	149493.6	149543.8
Gamma	1	77159.21	154322.4	154335.0
	2	75267.19	150544.4	150575.8
	3	75183.76	150383.5	150433.8
	4	75033.71	150089.4	150158.5
	5	74936.04	149900.1	149988.0
	6	74877.15	149788.3	149895.1
	7	74840.70	149721.4	149847.0
	8	**74788.23**	**149622.5**	**149766.9**
	9	74780.15	149612.3	149775.6
Birnbaum-Saunders	1	75725.19	151454.4	151466.9
	2	75002.98	150016	150047.4
	3	74933.42	149882.8	149933.1
	4	74845.65	149713.3	149782.4
	5	74785.21	149598.4	149686.4
	6	**74751.00**	**149536.0**	**149642.8**
	7	74749.97	149539.9	149665.6
Weibull	1	75830.63	151665.3	151677.8
	2	75283.79	150577.6	150609.0
	3	75237.39	150490.8	150541.0
	4	75132.79	150287.6	150356.7
	5	75033.06	150094.1	150182.1
	6	74950.18	149934.4	150041.2
	7	74886.95	149813.9	149939.5
	8	**74822.72**	**149691.4**	**149835.9**
	9	74834.14	149720.3	149883.6
Burr	**1**	**83590.17**	**167184.3**	**167196.9**
	2	83590.51	167191.0	167222.4

Note: The table provides results of the flexible mixture model fits to the loss severity data. Here M represents the number of components of the distribution that make up the mixture; NLL represents the Negative Log-Likelihood value; and AIC and BIC display the Akaike Information Criterion and the Bayesian Information Criterion respectively, used to identify the distribution and components that provide the most optimal fit for the data. The components with the lowest BIC value are highlighted in bold font.

The optimisation functions were tested on the Poisson distribution for the loss frequency data; and on five pre-specified distributions for the loss severity data, including the log-normal, gamma, birnbaum-saunders, weibull, and burr distributions. Each category of mixture model was tested, by increasing the mixture components within each distribution until the best fitting mixture was established for each distribution category. The best fitting mixture for a distribution was determined as the mixture that generated the lowest BIC values within said distribution. This was confirmed by testing that the next higher component-mixture for each distribution above the optimal mixture model's components would only produce worse fitting models, that is, higher BIC valued-models instead of lower BICs. These best-fitting mixtures under each distribution are subsequently highlighted in bold font in Tables 6.2 and 6.3. Finally, for the loss severity model, all the highlighted best-fit models were compared with each other to establish the overall best fitting model based on its low BIC. Following this, we can now finally deduce that, overall, the 3-component Poisson flexible mixture model and the 2-component log-normal flexible mixture model provide the best fit for the loss frequencies and the loss severities respectively.

The following table (Table 6.4) displays a comparison of the flexible mixture model fit with other comparable types of mixture models not based on the EM algorithm. The distributions tested are those that have been proposed in previous literature studying such composite models, including Cooray and Ananda (2005); Miljkovic and Grun (2016); and Grun and Miljkovic (2019), among others. We test General Composite Models (GCMs) that model mixtures as truncated distributions, and composite mixture models (CMMs) that fit the data to more than one type of distribution instead of just one, as we have done in flexible mixture modelling. The results are displayed in Table 6.4. Similar to Tables 6.2 and 6.3, the best-fitting models under each category are highlighted in bold font.

Table 6.4: *Model Comparisons: Loss Severity*

Flexible Mixture Model (EM)			
Distribution	NLL	AIC	BIC
2-Component Log-normal mixture	**74745.59**	**149501.2**	**149532.6**

General Composite Models (Newton-Raphson based)			
Distribution	NLL	AIC	BIC
Weibull-Loglogistic	80905.25	161818.5	161824.9
Weibull-Burr	81376.64	162763.3	162771.3
Weibull-Pareto	82317.72	164643.4	164649.8
Weibull-Paralogistic	**80050.61**	**160109.2**	**160115.6**
Lognormal-Pareto	83128.42	166264.8	166271.2

Composite Mixture Models (Newton-Raphson based)			
Distribution	NLL	AIC	BIC
Weibull-Loglogistic	82943.89	165897.8	165905.8
Weibull-Burr	**80849.74**	**161711.5**	**161721.1**
Weibull-Pareto	81098.48	162207.0	162214.9
Weibull-Paralogistic	81541.83	163093.6	163101.6
Lognormal-Pareto	81098.48	162207.0	162214.9

Note: The table gives comparisons between the fit characteristics of the flexible mixture models optimized via the EM algorithm, when compared to other mixture-type models based on Newton-Raphson algorithms, including general composite models and composite mixture models. The columns display the distributions analysed (Distribution), the Negative Log-Likelihood (NLL), and the Akaike Information Criterion (AIC) and Bayesian Information Criterion(BIC) which determine the most optimal models by fit.

Performance analytics for the best models chosen under each mixture type are further analysed and displayed in the table below, with factors including the model's estimate stability and reliability; its computational time; and finally its flexibility and adaptability characteristics.

Table 6.5: *Comparable Model Performance Analytics*

Mixture type	Estimate stability and reliability	Computational time	Model flexibility and adaptability
2-Component Log-normal Finite Mixture Model (EM)	Monotone: Stable and reliable estimates	0.06876183 seconds	Flexible, and the analysis of one distribution type per model ensures ease of distributional additions
Composite Weibull-Burr Mixture Model (Newton-Raphson)	Non-monotone: Reliability and stability of estimates not guaranteed	1.30968 seconds	Flexible, but adding more distributions to mixture model can be comparatively more complicated
Composite Weibull-Paralogistic Model (Newton-Raphson)	Non-monotone: Reliability and stability of estimates not guaranteed	1.231683 seconds	Flexible, but adding more distributions to mixture model can be comparatively more complicated

Note: The models derived from Table 6.4 are further compared in terms of their efficiency, reliability, and flexibility in this Table. The first column displays the type of mixture model, while the remaining three columns display the performance assessment factor, including the model estimates' stability and reliability characteristics, the model's computational time which represents the model's efficiency, and finally the model's flexibility and reliability.

From these two tables it is evident that the EM-based flexible mixture model possesses favourable performance statistics when compared to the other Newton-Raphson-based composite models. We therefore progress with the chosen flexible mixture models to the next section, that is, catastrophe bond valuation and pricing.

6.4.3 Model Application to Catastrophe Bond Valuation

Following the valuation framework detailed in section 2, the claim severity and the claim frequency models are applied to generate the final compound distribution for the underlying aggregate claims process. The parameters generated from the flexible mixture fitting processes in Table 6.2 and Table 6.3 above are displayed below for the overall best mixture models based on the BIC, for the respective loss frequency and loss severity distributions. The matrices display the weights and parameters of the individual component distributions making up the final mixture distributions.

For the loss frequency model i.e., the 3-component Poisson mixture

$$\begin{bmatrix} \text{component} & \text{weight} & \text{parameter} \\ 1 & 0.5913 & 0.7951 \\ 2 & 0.3468 & 1.8683 \\ 3 & 0.1230 & 2.7973 \end{bmatrix}$$

And for the 2-component log-normal mixture loss severity model, the parameters are;

$$\begin{bmatrix} \text{component} & \text{weight} & \mu & \sigma \\ 1 & 0.9760 & 17.2173 & 1.1095 \\ 2 & 0.0240 & 21.3226 & 0.9164 \end{bmatrix}$$

The aggregate distribution is a Compound Poisson Flexible Mixture Model (CPFMM), and this is used to represent the aggregate claims process $\{L_t : t \in [0, T]\}$ (defined in sub-section 6.2.4) in the pricing equation. The CIR model (as defined in sub-section 6.2.3) is applied to represent the interest rate process used to generate the discount factors.

The catastrophe bond valuation equation, previously defined in sub-section 6.2.5, is given as

$$\begin{aligned} V_t &= e^{-\int_t^T r_s ds}\mathbb{E}^{\mathcal{Q}}[P_{CAT}{}^{(1)}|\mathcal{F}_t] \\ &= B_{CIR}(t,T) \;\; \rho + (1-\rho) \times \sum_{n=0}^{\infty} e^{-\lambda_t(T-t)} \frac{(\lambda_t(T-t))^n}{n!} F^{*n}(D) \end{aligned} \tag{6.40}$$

for the *principal-at-risk bond*, given the catastrophe loss distribution $F(x)$ and the claim arrival process N_t, where $F^{*n}(D) = Pr(X_1 + X_2 + ... + X_n \leq D$ is the n-fold convolution of F and B_{CIR} represents the CIR discount rates. If $\rho(0 \leq \rho < 1)$ represents the proportion of principle recovered by the investor at maturity time T if the bond is triggered, then this bond is assumed have a payoff of 1 if it fails to trigger and a payoff of ρ if the bond is triggered. The bond value is then given by V_t, where T is the time to maturity and D is the triggering threshold.

On the other hand, the valuation equation for the *principal-and-coupon-at-risk CAT bond*, also previously defined in sub-section 6.2.5 is given as

$$\begin{aligned} V_t &= e^{-\int_t^T r_s ds}\mathbb{E}^{\mathcal{Q}}[P_{CAT}{}^{(2)}|\mathcal{F}_t] \\ &= B_{CIR}(t,T) \;\; \rho(c+1) + (1-\rho(c+1)) \times \sum_{n=0}^{\infty} e^{-\lambda_t(T-t)} \frac{(\lambda_t(T-t))^n}{n!} F^{*n}(D) \end{aligned} \tag{6.41}$$

given the catastrophe loss distribution $F(x)$ and the claim arrival process N_t. Similar to the principal-at-risk CAT bond equation above, $F^{*n}(D) = Pr(X_1+X_2+...+X_n \leq D$ is the n-fold convolution of F and B_{CIR} represents the CIR discount rates. $\rho(0 \leq \rho < 1)$ represents the proportion of principle and coupon recovered by the investor at maturity time T if the bond is triggered, and now there is the introduction of a fixed coupon c.This bond is thus assumed have a payoff of $c + 1$ if it fails to trigger and a payoff of $\rho(c + 1)$ if the bond is triggered. The bond value is also given by V_t, where T is the time to maturity and D is the triggering threshold.

We now assume an index-linked catastrophe bond with face value $Z = US\$1$, proportion $\rho = 0.7$ and coupon $c = 0.1$ at time $t = 0$. The prices are determined at different thresholds D, based on the annual average loss interval, with the lowest threshold representing a quarter of the average loss and the highest threshold representing three times the average loss; and for different terms to maturity T, ranging from 0.25 to 2.25 years. The the 3D plot of final CAT bond prices assuming the log-normal mixture model are given in figures 6.5a and 6.5b, for the principal-at-risk and the principal-and-coupon-at-risk catastrophe bonds respectively.

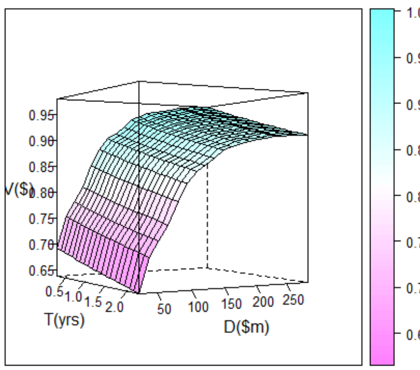

(a) *Principal-at-risk CAT bond prices*

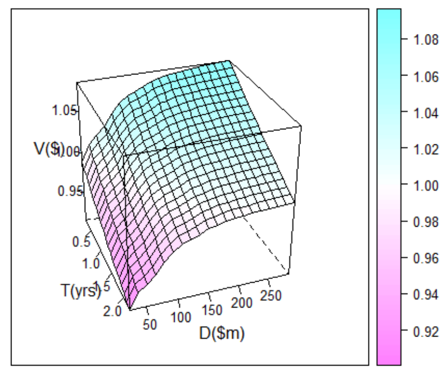

(b) *Principal-and-Coupon-at-risk CAT bond prices*

Note: The figures represent the 3D plots of final CAT bond prices assuming the compound Poisson-log-normal flexible mixture model. Final catastrophe bond prices for the pay-off structures considered are given in figure 6.5a, for the principal-at-risk CAT bond; and figure 6.5b for the principal-and-coupon-at-risk CAT bond. The plot includes the value of the bond in dollars (V($)), the bond term in years (T(yrs)), and the trigger threshold in millions of dollars (D($m)).

Final catastrophe bond prices for the pay-off structures considered are given in figure 6.5a, for the principal-at-risk CAT bond; and figure 6.5b for the principal-and-coupon-at-risk CAT bond. From these figures we can make the following general deductions; index-linked principal-at-risk CAT bond prices fall (higher risk for investors) with an increase in the term of the bond and a decrease in the threshold. This is because as the term increases, the amount of time available for the bond to be triggered also increases, thus increasing the bond's risk. A lower threshold implies that the bond could be triggered much faster (at a lower loss value) than an equivalent bond with a higher threshold. A decrease in the threshold therefore increases the risk of loss for an investor. The coupon bond's higher prices also imply that the penalty for risk is lower when investors receive higher interest payments. These figures prove that EM algorithm-based mixture processes can be efficiently applied to the modelling of catastrophic loss processes for their subsequent use as input to catastrophe bond valuation models.

The significant improvement in computational efficiency, flexibility, and robustness, as detailed in sub-section 6.4.2, also proves this model's superiority over other similar models for the modelling of heavy-tailed data. In addition, the model's flexibility in incorporating heavy-tail characteristics of catastrophic loss data without over-smoothing the tails of the distributions and losing vital information about the specific extreme value processes under consideration, and ensuring better modelling accuracy. In a world of increasing catastrophic losses as detailed in Section 6.1, which have led to more frequent heavier-tailed extreme loss processes (Swiss Re, 2023), the ability of a model to easily incorporate this structure for all types of heavy-tailed processes is especially useful. As these changes can no longer be ignored due to their key influence in determining the level of risk that disaster risk security investors will be taking on, and the high cost of mispricing due to incomplete incorporation of information, it is important that better models are found instead. These model improvements are necessary, especially if the catastrophe market expects to retain its investors and continue protecting its users from such high cost and often disastrous events.

6.5 Conclusion

This study set out to assess the suitability of the EM Algorithm in improving computational efficiency for catastrophe bond valuation. By formulating the convolution problem as an incomplete data problem, the EM Algorithm could be applied to the data to generate parameters for respective finite mixtures that could then be used to approximate the complex convolution function. The best-fitting mixture distribution based on the BIC, the 2-component log-normal mixture for loss severities; and the 3-component Poisson mixture for loss frequencies, were chosen and used to construct the final aggregate loss distribution model, a Compound Poisson Flexible Mixture Model (CPFMM). This claims process was then used to approximate expected payoffs under different catastrophic loss observations. Finally, these expected payoffs are applied to estimate the final bond values of the two CAT bonds defined; a zero-coupon index-linked CAT bond and a coupon index-linked CAT (with both the coupon and principal at risk). Plots are then generated to display the price distribution under different term to maturity and threshold assumptions.

This study has confirmed that the EM Algorithm is a viable alternative for approximating the claim size distribution for heavy-tailed data, therefore contributing to the sparse literature on approximating heavy-tailed distributions. The approximation is also flexible in terms of weight distributions, as the practitioner can reallocate weights if their future assumptions differ form current catastrophic risk assumptions. The EM algorithm is also a numerically stable and fast machine learning technique, and thus more computationally efficient than some other techniques frequently applied to approximate the convolution e.g. Monte Carlo simulation techniques.

Even though this study has successfully applied the EM algorithm in approximating the convolution function, it was only conducted for five heavy-tailed distributions; the Burr, the log-normal, the gamma, the Birnbaum-Saunders and the Weibull. The EM Algorithm does not always converge for all distributions, and further tests still need to be conducted to assess such distributions further and propose extensions to the classical EM Algorithm that can improve the algorithm's convergence properties. Some of these techniques include the Stochastic EM Algorithm (Celeux et al., 1996) and the Monte Carlo EM (Wei and Tanner, 1990) for simulating the expectation step when the E-step is complex, either because it is a large sum or a high-dimensional integral (Nielsen, 2000); and the Generalized EM (GEM) and the Expectation-Conditional Maximization (ECM) (Ng et al., 2011) to facilitate simulation of the M-step.

In conclusion, this study has been able to recommend an alternative efficient technique for approximating the convolution that is both flexible and fast. This is useful especially for those practitioners looking to reduce their computational costs while still retaining flexibility of assumptions. The EM Algorithm also includes numerous extensions that could be alternatively applied if the classical EM fails for a given model, thus providing robust and extensive application options.

Chapter 7

Moving Beyond 'Independent and Identically Distributed' Catastrophe Loss Processes via Hidden Markov Models and the Baum-Welch Algorithm

In the recent years, shifting climate and demographic trends have led to a general rise in the occurrence and severity of catastrophe events. This has increased the need for extensive and efficient risk models to aid the risk assessment and decision-making process. Due to the complexity of the catastrophe loss modelling process, however, there has been a heavy reliance on simplifying assumptions, key among these being that observations are independent and identically distributed. Many catastrophe loss processes rarely meet this assumption, however, and this effect has been further expounded by the changing climate and demographic trends. It is therefore important to find methods that incorporate both dependencies and seasonality into loss models. This study proposes a standardized approach that models loss clusters generated from dependent and non-stationary processes as catastrophe 'states' through the use of Hidden Markov Models and the Baum-Welch algorithm, a special case of Expectation-Maximisation algorithms. We assess the presence, extent and distribution of clusters through extreme

value techniques, and thereafter use hidden markov models to identify the optimal dependent mixture loss models for both loss severity and frequency. A compound markov-dependent (CMDMM) mixture model is then generated for the chosen mixtures and used to generate aggregate losses that serve as input for a catastrophe bond valuation process.

7.1 Introduction

Climate change effects arising chiefly from human-activity-linked global warming and demography-based trends related to economic growth, urbanisation, asset accumulation, and rising population densities, especially in high natural-peril exposure localities have continued to worsen the frequencies and magnitudes of losses stemming from catastrophic events, especially those linked to natural disaster events. According to Swiss Re's Research Institute Sigma, such effects contributed to record losses within the past two decades, with the highest insured loss years all falling within the most recent two decades. These include the years 2022 ($125billion), 2005($155billion), 2011($158billion), and finally the year 2017($173 billion), which had the highest insured loss values as of 2023 (Pande, 2023). This trend is expected to continue in the long-term, especially since projected long-term increases in global population from the current estimate of 8 billion to 10 billion in 2060 are expected to cause further increases in emissions and warming levels, according to the European Commission's Joint Research Committee (Vesnic, 2023). This implies that, unless there is drastic intervention, the world will continue to bear heavier costs from catastrophic events as losses mount.

So far, disaster risk insuring and financing institutions have had to bear the brunt of these rising costs, especially in more developed economies where insurance is a popular risk transfer option for individuals and institutions. As insurers generally rely on the pooling and diversification of risks to allow them to take on greater risk (see e.g., Rejda and McNamara, 2005), any extreme concentrations of risk can render such institutions insolvent. It is therefore crucial, for their own survival, that institutions in the business of taking on such extreme losses make such decisions only after thorough due diligence and analysis of the risks involved and the costs borne in the worst-case scenarios. In addition, and due to the aforementioned changes in climate and demographics, the need for efficiency in comprehensive risk assessment and modelling in light of these changes and trends is even greater, due to increasing volatility of losses introduced by trends (Swiss Re, 2023). For this reason, researchers have dedicated great effort over the years to the modelling of extreme loss events, to allow better risk incorporation for decision making. Some of these key studies on extreme event loss modelling are summarized below.

Starting from the late 1980s and early 1990s, theoretical developments in the modelling of univariate time series extremes proposed the most common approaches applied to date in catastrophe loss modelling. The most popular of these include the Fisher-Tippett Theorem for block maxima modelling via the generalized extreme value (GEV) distribution(Fisher and Tippett, 1928; Falk, 1994; Gumbel, 1958) and the Pickands-Balkema-de Haan Theorem for the exceedances over thresholds modelling via the generalized pareto distribution (GPD) (Gnedenko, 1943; Balkema and Haan, 1974; Pickands, 1975). Both approaches, though different, lead to closely related descriptions of extremes (Chavez-Demoulin and Davison, 2012). These techniques relied heavily on the assumption of independent and identically distributed data; and an implied data sufficiency above a given high threshold for their asymptotic theories of sample extremes to continue to hold (see e.g. McNeil (1997), Embrechts et al. (1997) and Resnick (1997)).

The 'independence and identical distribution' (IID) assumption was essential to the simplification of the extreme value modelling process, making it straightforward to generate estimates and model heavy-tailed data via extreme value theory (McNeil, 1997) for an otherwise complex process. It is not always the case, however, that catastrophic events generate independent or even identically distributed data (Fawcett, 2013). Recent climate trends and demographic changes, previously discussed in this section's first paragraph, however, have meant that relying on such simplifying assumptions can no longer aid in generating models that serve as reliable representations of reality. Assuming independence for dependent data would mean the under-estimation of standard errors for such a process (Davison and Smith, 1990), and assuming non-identically distributed observations possess identical distributions would lead to unreliable and even erroneous estimates.

This diversion is especially evident in events that are seasonal by nature e.g., meteorological events like windstorms and hurricanes that lead to the clustering of losses within the time of the year when the event is said to occur most frequently. The Atlantic and the East Pacific seasons in the US, for example, imply higher meteorological event occurrences between June 1st and November 30th of every year, according to the US National Oceanic and Atmospheric Administration (NOAA) (NOAA, 2022). In addition, and according to Simpson et al. (2020), even in cases where the event is non-seasonal, there can be instances of clustering in the tails of the distribution, implying that extreme losses tend to occur together. This can complicate the analysis, since new analysis techniques then need to be generated to match with the event under consideration, and since these events are rarely similar in nature, this can lead to a myriad of models without a single standardized approach.

Previously, researchers attempted to address these issues by focusing on the origin of the clustering and developing techniques to model such sources. This means that, of the two main sources of clustering historically identified, i.e., seasonality and temporal dependence (see e.g., Davison and Smith (1990) and Fawcett (2013)), the developed modelling approaches focused only on one or the other. Studies that focused on addressing temporal dependence issues include Davison and Smith (1990) and Simpson et al. (2020), while those that studied seasonality include Davison and Smith (1990)(this was modelled as a separate issue from temporal dependence); Smith (1989), Towe et al. (2019), and Herrmann and Hibbeln (2021). These studies are further discussed in the subsequent literature review section. These two issues were rarely considered in tandem, even though it has been shown that it is possible to encounter both in extreme event loss modelling (see e.g., Davison and Smith (1990) and Fawcett (2013)). In cases where both sources underly the clustered nature of loss observations, addressing only one aspect leads to an incomplete loss model and subsequently inefficient valuation of disaster risk instruments. This can be costly, not only to the issuer, who then has to pay for the model-based risks that their investors have to take on due to model reliability limitations and any other perceived information asymmetries introduced by incomplete models.

Furthermore, since these approaches focused heavily on modelling the tail dependencies in the dataset by assuming this was an independent phenomenon, the possible causalities between tail dependence and main sample dependence were ignored. These dependencies are a real possibility, however, since some of the seasonal characteristics of an event, which we assume are the main cause of in-sample clustering, can magnify its heavier (tail) losses . It is widely understood, for example, that specific events display heavier losses during specific times of the year, like the previously mentioned US hurricane season between June 1st and November 30th (NOAA, 2022), or wildfire events that mainly occur during dry periods. In addition, it is within such seasons that heaviest event losses are observed, based on historical data (see e.g., NOAA, 2022; Swiss Re, 2023), and catastrophic tail risk increases significantly.

To adequately address these issues therefore, we would need a more standardized technique that would focus on the typical structure of a non-IID dataset and attempts to adequately model this structure. Thereafter, the assumed origin of the observed structures could be used to explain the clustering structure or distributions observed for different processes, thereby accounting for most of the sources of such phenomena. We accomplish this by applying Hidden Markov Models (HMMs) and the Baum-Welch algorithm (a special case of Expectation-Maximisation algorithms) to model ‘clusters’ for a heavy-tailed loss process that exhibits both the characteristics of non stationarity/seasonality and tail dependence. We also model this ‘clustering’ structure for both the underlying loss frequency and loss severity processes, as these both determine the extent of aggregate losses. We investigate the differences in the clustering distributions, length of clusters, and the total number of required states to accurately account for the cluster distributions. Thereafter, the recommended Hidden Markov Models (HMMs) are used to develop a Compound Markov-Dependent Mixture Model (CMDM) for the aggregate catastrophic loss process, whose estimates are then used as inputs in a catastrophe bond valuation model.

Hidden Markov models, developed in the 1960s by Baum and Petrie (1966) and Baum and Eagon (1967), are a numerically efficient maximum likelihood optimization technique that have been shown to be reliable for modelling heterogeneous dataset, especially when the heterogeneity is unobserved (Zucchini et al., 2016). Since we assume that each cluster represents a 'state' of the loss process, Hidden Markov Models are useful for the identification of a loss process's underlying states that drive the observed loss estimates. This technique also focuses on 'general clustering', whether due to dependence and stationarity, since both lead to non-IID observations. The flexibility in the state distributions and weights also guarantees that heavier tails can be incorporated into the model to account for increased loss severity due to climate and demographic trends on loss distributions.

Our contribution is therefore as follows. First, we identify and assess the extent of 'clustering' in heavy-tailed catastrophe loss data. Thereafter, we apply Hidden Markov models and the Baum-Welch algorithm (a special case of Expectation Maximisation Algorithms) to model these 'clusters' and propose fitting dependent mixture models for both the catastrophe loss severity and loss frequency processes. The proposed models, which, in our case are the 4-state Log-normal and the 3-state Poisson HMMs for the loss severity and loss frequency models respectively, are then used to formulate a compound mixture distribution for aggregate losses. These aggregate losses are then applied for catastrophe bond valuation and the respective price estimates plotted.

The development of a Compound Poisson Markov-Dependent Model (CPMM) for the incorporation of seasonality and time-based dependence is of significant consequence, especially now in the face of developing climate and demographic trends that have led to increased catastrophic loss frequencies and loss severities. Models that are able to incorporate changes introduced by these trends, especially those related to dependence of losses and more extreme seasonality elements of disaster events are particularly necessary to allow for more comprehensive and fair pricing of disaster risk financing instruments, including catastrophe bonds.

This study's contributions are therefore of particular use to risk and catastrophe loss modellers, who are tasked with the role of incorporating all elements underlying catastrophic risk processes as comprehensively as possible; disaster risk financing security issuers, who use the results of such analysis to determine their disaster risk financing options and estimate market prices; and finally, disaster risk security investors, who then rely on these models to set the prices offered under each security based on its overall implied risks. This study therefore allows improvements in the overall disaster risk modelling, and ultimately financing, and risk management fields for catastrophic events in a changing climate and demographic landscape.

The rest of this article is structured as follows: Section 7.2 summarises key literature in dependence and non-stationarity modelling, Section 7.3 specifies the model and the algorithms; Section 7.4 details the numerical analysis and model estimation process, including the model application to catastrophe bond valuation; and Section 7.5 concludes the study.

7.2 Previous Literature

Prior to the turn of the century, heavy-tailed losses models had garnered considerable interest due to the increase in severity of high-loss events observed in the early 1990's, especially, with Hurricane Andrew and the Northridge earthquake [1]. This led to growing need for insurance securities that could address the capital flight from insurance and reinsurance markets due to the increase in event risk. Researchers during this time therefore proposed and applied extreme value models to the available heavy-tailed loss

[1] https://www.verisk.com/verisk-review/archived-articles/top-10-historical-hurricanes-and-earthquakes-in-the-u-s/

data, mainly Danish Fire Insurance data [2], to provide a reference point for practitioners to base their own risk assessment and quantification models. These extreme value theories were neatly summarized by several authors, including McNeil (1997), Resnick (1997) and Embrechts et al. (1997).

Original parametric techniques were heavily based on extreme value theories due to such developments in extreme event modelling theory and its applications. These include the Fisher-Tippett-Gnedenko theorem for Generalized Extreme Value distributions (Fisher and Tippett, 1928; Falk, 1994; Gumbel, 1958) and the Pickands Balkema-De Haan theorem for the Generalised Pareto distributions (GPD)(Gnedenko, 1943; Balkema and Haan, 1974; Pickands, 1975). These theories all relied on the assumption that data was independent and identically distributed; and on the assumed sufficiency of the samples in analysis, especially after accounting for the reduction in available sample sizes due to the high thresholds (McNeil, 1997). In cases of data insufficiency however, these theories fall apart due to the low thresholds. Data insufficiency is, unfortunately a common problem plaguing extreme value analysis problems, due to the long waiting intervals before extreme events occurred in the past, and limited access to the available data due to heavy costs of data collection and modification. Because of this, extreme event data is rarely available in sufficiency, and rarely independent and identically distributed when available. The lack of independence and/or stationarity can be due to either the underlying seasonal nature of the events; or temporal dependence characteristics, or both (Davison and Smith, 1990).

To address these issues, past researchers focused on addressing each source of deviation separately. One of these sources; temporal dependencies as a result of serial correlation, has received considerable attention compared to other sources like seasonality. Leadbetter et al. (1983) addressed extreme dependent processes by developing a theory to derive the maxima of dependent, but stationary extremes. The Leadbetter's condition allowed the long-range dependence of an extreme process to be weak

[2] This data comprises of loss observations describing large fire insurance claims in Denmark between 3rd January 1980 and 31st December 1990 (see e.g., McNeil (1997))

enough, thus lessening its impact on the asymptotics of an extreme value analysis (Fawcett, 2013).

Due to this condition, tail dependence is rarely an issue in the block maxima approaches (Charpentier, 2016). This is because in most cases, we can comfortably assume that long-range dependence is weak and model the process as independent (Fawcett, 2013). Block maxima, however, wastes a lot of data in an already data-scarce process, and is therefore a less preferred approach when compared to the threshold exceedances approaches (Charpentier, 2016).

For threshold exceedances, however, serial correlation is a major challenge, and the data would require modifications to allow the application of Generalised Pareto Models for parameter estimation. This is because serial correlation is mainly observed in threshold exceedances, due to the structure of this approach; while the underlying theory assumes independent observations. This can be addressed through a number of techniques summarized in Fawcett (2013) and listed below.

The first approach involves extracting an approximately independent sample of threshold exceedances through a declustering approach e.g., the runs declustering method (Davison and Smith, 1990). This approach, though popular, has been shown by Fawcett and Walshaw (2012) to be sensitive to the choice of 'declustering parameter'. The second approach ignores this dependence and fits the Generalised Pareto Distribution, thereafter the estimates are adjusted to reflect the effects of dependence. The third approach directly models these dependencies through multivariate extreme value techniques (e.g., Simpson et al., 2020).

The second source of deviation; non-stationarity in catastrophe loss processes, arises mainly due to inherent seasonality in catastrophic events; or due to changing climate trends (Davison and Smith, 1990; Smith, 1989). These effects have been shown to affect security valuation and yield volatilities for the respective events (e.g., Herrmann and Hibbeln, 2021). In addition, it has been shown that incorporating this non-stationarity could significantly improve models used in the risk assessment process (Towe et al., 2019).

Contrary to temporal dependencies; there are no general theories to describe non-stationary extremes. This means that non-stationarity is generally modelled by analysing the seasonal structures of the events under consideration (e.g., Rootzén and Katz, 2013) and most models are therefore specific to the event under consideration. Some approaches have been proposed in literature to address seasonality (Fawcett, 2013), and are summarised below.

The first approach involves fitting the model only to the season that displays the most extreme behaviour. This approach assumes that seasonal stationarity holds for these extreme seasons, which can be a limitation. In addition, the approach leads to significant wastage of data. The second approach attempts to ensure that seasonal stationarity holds better by assuming a longer timeline for the seasonal event. This approach picks an 'extreme time of the year' e.g., the Atlantic season for meteorological events in the US that runs from June 1st to November 30th. Even though this approach fits the 'seasonal stationarity' assumption better than the single season approach, it faces limitations in a changing climate, as this assumption then no longer holds. In addition, the approach relies on the assumption that we can safely ignore the non-extreme period as it is assumed to add little information to observed extremes. However, this can be a dangerous assumption, especially given current climate trends. It has been observed that some events, for example, wildfires[3] are now occurring further and further away from their expected 'season'; and lasting longer than their seasonal timelines. The third approach, analysed in Fawcett and Walshaw (2006), focuses on the application of smoothly varying seasonal parameters for the Generalised Pareto process. The authors found little improvement over the 'extreme time' seasonal approach above, however.

Alternative approaches (Davison and Smith, 1990) include 'pre-whitening' (e.g., Pugh and Vassie, 1980; Tawn et al., 1989), which removes the identified seasonal components before modelling the observations; and the 'separate seasons' approach (e.g.,

[3]https://www.theguardian.com/world/2021/oct/10/wildfire-climate-emergency-us-west

Smith, 1989; Carter and Challenor, 1981); where the year is split into its respective seasons and separate models fitted to each season. This is the approach that is most similar to this study's, with the exception that this study fits the season-states by optimization, and this fit is accomplished for both temporal dependencies and seasonality. Other approaches include the use of a periodic function in the intensity parameter estimation process to account for seasonality (Hainaut, 2012) and the use of pre-season indicators (Zhang et al., 2022).

Aside from models focusing on the sources of deviation; general 'clustering' approaches have also been applied in literature. The main approaches focused on modelling the number of clusters and thereafter determining the underlying cluster distribution. This distribution was then merged with a suitable claim severity distribution and its cluster maxima derived (e.g., Mendes and Lima, 2005; Mendes, 2006). These approaches can be linked to Leadbetter's approach for deriving cluster maxima (Leadbetter et al., 1983; Davison and Smith, 1990), and are therefore assumed to be particularly useful for temporally dependent processes.

This study adopts a 'general clustering' approach as well, but instead of modelling the number of clusters, we assume the clusters are generated from interrelated processes, and can therefore be grouped into descriptive states. These states would be much fewer than the number of clusters, since some clusters are seasonally recurrent. We model these states instead, through maximum likelihood optimization techniques, assuming they are the real drivers of the observed extremes. The next section details the hidden markov model that is used to accomplish this task.

7.3 Model Specification

7.3.1 The Hidden Markov Model

A Hidden Markov Model (HMM) is an unsupervised machine learning technique that was developed as a way to handle processes displaying considerable heterogeneity in observations. These include instances of over-dispersion from typically assumed distributions; or cases of serial dependence (Zucchini et al., 2016). In addition, HMMs allowed researchers to model unobserved 'cycles' or 'hidden states' in cases where observations were assumed to be generated from underlying hidden processes, effectively ensuring all underlying information was incorporated into the final model. Over time, HMMs have found applicability in signal processing, especially in speech recognition (Juang and Rabiner, 1991); in biological gene sequencing (Durbin et al., 1999); hydrological event modelling; and in financial returns tracking.

Under HMMs, observations are assumed to have been generated from an underlying unobserved state process satisfying the Markov property. The observation X_t at time t is stochastically generated, but the state S of this process is hidden, that is, it is not directly observable. The states are only observable through their observations. These hidden state process satisfies the Markov property, meaning that the state S_t at time t depends only on the previous state S_{t-1} at time $t-1$; assuming a first-order Markov model. As the complete state sequence is not known, the expected log-likelihood is maximized as opposed to the direct log-likelihood maximization. To accomplish this, the Expectation-Maximization algorithm thus needs to be employed. For this specific study, the observed data is represented by the catastrophic loss data, and the unobserved or hidden states are derived based on seasonal and time-dependent groupings of the data via the Expectation-Maximization (Baum-Welch in this case) algorithm.

The joint distribution of the hidden state process and its respective observations process for this first order HMM is expressed as (see e.g., Degirmenci (2014) and Rabiner (1989));

$$P(S_{1:N}, X_{1:N}) = P(S_1)P(X_1|S_1)\prod_{t=2}^{N} P(S_t|S_{t-1})P(X_t|S_t) \tag{7.1}$$

where $S_{1:N} = S_1, ..., S_N$. Alternatively, Equation 1 can be written as;

$$P(X_{1:N}, S_{1:N}) = P(S_1)\prod_{t=1}^{N} P(S_t|S_{t-1})\prod_{t=2}^{N} P(X_t|S_t) \tag{7.2}$$

The HMM is characterised by five elements (see e.g., Helske and Helske (2019), Degirmenci (2014), and Rabiner (1989));

1 The *observed state sequence* $X = (X_1, X_2, ..., X_T)$ with distinct observations $\omega \in \{1, ..., \Omega\}$.

2 The *hidden state sequence* $S = (S_1, S_2, ..., S_T)$ with hidden states $k \in \{1, ..., K\}$.

3 The *initial state distribution*, π, which is a $K \times 1$ vector of probabilities $\{\pi_k\}$. π_k gives the probability of starting from hidden state k;

$$\pi_k = P(S_1 = k); \qquad k \in \{1, ..., K\} \tag{7.3}$$

4 The *state transition matrix*, $\mathbf{A}$, a $K \times K$ matrix $\{A_{kj}\}$. A_{kj} is the probability of transitioning from hidden state k at time $t-1$ to hidden state j at time t;

$$A_{\{kj\}} = P(S_t = j | S_{t-1} = k); \qquad k, j \in \{1, ..., K\} \tag{7.4}$$

where $\ _j A_{kj} = 1$.

5 The *emission matrix*, $\mathbf{B}$, an $\Omega \times K$ matrix $\{B_k(\omega)\}$. $B_k(\omega)$ is the probability of the hidden state k emitting the observed sate ω;

$$B_k(\omega) = P(X_t = \omega | S_t = k); \qquad k \in \{1, ..., K\}; \quad \omega \in \{1, ..., \Omega\} \tag{7.5}$$

7.3.2 Model Considerations

Three considerations govern the applicability of HMMs to real-world applications, according to Rabiner (1989). These include

The Evaluation Problem

Given the model parameters defined above, define the HMM model θ as;

$$\theta = (A, B, \pi) \tag{7.6}$$

Given θ and the sequence of observations $X_1, ..., X_N$, this problem involves determining the probability that the observation sequence $X_1, ..., X_N$ was generated from the HMM model θ, that is;

$$P(X_{1:N}|\theta) \tag{7.7}$$

This problem can also be summarized as;

$$\text{Given} \qquad \theta, X_{1:N} \longrightarrow \text{Estimate} \qquad P(X_{1:N}|\theta) \tag{7.8}$$

This can be solved through the Forward Algorithm (see e.g. Murphy (2012), Degirmenci (2014)).

The Forward Algorithm

In this algorithm, forward filtering is applied to derive filtered marginals $P(S_t|X_{1:T})$ through a two-step process (Degirmenci, 2014). The 'prediction' step uses the current computed probability to estimate the probability of the proceeding time step, that is;

$$\begin{aligned} P(S_t|X_{1:t-1}) &= ... \\ &\sum_{i=1}^{K} = P(S_t = j|S_{t-1} = i)P(S_{t-1} = i|X_{1:t-1}) \end{aligned} \tag{7.9}$$

This probability then acts as the new prior for time t. The 'update' step then applies the Bayes rule to the observations at time t to generate the forward probabilities;

$$\begin{aligned} \alpha_t(j) &\triangleq P(S_t = j|X_{1:t}) \\ &= P(S_t = j|X_t, X_{1:t-1}) \\ &= \frac{P(X_t|S_t = j, X_{1:t-1})P(S_t = j|X_{1:t-1})}{{}_j\, P(X_t|S_t = j, X_{1:t-1})P(S_t = j|X_{1:t-1})} \\ &= \frac{1}{C_t} P(X_t|S_t = j)P(S_t = j|X_{1:t-1}) \end{aligned} \tag{7.10}$$

where C_t is a normalisation constant, given by;

$$C_t \triangleq P(X_t|X_{1:t-1}) = \sum_{j=1}^{K} = P(X_t|S_t = j)P(S_t = j|X_{1:t-1}) \tag{7.11}$$

$\alpha_t = P(S_t|X_{1:T})$ is a $K \times 1$ matrix.

The Decoding Problem

Given the HMM model θ and observations $X_1, ..., X_N$, in this problem we would seek to determine the most probable hidden state sequence $S_1, ..., S_N$ which would best explain the observations $X_1, ..., X_N$. This is solved using the Viterbi algorithm (see e.g. Murphy (2012), Degirmenci (2014)).

Viterbi Algorithm

The Forward Algorithm calculates $P(X_{1:N}|\theta)$ by summing over all state sequences; but the Viterbi Algorithm approximates $P(X_{1:N}|\theta)$ with $\hat{P}(X_{1:N}|\theta)$, which uses the most probable state sequence instead of all state sequences.

The Viterbi Algorithm finds the most likely state sequence;

$$\hat{P}(X_{1:N}|\theta) = max_S[P(X_{1:t}, S_{1:t}|\theta)] \tag{7.12}$$

where S is the most likely state sequence.

The probability of the most probable state of length t and ending at state j is given by

$$\delta_j(t) = max_{S_1,...,S_(t-1)}[P(X_{1:t}, S_t = j|\theta)] \tag{7.13}$$

Where $S_1, ..., S_{t-1}$ is the most probable state sequence. As with the forward algorithm, δ can be derived recursively;

$$\delta_j(t) = max_i[\delta_i(t-1)A_{ij}B_j(X_t)] \tag{7.14}$$

The Learning Problem

The final problem, and the most important and complex, focuses on adjusting the HMM parameters to optimize $P(X_{1:N}|\theta)$. This is solved through the Baum-Welch Algorithm (Baum et al., 1970; Baum, 1972; Welch, 2003), which also requires the forward and backward probabilities α and *beta* from the Forward-Backward algorithm as inputs. The Baum-Welch Algorithm is a special case of the EM Algorithm (Dempster et al., 1977) for hidden markov models, implying therefore, that this step is essentially completed via the EM Algorithm.

The Forward-Backward Algorithm

Using the forward probabilities α from the Forward Algorithm, we can compute the backward probabilities and derive the smoothed marginals. We begin this process by defining the probability that the hidden state at time t is j;

$$\begin{aligned} P(S_t = j|X_{1:N}) &\propto P(S_t = j.X_{t+1:N}|X_{1:t}) \\ &\propto P(S_t = j|X_{1:t}P(X_{t+1:N}|Z_t = j, X_{1:t}) \end{aligned} \tag{7.15}$$

If we define the smoothed posterior marginal by

$$\gamma_t(j) \triangleq P(Z_t = j|X_{1:N}) \tag{7.16}$$

Equation 7.3.2 above can then be rewritten as

$$\gamma_t(j) \propto \alpha_t(j)\beta_t(j) \tag{7.17}$$

with

$$\beta_t(j) \triangleq P(X_{t+1:N}|S_t = j) \tag{7.18}$$

representing the conditional likelihood of future observations. Through recursion, β can now be computed as;

$$\begin{aligned} \beta_{t-1}(i) &= P(X_{t:N}|S_{t-1} = i) \\ &= \sum_j P(S_t = j, X_t, X_{t+1:N}|S_{t-1} = i)...P(S_t = j, X_t|S_{t-1} = i) \\ &= \sum_j P(X_{t+1:N}|S_t = j)P(X_t|S_t = j, , S_{t-1} = i)...P(S_t = j|S_{t-1} = i) \\ &= \sum_j \beta_t(j)\psi_t(j)\mathbf{A}(i, j) \end{aligned} \tag{7.19}$$

The smoothed posterior γ_i is then given by

$$\gamma_i = \frac{\alpha_i \odot \beta_i}{_j(\alpha_i(j) \odot \beta_i(j))} \tag{7.20}$$

The Baum-Welch Algorithm

Given a sequence of observations $X_1, ..., X_N$ we would like to solve

$$argmax_\theta P(X;\theta) = argmax_\theta \sum_S P(X, S; \theta) \tag{7.21}$$

through maximum likelihood estimation. However, the summation function is computationally complex, and the model parameters are therefore estimated through the EM Algorithm instead. This involves two steps; the Expectation Step (E-step) and the Maximisation Step (M-Step).

The E-step is expressed as (Murphy, 2012; Degirmenci, 2014);

$$\begin{aligned}\gamma_{tk} &\triangleq P(S_{tk} = 1 | X, \theta^{old}) \\ &= \frac{\alpha_k(t)\beta_k(t)}{\sum_{j=1}^{N} \alpha_j(t)\beta_j(t)}\end{aligned} \tag{7.22}$$

$$\begin{aligned}\xi_{tjk} &\triangleq P(S_{t-1,j} = 1, S_{tk} = 1 | X, \theta^{old}) \\ &= \frac{\alpha_j(t) A_{jk} \beta_k(t+1) B_k(X_{t+1})}{\sum_{i=1}^{N} \alpha_i(t)\beta_i(t)}\end{aligned} \tag{7.23}$$

In the M-step, the parameters maximising $P(X_{1:N}|\theta)$ are determined as follows;

$$\hat{\pi}_k = \frac{\mathbb{E}[N_k^1]}{N} = \frac{\gamma_{1k}}{\sum_{j=1}^{K} \gamma_{1j}} \tag{7.24}$$

$$\hat{A}_{jk} = \frac{\mathbb{E}[N_{jk}]}{\sum_{k'} \mathbb{E}[N_{jk}]} = \frac{\sum_{t=2}^{N} \xi_{tjk}}{\sum_{l=1}^{K} \sum_{t=2}^{N} \xi_{tjl}} \tag{7.25}$$

$$\hat{B}_{jl} = \frac{\mathbb{E}[M_{jl}]}{\mathbb{E}[N_j]} = \frac{\sum_{t=1}^{N} \gamma_{tl} X_{tj}}{\sum_{t=1}^{N} \gamma_{tl}} \tag{7.26}$$

$$\theta^{new} = (\hat{A}, \hat{B}, \hat{\theta}) \tag{7.27}$$

This algorithm uses, as inputs, the forward and backward probabilities from the Forward-Backward Algorithm.

Baum-Welch Algorithm (Degirmenci, 2014)

1. Input: $X_{1:N}$, $\mathbf{A}$, $\mathbf{B}$, α, β
2. **for** $t = 1 : N$ **do**
3. $\gamma(:,t) = (\alpha(:,t) \odot \beta(:,t))./sum(\alpha(:,t) \odot \beta(:,t));$
4. $\xi(:,:,t) = ((\alpha(:,t) \odot A(t+1)) \star (\beta(:,t+1) \odot B(X_{t+1}))^T)./sum(\alpha(:,t) \odot \beta(:,t));$

5. $\hat{\pi} = \gamma(:,1)./sum(\gamma(:,1));$

6. **for** $j = 1 : K$ **do**

7. $\hat{A}(j,:) = sum(\xi(2:N,j,:),1)./sum(sum(\xi(2:N,j,:),1),2);$

8. $\hat{B}(j,:) = (X(:,j)^T\gamma)./sum(\gamma,1);$

9. Return $\hat{\pi}, \hat{A}, \hat{B}$

7.4 Numerical Analysis

7.4.1 Exploratory Data Analysis

We test Hidden Markov Models on meteorological event[4] data from the US's Property Claim Services (PCS), which provides industry loss estimates of historical catastrophic events. The data, which consists of 3143 observations between 12th January 1985 and 12th April 2014, [5] includes the affected states, the perils, and the loss estimates. This meteorological event data is extracted from a larger dataset of 3951 observations consisting of all major loss events including earthquakes and wildfires. The meteorological events i.e., hurricanes, tropical storms and other wind and thunderstorm events;[6] were chosen due to their common underlying drivers, their large sample size and the possible seasonal and tail dependent components in such events. The individual losses, which

[4]As defined by Munich Re in https://www.munichre.com/topics-online/en/climate-change-and-natural-disasters/natural-disasters.html

[5]The data is only used for applicational purposes. The timeline from January 1985 to April 2014 is a result of data unavailability due to extreme data costs for individual researchers after this period. The data was deemed acceptable to use as it was only used to fit the model and prove that the model could be applied to heavy-tailed data. Other recent studies have applied an even older dataset, the Danish Fire data, that spans the period beginning January 1980 and ending December 1990 for similar purposes (see e.g Miljkovic and Grün (2016)).

[6]As defined by Munich Re in https://www.munichre.com/topics-online/en/climate-change-and-natural-disasters/natural-disasters.html

were adjusted for inflation to their 2014 values using the US Consumer Price Index (CPI), range from approximately 1 million US dollars at minimum to over 30 billion US dollars at maximum, showing just how dispersed this dataset is.

The time series plot of this dataset is given in Figure 7.1 below;

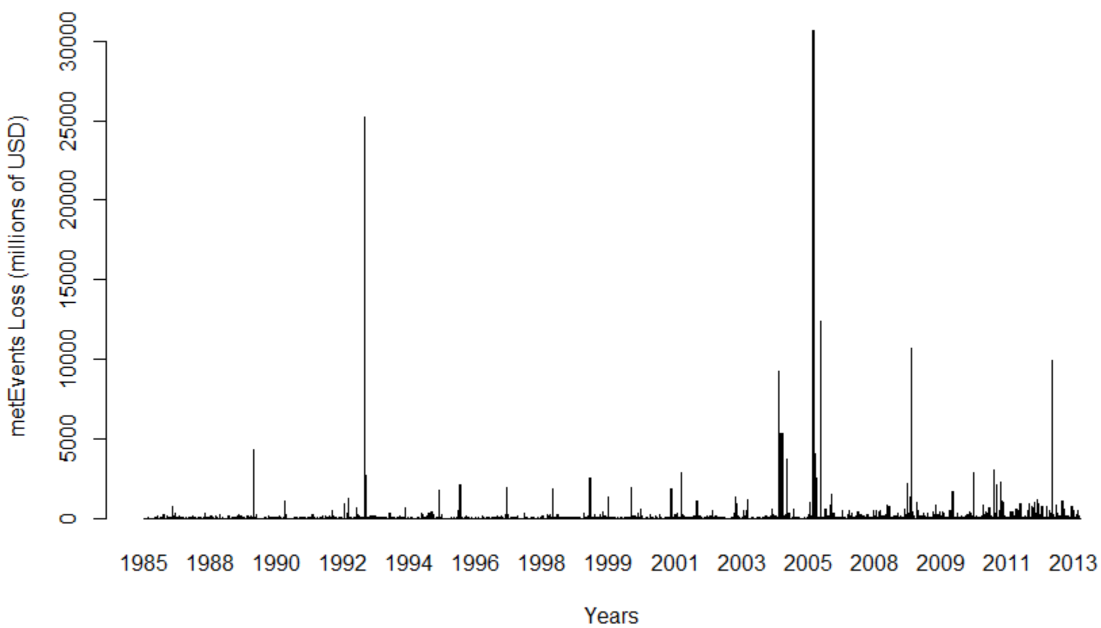

Figure 7.1: *Time Series Plot of Meteorological Catastrophe Losses*

Note: This time series plot provides a graphical summary of catastrophic industry loss estimates from meteorological loss events, including hurricanes, tropical storms and other extreme wind and thunderstorm events. The data was provided by the US's Property Claims Services (PCS) and spans the period from January 1985 to April 2014. The individual loss estimates were adjusted for inflation to their 2014 values using the US Consumer Price Index (CPI). Loss estimates are displayed in millions of US dollars on the y-axis, while the x-axis displays the respective dates.

The time series plot allows us to identify the periods of most extreme losses and any signs of data clustering, especially in large losses. From Figure 7.1 we can see that the years 1989, 1992, 2001, 2004-2005, 2008-2009, 2011 and 2012-2013 experienced the most extreme catastrophic events. This periods coincide with the following catastrophic events respectively; Hurricane Hugo, Hurricane Andrew, Tropical Storm Allison, Hurricanes Frances, Jeanne, Katrina and Wilma in the 2004-2005 period, Hurricane Ike in 2008, several extreme Wind and Thunderstorm events in 2011, and finally, Hurricane Sandy in 2012. This is further supported by Figure 7.2a and Figure 7.2b below, that summarise the annual losses and annual frequency of the observations over time.

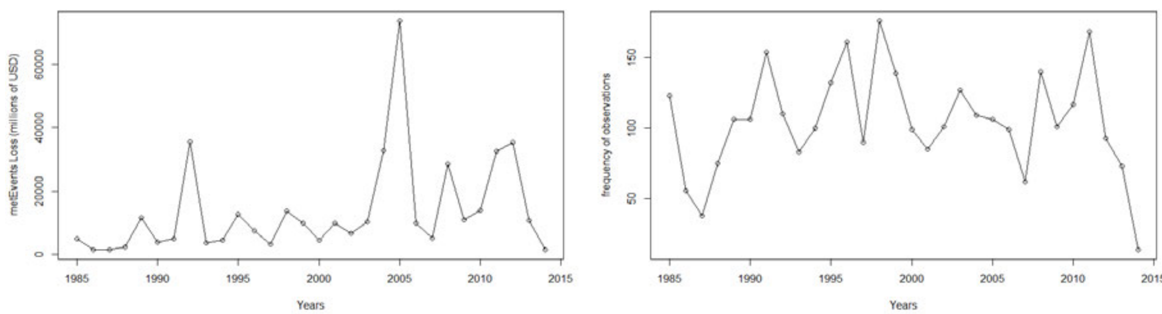

(a) *Annual Catastrophic Loss Severities* **(b)** *Annual Catastrophic Loss Frequencies*

Note: The two figures above display the aggregate annual loss severity (left) and annual loss frequency (right) estimates for PCS' meteorological industry loss data, for the period beginning January 1985 and ending April 2014. The Annual Loss Severities plot summarises the annual catastrophic loss severity values, while the Annual Loss Frequencies plot gives a summary of the annual catastrophic loss frequency values. Loss estimates in millions of US dollars are displayed on the y-axis while the x-axis displays the respective year.

From these plots, we can also see that some 'clustering' is evident. Further tests will prove that this is indeed the case, and provide an estimate of the extent of this clustering.

For the moment, we conduct tests on the data to determine that it is indeed a heavy-tailed process. The QQ plot and the plot of the sample mean excess function are used to support the heavy-tailed nature of the data.

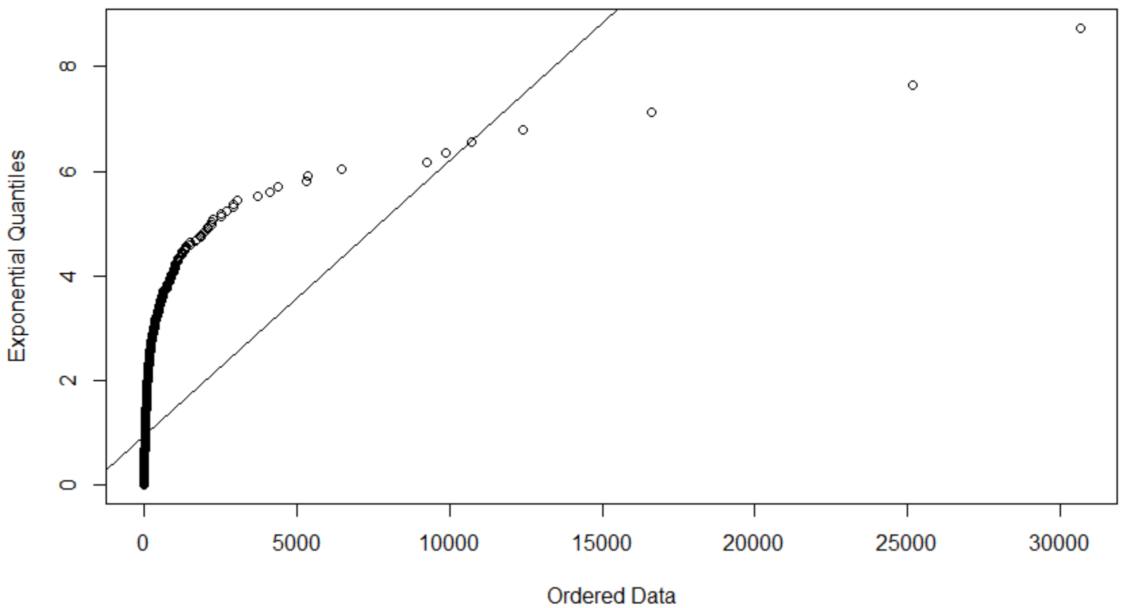

Figure 7.3: *Exploratory QQ plot*

Note: The figure displays the exploratory quantile-quantile plot against the exponential distribution (Exploratory QQ-plot), used to visually test the PCS meteorological data's heavy-tailed properties. Concave departures from the medium-tailed exponential distribution's straight line indicate that the data is heavy-tailed while Convex departures indicate shorter-tailed data.

The QQplot against the exponential distribution visually examines whether the data is derived from an exponential distribution i.e. a medium-tailed distribution. Any concave departures, as observed in Figure 7.3, indicate that our data is heavy-tailed while convex departures indicate shorter-tailed data. This plot proves that our data is heavy-tailed, and this is further reinforced by the plot of the sample mean excess function.

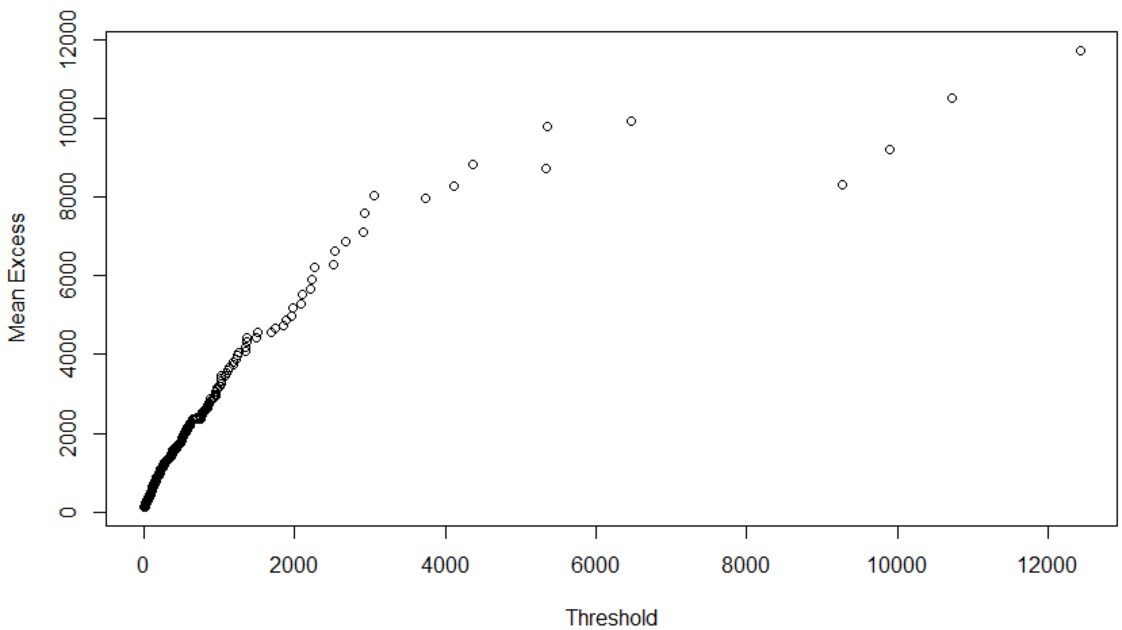

Figure 7.4: *Sample Mean Excess Plot*

Note: The plot of the sample mean excess function is used to further test and confirm heavy-tailed properties of the PCS meteorological data. As the medium-tailed exponential distribution would give an approximately horizontal line in this case, an upward trend in the line would indicate Pareto heavy-tailed behaviour.

In this plot, an upward trend indicates heavy-tailed behaviour, since the exponential data would give an approximately horizontal line. Figure 7.4 proves the heavy-tailed nature of our data through its reasonably straight line with positive gradient.

The next set of tests assesses the presence and extent of 'clustering' in our data. We apply a variety of tests, including the ACF for serial correlation; the Ljung-Box Test for Independence; and finally the extremal index for clustering extent quantification and plotting. The tests are described below.

We first test for independence of observations using the Ljung-Box test for independence (Ljung and Box, 1978). The results of this test i.e. a p-value $< 2.2e^{(-16)}$, lead to the rejection of the null hypothesis (independence of observations) in favour of the alternative hypothesis (evidence for dependence) at the 99.9999% confidence level. The presence of serial correlation is then tested through the sample autocorrelation function (ACF), and the results displayed in Figure 7.5.

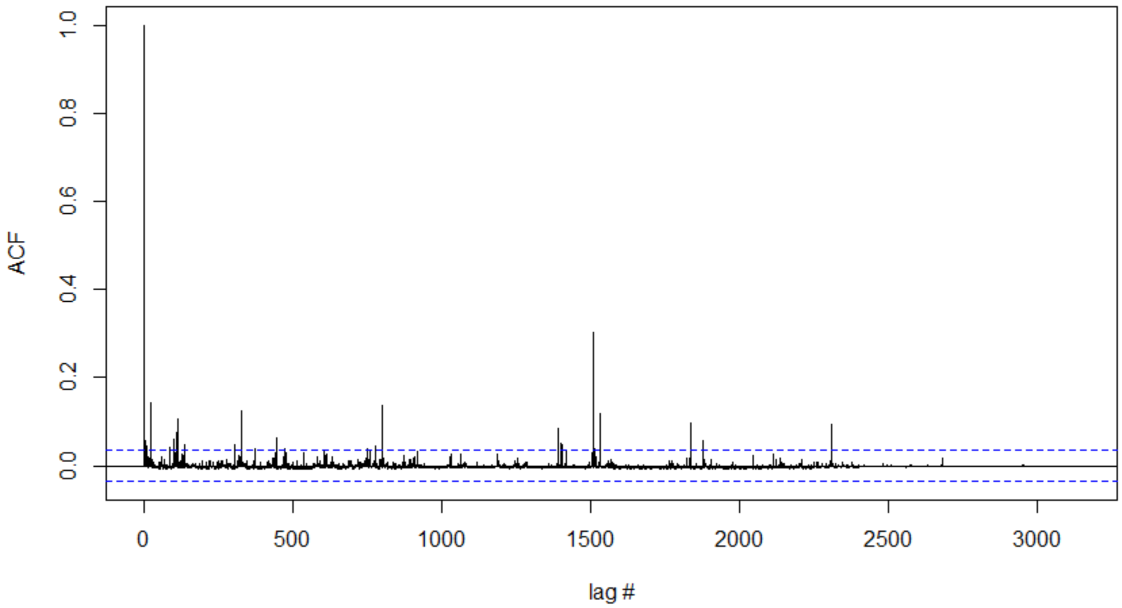

Figure 7.5: *Sample Autocorrelation Function*

Note: The sample autocorrelation function plot is used to test for serial correlation in the PCS meteorological data, as a preliminary step to determining the presence and extent of 'clustering' in the data. A larger number of spike points above the blue confidence band would be proof of serial correlation. Furthermore, the persistence of these spikes over higher and higher lags would also be an indication of long-range dependence as opposed to short-range dependence.

The large number of spikes falling above the blue confidence band indicate that the data is serially correlated. In addition, the persistence of the spikes over higher and higher lags is also an indication that we are dealing with long-range dependence as opposed to short-range dependence. This implies that we cannot assume independence by relying on the presence of only short-range dependence; and can only model the data as a dependent non-stationary process.

Finally, the extent of clustering is quantified and plotted through the use of the extremal index (Embrechts et al., 1997). Using the Ferro-Segers 'intervals method' (Ferro and Segers, 2003), we get an estimated index value of 0.4517447 (Confidence interval: 0.3703886 - 0.5610667) at the 95% confidence level. This proves our original deduction that clustering is evident in the data, since an independent dataset would give an extremal index of 1, with this value decreasing with the extent of clustering observed. We also compare different extremal index estimates to further support this deduction, including the blocks method, the reciprocal mean cluster size method and the runs method (see Embrechts et al. (1997) for further explanation). These methods give even lower estimates, further reinforcing our assumption. The summary plot is given in Figure 7.6, where the blocks, reciprocal and runs estimates are plotted by the black line, the green triangles, and the blue x's respectively.

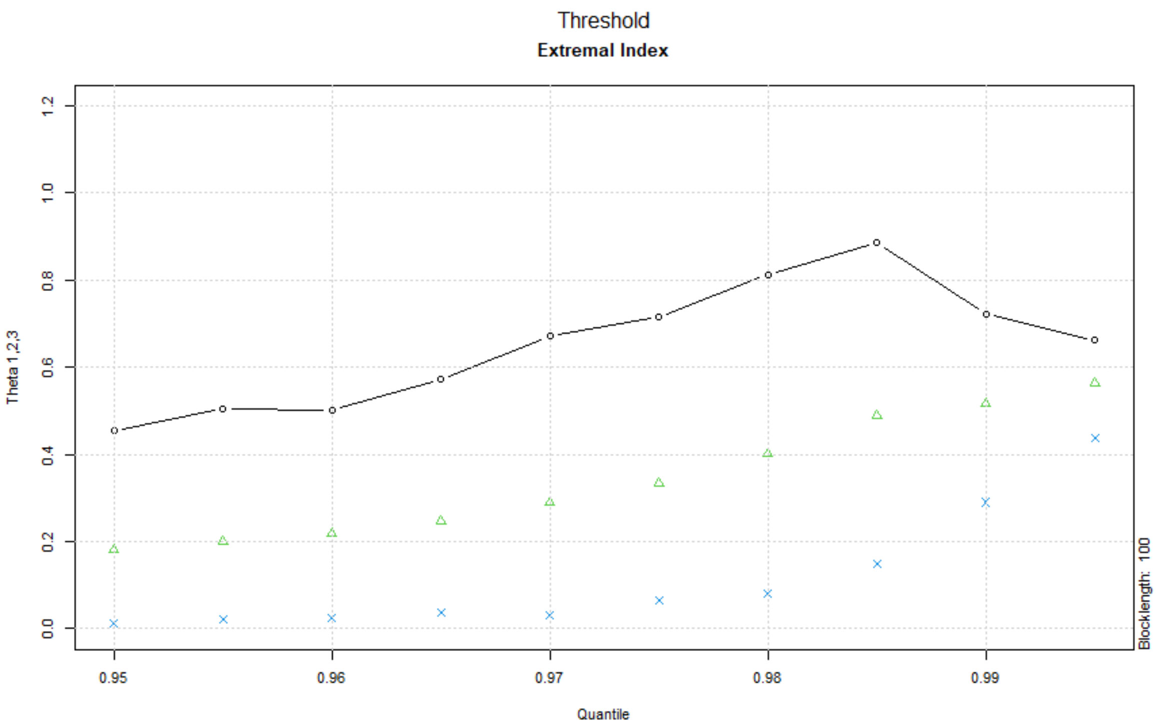

Figure 7.6: *Extremal Index Estimation*

Note: Once clustering has been established in data, its extent is quantified and plotted through the extremal index above. Three different techniques for extremal index estimation are used to arrive at these values, including the blocks method, the reciprocal mean cluster size method and the runs method (see e.g., Embrechts et al. (1997)). These results are displayed in the extremal index plot above, where the blocks, reciprocal and runs estimates are plotted by the black line, the green triangles, and the blue x's respectively.

7.4.2 Hidden Markov Model Fitting

Once the presence and extent of 'clustering' has been established, we model this using the hidden markov model and the Baum-Welch algorithm. For this purpose we apply the R packages **HiddenMarkov** (Harte, 2021) and **depmixs4** (Visser and Speekenbrink, 2010). We estimate two models; one representing the loss severity, and the other representing the loss frequency. Table 7.1 displays the model specification and fit results. The columns display the mixture distribution type (Distribution), the number of states of the distribution fitted to the data (No. of states (K)), the Negative Log-Likelihood, and the the Akaike Information Criterion (AIC) and Bayesian Information Criterion (BIC) to enable the identification of the most optimal fit distribution and states. The states with the lowest BIC values are highlighted in bold font, representing the hidden Markov models under each distribution that provides the best fit.

Table 7.1: *Hidden Markov Models fitted to Meteorological Loss Data*

	Loss Frequency Model			
Distribution	No. of states (K)	Negative Log-Likelihood	AIC	BIC
Poisson	1	2118.067	4238.134	4242.737
	2	1805.326	3620.653	3643.666
	3	**1774.287**	**3570.574**	**3621.202**
	4	1768.954	3575.954	3663.357
	Loss Severity Model			
Distribution	No. of states (K)	Negative Log-Likelihood	AIC	BIC
Exponential	**1**	**16247.96**	**32499.91**	**32512.02**
	2	16333.51	32673.02	32674.01
Lognormal	1	16247.96	36862.82	36,868.87
	2	15932.00	31874.00	31,870.99
	3	15779.48	31574.96	31574.96
	4	**15724.26**	**31470.52**	**31455.51**
	5	15724.26	31476.52	31455.51
Gamma	1	17607.62	35219.24	35231.35
	2	16252.21	32514.42	32511.41
	3	15992.87	32001.74	31992.73
	4	**15934.65**	**31891.3**	**31876.9**
	5	15934.65	31897.3	31876.9

Note: The table above shows the results of the Hidden Markov Models (HMMs) and the Baum-Welch Algorithm fit to both the loss severity and the loss frequency data via the R software packages HiddenMarkov and depmixs4. The table columns represent the mixture distribution type (Distribution), the number of states of the distribution fitted to the data (No. of states (K)), the Negative Log-Likelihood, and the the Akaike Information Criterion (AIC) and Bayesian Information Criterion (BIC) to enable the identification of the most optimal fit distribution and states. The states with the lowest BIC values are highlighted in bold font, representing the hidden Markov models under each distribution that provides the best fit.

For the frequency model, we use a Poisson mixture distribution to model the arrival times while for the loss severity model, several medium and heavy-tailed distributions are tested using the available packages, with the top three distributions by fit being included in the table.[7] The final loss frequency and loss severity HMMs are chosen with regards to the best fit characteristics based on the AIC and the BIC. These are the 3-state Poisson hidden markov model and the 4-state lognormal hidden markov model for loss frequency and loss severity respectively. The model parameters and their respective residual plots, which are generated as part of the model fitting process above, are given below.

For the Loss Frequency Model, that is, the 3-State Poisson HMM,

Parameter Estimates

Given the Hidden Markov Model as defined in Section 7.3, the model parameters are given as follows;

$$\theta = (A, B, \pi) \tag{7.28}$$

For the 737 loss frequency observations extracted from the individual loss severity data; the initial state probabilities are given by;

$$\pi = \begin{array}{ccc} 1.0000e^{+00} & 2.2657e^{-86} & 0.0000e^{+00} \end{array}$$

The transition matrix;

$$\mathbf{A} = \begin{bmatrix} 0.7076 & 0.2540 & 0.0384 \\ 0.4167 & 0.4776 & 0.1057 \\ 0.4755 & 0.4247 & 0.0999 \end{bmatrix}$$

And the state parameters defining the Emission matrix $\mathbf{B}$;

$$\begin{bmatrix} \text{State} & 1 & 2 & 3 \\ \lambda & 2.1695 & 6.0853 & 13.8355 \end{bmatrix}$$

Residual Plots

The histogram and normal QQ-plots of the loss frequency model are displayed below;

[7] This list is not yet exhaustive, and the author plans to extend the hidden markov models to other heavy-tailed distributions not currently included in the available statistical packages.

Figure 7.7: *Histogram and Normal QQ-plot of residuals for the Loss Frequency model*

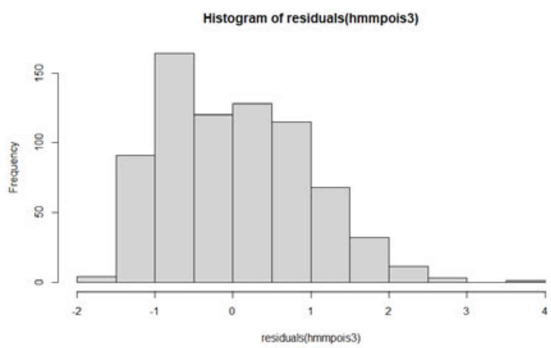

(a) *Histogram of Residuals*

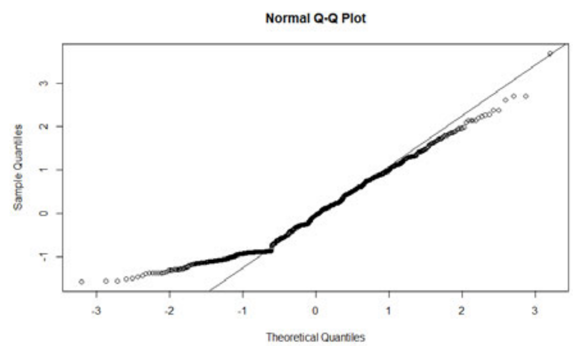

(b) *Normal QQ-Plot of Residuals*

Note: The histogram of residuals and Normal QQplot of residuals plots above are used to assess the fit of the chosen hidden markov model (i.e., the 3-state Poisson HMM) to the PCS loss frequency data. The better fitting models are expected to produce a histogram that is as close to the normal bell-shape as possible, and a normal QQ-plot that is as close to the diagonal line as possible.

And for the Loss Severity Model, that is, the 4-State Lognormal HMM

Parameter Estimates

With the Hidden Markov Model

$$\theta = (A, B, \pi) \tag{7.29}$$

The initial state probabilities are given by;

$$\pi = \begin{matrix} 0 & 1 & 0 & 0 \end{matrix}$$

The transition matrix;

$$\mathbf{A} = \begin{bmatrix} 9.0052e-01 & 7.9756e-05 & 0.0046 & 0.0948 \\ 2.6939e-12 & 9.8246e-01 & 0.0143 & 0.0033 \\ 1.7890e-06 & 3.8507e-02 & 0.6104 & 0.3511 \\ 7.9970e-02 & 5.2100e-03 & 0.0864 & 0.8285 \end{bmatrix}$$

And the state parameters defining the Emission matrix $\mathbf{B}$;

$$\begin{bmatrix} \text{State} & 1 & 2 & 3 & 4 \\ \mu & 3.1476 & 2.7594 & 5.3798 & 3.9922 \\ \sigma & 0.5928 & 1.1130 & 1.6622 & 0.9696 \end{bmatrix}$$

Residual Plots

The histogram and normal QQ-plot of residuals are displayed below;

Figure 7.8: *Histogram and Normal QQ-plot of residuals for the Loss Severity model*

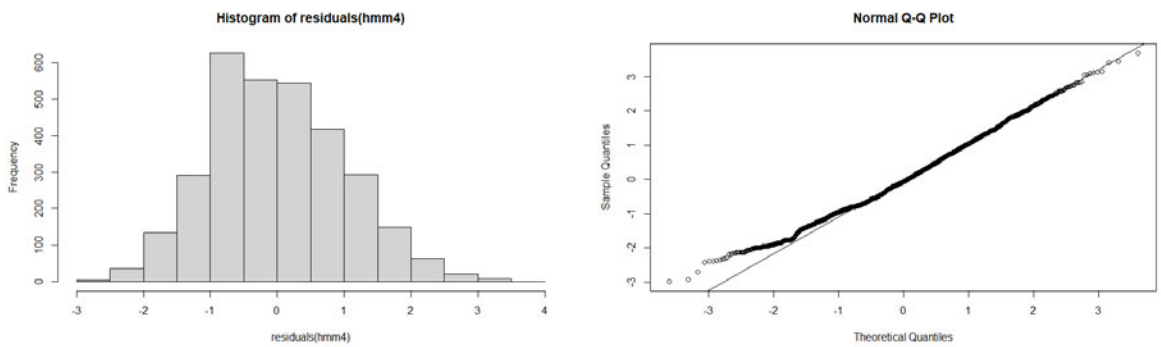

(a) *Histogram of Residuals* **(b)** *Normal QQ-Plot of Residuals*

Note: The histogram of residuals and Normal QQplot of residuals plots above are used to assess the fit of the chosen hidden markov model (i.e., the 4-state Lognormal HMM) to the PCS loss severity data. The better fitting models are expected to produce a histogram that is as close to the normal bell-shape as possible, and a normal QQ-plot that is as close to the diagonal line as possible.

The residual plots for the severity model indicate slightly better fits compared to the residual plots for the frequency model. It should be noted, however, that the multi-state frequency model is still a better fit for the data than a single-state frequency model i.e., the single Poisson distribution.

In addition, the multi-state frequency HMM's residuals were compared to a typical non-homogeneous Poisson process fit for the frequency data based on estimation of Poisson processes resulting from a peak-over-threshold approach (Cebrián et al., 2015), and these non-homogeneous plots found to be of a worse fit compared to the multi-state HMM fit. The multi-state HMM, is also, in its own right, a form of a finite non-homogeneous Poisson process, since its intensity functions are stochastic and state-dependent. Due to these advantages, we progress with the Poisson 3-state HMM for frequency modelling and the lognormal 4-state HMM for severity modelling in the application stage.

7.4.3 Model Application to Catastrophe Bond Valuation

The aggregate claims process

Assume the stochastic process N represents the number of claims occurring until time t; and $X_n, n = 1, ..., N$ the size of the individual claims to time t. X_n's have a common distribution function $P(x) = P\{X_n < x\}$, which, in our case, represents the HMM distribution.

Assuming the number of claims N is independent of the size of claims X_n, the aggregate loss process S can be defined as;

$$S = \sum_{n=0}^{N} X_n \tag{7.30}$$

and $S = 0$ when $N = 0$. S is assumed to follow a Compound Poisson Markov-dependent Mixture distribution. These assumptions are based on the Cramer-Lundberg collective risk model (Livshits, 1999; Boikov, 2003).

The Compound Poisson Markov-Dependent Mixture Distribution

The distribution of the random aggregate loss process $S = X_1 + X_2 + \cdot + X_N$ is termed a compound distribution (Teugels et al., 2004). Compound distributions are used to model aggregate losses, especially in insurance claims models. The distribution of N, also known as the primary distribution, generates the loss frequencies, values which are then used to generate individual losses for each loss frequency. These individual losses (X_n's), are then summed up to give the final aggregate loss values (S) that are used in pricing applications (Willmot and Lin, 2001).

The distribution of S, for the compound Poisson markov-dependent mixture distribution, can be expressed as

$$F_S(x) = \sum_{n=0}^{\infty} \sum_{i=1}^{M} w_i \frac{e^{\lambda_i} \lambda_i^n}{n!} \quad P^{*n}(x) \tag{7.31}$$

where $P^{*n}(x) = Pr(X_1 + X_2 + ... + X_n \leq x$. M represents the number of distributions included in the Markov-dependent mixture model; w_i denotes mixture component i's weight; and $\;{}_{i=1}^{M} w_i = 1$.

We generate this compound distribution using loss frequency observations from the 3-state Poisson HMM and individual loss severity observations from the 4-state Lognormal HMM. These loss severity values are then aggregated at each loss frequency to generate the final aggregate loss values used in the catastrophe bond valuation model.

The Catastrophe Bond Pricing Model

We consider two index-linked CAT bonds[8]; a zero-coupon CAT bond and a coupon-paying CAT with only the coupons at risk if a catastrophe occurs. The zero-coupon CAT bond with pay-off ($\text{Payoff}_{CAT}{}^{(1)}$) and maturity $T > 0$ can be expressed as;

$$\text{Payoff}_{CAT}{}^{(1)} = \begin{cases} 1, & \text{if } S_T < D. \\ \rho, & \text{if } S_T \geq D. \end{cases} \tag{7.32}$$

[8]an index linked CAT pays out to the issuer if the losses from the pre-specified event exceed losses on a certain catastrophe loss index

where S_T represents the aggregate claims at time T, D is the threshold level that triggers a payout, and $\rho(0 \leq \rho < 1)$ represents the proportion of principal recovered by the investor at time T if the bond is triggered. The value of this bond at time t given the catastrophe loss distribution $P(x)$ and the claim arrival process N_t is then given by (see e.g., Ma and Ma (2013));

$$
\begin{aligned}
V_t &= e^{-\int_t^T r_s ds}\mathbb{E}^{\mathcal{Q}}[\text{Payoff}_{CAT}{}^{(1)}|\mathcal{F}_t] \\
&= B_{CIR}(t,T)\left[\rho + (1-\rho) \times F_S(D)\right] \\
&= B_{CIR}(t,T) \quad \rho + (1-\rho) \times \sum_{n=0}^{\infty} \quad \sum_{i=1}^{M} w_i \frac{e^{\lambda_i}\lambda_i^n}{n!} \quad P^{*n}(D)
\end{aligned}
\tag{7.33}
$$

Under the risk-neutral probability measure $\mathcal{Q}$, $P^{*n}(D) = Pr(X_1 + X_2 + ... + X_n \leq D$ is the n-fold convolution of P; and

$$
\begin{aligned}
B_{CIR}(t,T) &= A(t,T)e^{-B(t,T)r_t}, \\
A(t,T) &= \quad \frac{2he^{(a+\lambda_r+h)(T-t)/2}}{2h + (a+\lambda_r+h)(e^{(T-t)h} - 1} \quad ^{\frac{2ab}{\sigma^2}}, \\
B(t,T) &= \quad \frac{2e^{(T-t)h} - 1}{2h + (a+\lambda_r+h)(e^{(T-t)h} - 1} \quad , \\
h &= \sqrt{(a+\lambda_r)^2 + 2\sigma^2}
\end{aligned}
\tag{7.34}
$$

is the Cox-Ingersoll-Ross interest rate process (Cox et al., 1985).

Next consider the coupon-paying CAT bond with a constant coupon $c > 0$ and the pay-off structure;

$$
\text{Payoff}_{CAT}{}^{(2)} = \begin{cases} c + 1, & \text{if } S_T < D. \\ \rho(c) + 1, & \text{if } S_T \geq D. \end{cases}
\tag{7.35}
$$

where S_T represents the aggregate claims at time T, D is the threshold level that triggers a payout, and $\rho(0 \leq \rho < 1)$ represents the proportion of coupon recovered by the investor at time T if the bond is triggered. The value of this bond at time t given the catastrophe loss distribution $P(x)$ and the claim arrival process N_t is then given by;

$$
\begin{aligned}
V_t &= e^{-\int_t^T r_s ds}\mathbb{E}^{\mathcal{Q}}[\text{Payoff}_{CAT}{}^{(2)}|\mathcal{F}_t] \\
&= B_{CIR}(t,T)\left[(\rho c+1)+\rho c\times F_S(D)\right] \\
&= B_{CIR}(t,T)\left[(\rho c+1)+\rho c\times\sum_{n=0}^{\infty}\left(\sum_{i=1}^{M} w_i\frac{e^{\lambda_i}\lambda_i^n}{n!}\right)P^{*n}(D)\right]
\end{aligned}
\tag{7.36}
$$

where $P^{*n}(D) = Pr(X_1 + X_2 + ... + X_n \leq D$ is the n-fold convolution of P and $B_{CIR}(t,T)$ represents the Cox-Ingersoll-Ross discount rates defined above.

Bond Valuation

Assuming an index-linked CAT bond with face value $Z = US\$1$, proportion $\rho = 0.7$ and coupon $c = 0.1$ at time $t = 0$. We estimate bond values at different thresholds D, determined on the annual average loss interval, with the lowest threshold representing a quarter of the average loss and the highest threshold representing three times the average loss (see e.g. Shao et al. (2017)); and for different terms to maturity T, ranging from 0.25 to 2.25 years.

The resulting 3D plots of final CAT bond values are given in figures 7.9 for the zero-coupon CAT bond (principal-at-risk) and 7.10 for the coupon paying CAT bond (principal-and-coupon-at-risk).

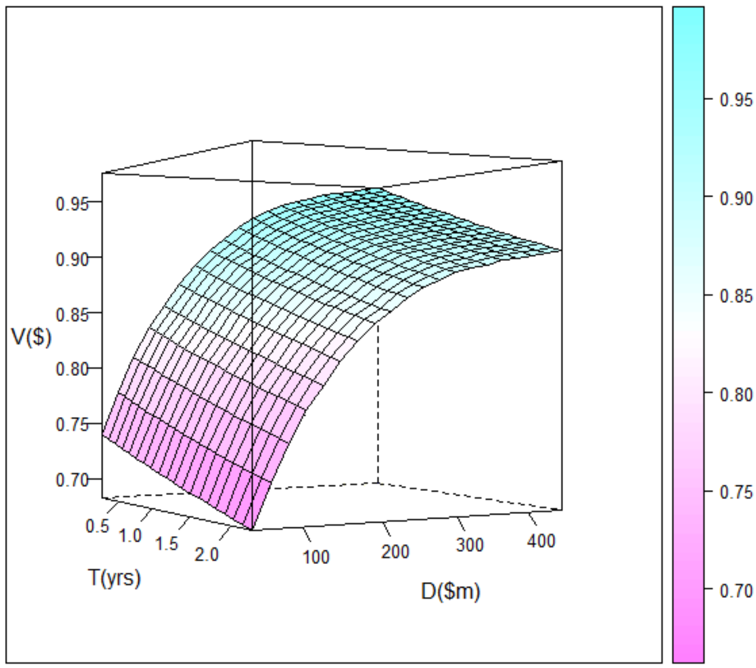

Figure 7.9: *Principal-at-risk CAT bond*

Note: The figure gives the 3D plot of catastrophe bond prices generated assuming a compound Markov dependent mixture model for the aggregate loss values and the CIR interest rate model for the discount rates. The payoffs are derived for the principal-at-risk catastrophe bond, and the plot displays the catastrophe bond value in US dollars (V($)), the catastrophe bond term in years (T(yrs)), and finally the catastrophe bond triggering threshold in millions of US dollars (D($m)).

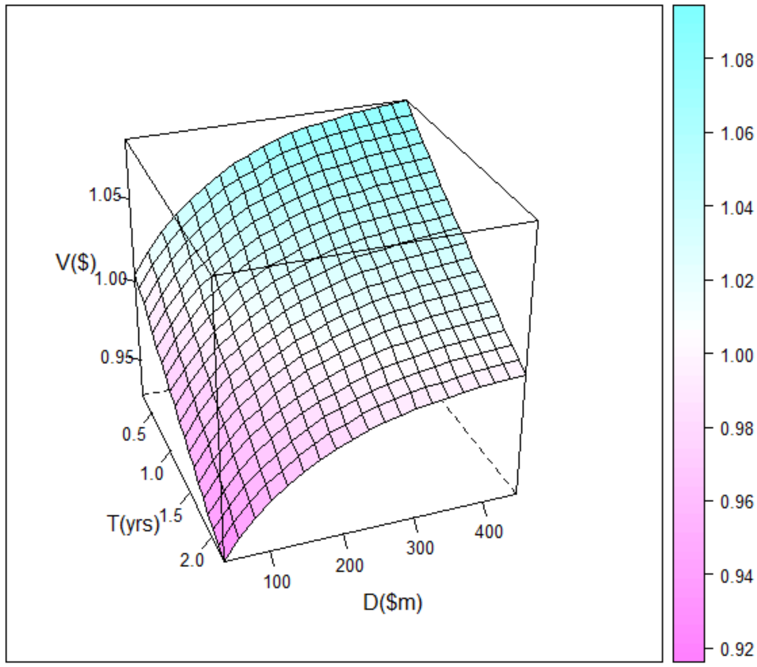

Figure 7.10: *Principal-and-coupon-at-risk CAT bond*

Note: The figure gives the 3D plot of catastrophe bond prices generated assuming a compound Markov dependent mixture model for the aggregate loss values and the CIR interest rate model for the discount rates. The payoffs are derived for the coupon-at-risk catastrophe bond, and the plot displays the catastrophe bond value in US dollars (V($)), the catastrophe bond term in years (T(yrs)), and finally the catastrophe bond triggering threshold in millions of US dollars (D($m)).

Figures 7.9 and 7.10 show that higher risk bonds i.e., lower bond prices are characterised by lower thresholds and longer time to maturities. These results are in line with observations from real catastrophe bond price regression models (see e.g. Braun (2016)). These 3D plots serve as proof that Hidden Markov Models and the Baum-Welch algorithm can be applied to incorporate effects of seasonality and temporal dependence in catastrophic loss datasets, especially for events that typically occur seasonally like meteorological events. It also shows that dependent and non-stationary processes can be efficiently modelled without incurring excessive computational costs or losing model robustness; and that these models can be applied to the valuation of catastrophe-linked securities to ensure completeness.

These results are crucial to providing the industry with a way to incorporate unique and often complex elements of dependent catastrophic loss processes into valuation models, in order to ensure that such unique elements are also efficiently priced into the final models used to determine the costs of catastrophic risk processes. This is especially important since, and similar to Chapter 6's conclusions, model accuracy, completeness, and efficiency, are key factors to ensuring that information asymmetries are reduced, and that investors and issuers can trust that the pricing process within the disaster risk financing market remains efficient to a reliable degree. Only in this way, can the market serve to both protect individuals, institutions, and even nations facing the threats of catastrophic losses, while ensuring that those investors who are willing to take on such risks are fairly compensated. Only this way can there be hope that those at risk can find protection against catastrophes which often are too costly for any other institutions to take on. Only this way can future survival be guaranteed against extreme losses.

7.5 Conclusion

This study set out to identify and quantify deviations from the 'independent and identical distribution' of observations assumption. This was accomplished through a standardised approach involving the application of Hidden Markov Models (Zucchini et al., 2016) and the Baum-Welch algorithm (Baum et al., 1970; Baum, 1972; Welch, 2003) to data 'clusters' in order to generate the best state-dependent distributions. The Hidden Markov Models were applied to both the loss frequency and loss severity data, and the model parameters then used as inputs in the generation of a compound mixture distribution for aggregate losses. These aggregate losses were then applied in a catastrophe bond valuation model to generate bond value estimates under different threshold and time to maturity assumptions.

The study's results show that, for extreme meteorological event data covering hurricanes, tropical storms and other related wind and thunderstorm events, individual loss severities can be modelled via a 4-state Log-normal hidden markov model; while loss frequencies can be modelled via a 3-state Poisson hidden markov model. A compound mixture distribution can also then be generated for these model combinations to estimate aggregate losses. The Hidden Markov Model (HMM) has been shown to be reliable for the modelling of 'clustered' data, and especially useful in the identification of underlying hidden catastrophic states determining catastrophe loss observations. In addition, the flexibility of the HMM implies that these models can be applied to a variety of distributions and state processes. This is especially useful in the changing catastrophe climate.

Future research opportunities include the comparison of seasonal events with non-seasonal events like earthquakes in order to establish the differences in the evolution of loss distributions or pricing factors, and the exploration of multivariate dependencies via 'correlated clustering' approaches. These cluster-based dependencies could then be compared to the popular multivariate dependence modelling approaches that focus on copula-based techniques. Other extensions focusing on further automating the HMM optimization process will be explored in future studies, to further improve efficiency.

In conclusion, this study has proposed a standardised hidden-markov-based approach to modelling both inherently seasonal and non-seasonal but tail dependent processes via the Baum-Welch algorithm. This is useful especially for practitioners looking to improve the precision of estimates used in model prediction, risk assessment and decision-making for events deviating from the 'independent and identically distributed' observations assumption.

Chapter 8

Conclusion

Through the application of mathematical optimization i.e., the Expectation-Maximization (EM) algorithm to climate-based catastrophic loss modelling and pricing disaster risk financing instruments i.e., the catastrophe bond, we have shown that these models can be applied to improve efficiency and tractability of current catastrophic loss models, thus improving model reliability for planning and decision making. This can then contribute to better priced financing options, subsequently boosting extreme disaster risk resilience and adaptation. To reach these aims, this study has followed the following structure.

A historical background of disaster occurrence and disaster risk management processes was analysed in Chapters 2 and 3, followed by a background of mathematical optimization and the EM algorithm in Chapter 4. These chapters provided a reference for the fit of this study with previous and present developments within the field, and gave this study a continuation point in the literature.

After the background was established, the study then focused on the modelling of catastrophic risk processes with Expectation-Maximization (EM) algorithms. The first of these tests, detailed in Chapter 5, focused on the modelling of volatility in catastrophe bond pricing among issuers whose bonds have similar characteristics. As the catastrophe bond's underlying risk is unrelated to the state of the issuer but rather dependent on the risk characteristics of the underlying catastrophe, there should not have been any significant differences in the prices of a bond with similar underlying but issued by different issuers in the market. Any differences would therefore have been a result of an inefficiency within the market, which could be a consequence of investor-based behavioural factors. The study therefore uses an EM-based random effects model to test for this effect on catastrophe bond prices available since market inception. The model identifies any collective volatility clustering effects between the different classes of data, with the 'class' representing a specific issuer, and finally its significance is determined. Our significant results prove that these effects still exist, signifying that the catastrophe bond market is still inefficient to some degree. Further analysis also shows that the effects are worse for less frequent issuers and for companies in the business of conducting insurance, as opposed to reinsurance or multi-business companies.

These results are particularly useful to new issuers seeking protection who may need to understand fully the factors that drive their pricing, including factors beyond the logical risk-based factors. In addition, market practitioners could benefit from these results as they give an indication of the state of the market and areas that may require improvement in order to make the market more attractive to both investors and bond issuers. This also gives a possible area for future research, where as time goes by, a larger dataset could enable this trend to be fully flushed out, and any improvements clearly identified within seasonal data splits. In addition, these behavioural factors could be assessed further to determine the exact cause of such pricing volatilities among the different classifications of issuers.

Next, in Chapter 6, the study shifts its focus to the actual modelling of the catastrophic loss processes that underly catastrophic risk pricing instruments, including catastrophe bonds. In this second project, analysis is focused on the application of an EM-based finite mixture model (FMM) to the modelling of heavy-tailed catastrophic loss processes, especially those that underly the catastrophic industry loss index provided by Property Claims Services (PCS), a US-based company that collects such claims data for extreme events. As heavy-tailed loss modelling can often be intractable and computationally inefficient due to the complexity of the final equations, the EM algorithm provides an optimization technique to enable efficient modelling techniques to be applied to the data, and reduce computational costs. The finite mixture models tests a number of heavy-tailed distributions to the data and determines the mixture distributions that best explain both the loss severity and the loss frequency observed, which in this case was the 2-component log-normal mixture and the 3-component Poisson mixture respectively. We then use these models to generate a compound distribution for the simulation of a complete dataset, which is then used to value catastrophe bonds with different payoff functions. The finite mixture models are also compared with other non-EM-based types of mixture models including composite models and composite mixture models and found to be superior. For this reason, the study is able to propose a computationally efficient and tractable modelling technique for catastrophic risk modelling and pricing.

Such results are useful for risk modellers looking to boost the efficiency of their recommended models and for market practitioners hoping to better understand or individually model such processes. The study also provides the possibility for further research on EM-type algorithms that can further improve efficiency, including some new algorithms that combine both Newton-based algorithms, Monte Carlo techniques etc., into their functionality to further improve the algorithm's speed. In addition, other loss frequency models apart from the popular Poisson could also be modelled and more efficient mixture models introduced for the loss frequency processes, which have seen little extension from the Poisson distribution-based models so far.

Finally in Chapter 7, the study tested the applicability of EM-based algorithms to the modelling of unique factors in catastrophic loss modelling processes, here focusing on the modelling of time-based dependencies in single event catastrophic loss observations. A Baum-Welch Hidden Markov Model (HMM), which relies on the EM algorithm for optimization, was used to accomplish this. The model was fit to meteorological event data from PCS and state-based distributions for the loss frequencies and loss severities derived, similarly to the techniques applied in the finite mixture modelling process above. In this case, the results showed that the 4-state lognormal HMM model and the 3-state Poisson HMM model provided the best fit for the loss severity and the loss frequency respectively. The model fits were then confirmed through residual models and QQ plots, and the loss frequency model fit further compared with a non-homogeneous Poisson model fit and found superior. The models were then applied to generate a Compound Poisson HMM model for the aggregate data, and this model used to simulate data for the valuation and finally pricing of catastrophe bonds with different payoff functions.

This study, like the FMM study above, also provides an efficient model for the analysis of dependencies and effects of seasonality on catastrophic loss observations, and finally pricing. This model is especially useful as it provides a starting point for practitioners seeking a way to incorporate unique elements of extreme event data into their pricing models for more efficient pricing of disaster risk. This also ensures that the previously-observed difficulty in incorporating loss dependencies in catastrophe models can finally be addressed more effectively. In addition, this study provides future research opportunities in multi-event dependence modelling, and other unique-trend modelling applications, especially with climate change and its effects on the pace and severity of disasters.

The three focused studies have shown that we can model both issuer-specific pricing volatility, tails and dependence structures in catastrophic loss observations with just one class of algorithms, and thus improve the efficiency of extreme loss modelling practices. These deductions are especially useful for catastrophic risk modelling due to the complexity of the models and equations applied to accomplish this process, which then often lead to computationally expensive solutions with little real-life applicability.

As climate change is an ongoing process, the field of climate modelling keeps expanding (see e.g., Froot, 1999a; Cummins, 2008; SOQS, 2019; Crutzen and Stoermer, 2021; Quéré et al., 2021), and this has increased the need for both practitioners and academics to find techniques that are better suited to adapt to new trends and observations in loss processes, as static models easily become obsolete with time. The EM provides a class of algorithms with significant adaptability potential (Dempster et al., 1977; Rabiner, 1989; McLachlan and Krishnan, 2007; Raudenbush and Bryk,

2010) and can therefore be a good option for modelling the dynamism of climate processes. It can also be easily modified and used in combination with other optimization algorithms including Monte Carlo and Quasi-Monte Carlo techniques in special-case situations, further boosting its potential.

Future studies will therefore focus on this ‘boost of potential’, aiming at introducing further possible applications, trends and special-case scenarios to make the EM algorithm a truly versatile optimization option for climate risk modelling and disaster risk financing. In addition, modified structures of disaster finance instruments better suited for specific disaster scenarios will also be created and modelled with such techniques to provide more financing and insurance options, especially for vulnerable communities that require such financing the most when extreme disasters strike. This will further contribute to the goal of improving disaster resilience, especially for vulnerable communities, thus supporting the goals of the Sendai Framework for Disaster Risk Reduction (SFDRR), and the efforts of the World Bank’s Disaster Risk Financing Facility to protect communities.

Bibliography

Abbott, Patrick L. (2022). *Natural Disasters*. McGraw-Hill Higher Education.

ADB (2018). *Disaster risk financing tools and approaches*. Asian Development Bank.

(2021). *Report: Climate Risk Country Profile: Mongolia*. Asian Development Bank/ World Bank Group.

Aguinis, H. et al. (2013). "Best-Practice Recommendations for Defining, Identifying, and Handling Outliers". In: *Organizational Research Methods* 16.2, pp. 270 301.

Akaike, H. (1974). "A New Look at the Statistical Model Identification". In: *IEEE Transactions on Automatic Control* 19.6, pp. 716 723.

Alagna, Magdalena (Dec. 2003). *The Great Fire of London of 1666*. en. The Rosen Publishing Group, Inc.

Albrecher, Hansjörg et al. (2004). "QMC Techniques for CAT Bond Pricing". In: *Monte Carlo Methods and Applications* 10.3-4.

Alexander, David (2020). *Disaster Risk Reduction*.

Allen, Greg (2012). "Hurricane Andrew's Legacy:'Like A Bomb'In Florida". In: *National Public Radio*.

Almgren Jr, F. J. and H. Montgomery (1974). "The 1974 Fields Medals (II): An Analyst and Number Theorist". In: *Science* 186.4159, pp. 130 131.

Ambraseys, N. N. (1963). "The Buyin-Zara (Iran) earthquake of September, 1962 a field report". In: *Bulletin of the Seismological Society of America* 53.4, pp. 705 740.

Antonopoulos, John (1992). “The great Minoan eruption of Thera volcano and the ensuing tsunami in the Greek Archipelago”. In: *Natural Hazards* 5.2, pp. 153 168.

Arneth, Almut et al. (2010). “Terrestrial biogeochemical feedbacks in the climate system”. In: *Nature Geoscience* 3.8, pp. 525 532.

Artemis (2023). *Catastrophe bonds, insurance linked securities, reinsurance capital and investment, risk transfer intelligence.* Artemis.bm.

Ashliman, D. L. (2002). “The Grimm Brothers’ Children’s and Household Tales (Grimms’ Fairy Tales)”. In: *Folktexts: A library of folktales, folklore, fairy tales, and mythology.*

Asselt, Harro van et al. (2015). *Assessment and review under a 2015 climate change agreement.*

Ayyub, Bilal M. et al. (2016). “Toward resilience to nuclear accidents: Financing nuclear liabilities via catastrophe risk bonds”. In: *ASCE-ASME J Risk and Uncert in Engrg Sys Part B Mech Engrg* 2.4.

Bagozzi, Richard (July 1994). *Advanced Marketing Research.* en. Google-Books-ID: bOxUEAAAQBAJ. John Wiley & Sons.

Bakar, Shaiful Anuar Abu et al. (2016). “Gendist: An R Package for Generated Probability Distribution Models”. In: *PLOS ONE* 11.6. Ed. by Duccio Rocchini, e0156537.

Baker, A. C. (1996). “Karl Theodor Wilhelm Weierstrass, the father of modern analysis. Math”. In: *Spectrum* 7, pp. 25 29.

Balkema, A. A. and L. de Haan (1974). “Residual Life Time at Great Age”. In: *The Annals of Probability* 2.5.

Bantwal, Vivek J. and Howard C. Kunreuther (2000). “A Cat Bond Premium Puzzle?” In: *Journal of Psychology and Financial Markets* 1.1, pp. 76 91.

Baryshnikov, Yuliy et al. (2001). “Pricing of CAT bonds”. In: *preprint.*

Baum, Leonard (1972). “An inequality and associated maximization technique in statistical estimation of probabilistic functions of a Markov process”. In: *Proc. Third Symposium on Inequalities.*

Baum, Leonard E. and J. A. Eagon (1967). “An inequality with applications to statistical estimation for probabilistic functions of Markov processes and to a model for ecology”. en. In: *Bulletin of the American Mathematical Society* 73.3, pp. 360 363.

Baum, Leonard E. and Ted Petrie (1966). “Statistical Inference for Probabilistic Functions of Finite State Markov Chains”. In: *The Annals of Mathematical Statistics* 37.6, pp. 1554 1563.

Baum, Leonard E. et al. (1970). “A Maximization Technique Occurring in the Statistical Analysis of Probabilistic Functions of Markov Chains”. In: *The Annals of Mathematical Statistics* 41.1, pp. 164 171.

Bayissa, Yared A. et al. (Nov. 2015). “Spatio-temporal assessment of meteorological drought under the influence of varying record length: the case of Upper Blue Nile Basin, Ethiopia”. In: *Hydrological Sciences Journal* 60.11, pp. 1927 1942.

Bellman, R. (Aug. 1952). “On the Theory of Dynamic Programming”. eng. In: *Proceedings of the National Academy of Sciences of the United States of America* 38.8, pp. 716 719.

Bellman, Richard (1956). “On the Theory of Dynamic Programming-A Warehousing Problem”. In: *Management Science* 2.3, pp. 272 275.

Ben Hassen, Tarek and Hamid El Bilali (Aug. 2022). “Impacts of the Russia-Ukraine War on Global Food Security: Towards More Sustainable and Resilient Food Systems?” In: *Foods* 11.15, p. 2301.

Bentzen, Jeanet Sinding (Feb. 2013). *Origins of Religiousness: The Role of Natural Disasters*. en. Tech. rep. 2221859. Rochester, NY.

Biggs, Norman (2021). “Linear programming from Fibonacci to Farkas”. In: *Annals of Science* 78.1, pp. 1 21.

Bodie, Z. et al. (2014). *Investments*. 10. ed. The McGraw-Hill/Irwin series in finance, insurance and real estate. New York, NY: Mc-Graw-Hill Education.

Bodoff, N.M. and Y. Gan (2009). “An Analysis of the Market Price of Cat Bonds”. In: *CAS E-Forum*.

Bogucki, Peter (2008). *Encyclopedia of society and culture in the ancient world. Volume 1.* Facts On File.

Boikov, A. V. (2003). "The Cramer Lundberg Model with Stochastic Premium Process". In: *Theory of Probability and Its Applications* 47.3, pp. 489 493.

Boldyrev, Ivan and Till Düppe (2020). "Programming the USSR: Leonid V. Kantorovich in context". In: *The British Journal for the History of Science* 53.2, pp. 255 278.

Bonola, Roberto (1955). *Non-Euclidean geometry: A critical and historical study of its development.* Courier Corporation.

Borovik, Alexandre and Mikhail G. Katz (2012). "Who gave you the Cauchy Weierstrass tale? The dual history of rigorous calculus". In: *Foundations of Science* 17.3, pp. 245 276.

Botzen, W. J. W. et al. (2010). "Climate change and increased risk for the insurance sector: a global perspective and an assessment for the Netherlands". In: *Natural hazards* 52, pp. 577 598.

Boyles, Russell A. (1983). "On the Convergence of the EM Algorithm". en. In: *Journal of the Royal Statistical Society: Series B (Methodological)* 45.1, pp. 47 50.

Braun, A. (2016). "Pricing in the Primary Market for Cat Bonds: New Empirical Evidence". In: *Journal of Risk and Insurance* 83.4, pp. 811 847.

Brenier, Yann (1987). "Décomposition polaire et réarrangement monotone des champs de vecteurs". In: *CR Acad. Sci. Paris Sér. I Math.* 305, pp. 805 808.

Brigo, Damiano and Fabio Mercurio (Sept. 2007). *Interest Rate Models - Theory and Practice.* Springer-Verlag GmbH.

Brown, Adger W. Neil; Katrina (1994). *Land Use and the Causes of Global Warming.* Wiley, p. 271.

Brown, M E (2008). *Remote Sensing for Food Security Monitoring in Afghanistan.* NASA.

Brue, Stanley L (1993). "Retrospectives: The Law of Diminishing Returns". In: *Journal of Economic Perspectives* 7.3, pp. 185 192.

Bryk, A. S. and S. W. Raudenbush (1987). "Application of Hierarchical Linear Models to Assessing Change". In: *Psychological Bulletin* 101.1, pp. 147 158.

Burnecki, Krzysztof and Mario Giuricich (2017). "Stable Weak Approximation at Work in Index-Linked Catastrophe Bond Pricing". en. In: *Risks* 5.4, p. 64.

Burnecki, Krzysztof and Grzegorz Kukla (Oct. 2003). "Pricing of Zero-Coupon and Coupon Cat Bonds". In: *Applicationes Mathematicae* 30.3, pp. 315 324.

Burnecki, Krzysztof et al. (2005). "Pricing of Catastrophe Bonds". In: *Statistical Tools for Finance and Insurance*. Springer-Verlag, pp. 93 114.

Burnecki, Krzysztof et al. (2019). "Valuation of Contingent Convertible Catastrophe Bonds The Case for Equity Conversion". In: *Insurance: Mathematics and Economics* 88, pp. 238 254.

Burnside, R R (1975). "Convexity and Jensen's Inequality". In: *The American Mathematical Monthly* 82.10, pp. 1005 1005.

Burton, Philip J. et al. (2008). "Large fires as agents of ecological diversity in the North American boreal forest". In: *International Journal of Wildland Fire* 17.6, pp. 754 767.

Busing, F. M. T. A. (1993). "Distribution Characteristics of Variance Estimates in Two-Level Models: A Monte Carlo study". en. In: *Leiden psychological reports: Psychometrics and research methodology* 4.

Caflisch, Russel E. (1998). "Monte Carlo and quasi-Monte Carlo methods". In: *Acta Numerica* 7, pp. 1 49.

Campbell, Josette and Chris Hayhurst (2015). *Euclid: The Father of Geometry*. The Rosen Publishing Group, Inc.

Cannan, Edwin (1892). "The Origin of the Law of Diminishing Returns, 1813-15". In: *The Economic Journal* 2.5, p. 53.

Canter, Michael S. et al. (1996). "Insurance derivatives: a new asset class for the capital markets and a new hedging tool for the insurance industry". In: *The Journal of Derivatives* 4.2, pp. 89 104.

Carayannopoulos, P. and F. M. Perez (2015). “Diversification through Catastrophe Bonds: Lessons from the Subprime Financial Crisis”. In: *The Geneva Papers on Risk and Insurance - Issues and Practice* 40.1, pp. 1 28.

Carayannopoulos, Peter et al. (2022). “Pricing dynamics in the market for catastrophe bonds”. In: *The Geneva Papers on Risk and Insurance-Issues and Practice*, pp. 1 31.

Carter, D. J. T. and P. G. Challenor (1981). “Estimating return values of environmental parameters”. In: *Quarterly Journal of the Royal Meteorological Society* 107.451, pp. 259 266.

Carter, R. L. (1983). “The role and development of reinsurance”. en. In: ed. by R. L. Carter. Dordrecht: Springer Netherlands, pp. 1 21.

Carter, Walter H. and Raymond H. Myers (Mar. 1973). “Maximum Likelihood Estimation from Linear Combinations of Discrete Probability Functions”. In: *Journal of the American Statistical Association* 68.341, pp. 203 206.

Cashman, Katharine V. and Shane J. Cronin (Oct. 2008). “Welcoming a monster to the world: Myths, oral tradition, and modern societal response to volcanic disasters”. en. In: *Journal of Volcanology and Geothermal Research*. Volcanoes and Human History 176.3, pp. 407 418.

Cauchy, Augustin (1847). “Méthode générale pour la résolution des systemes d’équations simultanées”. In: *Comp. Rend. Sci. Paris* 25.1847, pp. 536 538.

Cebrián, Ana C. et al. (2015). “NHPoisson: An R Package for Fitting and Validating Nonhomogeneous Poisson Processes”. In: *Journal of Statistical Software* 64.6.

Celeux, Gilles. et al. (1996). “Stochastic versions of the em algorithm: an experimental study in the mixture case”. In: *Journal of Statistical Computation and Simulation* 55.4, pp. 287 314.

Ceppellini, By R. et al. (1955). “The Estimation of Gene Frequencies in a Random-Mating Population”. en. In: *Annals of Human Genetics* 20.2, pp. 97 115.

CFGB (2006). *Principle of Least Action: Maupertuis Leibniz Fermat Lagrange Euler Hamilton*. Cambridge Forecast Group Blog.

Chakraborty, Atlanta et al. (2020). “A linear programming primer: from Fourier to Karmarkar”. In: *Annals of Operations Research* 287, pp. 593 616.

Chamberlain, Basil H. (1982). *The Kojiki: Records of Ancient Matters*. en. Google-Books-ID: QZfYAAAAMAAJ. C.E. Tuttle Company.

Chandler, David (2003). “The Civilization of Angkor”. In: *Journal of Interdisciplinary History* 33.4, pp. 690 691.

Chao, Wen and Huiwen Zou (2018). “Multiple-Event Catastrophe Bond Pricing Based on CIR-Copula-POT Model”. In: *Discrete Dynamics in Nature and Society* 2018, pp. 1 9.

Charpentier, Arthur (2016). *Computational Actuarial Science with R*. Taylor and Francis Group.

Chaston, Joel (2001). “The Wizard of Oz: The Shaping of an Imaginary World, and: Oz and Beyond: The Fantasy World of L. Frank Baum (review)”. In: *The Lion and the Unicorn* 25.1, pp. 157 160.

Chavez-Demoulin, V. and A. Davison (2012). “Modelling Time Series Extremes”. In.

Chen, B-S. and C-W. Li (2017). *Big Mechanisms in Systems Biology*. Elsevier.

Chen, Gang (2016). *The politics of disaster management in China: Institutions, interest groups, and social participation*. Springer.

Chen, Yongxin et al. (2020). “On the matrix Monge Kantorovich problem”. In: *European Journal of Applied Mathematics* 31.4, pp. 574 600.

Childe, V G (Oct. 1936). “Man makes Himself”. en. In: *Nature* 138.3495, pp. 699 700.

Cissé, Jennifer D. (May 2021). “Climate and Disaster Risk Financing Instruments: An Overview”. eng. In.

Cohen, J. (1992). “Statistical Power Analysis”. In: *Current Directions in Psychological Science* 1.3, pp. 98 101.

Cole, Benjamin (June 2019). *Catastrophe bonds: An asset whose time has come*. IREI.

Cook, R. D. (1977). “Detection of Influential Observation in Linear Regression”. In: *Technometrics* 19.1, pp. 15 18.

Coppola, Damon PP (2006). *Introduction to international disaster management*. Elsevier.

Courant, Richard (1943). "Variational methods for the solution of problems of equilibrium and vibrations". In.

Couvreur, Christophe (1997). "The EM Algorithm: A Guided Tour". In: *Computer Intensive Methods in Control and Signal Processing*. Birkhäuser Boston, pp. 209 222.

Cox, John C. et al. (1985). "A Theory of the Term Structure of Interest Rates". In: *Econometrica* 53.2, p. 385.

Cox, S. H. and H. W. Pedersen (2000). "Catastrophe Risk Bonds". In: *North American Actuarial Journal* 4.4, pp. 56 82.

Cox, Samuel H. and Robert G. Schwebach (1992). "Insurance futures and hedging insurance price risk". In: *Journal of Risk and Insurance*, pp. 628 644.

Crutzen, Paul J. and Eugene F. Stoermer (2021). "The 'Anthropocene' (2000)". In: *Paul J. Crutzen and the Anthropocene: A New Epoch in Earth's History*. Springer International Publishing, pp. 19 21.

Cummins, D. J. and O. Mahul (2009). *Catastrophe Risk Financing in Developing Countries : Principles for Public Intevrvention*. Washington, D.C: The World Bank.

Cummins, J. D. (2008). "CAT Bonds and Other Risk-Linked Securities: State of the Market and Recent Developments". en. In: *Risk Management & Insurance Review* 11.1, pp. 23 47.

Cummins, J. D. and M. A. Weiss (2009). "Convergence of Insurance and Financial Markets: Hybrid and Securitized Risk-Transfer Solutions". en. In: *Journal of Risk and Insurance* 76.3, pp. 493 545.

Cummins, J. David et al. (Mar. 2002). "Can insurers pay for the "big one"? Measuring the capacity of the insurance market to respond to catastrophic losses". en. In: *Journal of Banking & Finance* 26.2, pp. 557 583.

Cummins, John et al. (2004). "The basis risk of catastrophic-loss index securities". In: *Journal of Financial Economics* 71.1, pp. 77 111.

Cuomo, Serafina (2007). *Pappus of Alexandria and the mathematics of late antiquity.* Cambridge University Press.

Dacorogna, Bernard (2007). *Direct methods in the calculus of variations.* Vol. 78. Springer Science & Business Media.

D'Agostino, Davi (2002). *Catastrophe Insurance Risks: The Role of Risk-Linked Securities and Factors Affecting Their Use.* US GAO.

Dalley, Stephanie (1998). *Myths from Mesopotamia: creation, the flood, Gilgamesh, and others.* Oxford University Press, USA.

D'arcy, Stephen P. and Virginia Grace France (1992). "Catastrophe futures: A better hedge for insurers". In: *Journal of Risk and Insurance*, pp. 575 600.

Darwin, Charles (1859). *On the origin of species by means of natural selection, or the preservation of favoured races in the struggle for life.* London: Murray.

Daugherty, Gregory N. (1992). "The Cohortes Vigilum and the Great Fire of 64 AD". In: *The Classical Journal* 87.3, pp. 229 240.

Davison, A. C. and R. L. Smith (1990). "Models for Exceedances Over High Thresholds". In: *Journal of the Royal Statistical Society: Series B (Methodological)* 52.3, pp. 393 425.

Degirmenci, Alpen (2014). "Introduction to Hidden Markov Models". In: *Lecture Notes: MIT Machine Learning.*

Dempster, A. P. et al. (1977). "Maximum Likelihood from Incomplete Data Via the EM Algorithm". en. In: *Journal of the Royal Statistical Society: Series B (Methodological)* 39.1, pp. 1 22.

Deng, Guoqu et al. (2020). "Research on the Pricing of Global Drought Catastrophe Bonds". In: *Mathematical Problems in Engineering* 2020, pp. 1 7.

Dieckmann, S. (Mar. 2010). "By Force of Nature: Explaining the Yield Spread on Catastrophe Bonds". en. In: *SSRN Electronic Journal* 1082879.

Dietz, K. (1997). "Introduction to McKendrick (1926) Applications of Mathematics to Medical Problems". en. In: ed. by Samuel Kotz and Norman L. Johnson. Springer Series in Statistics. New York, NY: Springer, pp. 17 57.

Difiore, Peter et al. (2021). “Catastrophe bonds: Natural diversification”. In: *Neuberger Bergman White Paper, 29th January.*

Doherty, Neil A. (1997). “Innovations in managing catastrophe risk”. In: *The Journal of risk and insurance* 64.4, pp. 713 718.

(2000). “Innovation in corporate risk management: the case of catastrophe risk”. In: *Handbook of Insurance*, pp. 503 539.

Doherty, Neil A. and Andreas Richter (2002). “Moral Hazard, Basis Risk, and Gap Insurance”. In: *Journal of Risk and Insurance* 69.1, pp. 9 24.

Duncan, Angus M. et al. (1996). “The 1928 Eruption of Mount Etna Volcano, Sicily, and the Destruction of the Town of Mascali”. en. In: *Disasters* 20.1, pp. 1 20.

Durbin, Richard et al. (1999). *Biological Sequence Analysis. Probabilistic Models of Proteins and Nucleic Acids.* Cambridge University Press, p. 356.

Efron, B (1967). “The two sample problem with censored data.” In: *Proceedings of the fifth Berkeley symposium on mathematical statistics and probability* 4.

Egami, Masahiko and Virginia R. Young (2008). “Indifference prices of structured catastrophe (CAT) bonds”. In: *Insurance: Mathematics and Economics* 42.2, pp. 771 778.

Embrechts, Paul et al. (1997). *Modelling Extremal Events.* Springer Berlin Heidelberg.

Embrechts, Paul et al. (1999). “Extreme Value Theory as a Risk Management Tool”. In: *North American Actuarial Journal* 3.2, pp. 30 41.

Ermoliev, Yuri M et al. (2000). “A System Approach to Management of Catastrophic Risks”. In: *European Journal of Operational Research* 122.2, pp. 452 460.

Euler, Leonhard (1744). *Methodus inveniendi lineas curvas maximi minimive proprietate gaudentes sive solutio problematis isoperimetrici latissimo sensu accepti.* Vol. 1. Springer Science & Business Media.

Evans, Steve (Dec. 2021). *George Town Re silver jubilee* 135*bnofcatastrophebondstracked*. Artemis.bm.

Everson, Jane E. (2012). “The melting pot of science and belief: studying Vesuvius in seventeenth-century Naples”. en. In: *Renaissance Studies* 26.5, pp. 691 727.

Eyring, Veronika et al. (Apr. 2021). “Reflections and projections on a decade of climate science”. en. In: *Nature Climate Change* 11.4, pp. 279 285.

Falk, Michael (1994). “Efficiency of convex combinations of pickands estimator of the extreme value index”. In: *Journal of Nonparametric Statistics* 4.2, pp. 133 147.

Falkner, Robert (2016). “The Paris Agreement and the new logic of international climate politics”. In: *International Affairs* 92.5, pp. 1107 1125.

Farand, Chloe (Oct. 2020). *Nigeria, Jamaica bring closure to the Kyoto Protocal era, in last-minute dash*. Climate Change News.

Farkas, Gyula (1894). “A Fourier-féle mechanikai elv alkalmazásai”. In: *Mathematikai és Természettudományi Ertesito* 12, pp. 457 472.

(1896). “A Fourier-féle mechanikai elv alkalmazásainak algebrai alapjáról (The algebraic basis of the applications of the mechanical principle of Fourier)”. In: *Mathematikai és Physikai Lapok* 5.49-54.

(1898). “A Fourier-féle mechanikai elv algebrai alapja”. In: *Mathématikai és Természettudományi Ertesito* 16, pp. 361 364.

Farkas, J. (1901). “Uber die Theorie des einfachen Ungleichungen, J”. In: *Reine Angew.*

Farkas, Julius (1895). *Über die Anwendungen des mechanischen Princips von Fourier*. Friedlander.

Fawcett, Lee (2013). “Topics in Statistics; Environmental Extremes”. In: *Newcastle University Lecture Notes*.

Fawcett, Lee and David Walshaw (2006). “A hierarchical model for extreme wind speeds”. In: *Journal of the Royal Statistical Society: Series C (Applied Statistics)* 55.5, pp. 631 646.

(2012). “Estimating return levels from serially dependent extremes”. In: *Environmetrics* 23.3, pp. 272 283.

Ferguson, James (2004). “A Brief Survey of the History of the Calculus of Variations and its Applications”. In: *arXiv preprint math/0402357*.

Ferguson, Thomas S. (1989). “Who solved the secretary problem?” In: *Statistical science* 4.3, pp. 282 289.

Ferro, Christopher A. T. and Johan Segers (2003). “Inference for clusters of extreme values”. In: *Journal of the Royal Statistical Society: Series B (Statistical Methodology)* 65.2, pp. 545 556.

Findlay, Ronald et al. (2002). *Bertil Ohlin: A Centennial Celebration, 1899-1999*. en. Google-Books-ID: Vz90T4yb4HoC. MIT Press.

Fisher, R. A. and L. H. C. Tippett (1928). “Limiting forms of the frequency distribution of the largest or smallest member of a sample”. In: *Mathematical Proceedings of the Cambridge Philosophical Society* 24.2, pp. 180 190.

Fitzpatrick, Richard (2008). “Euclid’s elements of geometry”. In.

Ford, L. R. and D. R. Fulkerson (1956). “Maximal Flow Through a Network”. In: *Canadian Journal of Mathematics* 8, pp. 399 404.

Ford, Lester Randolph and D. R. Fulkerson (Apr. 1962). *Flows in Networks*. en. Princeton University Press.

Forman, J. (Nov. 2019). “Introduction to Linear Mixed Models for Repeated Measurements Data: Analysis of Single Group Studies with SAS PROC MIXED”. Section of Biostatistics, University of Copenhagen.

Fourier, J B J (1798). “Mémoire sur la statique contenant la démonstration du principe des vitesses virtuelles et la théorie des moments”. In: *Journal de l’École polytechnique, Ve Cahier, p. 20,*

(1826). “Solution d’une question particuliere du calcul des inégalités.” In: *Nouveau Bulletin des Sciences par la Société philomatique de Paris* 99.100.

Fraser, Craig G. (2005). “Leonhard Euler, book on the calculus of variations (1744)”. In: *Landmark Writings in Western Mathematics 1640-1940*. Elsevier, pp. 168 180.

Froot, K. A. (1999a). “The Evolving Market for Catastrophic Event Risk”. In: *Risk Management & Insurance Review* 2.3, pp. 1 28.

Froot, Kenneth A. (Dec. 1999b). *The Financing of Catastrophe Risk*. en. Google-Books-ID: 6kXph_NvBFMC. University of Chicago Press.

(2001). “The market for catastrophe risk: a clinical examination”. In: *Journal of Financial Economics* 60.2-3, pp. 529 571.

Froot, Kenneth A. and Paul G. J. O'Connell (Apr. 1997). *On The Pricing of Intermediated Risks: Theory and Application to Catastrophe Reinsurance*. Working Paper 6011. National Bureau of Economic Research.

Froot, Kenneth A. and Paul GJ O'Connell (1999). "The pricing of US catastrophe reinsurance". In: *The financing of catastrophe risk*. University of Chicago Press, pp. 195 232.

Froot, Kenneth A. and Steven Posner (2000). "Issues in the Pricing of Catastrophe Risk". In: *Marsh and McLennan*.

Funk, Chris et al. (2019). "Recognizing the Famine Early Warning Systems Network: Over 30 Years of Drought Early Warning Science Advances and Partnerships Promoting Global Food Security". In: *Bulletin of the American Meteorological Society* 100.6, pp. 1011 1027.

Galeotti, M. et al. (2013). "Accuracy of Premium Calculation Models for CAT Bonds-An Empirical Analysis". In: *Journal of Risk and Insurance* 80.2, pp. 401 421.

Galloway, J. N. et al. (2014). "Ch. 15: biogeochemical cycles". In: *Climate change impacts in the United States: the third national climate assessment. US Global Change Research Program, Washington, DC, USA*, pp. 350 368.

Gamper, C (2018). *The cost of catastrophe: Why putting a price-tag on disaster is our best protection.* en. Organisation for Economic Cooperation and Development. The OECD Observer, 1-3.

Gates, David (2011). *The Napoleonic Wars 1803-1815*. Random House.

Gelman, A. and J. Hill (June 1, 2007). *Data Analysis Using Regression and Multilevel / Hierarchical Models: Analytical Methods for Social Research*. Cambridge University Press. 648 pp.

Gerber, Hans U. and Elias S. W. Shiu (Nov. 1996). "Actuarial bridges to dynamic hedging and option pricing". en. In: *Insurance: Mathematics and Economics* 18.3, pp. 183 218.

Ghesquiere, Francis et al. (2006). “Caribbean Catastrophe Risk Insurance Facility: A solution to the short-term liquidity needs of small island states in the aftermath of natural disasters”. In: *World Bank, Washington DC*.

Gnedenko, B. (1943). “Sur La Distribution Limite Du Terme Maximum D'Une Serie Aleatoire”. In: *The Annals of Mathematics* 44.3, p. 423.

Goetze, T. and M. Gürtler (2020). “Hard markets, Hard times: On the Inefficiency of the CAT bond market”. In: *Journal of Corporate Finance* 62, p. 101553.

Goldammer, Johann G. et al. (2005). “The current fire situation in the Russian Federation: implications for enhancing international and regional cooperation in the UN framework and the global programs on fire monitoring and assessment”. In: *Int. Forest Fire News* 32, pp. 13 42.

Goldstine, Herman Heine (2012). *A History of the Calculus of Variations from the 17th through the 19th Century*. Vol. 5. Springer Science & Business Media.

Gong, Xiaoli et al. (2019). “Yu the Great Managed the Flood”. In: *Children and Mother Nature*. BRILL, pp. 25 31.

Grabiner, Judith V. (1983). “The changing concept of change: the derivative from Fermat to Weierstrass”. In: *Mathematics magazine* 56.4, pp. 195 206.

Granados, Hugo Delgado and Susanna Jenkins (Jan. 2015). “Chapter 13 - Extreme Volcanic Risks 1: Mexico City”. en. In: ed. by John F. Shroder and Paolo Papale. Hazards and Disasters Series. Boston: Elsevier, pp. 315 354.

Grattan-Guinness, I. (Sept. 1970). “Joseph Fourier’s Anticipation of Linear Programming”. In: *Journal of the Operational Research Society* 21.3, pp. 361 364.

Graves, Robert (1955). *The Greek myths*. eng. Penguin books (Series). OCLC: 656544. Baltimore: Penguin Books.

GRFF (Jan. 2021). *Literature review of evidence on disaster risk finance | PreventionWeb*. en. Global Risk Financing Facility, World Bank.

Grün, Bettina and Friedrich Leisch (2008). “FlexMix Version 2: Finite Mixtures with Concomitant Variables and Varying and Constant Parameters”. In: *Journal of Statistical Software* 28.4.

Gumbel, E. J. (1958). *Statistics of Extremes*. Columbia University Press.

Gürtler, M. et al. (2016). "The Impact of the Financial Crisis and Natural Catastrophes on CAT Bonds". In: *Journal of Risk and Insurance* 83.3, pp. 579 612.

Gårding, Lars (1977). "The Heroic Century". en. In: ed. by Lars Gårding. New York, NY: Springer US, pp. 124 133.

Hadamard, J. (1907). "Memoire sur les problemes de fonctions holomorphes relatifs a l'equilibre des plaques elastiques encastrees". In: *Memoires presentes par divers savants a l'Academie des science* 33.

Hainaut, Donatien (2012). "Seasonality modelling for catastrophe bond pricing". In.

Han, S. P. (July 1977). "A globally convergent method for nonlinear programming". en. In: *Journal of Optimization Theory and Applications* 22.3, pp. 297 309.

Han, Shih-Ping (Dec. 1976). "Superlinearly convergent variable metric algorithms for general nonlinear programming problems". en. In: *Mathematical Programming* 11.1, pp. 263 282.

Hansen, James et al. (2016). "Ice melt, sea level rise and superstorms: evidence from paleoclimate data, climate modeling, and modern observations that 2 °C global warming could be dangerous". In: *Atmospheric Chemistry and Physics* 16.6, pp. 3761 3812.

Harper, Robert Francis (1999). *The Code of Hammurabi, King of Babylon: About 2250 B.C. : Autographed Text, Transliteration, Translation, Glossary Index of Subjects, Lists of Proper Names, Signs, Numuerals ...* en. Google-Books-ID: jeLz_BYUoeQC. The Lawbook Exchange, Ltd.

Harrington, Scott and Greg Niehaus (1999). "Basis risk with PCS catastrophe insurance derivative contracts". In: *Journal of Risk and Insurance*, pp. 49 82.

Harrison, Jenny (2014). "Soap film solutions to Plateau's problem". In: *Journal of Geometric Analysis* 24, pp. 271 297.

Hart-Davis, A (2012). *History: The Definitive Visual Guide (From The Dawn of . . .* en.

Harte, David (2021). "HiddenMarkov: Hidden Markov Models. R package version 1.8-13". In: *Statistics Research Associates*.

Hartley, H. O. (1958). "Maximum Likelihood Estimation from Incomplete Data". In: *Biometrics* 14.2, p. 174.

Hartshorne, Robin (2013). *Geometry: Euclid and beyond*. Springer Science & Business Media.

Hauksson, Egill et al. (1995). "The 1994 Northridge earthquake sequence in California: Seismological and tectonic aspects". In: *Journal of Geophysical Research: Solid Earth* 100.B7, pp. 12335 12355.

Hayter, Cox F (1949). *The Oldest Accident Office in the World. The Railway Passenger Assurance Company, 1849-1949*. Barter Books Ltd.

Healy, Michael and Michael Westmacott (1956). "Missing values in experiments analysed on automatic computers". In: *Journal of the Royal Statistical Society: Series C (Applied Statistics)* 5.3, pp. 203 206.

Heath, Thomas Little (1956). *The thirteen books of Euclid's Elements*. Courier Corporation.

Hellmann, Martin (2019). *Johannes Kepler: Nova stereometria doliorum vinariorum/New solid geometry of wine barrels. Accessit Stereometriæ Archimedeæ supplementum/A supplement to the Archimedean solid geometry has been added: Edited and translated, with an Introduction, by Eberhard Knobloch (Sciences et Savoirs. Bibliothèque de science, tradition et savoirs humanistes 4). Les Belles Lettres, Paris 2018, 348 S., ISBN 978-2-251-44832-9, ISSN 0184-7155,€ 95.*

Helske, Satu and Jouni Helske (2019). "Mixture Hidden Markov Models for Sequence Data: The seqHMM Package in R". In: *Journal of Statistical Software* 88.3.

Hemphill, R S (2012). "Peruvian Inca structural engineering". In: *Australasian Structural Engineering Conference 2012: The past, present and future of Structural Engineering*.

Hennings, Juli and Harry Lynch (2022). *Finding Faults with the Inca*. EarthDate.

Herrmann, Markus and Martin Hibbeln (2021). “Seasonality in catastrophe bonds and market-implied catastrophe arrival frequencies”. In: *Journal of Risk and Insurance* 88.3, pp. 785 818.

(2023). “Trading and liquidity in the catastrophe bond market”. In: *Journal of Risk and Insurance* 90.2, pp. 283 328.

Hirono, Tatsushi and Michelle Emery Blake (2017). “The role of religious leaders in the restoration of hope following natural disasters”. In: *Sage open* 7.2, p. 2158244017707003.

Hodder, Ian (Aug. 2010). *Religion in the Emergence of Civilization: Çatalhöyük as a Case Study*. en. Cambridge University Press.

Holder, O (1889). “Uber einen Mittelwertssatz”. In: *Nachr. Akad. Wiss. Gottingen Math.-Phys. Kl.*

Holland, David M. (2009). “A brief history of reinsurance”. In: *Reinsurance News* 65.19, pp. 4 29.

Hughes, J. Donald (2013). “Responses to Natural Disasters in the Greek and Roman World”. en. In: ed. by Katrin Pfeifer and Niki Pfeifer. Dordrecht: Springer Netherlands, pp. 111 137.

Hull, John C. (Sept. 2017). *Options, Futures, and Other Derivatives, Global Edition*. Pearson. 896 pp.

Hyndman, Donald and David Hyndman (2016). *Natural hazards and disasters*. Cengage Learning.

Härdle, Wolfgang Karl and Brenda López Cabrera (2010). “Calibrating CAT Bonds for Mexican Earthquakes”. In: *Journal of Risk and Insurance* 77.3, pp. 625 650.

Ibrahim Dincer Can Ozgur Colpan, Fethi Kadioglu, ed. (2013). *Causes, Impacts and Solutions to Global Warming*. Springer New York.

ICMIF (July 2020). *A practical guide tounderstanding mutual insurance*. International Cooperative and Mutual Insurance Federation.

ICRC (2021). *Somali Herders Defenceless Against The Climate Crisis*. https://www.icrc.org/en/docume herders-climate-change-conflict-crisis.

Intergovernmental Panel on Climate Change (2018). *Global warming of 1.5° C: An IPCC special report on the impacts of global warming of 1.5° C above pre-industrial levels and related global greenhouse gas emission pathways, in the context of strengthening the global response to the threat of climate change, sustainable development, and efforts to eradicate poverty.* Intergovernmental Panel on Climate Change.

Ivanov, A. et al. (Sept. 2022). “The Grain Market in India and the Creation of the BRICS Grain Union”. In: *BRICS Law Journal* 9.3, pp. 117 143.

Jacobs, J (2005). *English Fairy Tales.* Pennsylvania: A Penn State Electronic Classics Series Publication.

Jensen, Johan Ludwig William Valdemar (1906). “Sur les fonctions convexes et les inégalités entre les valeurs moyennes”. In: *Acta mathematica* 30.1, pp. 175 193.

Johnson, Nils P. (2004). “The brachistochrone problem”. In: *The College Mathematics Journal* 35.3, pp. 192 197.

Jones Lucile M.; Aki, Keiti; Boore David M.; Çelebi Mehmet; Donnellan Andrea; Hall John F.; Harris Ruth A.; Hauksson Egill; Heaton Thomas H.; Hough S.E.; Hudnut Kenneth W.; Hutton Kate; Johnston Malcolm J. S.; Joyner William B.; Kanamori Hiroo; Marshall Grant A.; Michael Andrew J.; Mori Jim; Murray Mark H.; Ponti Daniel J.; Reasenberg Paul A.; Schwartz David C.; Seeber Leonardo; Shakal A.; Simpson Robert W.; Thio Hong-Kie; Tinsley John C.; Todorovska Maria I.; Trifunac Mihailo D.; Wald David J.; Zoback Mary Lou (1994). “The Magnitude 6.7 Northridge, California, Earthquake of 17 January 1994”. In: *Science* 266.5184, pp. 389 397.

Juang, B. H. and L. R. Rabiner (1991). “Hidden Markov Models for Speech Recognition”. In: *Technometrics* 33.3, pp. 251 272.

Kafafi, Zeidan (June 2014). “Ayn Ghazal. A 10,000 year-old Jordanian village”. en. In: *Atlas of Jordan : History, Territories and Society.* Ed. by Myriam Ababsa. Contemporain publications. Beyrouth: Presses de l’Ifpo, pp. 111 113.

Kantorovich, L. V. (1960). “Mathematical Methods of Organizing and Planning Production”. In: *Management Science* 6.4, pp. 366 422.

Kantorovich, Leonid V. (1942). “On the translocation of masses”. In: *Dokl. Akad. Nauk. USSR (NS)*. Vol. 37, pp. 199 201.

Karmarkar, Narendra (1984). “A new polynomial-time algorithm for linear programming”. In: *Proceedings of the sixteenth annual ACM symposium on Theory of computing*, pp. 302 311.

Kennett, Douglas J. and James P. Kennett (2006). “Early state formation in southern Mesopotamia: Sea levels, shorelines, and climate change”. In: *Journal of Island & Coastal Archaeology* 1.1, pp. 67 99.

Khachiyan, L. G. (1979). “A polynomial algorithm in linear programming”. In: *Dokl. Akad. Nauk SSSR* 244.5, 1093 1096.

Kijima, Masaaki (2006). “A multivariate extension of equilibrium pricing transforms: The multivariate Esscher and Wang transforms for pricing financial and insurance risks”. In: *ASTIN Bulletin: The Journal of the IAA* 36.1, pp. 269 283.

King, L W (2005). *The Code of Hammurabi*. Yale University.

Knobloch, Eberhard (2017). “The Hellenistic mathematician Archimedes and his Renaissance admirer Kepler”. In: *Hellenistic Alexandria* 13, p. 249.

Kohn, Meir (Feb. 1999). *Risk Instruments in the Medieval and Early Modern Economy*. en. Tech. rep. 151871. Rochester, NY.

Koopmans, Tjalling C. (1960). “A Note About Kantorovich's Paper, “Mathematical Methods of Organizing and Planning Production””. In: *Management Science* 6.4, pp. 363 365.

Korn, Ralf et al. (2010). *Monte Carlo Methods and Models in Finance and Insurance*. CRC Press.

Kovalchuk, Igor et al. (2004). “Molecular Aspects of Plant Adaptation to Life in the Chernobyl Zone”. In: *Plant Physiology* 135.1, pp. 357 363.

Kreft, I. and J. de Leeuw (1998). *Introducing Multilevel Modeling*. 1 Oliver’s Yard, 55 City Road, London England EC1Y 1SP United Kingdom: SAGE Publications, Ltd.

Kreyszig, Erwin (1994a). “On the Calculus of Variations and Its Major Influences on the Mathematics of the First Half of Our Century. Part I.” In: *The American Mathematical Monthly* 101.7, pp. 674 678.

(1994b). “On the Calculus of Variations and Its Major Influences on the Mathematics of the First Half of Our Century. Part II.” In: *The American Mathematical Monthly* 101.9, pp. 902 908.

Krtinic, Djordje and Marija Mikic (2018). “Refinement of Hermite Hadamard type inequalities for s -convex functions”. In: *Miskolc Mathematical Notes* 19.2, pp. 997 1005.

Krutov, A. (2010). *Investing in Insurance Risk: Insurance-Linked Securities ; a Practitioner’s Perspective*. London: Risk Books.

Kuhn, H. W. and A. W. Tucker (Jan. 1951). “Nonlinear Programming”. In: *Proceedings of the Second Berkeley Symposium on Mathematical Statistics and Probability*. Vol. 2. University of California Press, pp. 481 493.

Kunkel, Paul (2016). *Hanging With Galileo*. Whistler Alley Mathematics.

Kunreuther, Howard and Geoffrey Heal (2012). *Managing catastrophic risk*. Tech. rep. National Bureau of Economic Research.

Kuznetsova, A. et al. (2017). “lmerTest Package: Tests in Linear Mixed Effects Models”. In: *Journal of Statistical Software* 82.13.

Lambert, Simon and John Scott (2019). “International Disaster Risk Reduction Strategies and Indigenous Peoples”. In: *International Indigenous Policy Journal* 10.2, pp. 1 21.

Lane, M. and O. Mahul (2008). “Catastrophe Risk Pricing: An Empirical Analysis”. In: *Policy Research Working Papers*.

Lane, M. N. (2000). “Pricing Risk Transfer Transactions”. In: *ASTIN Bulletin* 30.2, pp. 259 293.

(2018). *Pricing Cat Bonds: Regressions and Machine Learning: Some Observations, Some Lessons*.

Lane, M. N. and R. G. Beckwith (2007). *That Was the Year that Was! The 2007 Review of the Insurance Securitization Market*.

(2008). *The 2008 Review of ILS Transactions: What Price ILS? A Work in Progress*.

(June 2009). *Classic Hard Market? Lane Financial Insurance Return Index Quarterly Market Performance Report - Q2 2009*. Lane Financial LLC Trade Notes.

(2020). *"Ceteris Paribus" ... is on hold: Annual Review and Commentary for the Four Quarters, Q2 2019 to Q1 2020*.

Lane, Morton (2021). *History and Analysis of Natural Catastrophe ILS Issues 2001-2020*. Lane Financial LLc.

Lauer, Matthew (2012). "Oral traditions or situated practices? Understanding how indigenous communities respond to environmental disasters". In: *Human Organization* 71.2, pp. 176 187.

Lay, T. et al. (2013). "Introduction to the special issue on the 2011 Tohoku earthquake and tsunami". In: *Bulletin of the Seismological Society of America* 103.2B, pp. 1165 1170.

Le Treut, H. et al. (Sept. 2007). "Historical Overview of Climate Change Science. Chapter 1". English. In.

Leadbetter, M. R. et al. (1983). *Extremes and Related Properties of Random Sequences and Processes*. Springer New York.

Lee, Jin-Ping and Min-Teh Yu (2002). "Pricing default-risky CAT bonds with moral hazard and basis risk". In: *Journal of Risk and Insurance*, pp. 25 44.

Leeden, R. van der et al. (Dec. 26, 2007). "Handbook of Multilevel Analysis". In: ed. by Jan de Leeuw and Erik Meijer. Springer, New York, NY. Chap. 11, pp. 401 433.

Legendre, Adrien Marie (1806). *Nouvelles méthodes pour la détermination des orbites des comètes; par A.M. Legendre ...* fr. Google-Books-ID: n8rYPgqgt_AC. chez Firmin Didot, libraire pour lew mathematiques, la marine, l'architecture, et les editions stereotypes, rue de Thionville.

Leisch, Friedrich (2004). “FlexMix: A General Framework for Finite Mixture Models and Latent Class Regression iniR/i”. In: *Journal of Statistical Software* 11.8.

Lemaréchal, Claude (2012). “Cauchy and the gradient method”. In: *Doc Math Extra* 251.254, p. 10.

Leroy, Suzanne AG (2020). “Natural hazards, landscapes and civilizations”. In: *Reference Module in Earth Systems and Environmental Sciences*.

Leroy, Suzanne A.G. (2022). “Natural Hazards, Landscapes and Civilizations”. In: *Treatise on Geomorphology*. Elsevier, pp. 620 634.

Lin, Faqin et al. (Mar. 2023). “The impact of Russia-Ukraine conflict on global food security”. In: *Global Food Security* 36, p. 100661.

Litzenberger, R. H. et al. (1996). “Assessing Catastrophe Reinsurance-Linked Securities as a New Asset Class”. In: *The Journal of Portfolio Management* 23.5, pp. 76 86.

Livshits, K. I. (1999). “Probability of ruin of an insurance company for the poisson model”. In: *Russian Physics Journal* 42.4, pp. 394 399.

Ljung, G. M. and G. E. P. Box (1978). “On a measure of lack of fit in time series models”. In: *Biometrika* 65.2, pp. 297 303.

Longo, Bernadette M. and Anthony A. Longo (Aug. 2013). “Volcanic ash in the air we breathe”. en. In: *Multidisciplinary Respiratory Medicine* 8.1, p. 52.

Lorah, J. (2018). “Effect Size Measures for Multilevel Models: Definition, Interpretation, and TIMSS example”. In: *Large-scale Assessments in Education* 6.8.

Ma, Zong-Gang and Chao-Qun Ma (2013). “Pricing Catastrophe Risk Bonds: A Mixed Approximation Method”. In: *Insurance: Mathematics and Economics* 52.2, pp. 243 254.

Maas, Cora J. M. and Joop J. Hox (2005). “Sufficient Sample Sizes for Multilevel Modeling”. In: *Methodology* 1.3, pp. 86 92.

Maeterlinck, Maurice (1901). *The Life of the Bee*. en. Google-Books-ID: KYEVAAAAMAAJ. Dodd, Mead.

Mahoney, Michael Sean (1994). *The Mathematical Career of Pierre de Fermat, 1601-1665*. en. Google-Books-ID: iuM9DwAAQBAJ. Princeton University Press.

Maizland, Lindsay (Nov. 2022). *Global Climate Agreements: Successes and Failures.* Council on Foreign Relations (CFR).

Major, J. A. (2019). "Methodological Considerations in the Statistical Modeling of Catastrophe Bond Prices". In: *Risk Management and Insurance Review* 22.1, pp. 39 56.

Major, J. A. and R. E. Kreps (2002). "Catastrophe Risk Pricing in the Traditional Market". In: *Alternative Risk Strategies.* Risk Waters Group, pp. 201 220.

Manes, Alfred (1942). "Outlines of a general economic history of insurance". In: *The Journal of Business of the University of Chicago* 15.1, pp. 30 48.

Markowitz, Harry (1952). "Portfolio Selection". In: *The Journal of Finance* 7.1, p. 77.

Marschak, J. (1938). "Money and the Theory of Assets". In: *Econometrica* 6.4, pp. 311 325.

Masci, P (2011). *The history of insurance: risk, uncertainty and entrepreneurship.* Business and Public Administration Studies.

Mauch, Christof and Christian Pfister (2009). *Natural Disasters, Cultural Responses: Case Studies Toward a Global Environmental History.* en. Google-Books-ID: VpI-jAQAAIAAJ. Lexington Books.

Maupertuis, Pierre Louis Moreau de (1744). "Accord de différentes lois de la nature qui avaient jusqu'ici paru incompatibles (Eng. trans." In: *Accord between different laws of nature that seemed incompatible")," presented at the Mémoires l'Acad. Sci. Paris, Paris, France*, p. 417.

(1746). "Les lois du mouvement et du repos, déduites d'un principe de métaphysique (Eng. trans." In: *Derivation of the laws of motion and equilibrium from a metaphysical principle"")," presented at the Mémoires l'Acad. Sci. Paris, Berlin, Germany*, p. 267.

Mays, Larry W. (2010). *Ancient Water Technologies.* Springer, p. 280.

McDaniel, Thomas F. (1968). "The alleged Sumerian influence upon Lamentations". In: *Vetus Testamentum* 18.1-4, pp. 198 209.

McDermott, Gerald (1987). *Anansi the Spider: A Tale from the Ashanti. A Tale from the Ashanti (An Owlet Book)*. Henry Holt and Co. (BYR), p. 48.

McLachlan, Geoffrey J. and Thriyambakam Krishnan (Nov. 2007). *The EM Algorithm and Extensions*. en. Google-Books-ID: NBawzaWoWa8C. John Wiley & Sons.

McLachlan, Krishnan (Feb. 2008). *The EM Algorithm and Extensions (2nd ed.)* John Wiley Sons. 400 pp.

McNeil, Alexander J. (1997). "Estimating the Tails of Loss Severity Distributions Using Extreme Value Theory". In: *ASTIN Bulletin* 27.1, pp. 117 137.

Mendes, B. (2006). "A Bayesian analysis of clusters of extreme losses". In.

Mendes, B. and Juliana Sa Freire de Lima (2005). "Modeling Clusters of Extreme Losses". In.

Mendia-Landa, Pedro (2008). "Myths and Legends on Natural Disasters: Making Sense of our World". In: *Diakses pada*, pp. 02 05.

Meng, Xiao-Li and David Van Dyk (1997). "The EM Algorithm an Old Folk-song Sung to a Fast New Tune". In: *Journal of the Royal Statistical Society Series B: Statistical Methodology* 59.3, pp. 511 567.

Milfont, Taciano L. et al. (2021). "Scepticism of anthropogenic climate change: Additional evidence for the role of system-justifying ideologies". In: *Personality and Individual Differences* 168, p. 110237.

Miljkovic, Tatjana and Bettina Grün (2016). "Modeling loss data using mixtures of distributions". In: *Insurance: Mathematics and Economics* 70, pp. 387 396.

Minkowski, H L (1910). "Geometrie der Zahlen". In.

— (1911). "Theorie der konvexen Korper. insbesondere Begründung ihres Oberflachenbegriffs." In: *Gesammelte Abhandlungen II, Teubner, Leipzig*.

MIS (2023). *Reinsurers defend against rising tide of natural catastrophe losses, for now.* Tech. rep. Moody's Investor Service.

MMC Securities (2007). *The Catastrophe Bond Market at Year-End 2006: Ripples Into Waves*.

Monge, Gaspard (1781). “Mémoire sur la théorie des déblais et des remblais”. In: *Mem. Math. Phys. Acad. Royale Sci.*, pp. 666 704.

Motzkin, Theodore Samuel (1936). “Beiträge zur Theorie der linearen Ungleichungen”. In: *(No Title)*.

Muhammad, Ameer et al. (Aug. 2017). “Drought Characterization for a Snow-Dominated Region of Afghanistan”. EN. In: *Journal of Hydrologic Engineering* 22.8, p. 05017014.

Murphy, Kevin P. (2012). *Machine learning a probabilistic perspective. a probabilistic perspective*. MIT Press.

Nahin, Paul J. (2003). *When Least is Best: How Mathematicians Discovered Many Clever Ways to Make Things as Small (or as Large) as Possible*. en. Google-Books-ID: flz0m86ZUPUC. Princeton University Press.

Nakagawa, S. and H. Schielzeth (2012). “A General and Simple Method for Obtaining R2 from Generalized Linear Mixed-effects Models”. In: *Methods in Ecology and Evolution* 4.2. Ed. by Robert B. O'Hara, pp. 133 142.

Nance, R. Damian et al. (2014). “The supercontinent cycle: a retrospective essay”. In: *Gondwana Research* 25.1, pp. 4 29.

NASA (Sept. 2023). *Global Climate Change: Vital Signs of the Planet*. https://climate.nasa.gov/effects/.

Nazareth, John L. (1994). “The Newton and Cauchy perspectives on computational nonlinear optimization”. In: *SIAM review* 36.2, pp. 215 225.

NCEI (Mar. 2021). *On This Day: 2011 Tohoku Earthquake and Tsunami*. National Oceanic and Atmospheric Administration.

Neunzert, Helmut and Abul Hasan Siddiqi (2000). *Topics in industrial mathematics: case studies and related mathematical methods*. Vol. 42. Springer Science & Business Media.

Newcomb, Simon (1886). “A Generalized Theory of the Combination of Observations so as to Obtain the Best Result”. In: *American Journal of Mathematics* 8.4, pp. 343 366.

Nezlek, J. B. (2012). “Multilevel Modeling for Psychologists”. In: *APA Handbook of Research Methods In Psychology, Volume 3: Data Analysis and Research Publication*. American Psychological Association, pp. 219 241.

Ng, Shu Kay et al. (2011). “The EM Algorithm”. In: *Handbook of Computational Statistics*. Springer Berlin Heidelberg, pp. 139 172.

Niebyl, Donald (2021). *Skopje’s 1963 Quake: From Ruins to Modernist Resurrection*. Spomenik Database.

Niehaus, Greg and Steven V. Mann (1992). “The Trading of Underwriting Risk: An Analysis of Insurance Futures Contracts and Reinsurance”. In: *The Journal of Risk and Insurance* 59.4, pp. 601 627.

Nielsen, Søren Feodor (2000). “The Stochastic EM Algorithm: Estimation and Asymptotic Results”. In: *Bernoulli* 6.3, p. 457.

NOAA (May 2022). *NOAA predicts above-normal 2022 Atlantic Hurricane Season*. National Oceanic and Atmospheric Administration.

Nordell, Bo (Sept. 2003). “Thermal pollution causes global warming”. In: *Global and Planetary Change* 38.3 4, pp. 305 312.

Nowak, Piotr and Maciej Romaniuk (2013). “Pricing and Simulations of Catastrophe Bonds”. In: *Insurance: Mathematics and Economics* 52.1, pp. 18 28.

(2016). “Valuing Catastrophe Bonds Involving Correlation and CIR Interest Rate Model”. In: *Computational and Applied Mathematics* 37.1, pp. 365 394.

Nunn, Patrick D. (2003). “Fished up or thrown down: The geography of Pacific Island origin myths”. In: *Annals of the Association of American Geographers* 93.2, pp. 350 364.

O’Connor, J J and E F Roberston (1999). *Heron of Alexandria - Biography*. en.

O’Connor, J J and E F Robertson (2003). *The Berlin Academy and forgery*. en.

OECD (2017). *OECD Recommendation on Disaster Risk Financing Strategies - OECD*.

(2021). *Financial Management of Catastrophe Risks: Approaches to Building Financial Resilience - OECD*.

Oki, Taikan (2006). “The hydrologic cycles and global circulation”. In: *Encyclopedia of hydrological sciences*.

Omtatah, Okoiti (1991). *Lwanda Magere*. Heinmann Kenya.

Orchard, Terence and Max A. Woodbury (Apr. 1972). “A missing information principle: theory and applications”. en. In: *Volume 1 Theory of Statistics*. University of California Press, pp. 697 716.

Oskin, Becky (Feb. 2022). *Japan Earthquake & Tsunami of 2011: Facts and Information*. en. LiveScience.

O’Rourke, Kevin H. (Mar. 2006). “The worldwide economic impact of the French Revolutionary and Napoleonic Wars, 1793 1815”. en. In: *Journal of Global History* 1.1, pp. 123 149.

Pande, Mohit (May 2023). *The State of the Reinsurance Property Catastrophe Market*. Swiss Re.

Papachristou, D. (2009). “Statistical Analysis of the Spreads of Catastrophe Bonds at the Time of Issue”. In: *ASTIN Colloquia*.

PartnerRe (2015). *The Drivers of CatastropheBond Pricing*. Partner Reviews.

Patel, N. (2015). *The Drivers of Catastrophe Bond Pricing*.

Pearce II, J. A. and I. A. Lipin (2011). “Special Purpose Vehicles in Bankruptcy Litigation”. In: *Hofstra Law Review* 40.1.

Pearson, Karl (1894). “Contributions to the Mathematical Theory of Evolution”. In: *Philosophical Transactions of the Royal Society of London. A* 185, pp. 71 110.

Penny, Dan et al. (2019). “Geoarchaeological evidence from Angkor, Cambodia, reveals a gradual decline rather than a catastrophic 15th-century collapse”. In: *Proceedings of the National Academy of Sciences* 116.11, pp. 4871 4876.

Peyré, Gabriel and Marco Cuturi (Mar. 2019). *Computational Optimal Transport*. Tech. rep. arXiv:1803.00567 [stat] type: article. arXiv.

Piantedosi, Ilaria (2020). “CAT bonds and pandemic bonds: the world bank unique experience and the new challenge for the insurance industry”. In.

Pickands, James (1975). “Statistical Inference Using Extreme Order Statistics”. In: *The Annals of Statistics* 3.1.

Pinch, Geraldine (2004). *Egyptian Mythology. A Guide to the Gods, Goddesses, and Traditions of Ancient Egypt*. Oxford University Press, USA, p. 272.

Pontryagin, L. S. (Mar. 1987). *Mathematical Theory of Optimal Processes*. en. Google-Books-ID: kwzq0F4cBVAC. CRC Press.

Powell, M. J. D. (1978a). “A fast algorithm for nonlinearly constrained optimization calculations”. In: *Lecture Notes in Mathematics*. Springer Berlin Heidelberg, pp. 144 157.

(Jan. 1978b). “The convergence of variable metric methods for nonlinearly constrained optimization calculations”. en. In: ed. by Olvi L. Mangasarian et al. Academic Press, pp. 27 63.

Powell, Michael JD (1978c). “Algorithms for nonlinear constraints that use Lagrangian functions”. In: *Mathematical programming* 14, pp. 224 248.

Prudential Insurance Company of America (1915). *The Documentary History of Insurance, 1000 B. C. - 1875 A. D.* en. Google-Books-ID: RDHMPgAACAAJ.

Prékopa, András (Aug. 1980). “On the Development of Optimization Theory”. In: *The American Mathematical Monthly* 87.7, pp. 527 542.

Pugh, D.T. and J. M. Vassie (1980). “Applications of the Joint Probability Method for Extreme Sea Level Computations”. In: *Proceedings of the Institution of Civil Engineers* 69.4, pp. 959 975.

Quéré, Corinne Le et al. (2021). “Fossil CO2 emissions in the post-COVID-19 era”. In: *Nature Climate Change* 11.3, pp. 197 199.

Rabiner, L.R. (1989). “A tutorial on hidden Markov models and selected applications in speech recognition”. In: *Proceedings of the IEEE* 77.2, pp. 257 286.

Rappaport, Edward (1993). *Preliminary Report Hurricane Andrew, 16 - 28 August, 1992*. Tech. rep. U.S. Department of Commerce, National Oceanic and Atmospheric Administration, National Weather Service, National Hurricane Center.

Raudenbush, S. W. and A. S. Bryk (2010). *Hierarchical Linear Models: Applications and Data Analysis Methods*. 2. ed., [Nachdr.] Vol. 1. Advanced quantitative techniques in the social sciences. Thousand Oaks, California.: SAGE Publications Ltd.

Raup, David M. (1994). “The role of extinction in evolution.” In: *Proceedings of the National Academy of Sciences* 91.15, pp. 6758 6763.

Redner, Richard A. and Homer F. Walker (1984). “Mixture densities, maximum likelihood and the EM algorithm”. In: *SIAM review* 26.2, pp. 195 239.

Reid, Kathryn (Nov. 2019). *2005 Hurricane Katrina: Facts and FAQs*. World Vision.

Rejda, George E. and Michael McNamara (2005). *Principles of Risk Management and Insurance*. Pearson, p. 748.

Renn, Jürgen and Peter Damerow (2003). “The Hanging Chain: A Forgotten “Discovery” Buried in Galileo’s Notes on Mition”. In: *Reworking the Bench: Research Notebooks in the History of Science*, pp. 1 24.

Resnick, Sidney I (1997). “Discussion of the Danish Data on on Large Fire Insurance Losses”. In: *ASTIN Bulletin* 27.1, pp. 139 151.

Ring, Michael J et al. (2012). “Causes of the Global Warming Observed since the 19th Century”. In: *Atmospheric and Climate Sciences* 02.04, pp. 401 415.

RMS (2004). *The Northridge, CaliforniaEarthquake: RMS 10-year Retrospective*. Tech. rep. Risk Management Solutions.

Rodkinson, Michael Levi et al. (1903). *New Edition of the Babylonian Talmud: Tracts Betzah, Succah, and Moed katan*. en. Google-Books-ID: DkcWAAAAYAAJ. New Talmud Publishing Company.

Rodríguez-Camilloni, Humberto (2009). “Review of Machu Picchu: Unveiling the Mystery of the Incas”. In: *Journal of Latin American Geography* 8.2, pp. 230 232.

Rootzén, Holger and Richard W. Katz (2013). “Design Life Level: Quantifying risk in a changing climate”. In: *Water Resources Research* 49.9, pp. 5964 5972.

Rosenberg, Donna (Jan. 1997). *Folklore, Myths, and Legends: A World Perspective, Hardcover Student Edition*. en. Google-Books-ID: 7AfungEACAAJ. McGraw-Hill Companies,Incorporated.

Roy, Andrew Donald (1952). “Safety first and the holding of assets”. In: *Econometrica: Journal of the econometric society*, pp. 431 449.

Ruijven, Bas J. van et al. (2019). “Amplification of future energy demand growth due to climate change”. In: *Nature Communications* 10.1.

Sargent, R. W. H. (2000). “Optimal control”. In: *Journal of Computational and Applied Mathematics* 124.1-2, pp. 361 371.

Sasaki, Daisuke and Mikio Ishiwatari (2022). “Recent trends in disaster risk reduction investments: a literature review”. In: *Financing Investment in Disaster Risk Reduction and Climate Change Adaptation*, pp. 37 47.

Sassa, Kyoji et al. (Jan. 2005). “Landslide Investigation in Machu Picchu World Heritage, Cusco, Peru (C101-1)”. In: pp. 25 38.

Schalatek, Liane et al. (2019). *The green climate fund.* Tech. rep. Overseas Development Institute and Heinrich Böll Stiftung North America, 1-8.

Schrijver, Alexander (1998). *Theory of linear and integer programming.* John Wiley & Sons.

Schwarcz, Steven L. (Oct. 2020). *Insuring the 'Uninsurable': Catastrophe Bonds, Pandemics, and Risk Securitization.* en. Tech. rep. 3712534. Rochester, NY.

Schwarz, Gideon (1978). “Estimating the Dimension of a Model”. In: *The Annals of Statistics* 6.2.

Scott, Anthony (2008). “Faustmann, Martin (1822 1876)”. In: *The New Palgrave Dictionary of Economics.* Palgrave Macmillan UK, pp. 1 2.

SDDG (2011). *The Kyoto Protocol.* Tech. rep. Statistiques Developpement Durable Gouv Fr.

Selya, A. S. et al. (2012). “A Practical Guide to Calculating Cohen’s f2, a Measure of Local Effect Size, from PROC MIXED”. In: *Frontiers in Psychology* 3.

Sezer, Sevda (2021). “The Hermite-Hadamard inequality for s-Convex functions in the third sense”. In: *AIMS Math* 6.7, pp. 7719 7732.

Shao, Jia et al. (2017). "Pricing and Simulating Catastrophe Risk Bonds in a Markov-Dependent Environment". In: *Applied Mathematics and Computation* 309, pp. 68 84.

Sialaros, Michalis (2015). "Euclid". In: *Oxford Classical Dictionary.*

Sibbett, Trevor (2006). *History of Insurance.*

Sieczkowska, Dominika et al. (Jan. 2022). "Inca water channel flow analysis based on 3D models from terrestrial and UAV laser scanning at the Chachabamba archaeological site (Machu Picchu National Archaeological Park, Peru)". In: *Journal of Archaeological Science* 137, p. 105515.

Simic, Milan (Sept. 2019). *Putting Jebi's Insured Losses in Context: A Look Back at Historic Japan Typhoons.* AIR Worldwide.

Simmons, George F. (2007). *Calculus gems: brief lives and memorable mathematics.* Vol. 55. MAA.

Simpson, E S et al. (2020). "Determining the dependence structure of multivariate extremes". In: *Biometrika* 107.3, pp. 513 532.

Sinadinovski, C and KF McCue (Nov. 2013). *50 years since the Skopje 1963 Earthquake: Implications for Australian building standards.* Tech. rep. In Australian Earthquake Engineering Society 2013 Conference. Hobart Tasmania.

Sitek, Grzegorz (2016). "Loss Modeling with Mixtures Distributions in R package". In: *Śląski Przegląd Statystyczny* 15, pp. 183 199.

Smit, Jana Louise (Dec. 2019). *Ancient Civilizations Timeline: The Complete List from Aboriginals to Incans | History Cooperative.* en-US.

Smith, A. Mark (1999). *Ptolemy and the Foundations of Ancient Mathematical Optics: A Source Based Guided Study.* en. Google-Books-ID: ASILAAAAIAAJ. American Philosophical Society.

Smith, C. a. B. (1957). "Counting Methods in Genetical Statistics". en. In: *Annals of Human Genetics* 21.3, pp. 254 276.

Smith, Richard L. (1989). "Extreme Value Analysis of Environmental Time Series: An Application to Trend Detection in Ground-Level Ozone". In: *Statistical Science* 4.4.

Smyth, William Henry (Aug. 2013). *The Sailor's Word-Book: An Alphabetical Digest of Nautical Terms*. en. Google-Books-ID: lVTGyMaGrHwC. Cambridge University Press.

SOQS (2019). *Results of Finding Vote by AWG*. Tech. rep. Anthropocene Working Group.

Soroush, Mehrnoush and Lee Mordechai (2018). "Adaptation to short-term cataclysmic events: flooding in premodern riverine societies". In: *Human Ecology* 46, pp. 349 361.

Spencer, Herbert (1872). "The survival of the fittest". In: *Nature* 5.118, pp. 263 264.

Spry, J. (2009). "Non-Life Insurance Securitization: Market Overview, Background and Evolution". In: *Handbook of Insurance Linked Securities*. John Wiley and Sons Ltd., pp. 7 18.

Stander, Daniel (July 2017). *The Role of Catastrophe Risk Finance in Developing Nations*. Risk Management Solutions (RMS).

Stigler, Stephen M (Feb. 1977). "An attack on Gauss, published by Legendre in 1820". en. In: *Historia Mathematica* 4.1, pp. 31 35.

Stigler, Stephen M. (1981). "Gauss and the Invention of Least Squares". In: *The Annals of Statistics* 9.3, pp. 465 474.

Stimpson, Ian (2011). "Japan's Tohoku earthquake and tsunami". In: *Geology Today* 27.3, pp. 96 98.

Sundberg, Rolf (1974). "Maximum Likelihood Theory for Incomplete Data from an Exponential Family". In: *Scandinavian Journal of Statistics* 1.2, pp. 49 58.

(Jan. 1976). "An iterative method for solution of the likelihood equations for incomplete data from exponential families". In: *Communications in Statistics - Simulation and Computation* 5.1, pp. 55 64.

Suñe-Puchol, Ivan et al. (Feb. 2019). "The Ilopango caldera complex, El Salvador: Origin and early ignimbrite-forming eruptions of a graben/pull-apart caldera structure". en. In: *Journal of Volcanology and Geothermal Research* 371, pp. 1 19.

Swiss Re (Sept. 2012). *What are Insurance Linked Securities (ILS), and Why Should they be Considered?*

(2017). *A History of Insurance*. Tech. rep. https://www.swissre.com/dam/jcr:638f00a0-71b9-4d8e-a960-dddaf9ba57cb/150_history_of_insurance.pdf: Swiss Re.

(2019). *ILS Market Update : September 2019*.

(2023). *Natural Catastrophes and Inflation in 2022: A Perfect Storm*. Tech. rep. Sigma Research Institute.

Syahputra, Hendra (2019). "Indigenous knowledge representation in mitigation process: A study of communities' understandings of natural disasters in Aceh Province, Indonesia". In: *Collection and Curation* 38.4, pp. 94 102.

Tang, Weiyi et al. (2021). "Widespread phytoplankton blooms triggered by 2019 2020 Australian wildfires". In: *Nature* 597.7876, pp. 370 375.

Tawn, J. A. et al. (1989). "Extreme Sea Levels; The Joint Probabilities Method Revisited and Revised". In: *Proceedings of the Institution of Civil Engineers* 87.3, pp. 429 442.

Teimouri, Mahdi et al. (2020). "ForestFit: An R package for modeling plant size distributions". In: *Environmental Modelling &amp Software* 131, p. 104668.

Teugels, Jef L. et al. (2004). *Encyclopedia of Actuarial Science*. Wiley, p. 1944.

Thompson d'Arcy, W. (1917). "On growth and form". In: *Cambridge: Cambridge University Press* 16, p. 794.

Titterington, D. Michael (1984). "Recursive parameter estimation using incomplete data". In: *Journal of the Royal Statistical Society: Series B (Methodological)* 46.2, pp. 257 267.

Tobin, James (1958). "Liquidity preference as behavior towards risk". In: *The review of economic studies* 25.2, pp. 65 86.

Tolmie, A. et al. (2011). *Quantitative Methods in Educational and Social Research Using SPSS*. Maidenhead: Open University Press.

Toomer, G. J. (1976). “On Burning Mirrors”. en. In: ed. by G. J. Toomer. Sources in the History of Mathematics and Physical Sciences. Berlin, Heidelberg: Springer, pp. 34 216.

Towe, Ross et al. (2019). “Modelling the Clustering of Extreme Events for Short-Term Risk Assessment”. In: *Journal of Agricultural, Biological and Environmental Statistics* 25.1, pp. 32 53.

Trenerry, Charles Farley (1926). *The Origin and Early History of Insurance: Including the Contract of Bottomry.* en. Google-Books-ID: v_xCAAAAIAAJ. P. S. King & son, Limited.

Turnbull, Bruce W. (1976). “The Empirical Distribution Function with Arbitrarily Grouped, Censored and Truncated Data”. en. In: *Journal of the Royal Statistical Society: Series B (Methodological)* 38.3, pp. 290 295.

UNCDF (2021). *Climate and Disaster Risk Financing Instruments - UN Capital Development Fund (UNCDF).* en. UN Capital Development Fund (UNCDF).

UNDP (May 2023). *Impacts of Changing Climate on Mongolia’s nomadic herder.*

UNDRR (Dec. 2016). “Report of the Open-ended Intergovernmental Expert Working Group on Indicators and Terminology relating to Disaster Risk Reduction :: note /: by the Secretary-General”. en. In.

(2022). *Global Assessment Report on Disaster Risk Reduction 2022: Our World at Risk: Transforming Governance for a Resilient Future.* en. Google-Books-ID: LQB0EAAAQBAJ. United Nations Office for Disaster Risk Reduction.

(2023a). *2022 The invisible toll of disasters.* United Nations Office for Disaster Risk Reduction.

(May 2023b). *DRR and UNDRR’s history | UNDRR.* en.

UNESCO (Nov. 2015). *UNESCO science report: towards 2030.* en. Google-Books-ID: SDHwCgAAQBAJ. UNESCO Publishing.

UNISDR (2004). “Living with risk: A global review of disaster reduction initiatives”. In: *United Nations International Strategy for Disaster Reduction.*

Vaughan, Emmett J. (1997). “Risk management”. In: *(No Title).*

Vaugirard, Victor E. (2003a). “Pricing Catastrophe Bonds by an Arbitrage Approach”. In: *The Quarterly Review of Economics and Finance* 43.1, pp. 119 132.

(2003b). “Valuing Catastrophe Bonds by Monte Carlo Simulations”. In: *Applied Mathematical Finance* 10.1, pp. 75 90.

Vesnic, Christoph Deuster; Nina Kajander; Stefan Muench; Fabrizio Natale; Astrid Nedee; Fabiana Scapolo; Philipp Ueffing; Lucia Alujevic (2023). *Demography and Climate Change*. Tech. rep. Publications Office of the European Union.

Viitala, Esa-Jussi (2006). “An early contribution of Martin Faustmann to natural resource economics”. In: *Journal of Forest Economics* 12.2, pp. 131 144.

Visser, Ingmar and Maarten Speekenbrink (2010). “depmixS4: An R Package for Hidden Markov Models”. In: *Journal of Statistical Software* 36.7.

Vitaliano, Dorothy B. (1968). “Geomythology: The Impact of Geologic Events on History and Legend with Special Reference to Atlantis”. In: *Journal of the Folklore Institute* 5.1, pp. 5 30.

(1973). *Legends of the Earth: Their Geologic Origins*. en. Google-Books-ID: FwjgAAAAMAAJ. Indiana University Press.

Wahlström, Margareta (2015). “New Sendai framework strengthens focus on reducing disaster risk”. In: *International Journal of Disaster Risk Science* 6, pp. 200 201.

Wang, J. et al. (Dec. 23, 2011). *Multilevel Models: Applications using SAS*. Walter de Gruyter.

Wang, Shaun (1996). “Premium calculation by transforming the layer premium density”. In: *ASTIN Bulletin: The Journal of the IAA* 26.1, pp. 71 92.

Wang, Shaun S. (2000). “A Class of Distortion Operators for Pricing Financial and Insurance Risks”. In: *Journal of Risk and Insurance* 67.1, p. 15.

(2002). “A Universal Framework for Pricing Financial and Insurance Risks”. In: *ASTIN Bulletin* 32.2, pp. 213 234.

Webster, Colin (2014). “Euclid’s Optics and geometrical astronomy”. In: *Apeiron* 47.4, pp. 526 551.

Wei, Greg C. G. and Martin A. Tanner (1990). “A Monte Carlo Implementation of the EM Algorithm and the Poor Man's Data Augmentation Algorithms”. In: *Journal of the American Statistical Association* 85.411, pp. 699 704.

Welch, Lloyd R (2003). “Hidden Markov Models and the Baum-Welch Algorithm”. In: *IEEE Inforamation Theory Society Newsletter* 53.4.

White, L. J. (2013). “Credit Rating Agencies: An Overview”. In: *Annual Review of Financial Economics* 5.1, pp. 93 122.

WHO (2023). *WHO Somalia: Technical Programme Update (January - April 2023)*. World Health Programme.

Willmot, Gordon E. and X. Sheldon Lin (2001). “Compound distributions”. In: *Lundberg Approximations for Compound Distributions with Insurance Applications*. Springer New York, pp. 51 80.

Wilson, R B (1963). “A simplicial algorithm for concave programming”. PhD thesis. Graduate School of Bussiness Administration, Harvard University.

World Bank Group (2017). *Sovereign Catastrophe Risk Pools: World Bank Technical Contribution to the G20*. World Bank.

Wu, C. F. Jeff (1983). “On the Convergence Properties of the EM Algorithm”. In: *The Annals of Statistics* 11.1, pp. 95 103.

Zeller, Wilhelm (2007). “Securitization and Insurance Characteristics of Hannover Re's Approach”. In: *The Geneva Papers on Risk and Insurance - Issues and Practice* 33.1, pp. 7 11.

Zhang, Oscar Y. W. et al. (2022). “Statistical Seasonal Forecasting of Tropical Cyclone Landfall on South China Utilizing Preseason Predictors”. In: *Frontiers in Earth Science* 9.

Zhang, Yang and Walter Gillis Peacock (2009). “Planning for housing recovery? Lessons learned from Hurricane Andrew”. In: *Journal of the American Planning Association* 76.1, pp. 5 24.

Zimbidis, A. A. et al. (2007). "Modeling earthquake risk via extreme value theory and pricing the respective catastrophe bonds". In: *ASTIN Bulletin: The Journal of the IAA* 37.1, pp. 163 183.

Zolkos, Rodd (Dec. 1997). *1997 Risk Management: Catastrophe Bonds Take Risk Financing by Storm*. Business Insurance.

Zoutendijk, G. (1960). *Methods of Feasible Directions: A Study in Linear and Nonlinear Programming*. en. Elsevier Publishing Company.

Zucchini, W. et al. (2016). *Hidden Markov Models for Time Series*. Taylor and Francis Group.

Ünüvar, Burcu (2019). "Financing the green economy". en. In: pp. 163 181.

.1 Summary of Issuer Characteristics

Table 1: *Catastrophe bonds by issuer*

Issuer	Size ($m)	% Size	Obs. (No)	% Obs.	Premium (%)	EL (%)	P/EL	EER (%)	Term
Achmea Re	54.70	0.06%	1	0.14%	3.30%	1.29%	2.56	2.01%	36.00
AGF	129.00	0.13%	2	0.28%	4.29%	0.69%	8.56	3.60%	60.00
AIG	1,325.00	1.37%	8	1.10%	6.53%	1.72%	4.03	4.81%	29.25
Aioi Nissay Dowa Insurance	167.90	0.17%	2	0.28%	3.00%	0.83%	4.00	2.17%	41.50
Allianz SE	1,755.00	1.81%	16	2.21%	10.36%	3.24%	4.80	7.12%	37.50
Allstate Insurance Company	2,725.00	2.81%	12	1.66%	5.30%	1.04%	5.06	4.27%	46.58
Am Family Mutual	200.00	0.21%	2	0.28%	7.48%	2.72%	3.04	4.76%	37.50
Am Re	176.80	0.18%	2	0.28%	4.24%	0.40%	13.14	3.84%	17.00
American Coastal Insurance	383.00	0.40%	2	0.28%	4.19%	0.46%	9.29	3.73%	21.00
American Modern Insurance	75.00	0.08%	1	0.14%	3.55%	0.57%	6.23	2.98%	36.00
American Re	116.40	0.12%	1	0.14%	5.58%	0.75%	7.44	4.83%	12.00
American Strategic Insurance	600.00	0.62%	4	0.55%	5.07%	1.85%	2.98	3.22%	38.25
Amlin AG	500.00	0.52%	3	0.41%	10.06%	3.63%	2.91	6.42%	44.00
AmTrust Financial Services	100.00	0.10%	1	0.14%	3.80%	1.19%	3.19	2.61%	47.00
Argo Re	372.00	0.38%	5	0.69%	13.44%	5.25%	2.82	8.19%	39.60
Arrow Re	162.80	0.17%	3	0.41%	3.95%	0.59%	34.68	3.37%	12.00
Arrow Re/St Farm	52.20	0.05%	1	0.14%	4.62%	0.63%	7.33	3.99%	12.00
Aspen Insurance Holdings	325.00	0.34%	2	0.28%	5.83%	2.29%	2.64	3.54%	30.00
Assicurazioni Generali	486.60	0.50%	2	0.28%	2.66%	1.66%	1.73	1.00%	42.00
Assurant	605.00	0.62%	9	1.24%	8.82%	2.06%	4.78	6.76%	36.00

Continued on next page

Table 1 – continued from previous page

Issuer	Size ($m)	% Size	Obs.	% Obs.	Premium (%)	EL (%)	P/EL	EER (%)	Term
Avatar P&C	100.00	0.10%	3	0.41%	8.45%	4.68%	2.66	3.77%	35.00
AXA Global Re	1,105.30	1.14%	4	0.55%	3.32%	1.28%	2.68	2.04%	41.75
AXIS Re	915.00	0.94%	4	0.55%	7.53%	3.73%	2.22	3.80%	41.25
Balboa Insurance Company.	50.00	0.05%	1	0.14%	3.04%	0.82%	3.71	2.22%	36.00
Bayview Opp Fd	225.00	0.23%	2	0.28%	4.57%	1.75%	3.16	2.82%	35.00
Brit Insurance Holdings plc	140.00	0.14%	2	0.28%	4.57%	0.78%	12.60	3.79%	36.00
California Earthquake Authority (CEA)	3,725.00	3.85%	13	1.80%	5.14%	2.09%	2.80	3.05%	37.85
California State Compensation Insurance Fund	660.00	0.68%	3	0.41%	2.75%	0.25%	11.90	2.51%	45.33
Castle Key Insurance & Indemnity	700.00	0.72%	2	0.28%	4.44%	0.78%	5.89	3.67%	41.50
Catlin Group	1,041.80	1.08%	6	0.83%	7.48%	2.42%	6.91	5.06%	36.50
Central Re Corp	100.00	0.10%	1	0.14%	4.11%	0.73%	5.63	3.38%	34.00
Centre Solutions (Bermuda) Ltd (Zurich Group)	113.15	0.12%	2	0.28%	3.75%	0.80%	4.69	2.95%	12.00
Chubb Group	1,745.00	1.80%	12	1.66%	7.60%	1.78%	4.90	5.81%	44.00
Citizen's Property Insurance	3,350.00	3.46%	6	0.83%	8.48%	2.47%	3.33	6.00%	33.67
Converium	100.00	0.10%	1	0.14%	5.48%	1.07%	5.12	4.41%	60.00
Dominion Resources	50.00	0.05%	1	0.14%	20.78%	1.54%	13.49	19.24%	7.00
Electricite de France	232.50	0.24%	2	0.28%	2.74%	0.28%	41.66	2.46%	60.00
Endurance Specialty Holdings	125.00	0.13%	1	0.14%	8.11%	1.13%	7.18	6.98%	18.00
Equator Re Ltd	250.00	0.26%	1	0.14%	3.80%	1.34%	2.84	2.46%	36.00
Everest Re	4,200.00	4.34%	19	2.62%	8.58%	4.78%	1.99	3.80%	52.32
First Mutual Transportation Assurance (MTA)	325.00	0.34%	2	0.28%	4.16%	2.07%	2.12	2.09%	35.50

Continued on next page

Table 1 – continued from previous page

Issuer	Size ($m)	% Size	Obs.	% Obs.	Premium (%)	EL (%)	P/EL	EER (%)	Term
Flagstone Re	489.00	0.50%	7	0.97%	12.07%	3.37%	4.74	8.69%	36.00
FM Global	300.00	0.31%	1	0.14%	3.17%	0.71%	4.46	2.45%	36.00
FONDEN, Mexico	315.00	0.33%	3	0.41%	7.86%	3.71%	2.23	4.15%	38.00
Frontline	350.00	0.36%	2	0.28%	9.51%	5.77%	1.70	3.74%	47.00
Gerling	180.00	0.19%	2	0.28%	4.41%	0.60%	7.77	3.81%	48.00
Glacier Re	255.00	0.26%	4	0.55%	10.05%	2.80%	3.87	7.25%	36.00
Great American Insurance Co.	285.00	0.29%	3	0.41%	4.99%	1.67%	3.24	3.32%	39.00
Groupama	292.00	0.30%	1	0.14%	3.65%	0.89%	4.10	2.76%	36.00
Gulfstream Ins.(for Vivendi)	175.00	0.18%	2	0.28%	6.64%	1.18%	6.35	5.46%	43.00
Hannover Re	5,081.20	5.25%	26	3.59%	7.51%	3.11%	3.03	4.40%	40.81
Hartford Fire Insurance	915.00	0.94%	7	0.97%	5.88%	0.93%	6.99	4.95%	45.00
Heritage P&C	852.50	0.88%	8	1.10%	6.56%	3.22%	2.38	3.34%	42.00
Hiscox Syndicate	33.00	0.03%	1	0.14%	6.84%	1.14%	6.00	5.70%	36.00
IBRD - Chile	500.00	0.52%	1	0.14%	2.53%	0.86%	2.94	1.67%	36.00
IBRD - Colombia	400.00	0.41%	1	0.14%	3.04%	1.56%	1.95	1.48%	36.00
IBRD - Mexico	1,105.00	1.14%	9	1.24%	6.70%	4.11%	1.98	2.58%	36.44
IBRD - Peru	200.00	0.21%	1	0.14%	6.08%	5.00%	1.22	1.08%	36.00
IBRD - Philippines	225.00	0.23%	2	0.28%	5.66%	2.97%	1.90	2.69%	36.00
ICAT Syndicate 4242	164.50	0.17%	2	0.28%	5.07%	2.89%	2.03	2.19%	37.00
Kemper	80.00	0.08%	1	0.14%	3.74%	0.50%	7.48	3.24%	37.00
Lehman Re	499.50	0.52%	3	0.41%	4.39%	0.49%	10.20	3.83%	18.67

Continued on next page

Table 1 – continued from previous page

Issuer	Size ($m)	% Size	Obs.	% Obs.	Premium (%)	EL (%)	P/EL	EER (%)	Term
Liberty Mutual	1,175.00	1.21%	7	0.97%	9.46%	1.53%	7.04	7.93%	34.29
Louisiana Citizens	565.00	0.58%	5	0.69%	6.13%	2.23%	2.62	3.90%	38.40
Markel Bermuda	100.00	0.10%	1	0.14%	2.79%	0.14%	19.93	2.65%	37.00
Mitsui Sumitomo	640.00	0.66%	5	0.69%	2.69%	0.97%	2.81	1.72%	52.80
MMM IARD SA+	239.22	0.25%	3	0.41%	6.64%	5.31%	1.28	1.33%	48.33
Montpelier Re	150.00	0.15%	2	0.28%	13.31%	3.51%	3.80	9.80%	36.00
Munich Re	4,051.40	4.18%	30	4.14%	7.12%	1.99%	4.26	5.14%	39.50
National Union Fire Insurance	1,850.00	1.91%	8	1.10%	9.19%	1.86%	5.38	7.33%	34.50
Nationwide Mutual	2,640.00	2.73%	18	2.49%	6.58%	2.40%	3.34	4.18%	38.78
Natixis SA	214.60	0.22%	2	0.28%	7.36%	3.56%	2.09	3.80%	57.00
NC Insurance Underwriting Association	550.00	0.57%	2	0.28%	5.58%	2.02%	2.79	3.56%	35.00
Nephila Capital Ltd.	240.00	0.25%	3	0.41%	3.85%	0.65%	29.30	3.21%	32.00
Oak Tree Assurance	400.00	0.41%	1	0.14%	2.79%	0.80%	3.49	1.99%	39.00
OCIL (Oil Casualty Insurance Ltd.)	405.00	0.42%	3	0.41%	4.55%	0.89%	16.17	3.66%	36.00
Oriental Land	100.00	0.10%	1	0.14%	3.14%	0.42%	7.48	2.72%	60.00
Palomar Specialty Ins.	166.00	0.17%	3	0.41%	4.39%	2.49%	1.92	1.90%	36.00
Passenger Railroad Ins.	275.00	0.28%	1	0.14%	4.56%	1.99%	2.29	2.57%	38.00
Platinum	200.00	0.21%	1	0.14%	4.82%	0.56%	8.61	4.26%	36.00
PXRE	550.00	0.57%	4	0.55%	7.10%	1.18%	7.33	5.92%	48.00
Renaissance Re	550.00	0.57%	3	0.41%	7.70%	2.95%	2.73	4.75%	39.33
Safepoint Insurance	435.00	0.45%	7	0.97%	7.71%	3.68%	3.08	4.04%	35.86

Continued on next page

Table 1 – continued from previous page

Issuer	Size ($m)	% Size	Obs.	% Obs.	Premium (%)	EL (%)	P/EL	EER (%)	Term
SCOR	2,716.60	2.80%	21	2.90%	9.00%	2.47%	8.15	6.53%	39.43
Sempra En, SD G&E, S C	125.00	0.13%	1	0.14%	4.06%	0.21%	19.33	3.85%	36.00
Sompo Japan Nipponkoa	878.00	0.91%	4	0.55%	2.53%	0.88%	3.02	1.65%	48.25
Sorema	34.00	0.04%	2	0.28%	5.07%	0.43%	16.30	4.66%	24.00
State Farm	3,158.60	3.26%	10	1.38%	2.37%	0.28%	51.80	2.09%	35.90
Swiss Re	10,868.00	11.22%	173	23.90%	9.51%	2.96%	8.07	6.56%	29.56
Texas Windstorm Insurance Association (TWIA)	600.00	0.62%	2	0.28%	3.93%	1.89%	2.07	2.04%	36.00
Tokio Marine	985.00	1.02%	6	0.83%	2.53%	0.62%	6.95	1.91%	49.67
Tokio Millenium Re	630.00	0.65%	3	0.41%	5.66%	1.47%	4.94	4.19%	43.33
Transatlantic Re	500.00	0.52%	3	0.41%	6.00%	2.49%	2.59	3.51%	47.00
Travellers Group	2,350.00	2.43%	7	0.97%	4.72%	1.01%	5.03	3.70%	39.29
Turkish Cat Ins Pool	500.00	0.52%	2	0.28%	2.92%	1.23%	2.40	1.69%	36.00
UnipolSai Assicurazioni	276.11	0.29%	2	0.28%	3.37%	0.38%	8.58	2.99%	39.50
United P&C & affiliates	300.00	0.31%	5	0.69%	8.60%	5.02%	2.22	3.58%	19.40
US Fidelity and Guaranty	65.30	0.07%	3	0.41%	6.88%	2.00%	5.22	4.88%	12.00
USAA	8,199.18	8.46%	74	10.22%	9.24%	3.62%	4.69	5.61%	38.30
Validus Re	400.00	0.41%	3	0.41%	9.21%	5.01%	1.85	4.20%	48.00
Vesta Fire Ins.	41.50	0.04%	1	0.14%	4.16%	0.70%	5.94	3.46%	36.00
XL Insurance (Bermuda)	2,200.00	2.27%	18	2.49%	9.09%	4.97%	2.11	4.12%	41.50
Zenkyoren (Japan)	3,445.00	3.56%	15	2.07%	2.68%	0.69%	4.93	1.99%	56.13
Zurich Insurance Group	842.00	0.87%	5	0.69%	6.70%	1.33%	5.33	5.38%	34.40

Continued on next page

Table 1 – continued from previous page

Issuer	Size ($m)	% Size	Obs.	% Obs.	Premium (%)	EL (%)	P/EL	EER (%)	Term
Grand Total	96,871.36	100.00%	724	100.00%	7.64%	2.60%	6.35	5.04%	37.02

Note: This table shows the aggregate characteristics of CAT bonds issued by all the issuers in the CAT bond market since inception. The table displays the total issue size (in millions of US dollars), total number of issues (Obs), the average premium, average expected loss (EL), the average multiple of the premium with respect to the expected loss (P/EL), the expected excess return (EER) and the average bond term in months for each issuer. In addition, the total issue size and number of observations for each issuer are displayed as a percentage of the total. These characteristics are given for CAT bonds issued between June 1997 and March 2020 in the primary market.

.2 Multilevel Analysis

Multilevel models are an extension of linear or generalised linear models (Gelman and Hill, 2007) that are used to assess the extent of grouping in a sample. With multilevel models, however, the assumption of independent observations applied to ordinary least squares models no longer holds. Depending on the dependence structure, we can vary either the intercept, the slope, or both the intercept and the slope. The choice of this random effect depends on the underlying theoretical support. In the random intercept model, only the intercept varies by group while all the other predictors are fixed. The between-group variability is assumed to only affect the baseline or mean values of the dependent variable, depending on how the data is centred. It does not affect the manner in which the other predictors affect the dependent variable. For a two-level model, the equation then becomes (Raudenbush and Bryk, 2010),

$$Y_{ij} = \beta_{0j} + \sum_{k=1}^{p} \beta_{kj} X_{ijk} + \varepsilon_{ij} \tag{1}$$
$$\beta_{0j} = \gamma_{00} + u_{0j},$$
$$\beta_{kj} = \gamma_{k0},$$

with $\varepsilon_{ij} \sim N(0, {\sigma^2}_e)$ and $u_{0j} \sim N(0, {\sigma^2}_{u0})$, assuming the error terms are random and uncorrelated (Tolmie et al., 2011). The additional level, representing the group (the issuers), is introduced by the subscript j. With a random slope model, only the slope varies while the intercept and other predictor effects remain fixed. The assumption is that the group effect only affects the strength of the relationship between the other predictors and the dependent variable, but the mean or base value of the dependent variable remains fixed. The structure is given by Eq. (1) with

$$\beta_{0j} = \gamma_{00},$$
$$\beta_{kj} = \gamma_{k0} + u_{kj},$$

and $u_{kj} \sim N(0, {\sigma^2}_{uk})$. When we allow both intercept and slope to vary by group, then we get Eq. (1) with

$$\beta_{0j} = \gamma_{00} + u_{0j},$$
$$\beta_{kj} = \gamma_{k0} + u_{kj},$$

and $u_{kj} \sim N(0, \sigma^2{}_{uk})$. In all three cases, the overall equation remains the same, but the parameters are either fixed or random depending on the model assumption.

.3 EM Algorithm for Multilevel Analysis

Following from the equations in Appendix .2, we get the following linear mixed effects model for a random intercept model;

$$Y_{ij} = \gamma_{00} + u_{0j} + x_{ijk}{}^T \gamma_{k0} + \varepsilon_{ij} \tag{2}$$

with $\varepsilon_{ij} \sim N(0, \sigma^2{}_e)$ and $u_{0j} \sim N(0, \sigma^2{}_{u0})$, assuming the error terms are random and uncorrelated; and j represents the additional level introduced by issuer variance. In this case, the unknown parameters are given by $\delta = (\gamma_{00}, \gamma_{k0}, \sigma^2{}_e, \sigma^2{}_{u0})$, and their joint likelihood is

$$\begin{aligned} L(\delta) &= \prod_{i=1}^{m} f(y_i) = \prod_{i=1}^{m} \int f(y_i, u_{oj}) du_{oj} \\ &= \prod_{i=1}^{m} \int \prod_{j=1}^{n_i} f(y_i|u_{oj}) f(u_{oj}) du_{oj} \\ &= \prod_{i=1}^{m} \int \prod_{j=1}^{n_i} \frac{1}{\sqrt{2\pi}\sigma_e} exp \quad -\frac{(y_{ij} - \gamma_{00} - u_{oj} - x_{ijk}{}^T \gamma_{k0})^2}{2\sigma_e^2} \quad \times \frac{1}{\sqrt{2\pi}\sigma_u} exp \quad -\frac{u_{oj}{}^2}{2\sigma_u^2} \quad du_{oj} \end{aligned} \tag{3}$$

This joint likelihood can now be written as

$$L(\delta) = \prod_{i=1}^{m} c_i \sqrt{2\pi a_i} exp \left\{ -\frac{1}{2\sigma_e^2} \sum_{j=1}^{n_i} (y_{ij} - \gamma_{00} - x_{ijk}{}^T \gamma_{k0})^2 \right\} exp \quad \frac{a_i b_i^2}{2} \tag{4}$$

where

$$c_i = \quad \tfrac{1}{\sqrt{2\pi}\sigma_e} \quad ^{n_i} \tfrac{1}{\sqrt{2\pi}\sigma_u},$$
$$a_i^{-1} = \tfrac{n_i}{\sigma_e{}^2} + \tfrac{1}{\sigma_u{}^2},$$
$$b_i = \tfrac{1}{\sigma_e{}^2} \quad {}^{n_i}_{j=1} (y_{ij} - \gamma_{00} - x_{ijk}{}^T \gamma_{k0}),$$

The maximum likelihood estimator of δ is therefore;

$$\hat{\delta} = \underset{\delta}{\operatorname{argmax}} \quad L(\delta) \tag{5}$$

The complete data is then given by (y_i, u_{oj}), and the observed data is (y_i). The complete data log-likelihood is then;

$$l(\delta; y, u) = -\frac{1}{2}(\sum_{i=1}^{m} n_i)\log(2\pi\sigma_e^2) - \frac{m}{2}\log(\sigma_u^2) - \frac{1}{2\sigma_e^2}\sum_{i=1}^{m}\sum_{j=1}^{n_i}(y_{ij} - \gamma_{00} - u_{oj} - x_{ijk}{}^T\gamma_{k0})^2 - \frac{1}{2\sigma_u^2}\sum_{j=1}^{n_i} u_{oj}{}^2 \tag{6}$$

.4 ANOVA Test for Homogeneity of Variance

Table 2: *ANOVA Table for Homoscedasticity*

	Dof	Sum Sq.	Mean Sq.	F value	Pr(>F)
Issuers	100	2388.3	23.883	0.6977	0.9867
Residuals	603	20640.7	34.23		

Note: This table displays the results of the Analysis of Variance (ANOVA) test for homoscedasticity of level 1 (individual catastrophe bonds) residual variance. The columns dispay the degrees of freedom applied in the test (Dof), the sum of squares (Sum Sq.) and mean square (Mean Sq.) values, and finally the F value and its corresponding p-value (Pr(>F)). The significance of each of these values is also indicated. Significance at 90%, 95%, and 99% confidence levels are indicated by *, **, and ***, respectively. It is assumed, for this test, that the variance is equal across the level 1 subjects. This is tested through the F test, which in this case is insignificant.

Low Risk Research Ethics Approval

Project title

Final Thesis: Mathematical Optimization of Catastrophic Risk Processes via Expectation-Maximization(EM) Algorithms

Record of Approval

Principal Investigator's Declaration

I request an ethics peer reviewI confirm that I have answered all relevant questions in this application honestly	X
I confirm that I will carry out the project in the ways described in this application. I will immediately suspend research and request an amendment or submit a new application if the project subsequently changes from the information I have given in this application.	X
I confirm that I, and all members of my research team (if any), have read and agree to abide by the code of research ethics issued by the relevant national learned society.	X
I confirm that I, and all members of my research team (if any), have read and agree to abide by the University's Research Ethics Policies and Processes.	X
I understand that I cannot begin my research until this application has been approved and I can download my ethics certificate.	X

Name: Marian Chatoro (CFCI-PhD)

Date: 18/06/2023

Student's Supervisor (if applicable)

I have read this checklist and confirm that it covers all the ethical issues raised by this project fully and frankly.I also confirm that these issues have been discussed with the student and will continue to be reviewed in the course of supervision.

Name: Prof. Panagiotis Andrikopoulos

Date: 20/06/2023

Reviewer (if applicable)

Date of approval by anonymous reviewer: -

Low Risk Research Ethics Approval Checklist

Project Information

Project Ref	P161478
Full name	Marian Chatoro
Faculty	Faculty of Business and Law
Department	School of Economics, Finance and Accounting
Supervisor	Prof. Panagiotis Andrikopoulos
Module Code	CFCI-PhD
EFAAF Number	
Project title	Final Thesis: Mathematical Optimization of Catastrophic Risk Processes via Expectation-Maximization(EM) Algorithms
Date(s)	18 Sep 2022 - 01 Sep 2023
Created	18/06/2023 17:39

Project Summary

The study aggregates the results of previous years into a final thesis file

Names of Co-Investigators and their organisational affiliation(place of study/employer)	Prof Panos Andrikopoulos, CFCI
Is this project externally funded?	No
Are you required to use a Professional Code of Ethical Practice appropriate to your discipline?	No
Have you read the Code?	No

Project Details

What are the aims and objectives of the project?	This study intends to contribute to this long-term optimality, by first analysing the history, developments, and trends underlying climate processes, modelling these processes mathematically for the sake of comprehensiveness, and finally applying said models to not only improve climate-based catastrophic risk loss modelling, but also to price and analyse extreme disaster risk financing instruments.
Explain your research design and outline the principal method(s) you will use	The study focuses on the application of mathematical optimization, with the Expectation-Maximization (EM) algorithm in particular, to improve climate-based catastrophic loss modelling and pricing of catastrophic disaster risk financing instruments, and the catastrophe bond in particular. Three main studies are conducted, with the first aiming to assess the catastrophe bond market's efficiency by analysing the 'fairness' of its issuer specific prices through multi-level random effects modelling, the second to provide a better mathematical optimization model for the heavy-tailed nature of catastrophic losses through finite mixture modelling, while the third and final study proposes a model that better incorporates dependence single-peril dependence structure in observed catastrophic losses by applying hidden Markov models. Apart from these three main studies, historical timelines and developments in climate and financial disaster risk management are also extensively discussed in the remaining sections.
Are you proposing to use a validated scale or published research method/tool?	No

Data Analysis

Does the research seek to understand, identify, analyse and/or report on data/information on terrorism/terrorism policies?	No
Does your research seek to understand, identify, analyse and/or report on information for other activities considered illegal in the UK and/or in the country you are researching in?	No
Are you analysing Secondary Data?	Yes
Is this data publicly available?	Yes
Could an individual be identified from the data? e.g. identifiable datasets where the data has not been anonymised or there is risk of re-identifying an individual	No
Are you dealing with Primary Data involving people?	No
Are you dealing with personal data?	No
Are you dealing with special category data (formerly known as sensitive data)?	No

Is the project solely desk based secondary research?	Yes
Will the data collection, recruitment materials or any other project documents be in any language other than English?	No
Are there any other ethical issues or risks of harm raised by the study that have not been covered by previous questions?	No

External Ethics Review

Question		Yes	No
1	Will this project be submitted for ethical review to an external organisation?		X
	Name of external organisation		
2	Are you submitting to IRAS?		
3	Has this project previously been reviewed by an external organisation?		